

**A methodology for the measurement of distributed
agricultural sources of ammonia outdoors**

Denise Clare Welch, BSc (Hons)

**Thesis submitted to The University of Nottingham
for the degree of Doctor of Philosophy, March 2003**

TABLE OF CONTENTS

List of figures	<i>vi</i>
List of tables	<i>xi</i>
Abstract	<i>xii</i>
Acknowledgements	<i>xiii</i>
Notation	<i>xiv</i>
1 INTRODUCTION AND LITERATURE REVIEW	
1.1 AMMONIA	1
1.1.1 Mechanisms of ammonia emission	2
1.1.2 Emissions of ammonia from farm animals and their housing	3
1.1.3 Waste collection and storage	3
1.1.4 Application of animal manure and slurry	4
1.1.5 Emissions of ammonia from other sources	4
1.2 REDUCTION OF EMISSIONS FROM AGRICULTURAL SOURCES	5
1.3 PIG PRODUCTION	6
1.3.1 Outdoor pig production	6
1.3.2 Urine excretion	8
1.4 FACTORS AFFECTING AMMONIA EMISSION	9
1.4.1 Soil	9
<i>1.4.1.1 Moisture</i>	<i>9</i>
<i>1.4.1.2 pH</i>	<i>9</i>
<i>1.4.1.3 Cation Exchange Capacity</i>	<i>10</i>
1.4.2 Wind	11
1.4.3 Temperature	12
1.5 THE FATE OF AMMONIA IN THE ATMOSPHERE	13
1.5.1 Plant-atmosphere exchange	13
1.5.2 Dry deposition	14
1.5.3 Precipitation scavenging	14
1.6 ENVIRONMENTAL IMPACT	15
1.6.1 Direct effects	15
<i>1.6.1.1 Eutrophication</i>	<i>15</i>
1.6.2 Indirect effects	16
<i>1.6.2.1 Acidification</i>	<i>16</i>
<i>1.6.2.2 Opening of the canopy</i>	<i>17</i>
<i>1.6.2.3 Aerosol formation</i>	<i>18</i>
1.7 MEASUREMENT OF EMISSIONS	19
1.7.1 Ventilated volatilization chambers	20
1.7.2 Wind tunnels	21
1.7.3 Recovery of ¹⁵N	22
1.7.4 Micrometeorological methods	22
1.7.5 Tracer ratio method	26
1.7.6 Standard comparison method	27
1.7.7 Modelling	28

1.8 PASSIVE AMMONIA FLUX SAMPLERS	29
1.8.1 Principle of operation	29
<i>1.8.1.1 Acid coating</i>	33
1.8.2 Measurement of net horizontal flux	34
1.8.3 Variations on the Ferm tube	34
1.8.4 Advantages and disadvantages of PAF samplers	36
1.9 CONCLUSIONS	38
1.10 THESIS OUTLINE	38
2 MEASUREMENT OF THE COLLECTION EFFICIENCY OF PASSIVE AMMONIA FLUX SAMPLERS	
2.1 INTRODUCTION	40
2.2 MATERIALS AND METHODS	41
2.2.1 The fan test rig	41
2.2.2 Wind speed distribution	43
2.2.3 Ammonia supply system	43
2.2.4 Preparation and analysis of recurved PAF samplers	45
2.2.5 Experiment 1: Ammonia flux distribution	46
2.2.6 Experiment 2: Effect of orientation of sampler to air flow	47
2.3 RESULTS	48
2.3.1 Wind speed distribution	48
2.3.2 Experiment 1: Ammonia flux distribution	50
<i>2.3.2.1 Collection efficiency of recurved PAF samplers</i>	50
<i>2.3.2.2 Positional effect</i>	51
2.3.3 Experiment 2: Effect of orientation of sampler to air flow	52
2.3.4 Results at a wind speed of 10 m s⁻¹	54
2.3.5 Error analysis	55
2.3.6 Reference ammonia flux	55
2.4 DISCUSSION	55
2.4.1 Experiment 1: Ammonia flux distribution	55
2.4.2 Critical angle of incidence	56
2.4.3 Collection efficiency	58
2.5 CONCLUSIONS	59
3 VALIDATION OF THE FLUX FRAME METHOD IN THE ATMOSPHERIC FLOW LABORATORY	
3.1 INTRODUCTION	60
3.2 MATERIALS AND METHODS	61
3.2.1 The Atmospheric Flow Laboratory	61
3.2.2 Flux frame	62
3.2.3 Preliminary investigation	63
3.2.4 Ammonia release experiments	65
3.2.5 Turbulence intensity	67
3.2.6 Total error	68
3.2.7 Plume simulation	68

3.3 RESULTS	71
3.3.1 Preliminary investigation	71
3.3.1.1 Smoke release	71
3.3.1.2 Variations in wind speed along a lateral traverse of the AFL	72
3.3.2 Ammonia Release Experiments	79
3.3.3 Actual difference plots	87
3.3.4 Optimum sampling configuration	91
3.4 DISCUSSION	92
3.4.1 The use of the AFL	92
3.4.2 Loss of ammonia	93
3.4.3 Optimum sampling configuration	94
3.4.4 Agreement between ammonia release experiments	95
3.4.5 Agreement between measured and modelled plots	95
3.4.6 The use of ADMS 3.0 in the AFL	96
3.4.7 Saturation of samplers	97
3.4.8 Improvements and possibilities for future work	97
3.5 CONCLUSIONS	97
4 VALIDATION OF THE FLUX FRAME METHOD IN THE FIELD	
4.1 INTRODUCTION	99
4.2 MATERIALS AND METHODS	100
4.2.1 Flux frame	100
4.2.2 Field site	101
4.2.3 Ammonia point source	101
4.2.4 Ammonia line source	102
4.2.5 Modifications to the flux frame	103
4.2.6 ADMS modelling	104
4.2.7 Meteorological station	104
4.3 RESULTS	105
4.3.1 Run 1: Point source at 15 m	105
4.3.2 Runs 2 and 3: Point source at 25 m	108
4.3.3 Runs 4 and 5: Point source at 50 m	111
4.3.4 Modifications to the flux frame	114
4.3.5 Runs 10, 11 and 12: Line source length of 20 m	114
4.3.6 Run 8: Line source length of 40 m	119
4.3.7 Runs 6 and 7: Line source length of 80 m	120
4.3.8 Total error	123
4.3.9 Measured vs. modelled fluxes	123
4.3.10 Apparent vs. actual measured collection efficiencies	128
4.3.11 Collection efficiency using sections of the flux frame	129
4.4 DISCUSSION	132
4.4.1 Capture of the height of the plume	132
4.4.2 Agreement between ammonia release experiments	132
4.4.3 Agreement between measured and modelled plots	133

4.4.4	Collection efficiency using sections of the flux frame	134
4.4.5	Potential for loss of ammonia	134
4.4.6	Usefulness of flux frame method	135
4.4.7	Future work	136
4.3	CONCLUSIONS	136
5 MEASUREMENT OF AMMONIA EMISSIONS AT A FREE-RANGE SOW FARM		
5.1	INTRODUCTION	138
5.2	MATERIALS AND METHODS	140
5.2.1	Farm	140
5.2.2	Preliminary Investigation	142
5.2.3	Flux sampling	142
5.2.4	Soil Sampling	145
	5.2.4.1 <i>Moisture content</i>	145
	5.2.4.2 <i>pH</i>	146
5.2.5	Additional information	146
5.2.6	Meteorological station	146
5.3	RESULTS	147
5.3.1	Preliminary results	147
5.3.2	Flux sampling	147
	5.3.2.1 <i>Run 1</i>	148
	5.3.2.2 <i>Run 2</i>	151
	5.3.2.3 <i>Run 3</i>	154
5.3.3	Soil Sampling	157
5.3.4	Additional information	161
5.3.5	Source strength calculation	162
5.4	DISCUSSION	162
5.4.1	Limitations	162
5.4.2	pH vs. ammonia emission	164
5.4.3	Moisture vs. ammonia emission	164
5.4.4	Variability of wind direction	165
5.4.5	Nitrogen losses	165
5.4.6	Source strength comparison	166
5.4.7	Uses of flux samplers	166
5.4.8	Other possible methods	167
	5.4.8.1 <i>Micrometeorological methods</i>	167
	5.4.8.2 <i>Tracer techniques</i>	167
	5.4.8.3 <i>Measurements from other grazing animals</i>	168
5.5	CONCLUSIONS	169
6 GENERAL DISCUSSION AND CONCLUSIONS		
6.1	INTRODUCTION	170
6.2	VALIDATION OF RECURVED PASSIVE AMMONIA FLUX SAMPLERS	170
6.3	VALIDATION OF THE FLUX FRAME METHOD	172

6.4 AMMONIA EMISSIONS FROM FREE-RANGE SOWS	176
6.5 FURTHER WORK	179
6.6 CONCLUSIONS	181

BIBLIOGRAPHY	183
---------------------	-----

APPENDIX 1: CHEMICAL ANALYSIS OF SAMPLERS

APPENDIX 2: UNCERTAINTY OF FLUX MEASUREMENTS

APPENDIX 3: ADMS PARAMETERS

APPENDIX 4: AMMONIA DEPOSITION RATE CALCULATION

List of Figures

Figure 1.1: Mechanisms of transport and deposition of pollutants (ITE Edinburgh).	13
Figure 1.2: Passive ammonia flux sampler.	29
Figure 1.3: Sketch of the change in positive and negative pressure profiles over the ends of the tubes with an increased angle of incidence of the ambient wind.	33
Figure 1.4: a) Photograph of recurved passive ammonia flux sampler. b) Diagram of side view. c) Plan view.	36
Figure 2.1: The fan test rig.	41
Figure 2.2: Sketch showing sampler position (1-6) in wind tunnel extension. Black lines represent the recurved PAF samplers held at an angle whilst the red circles represent the sampling plane. Direction of air flow is out of the plane of the page.	42
Figure 2.3: Ammonia supply system and wind tunnel.	44
Figure 2.4: Photograph of mass flow controllers and control unit.	45
Figure 2.5: Bubbler system.	46
Figure 2.6: Wind speed distribution as a function of vertical position within the extension of the wind tunnel.	49
Figure 2.7: Collection efficiency of recurved PAF samplers.	50
Figure 2.8: Variation of the ratio of measured to nominal fluxes with orientation of the flux sampler to the flow direction. Each symbol represents the net flux measured by a sampler.	53
Figure 2.9: Average collection efficiency of recurved PAF samplers when orientated at angles 0-80°. Symbols represent the average measured flux for angles 0-80° for each of the 12 wind speed and ammonia concentration combinations.	54
Figure 2.10: Comparison of experimental data from this study (black line), cosine curve, Ferm (1986) - blue line, and Flint <i>et al.</i> (2000) - red line.	58
Figure 3.1: Working section of Atmospheric Flow Laboratory, viewed from downstream.	62
Figure 3.2: Schematic of AFL. Green dashed line represents the fan bank; blue lines show the positions of the curtain; dotted lines are mesh curtains; pink arrows show the direction of the air flow.	62
Figure 3.3: Smoke release in the AFL.	64
Figure 3.4: Cross-section of working section of AFL 17.6 m downwind of the fans. o indicate sampling locations, whilst the dashed lines indicate the three different sampling planes.	64

Figure 3.5: Variation in wind speed across a lateral traverse of the AFL. Blue lines and symbols represent the slowest nominal speed (2.4 m s^{-1}), pink the medium speed (3.4 m s^{-1}), and green the fastest (4.2 m s^{-1}). Diamonds represent measurements at the left side of the AFL, squares the centre and triangles the right. The lines represent the average profile and the error bars are one standard error of the mean.	72
Figure 3.6: Wind speed profiles for the slowest wind speed (2.4 m s^{-1}) before the curtain was added (blue diamonds), with extractors on (green triangles) and off (pink circles), and repeat measurements at the original measurement heights with the curtain fitted and extractors off (red squares).	73
Figure 3.7: Wind speed profile when checking sonic anemometer. The three different symbols represent the results from three repeats at the same measurement heights.	75
Figure 3.8: Wind speed profiles with original fan settings. Blue diamonds represent the fastest speed (2.8 m s^{-1} at a height of 2 m), pink squares the medium speed (2.3 m s^{-1} at 2 m) and green triangles the slowest (1.7 m s^{-1} at 2 m).	76
Figure 3.9: Turbulence intensity profiles with original fan settings. Legend as Figure 3.8.	76
Figure 3.10: Improved wind speed profiles. Legend as Figure 3.8.	77
Figure 3.11: Improved turbulence intensity profiles. Legend as Figure 3.8.	77
Figure 3.12: Turbulence intensity profile as reported by Hoxey <i>et al.</i> , (2000) measured at SRI wind engineering site.	78
Figure 3.13: Plot of wind speed against log height in the AFL to determine the aerodynamic roughness length for the AFL for each of the three speeds (blue is 2.8 m s^{-1} at a height of 2 m, pink is 2.3 m s^{-1} and green 1.7 m s^{-1}).	79
Figure 3.14: Contour plot of horizontal ammonia flux with position on flux frame using 80 recurved PAF samplers, Run 6.	80
Figure 3.15: Contour plot of Run 6, with saturation taken into account.	81
Figure 3.16: Contour plot of horizontal fluxes measured at 90 sampling locations, Run 16.	84
Figure 3.17: Contour plot of fluxes modelled at 90 sampling locations, Run 16.	84
Figure 3.18: Contour plot of horizontal fluxes measured at 87 sampling locations with a higher sampling density at the centre of the plume, Run 19.	85
Figure 3.19: Contour plot of fluxes modelled at 87 sampling locations with a higher sampling density at the centre of the plume, Run 19.	85
Figure 3.20: Contour plot when saturation has been taken into account, Run 19.	86
Figure 3.21: Actual differences between measured and modelled fluxes for each sampling position, plotted on flux frame area. Run 10 – ground level source, wind speed at 2 m = 2.8 m s^{-1} .	88

Figure 3.22: Actual differences between measured and modelled fluxes for each sampling position, plotted on flux frame area. Run 17 – source positioned centrally, wind speed at 2 m = 2.3 m s ⁻¹ .	88
Figure 3.23: Actual differences between measured fluxes for two replicate runs, plotted over the sampling area. Runs 11 and 12, ground level source, wind speed at 2m = 1.7 m s ⁻¹ .	89
Figure 3.24: Actual differences between measured fluxes for two replicate runs, plotted over the sampling area. Runs 14 and 15, ground level source, wind speed at 2m = 2.3 m s ⁻¹ .	90
Figure 3.25: Actual differences between measured fluxes for two replicate runs, plotted over the sampling area. Runs 22 and 23, ground level source, wind speed at 2m = 2.8 m s ⁻¹ .	90
Figure 3.26: Actual differences between measured fluxes for two replicate runs, plotted over the sampling area. Runs 16 and 17, source centrally positioned, wind speed at 2m = 2.3 m s ⁻¹ .	91
Figure 4.1: The flux frame viewed from upwind of the prevailing wind	101
Figure 4.2: Run 1: scale diagram.	107
Figure 4.3: Run 1: point source at 15 m from the flux frame: a) Fluxes measured at 132 sampling locations (Collection efficiency = 63.5%); b) fluxes modelled for the same sampling locations (C.E.=52.0%).	107
Figure 4.4: Run 2: scale diagram.	109
Figure 4.5: Run 2: point source at 25 m from the flux frame: a) Fluxes measured at 132 sampling locations (C.E.=47.6%); b) fluxes modelled for the same sampling locations (C.E.=30.0%).	109
Figure 4.6: Run 3: scale diagram.	110
Figure 4.7: Run 3: point source at 25 m from the flux frame: a) Fluxes measured at 132 sampling locations (C.E.=60.6%); b) fluxes modelled for the same sampling locations (C.E.=59.7%).	110
Figure 4.8: Run 4: scale diagram.	112
Figure 4.9: Run 4: point source at 50 m from the flux frame: a) Fluxes measured at 132 sampling locations (C.E.=63.5%); b) fluxes modelled for 132 sampling positions (C.E.=56.0%).	112
Figure 4.10: Run 5: scale diagram.	113
Figure 4.11: Run 5: point source at 50 m from the flux frame: a) Fluxes measured at 132 sampling locations (C.E.=46.7%); b) fluxes modelled for the same sampling positions (C.E.=57.8%).	113
Figure 4.12: Run 3: fluxes modelled for 156 sampling positions.	114
Figure 4.13: Run 10: scale diagram showing source position (green line) and wind conditions relative to flux frame (pink line).	116
Figure 4.14: Run 10: 20 m line source at 25 m from flux frame: a) Fluxes measured by 156 samplers (C.E.=81.2%); b) fluxes modelled for the same sampling locations (C.E.=82.6%).	116
Figure 4.15: Run 11: scale diagram.	117

Figure 4.16: Run 11: 20 m line source at 25 m from flux frame: a) Fluxes measured by 156 samplers (C.E.=113.9%); b) fluxes modelled for the same sampling locations (C.E.=88.0%).	117
Figure 4.17: Run 12: scale diagram.	118
Figure 4.18: Run 12: 20 m line source at 25 m from flux frame: a) Fluxes measured by 156 samplers (C.E.=97.8%); b) fluxes modelled for the same sampling locations (C.E.=86.3%).	118
Figure 4.19: Run 8: scale diagram.	119
Figure 4.20: Run 8: 40 m line source at 25 m from flux frame: a) Fluxes measured by 156 samplers (C.E.=45.3%); b) fluxes modelled for the same sampling locations (C.E.=82.6%).	119
Figure 4.21: Run 6: scale diagram.	121
Figure 4.22: Run 6: 80 m line source at 25 m from flux frame: a) Fluxes measured by 156 samplers (C.E.=15.9%); b) fluxes modelled for the same sampling locations (C.E.=48.6%).	121
Figure 4.23: Run 7: scale diagram.	122
Figure 4.24: Run 7: 80 m line source at 25 m from flux frame: a) Fluxes measured by 156 samplers (C.E.=34.2%); b) fluxes modelled for the same sampling locations (C.E.=62.6%).	122
Figure 4.25: a-k): Correlation plots of measured and modelled fluxes for each experimental run; l): All runs combined.	125-127
Figure 4.26: Correlation plot of all measured and modelled flux data, restricted to fluxes below 5 mg NH ₃ m ⁻² s ⁻¹ .	128
Figure 4.27: a) Run 7: Half frame; b) Run 7: Single mast of samplers at centre of plume.	130
Figure 4.28: Comparison of 'Half frame', 'Quarter frame' and 'Single mast' collection efficiencies with the collection efficiency of the full flux frame. Different symbols represent the results of the six experimental runs; Red symbols and lines refer to the relationship between the full frame and half frame, blue – full and quarter, and green – full and single mast.	131
Figure 5.1: Aerial photograph of farm (www.multimap.co.uk).	141
Figure 5.2: Typical conditions at farm.	141
Figure 5.3: Positions of sampling masts around farm perimeter on simplified diagram of the site.	143
Figure 5.4: Schematic of sampling mast.	143
Figure 5.5: Sampling mast in use at farm. (position 4 on Figure 5.3). Inset: Close-up of sampler holders lowered to enable samplers to be	144
Figure 5.6: Change in net flux with height for each sampling mast (1-6), Run 1.	149
Figure 5.7: Wind direction throughout the sampling period, Run 1.	150
Figure 5.8: Wind speed throughout the sampling period, Run 1.	150
Figure 5.9: Change in net flux with height for each sampling mast (1-6), Run 2.	152
Figure 5.10: Wind direction throughout the sampling period, Run 2.	153
Figure 5.11: Wind speed throughout the sampling period, Run 2.	153

Figure 5.12: Change in net flux with height for each sampling mast (1-6), Run 3.	155
Figure 5.13: Wind direction throughout the sampling period, Run 3.	156
Figure 5.14: Wind speed throughout the sampling period, Run 3.	156
Figure 5.15: Soil sampling positions, Run 1. Soil moisture content is marked for each position in dark blue, whilst pH is yellow.	158
Figure 5.16: Soil moisture content vs. Soil pH, Run 1.	159
Figure 5.17: Soil sampling positions, Run 2. Soil moisture content: dark blue; pH: yellow.	160
Figure 5.18: Soil sampling positions, Run 3. Soil moisture content: dark blue; pH: yellow.	161

List of Tables

Table 2.1: Reynolds numbers for air speeds to be used in experiments.	43
Table 2.2: Summary of multiple regression analysis results for wind speed distribution for each of the three wind speeds tested. Polynomial regressions were fitted to each data set; $y = a + bx + cx^2$ where y is the wind speed, x is the position and a , b and c are fitted parameters.	49
Table 2.3: Summary of simple regression analysis for positional effects on flux measurement.	52
Table 3.1: Maximum distance of smoke nozzle from frame at the three wind speeds.	71
Table 3.2: Comparison of wind speed once curtain added to AFL.	74
Table 3.3: AFL results summary sheet. (Green cells are runs performed at 1.7 m/s; orange 2.3 m/s; blue 2.8 m/s and pink with the source centrally located).	82
Table 3.4: Summary of optimum sampler configuration investigation.	92
Table 4.1: Summary of results for all experimental runs successfully performed and analysed.	106
Table 4.2: R^2 and O values for each experimental run.	124
Table 4.3: Collection efficiencies of sections of the flux frame.	129
Table 5.1: Comparison of reported ammonia emission rates.	139
Table 5.2: Net fluxes measured at each sampling position, Run 1.	148
Table 5.3: Fluxes measured on individual tubes of the sampler, Run 1.	149
Table 5.4: Net fluxes measured at each sampling position, Run 2.	151
Table 5.5: Fluxes measured on individual tubes of the sampler, Run 2.	152
Table 5.6: Net fluxes measured at each sampling position, Run 3.	154
Table 5.7: Fluxes measured on individual tubes of the sampler, Run 3.	155
Table 5.8: Wind direction proportions, all Runs.	157
Table 5.9: Summary of pig numbers and live weights.	161
Table 6.1: Total ammonia emission from pig production (from Pain <i>et al.</i> , 1998).	178
Table 6.2: Total ammonia emission from UK agriculture (from Pain <i>et al.</i> , 1998).	178

ABSTRACT

Ammonia is the most prevalent alkaline gas in the atmosphere and plays an important role in environmental pollution through acidification and eutrophication. Livestock are the largest source of ammonia in the UK, mainly originating during storage and spreading of animal manure. The aim of this study was to validate the collection efficiency of recurved passive ammonia flux (PAF) samplers and the flux frame method to provide a robust methodology for measurement of distributed agricultural sources of ammonia outdoors.

The collection efficiency of recurved PAF samplers was determined in a wind tunnel under controlled conditions of ammonia flux ($0.771 - 13.49 \text{ mg NH}_3 \text{ m}^{-2} \text{ s}^{-1}$), and at angles of orientation to the flow direction ($0, 30, 60, 70, 80, 90^\circ$). The samplers were effective up to a wind speed of 7 m s^{-1} and an angle of 80° , with a mean collection efficiency of 71%.

The flux frame method had a mean collection efficiency of 87.4% when used with ground level point sources under controlled conditions in the Atmospheric Flow Laboratory. However, in controlled field releases, the efficiency fell to 56.4%. The flux frame method was also suitable for line sources, although assumptions must be made about the source homogeneity and plume dispersion. ADMS modelling was used to predict the collection efficiencies for the flux frame method and these agreed with measured collection efficiencies to within 37.3%.

A comparison of source strengths determined using a full size flux frame and portions of the flux frame showed that a full size flux frame was unnecessary as one column of samplers produced a very similar estimate to that of the whole frame.

The validated method was then used to measure ammonia emissions from free-range pigs. The amount of ammonia emitted from this source was very low and less than $0.16 \text{ g (kg of sow)}^{-1} \text{ day}^{-1}$.

ACKNOWLEDGEMENTS

(and thank yous!)

I would like to thank my supervisors Dr. Jeremy Colls and Dr. Theo Demmers for their technical guidance and support throughout this project. I would particularly like to thank Prof. Christopher Wathes, who has not only been my supervisor, but also my mentor on more than just my academic career. Thank you for getting your hands dirty on so many occasions!

I must also give many thanks to John Rickatson, who allowed me to use his farm for my measurements and didn't complain when we dug up half his field and had 12 m high lighting columns, visible from miles around, attracting attention to his farm for 6 months!

Many thanks are due to most of the staff in the Environment Group at Silsoe Research Institute for their assistance with deploying samplers and hoisting masts, most notably Len Burgess, Dave Matthews and Annaclaire Richards, but thanks to all for every little bit of help received. The lab staff, past and present, (Christine O'Sullivan, Alison Bird, Colin Mitchell, Paul Rooney and Katie Bowden) also need thanking for their encouragement when the mountains of sampling tubes seemed never ending. Without their support I don't think the days spent washing and coating tubes would have been bearable. Thanks must also go to Rodger White for his patient explanations of statistics.

I would like to thank the many friends I have made here at the Institute, particularly my closest friends, who have kept me sane in times of need (and there have been many!). Last, but not least, I would like to thank my mum and Frank, and Roger (my partner and best friend) for all their constant encouragement and confidence that I had what it took to complete this project.

NOTATION

<i>F</i>	flux	$\mu\text{g m}^{-2} \text{s}^{-1}$
<i>C</i>	concentration	$\mu\text{g m}^{-3}$
<i>u</i>	wind velocity	m s^{-1}
<i>U</i>	wind speed	m s^{-1}
<i>Q</i>	source strength	$\mu\text{g s}^{-1}$
Δz	height difference	m
<i>d</i>	distance	m
<i>n</i>	number of masts	
<i>m</i>	number of sampling heights	
<i>x</i>	fetch	m
<i>z</i>	height of plume	m
z_0	roughness length	m
T_F	Transfer factor	
P_D	negative pressure	Pa
F_D	drag force	N
C_D	drag coefficient	
ρ	air density	kg m^{-3}
<i>A</i>	area	m^2
P_O	pressure drop over orifice meter	Pa
<i>B</i>	ratio of orifice diameter to tube diameter	
D_O	orifice diameter	m
D_T	tube diameter	m
<i>Y</i>	expansion factor	
C_O	orifice meter constant	
<i>K</i>	sampler constant	
<i>r</i>	radius	m
<i>t</i>	time	s
<i>M</i>	mass	μg
<i>Re</i>	Reynold's number	
<i>v</i>	coefficient of kinematic viscosity of air ($15.5 \times 10^{-6} \text{ m}^2 \text{ s}^{-1}$ at 20°C)	
<i>E</i>	dimension of system (area / perimeter)	

V	mass captured by the flux frame per unit time	mg s ⁻¹
H	height	m
H ₀	aerodynamic roughness length	m
<i>u</i> _*	turbulent velocity fluctuations	
κ		
W _m	moisture content	%
O	overall error	
I	Turbulence Intensity	%

INDICES

e	air entering
l	air leaving
d	downwind
u	upwind
i	mast number
o	sampling height
v	vertical
gas	pollutant
SF ₆	SF ₆
S	standard plot
E	experimental plot
A	measured
B	background
P	projected area
O	orifice
h	horizontal
F	flux frame
R	released
REF	reference measurements
M	modelled
Run 1	replicate 1

Run 2	replicate 2
W	wet sample plus container
D	dry sample plus container
T	empty dry container
j	sampling position
stream	in the streamwise direction
lat	in the lateral direction
vert	in the vertical direction

1. INTRODUCTION AND LITERATURE REVIEW

1.1 AMMONIA

Ammonia (NH_3) is the most abundant alkaline gas in the atmosphere. When it is emitted as gaseous NH_3 , it rapidly reacts with other gases such as SO_2 and NO_x to form ammonium aerosols (Singles *et al.*, 1998). As SO_2 emissions have decreased over recent years, concern over environmental pollution has switched to NH_3 and also NO_x , both of which contribute not only to acidification of ecosystems but also to eutrophication (Sutton *et al.*, 1998). Ammonia emissions to the atmosphere mainly originate from agriculture, especially from farm animals and their manures, and emissions have risen along with intensification of farming (Apsimon and Kruse-Plass, 1991, Hartung, 1991); in the UK, 90-95% of emissions originate from agricultural sources (Sutton *et al.*, 1995; Holman, 1999).

Approximately fifty percent of the total emissions from agriculture are estimated to arise from cattle production (Pain *et al.*, 1998; Holman, 1999). Whilst the majority of this occurs during slurry spreading, other losses from the housing of cattle and storage of their waste also contribute significant amounts (Pain *et al.*, 1998). Losses from sheep, poultry and pig production, and fertiliser applications to agricultural land make up the remainder; current estimates are sheep 5-7%, poultry 10-15%, pigs 10-12% and fertiliser production 16-25% (Pain *et al.*, 1998; Holman, 1999).

Ammonia emission is an environmental issue for three main reasons:

- NH_3 deposition on and around livestock farms can damage vegetation;
- Aerial deposition of ammonia and ammonium contributes to water and soil acidification;
- NH_3 deposition is one of the main sources of increased nitrogen supply to natural areas which can contribute to eutrophication of terrestrial and aquatic

ecosystems, leading to changes in species diversity, and increases in the fluxes of greenhouse gases (mainly N₂O) to the atmosphere (ECETOC, 1994).

Short and long range transport deposits atmospheric nitrogen in many natural and semi-natural ecosystems. Nitrogen deposition has been estimated to be as high as 20-60 kg N ha⁻¹ yr⁻¹ in non-forest ecosystems in Europe, in contrast to the estimated 1-5 kg N ha⁻¹ yr⁻¹ early this century (Bobbink, 1998). As ammonia has an atmospheric lifetime of the order of hours (Galperin and Sofiev, 1998) it is therefore deposited relatively close to the sources of emission. Ammonium ions (NH₄⁺), however, have low deposition velocities as they form complexes in the atmosphere, such as with nitrate ions forming NH₄NO₃, which then persist as aerosols with diameters around 2.5 μm (Fangmeier *et al.*, 1994). This enables long-range transport to take place.

The spatial distribution of ammonia sources reflects the distribution of livestock, particularly cattle, and as intensification of livestock production has occurred, the strength of sources has increased in recent decades (Holman, 1999). Ammonia emissions to the atmosphere from animal waste (stored and land-applied) represent losses of valuable nitrogen fertiliser for crop production, that should be minimised not only for environmental but also for economic reasons (Hartung, 1991; Amberger, 1991; McGinn and Janzen, 1998).

1.1.1 Mechanisms of ammonia emission

NH₃ is a gas at normal atmospheric temperatures and pressures with high solubility in water. NH₃ reacts with water and this reaction determines the concentration of NH₃ in the solution and hence the potential for NH₃ volatilization. NH₄⁺ in soil originates from manures, fertilisers, and from mineralisation (decomposition) of organic matter, e.g. plant residues. NH₃ can also be formed, e.g. in the rumen of animals and in the soil, by bacterial reduction of nitrate, notably in environments rich in degradable carbon compounds (Cole, 1988).

Enhanced NH_4^+ concentration in soil solution is removed within a few days by three major mechanisms: uptake by plants and microbes, biological oxidation of NH_4^+ to NO_3^- during nitrification, and by ion exchange reactions, whereby NH_4^+ can be retained by clays and organic matter. NH_4^+ in aqueous solution is in equilibrium with NH_3 ($\text{NH}_4^+ + \text{H}_2\text{O} \leftrightarrow \text{NH}_3 + \text{H}_3\text{O}^+$), and as either pH or temperature (or both) increases, the concentration of NH_3 increases and the concentration of NH_4^+ decreases (ECETOC, 1994).

1.1.2 Emissions of ammonia from farm animals and their housing

More than one third of the ammonia emissions from agriculture are from buildings and stores (Hartung, 1991). Pain *et al.* (1998) calculate that 64% of ammonia emissions from pigs in the UK are from housing. Since about 20% of the pig breeding herd are kept out of doors, and using an emission factor for grazing cattle, Pain *et al.* (1998) estimated that just 1% of ammonia losses were due to outdoor pigs.

In most inventories of national emissions from dairy cow housing, it has so far been assumed that emissions arise only over the winter when the cows are housed almost full-time, and that emissions for the remainder of the year are zero. However, variations in the practice of housing cows mean that some cows are housed during the summer and this leads to an increase in total ammonia emissions by at least another 9% in the UK (Phillips *et al.*, 1998a).

1.1.3 Waste collection and storage

As methods for storage of wastes and their removal from animal housing vary from country to country and from farm to farm, so do the amount of emissions from them (ECETOC, 1994). Emissions from slurry and urine pits used for storage can be very large. They can be reduced by covers and ensuring that the pit is full beneath the cover (Gustavsson, 1998).

1.1.4 Application of animal manure and slurry

Low-trajectory spreading, shallow injection, deep injection, ploughing after application to mix the manure with the soil or application of diluted slurry where the land must be left undamaged (e.g. grassland for grazing), are techniques that reduce emissions after spreading. Seasonal effects (temperature; rainfall) are also important (Amberger, 1991; Klarenbeek and Bruins, 1991; Phillips *et al.*, 1991; Malgeryd, 1998). When injected, losses have been reported to be as little as 2.5% (Hoff *et al.*, 1981). Incorporation of wastes into bare soils within four hours of application is recommended by Gustavsson (1998), and leads to a reduction of 80% of the ammonia volatilization if this is to a depth of 5 cm or greater (Kirchmann and Lundvall, 1998).

Up to 40% of the total ammonium nitrogen content of pig slurry was found by Vlassak *et al.* (1991) to be lost as NH_3 during the first four days after traditional surface application in the summertime. In winter, this was reduced to 23% due to the lower temperature. In both winter and summer, fifty per cent of total ammonia loss took place during the first twelve hours and a further 20% volatilised in the next twelve hours, leading to an overall figure of 70% in 24 hours (Vlassak *et al.*, 1991). This highlights the need for incorporation as soon as possible after spreading.

When applied under the same conditions, solid manure can give rise to much higher ammonia emissions than slurry and should therefore not be considered as a low-concentration nitrogen fertiliser (Malgeryd, 1998).

1.1.5 Emissions of ammonia from other sources

Industrial processes, including fertiliser production, are thought to be a significant source of ammonia with other minor sources including uncultivated soils, human respiration and traffic. Other potentially significant sources include low-temperature combustion, for example domestic bonfires, and decaying vegetation (Holman, 1999). Horses, wild animals, sea bird colonies, industry, sugar beet processing, household products, non-agricultural fertiliser use, land-spreading of

sewage sludge, direct human emissions (sweat, breath, smoking, infants), pets (cats and dogs) and fertiliser manufacture are the sources included in the 1996 estimate of 54 (27-106) kt of ammoniacal-N emitted from non-agricultural sources per year (Sutton *et al.*, 2000).

1.2 REDUCTION OF EMISSIONS FROM AGRICULTURAL SOURCES

Jarvis (1991) found that as the nitrogen content of an animal's diet increased, not only did the total quantity of urinary nitrogen increase but so also did the urea content. Therefore, the amount of N available for emission can be influenced through the diet of an animal. It is possible to reduce urea concentrations in urine, and thus ammonia emissions, by either feeding low protein diets or including more fibrous food in the diet. Fibrous food, or adding acidifying salts to the diet, can also lower the pH of slurry which lowers ammonia emission (van der Peet-Schwering *et al.*, 1999). These methods result in reductions of nitrogen excretion of between 15 and 54%, and thus ammonia emissions to the atmosphere (Canh *et al.*, 1998; Peterson *et al.*, 1998; Dourmad *et al.*, 1999).

Vlassak *et al.* (1991) found however that, although the emissions of ammonia were reduced, losses of other forms of nitrogen were increased through denitrification. This realisation has led to a new holistic approach to pollution abatement to avoid 'pollution swapping'. This is implemented, for example, in a computer-based decision support system for the application of manure, known as MANNER (MANure Nitrogen Evaluation Routine) (Chambers *et al.*, 2000). This allows more efficient use of manure to increase fertilisation whilst reducing losses of both ammonia gas and nitrate as leachate (Webb *et al.*, 2001).

A new international protocol is being developed to incorporate the contribution from ammonia to the overall nitrogen deposition in Europe. This uses the MARACCAS model (Model for the Assessment of Regional Ammonia Cost Curves for Abatement Strategies) which assesses the potential for the abatement of ammonia emissions and the overall economic cost of the reduction. The management of livestock wastes will be of major importance in the abatement measures. Whilst the reduction in emissions is limited, it is thought that the

abatement can be achieved at a low cost. However, due to uncertainties in the estimation of ammonia emissions, arising from the complexity and variability in the behaviour of ammoniacal compounds, and the incomplete data availability, a more flexible protocol may be the most appropriate strategy. Enforcing compliance on the large numbers of farms, along with ensuring the highest quality of work when applying the techniques means that guidelines for the most cost-effective measures rather than a strict regulatory protocol would be more appropriate (Cowell and ApSimon, 1998).

One of the potential abatement strategies would be to decrease the livestock production volume (Cowell and ApSimon, 1998). This could include the relocation of farms or even a reduction in the overall number of animals (Lekkerkerk, 1998).

1.3 PIG PRODUCTION

1.3.1 Outdoor pig production

Since the middle of the ninth century BC there is evidence that pigs were kept outdoors in Britain, scavenging and foraging in forests, woods and orchards, feeding on acorns, roots, fruit and seeds. This practice did not change very much until the eighteenth century when the human population began to increase and the first steps to full confinement and the mainly intensive pig industry seen today began (Thornton, 1988).

Recently, outdoor pig production has gained in popularity for a number of reasons. It has been relatively more profitable than the production of cereal crops, and consumers now demand that animal welfare issues are taken into consideration in livestock production. Also, compared with intensive systems, outdoor pig production is a much lower cost system and capital outlay is low (Riley, 1990). Successful outdoor pig production however requires a suitable soil type, i.e. a light, sandy free-draining soil (Thornton, 1988).

The main advantages of outdoor pig herds are outlined by Thornton (1988) as:

1. favourable profitability compared with indoor herds;
2. production of strong healthy store pigs, for which demand is high;
3. lower labour costs compared with indoor herds;
4. no slurry problem and
5. low capital outlay.

Many of the disadvantages of outdoor pig production evident at the end of the 1970's have since been overcome leading to a system that can compete with intensive production. Currently in the UK around 25% of the pig breeding herd is kept outdoors on an estimated land area of 8,000 ha, principally based in eastern, central, southern and south west England (Chambers, 1998).

Whilst 25% of the pig breeding herd are kept out of doors, there is very little literature on the contribution of this source to ammonia emissions and other forms of pollution such as nitrate leaching. One study available, carried out by Chambers (1998), suggests that nitrogen inputs to outdoor pig systems can be considerable. Calculated annual N inputs in feed for systems stocked at 14 dry sows ha⁻¹ are 625 kg ha⁻¹ N, whilst estimated outputs in pig meat are 119 kg ha⁻¹ N. The surplus N is largely returned to the soil via faeces and urine which is then potentially available for volatilisation or leaching (Chambers, 1998).

Most emission rates in literature are for intensively housed pigs. For example, estimated ammonia emission rates from livestock buildings, measured using chemiluminescence were found to be 46.9 kg lu⁻¹ yr⁻¹ (lu = livestock unit = 500 kg) for a fattening pig unit (Demmers *et al.*, 1999). However, Williams *et al.* (2000) measured an ammonia emission rate of 11 g NH₃ sow⁻¹ day⁻¹ and Sommer *et al.* (2001) calculated an annual ammonia volatilisation of 4.8 kg NH₃ sow⁻¹ (with piglets). A study by Groot Koerkamp *et al.* (1998) based on a large number of buildings in a number of countries found emission rates ranging from 22 – 1298 mg NH₃ hr⁻¹ animal⁻¹. These emission rates are discussed further in Chapter 5, and standardised in Table 5.1.

1.3.2 Urine excretion

On average 67% of dietary nitrogen consumed by pigs is excreted, 17% in faeces and 50% in urine (Dourmad *et al.*, 1999). Nitrogen in faeces is mainly present in the form of protein; in urine it is mainly urea (van der Peet-Schwering *et al.*, 1999). Doak (1952) found that 75% of the urinary nitrogen was urea, whilst Petersen *et al.* (1998) measured 64-94%.

Urea undergoes rapid hydrolysis to ammonia and carbonate, catalysed by the enzyme urease which is produced by a wide variety of microbial organisms present in faeces but not in urine (van der Peet-Schwering *et al.*, 1999). This produces a high pH in the surface soil and leads to volatilization of ammonia (Doak, 1952). This hydrolysis is almost complete within 24 hours and scorching was an indication of ammonia release (Petersen *et al.*, 1998).

The enzyme urease is also widely distributed in plants, micro-organisms and soils. Its activity varies from soil to soil, tending to increase with organic matter content. Thus, sandy or calcareous soils tend to have lower activities. Urease activity also decreases with soil depth, in relation to the organic matter content (Freney *et al.*, 1983).

Sherlock and Goh (1984) found that after repeated applications of urine or aqueous urea to the same area of land, significantly greater subsequent volatilisation was measured. Compared with initial ammonia release, 20.5%, repeated applications produced significantly higher losses averaging 29.6% and 37.5% from the second and third applications respectively. These higher subsequent losses were attributed to the high soil pH at the time of application, which favours the formation of ammonia from ammonium, thereby increasing the amount of ammonia available for volatilisation in the soil.

Urea is not the only factor affecting ammonia volatilisation since pH, wind speed and temperature also affect the volatilisation from a urine patch (Sherlock and Goh, 1984). These factors are considered in detail in the next section.

1.4 FACTORS AFFECTING AMMONIA EMISSION

1.4.1 Soil

1.4.1.1 Moisture

Emission from soil is governed by physical and chemical reactions. Volatilization of ammonia from the topsoil layer depends on the concentration available in this layer. The soil moisture content and the water supply to the soil influence transport of ammonia in the upper soil layers. Vertregt and Rutgers (1991) found no clear relation between soil moisture content and volatilization level, though Freney *et al.* (1983) reported that soil moisture (along with other physical properties of soil) affected urease activity, and thus ammonia volatilisation.

The rate of hydrolysis increases with increasing water content following rain, then decreases as the soil dries. Soil water content can limit urea hydrolysis and most urea in the soil remains unhydrolysed until rain or irrigation. Urea diffuses into moist soil, but if there is a high evaporative demand, it can return to the soil surface due to mass flow. Urea concentrated at the dry soil surface is, however, relatively protected from volatile losses of ammonia since the water content at the soil surface can be too low to allow urea hydrolysis (Ferguson *et al.*, 1988). Faster hydrolysis of urea was proposed by Black *et al.* (1985) to be due to higher moisture conditions in the soil, whilst Vallis *et al.* (1982) and Harper *et al.* (1983) suggested that a lack of water for evaporation restricts volatilization.

1.4.1.2 pH

Maximum soil pH coincides with the maximum ammonia emission; conversely, ammonia emission decreases with decreasing soil pH (Freney *et al.*, 1983; Sherlock and Goh, 1984). The potential for ammonia emission from soil is increased at higher pH as this increases the concentration of ammonia present in the soil solution and the air contained within soil (Freney *et al.*, 1983). Vallis *et al.* (1982) found that the greatest increase in pH occurred in the top layer of soil (0-0.5 cm) where maximum values were measured 2-6 h after urine application.

A study performed by Hoff *et al.* (1981) supports these findings. For the same time period, 65% of applied ammoniacal-N was volatilised from a soil and manure combination with a high pH (>7), whilst only 14% from a soil and manure combination with a pH of 6.4.

1.4.1.3 Cation Exchange Capacity

Losses of ammonia have been found to be highest on light sandy soil and lowest on silty loam. Incorporation into the soil reduced the amount of ammonia volatilised from the slurry (Amberger, 1991). Döhler (1991) found that whilst pig slurry had similar flow properties to water, cattle slurry was more viscous. Therefore, infiltration of pig slurry into the soil is more rapid and slurry ammonium ions are sorbed to the soil complex. The more viscous cow slurry only partially infiltrates and ammonia was found to volatilise from the slurry liquid on the soil surface. When pig slurry was applied to a sandy soil, a loamy soil and a plastic sheet, slurry infiltration into the soil was altered. The plastic sheet stopped infiltration into the soil and almost all the ammoniacal nitrogen was lost through volatilization (81%). Losses were higher from the sandy soil than the loamy soil (22% and 14% respectively) and this was suggested to be due to the higher CEC (Cation Exchange Capacity) of the loamy soil. A similar result is seen when slurry is applied to well structured soil and compacted soil. Losses of 14% and 22% of the applied ammoniacal nitrogen have been seen after two days when applied to well structured and compacted soils respectively. The same trend is seen after four days with losses of 19% and 32%, respectively (Döhler, 1991).

As ammonium ions are positively charged, they readily react with the cation exchange complex in soils. There is a continual process of sorption and desorption which is dependent upon the pressure of ammonia in the soil: when pressure in the gaseous phase decreases, adsorbed ammonia desorbs. The effect of CEC on volatilisation is unclear as conflicting results have been found (Freney *et al.*, 1983).

Adsorption is also related to the surface area of the soil. For example, clay soils have a greater surface area per unit weight than sandy soils and absorb more

ammonia (Freney *et al.*, 1983). The ambiguity found in experiments may be due to the complex interaction of all the soil properties that affect ammonia volatilisation.

1.4.2 Wind

“Variations in the physical and dynamic properties of the atmosphere, on time scales from hours to days, can play a major role in influencing air quality” (McGregor, 1999). Ammonia released from the soil or its surface into the atmosphere after application of manure or excretion by grazing animals is transported horizontally by the wind whilst spreading laterally and vertically by turbulent diffusion. This leads to an increased ammonia concentration in the air downwind (Denmead *et al.*, 1977).

The direction of the wind controls the direction of pollutant transport: a persistent wind direction results in pollutant transport in a well-defined direction, whilst variable wind directions, often experienced in near calm conditions, result in pollutants being spread over a wide area. As wind flows over a surface, friction slows down the air close to the surface. A deeper layer of air is affected by a rougher surface. Fluctuations in wind speed and direction lead to turbulence which greatly influences the diffusion of pollutants (McGregor, 1999).

The removal of volatilised gas from above the soil surface by wind influences the further loss of gas from the soil by encouraging more rapid transport of ammonia away from the air-surface interface and increasing net upward diffusion. The rate of volatilization of ammonia is determined by the difference in ammonia partial pressure between the soil solution and the atmosphere. As atmospheric ammonia concentrations are usually found to be very low, there is no evidence to suggest that this would limit volatilization rates in the field (Freney *et al.*, 1983). Indirectly, wind velocity affects ammonia emission by influencing the rate of evaporation of soil water and surface temperature (Freney *et al.*, 1983; Simpson and Steele, 1983). However, little evidence is available to confirm this.

Sommer *et al.* (1991) found that although ammonia loss rates in the first twelve hours after application of slurry increased with wind speeds up to 2.5 m s^{-1} , no further increase was observed when the wind speed was increased to 4 m s^{-1} . Ammonia losses during 12-24 hours were constant with increasing wind speed, which is believed to be due to crust formation which was accelerated at higher wind speeds through a faster rate of evaporation. Water evaporation is also dependent on other factors, such as temperature. Therefore, the results showed no apparent relationship between volatilization and wind speed, apart from a small change at higher wind speeds. The effects of wind speed are difficult to separate from the effects of other factors, such as high pH (Freney *et al.*, 1983).

1.4.3 Temperature

According to Arrhenius' law of reaction kinetics, physical processes such as volatilisation roughly double in rate for every 10°C rise in temperature. Therefore the factor expected to influence ammonia emission rate most is temperature of the waste (Phillips *et al.*, 1997). Higher temperatures give a greater potential for ammonia loss due to an increase in the relative proportion of ammonia to ammonium, a decrease in the solubility of ammonia in water and an increase in diffusion of ammonia through the soil. Temperature also affects the urease activity and the rate of microbial transformations of ammonia in the surface soil, which determine the rate of ammonia emission (Freney *et al.*, 1983; Simpson and Steele, 1983).

An experiment by Sommer *et al.* (1991), investigating the effect of air temperature on ammonia loss from slurry, demonstrated that ammonia loss increased with increasing temperature. An exponential relationship between loss rate and temperature was observed during the first six hours after field application of the slurry. After this period, no such relationship was found and the effect of temperature decreased with time. Crust formation is a possible explanation, as this would limit availability for emission. They also found that the rate of loss followed a strong diurnal pattern with maxima occurring at about midday, when the solar radiation and temperature would have been the highest. Air temperature

appeared to be closely related to loss rate in the first two or three days after application of slurry. However, scatter in the results suggested that other parameters became increasingly important after this period. Hoff *et al.* (1981) also found that the rate of ammonia loss increased with increasing temperature, and also with air movement.

1.5 THE FATE OF AMMONIA IN THE ATMOSPHERE

Figure 1.1 shows the different mechanisms of transport and uptake of pollutants including ammonia and the complexes it forms. These mechanisms are described further in this section.

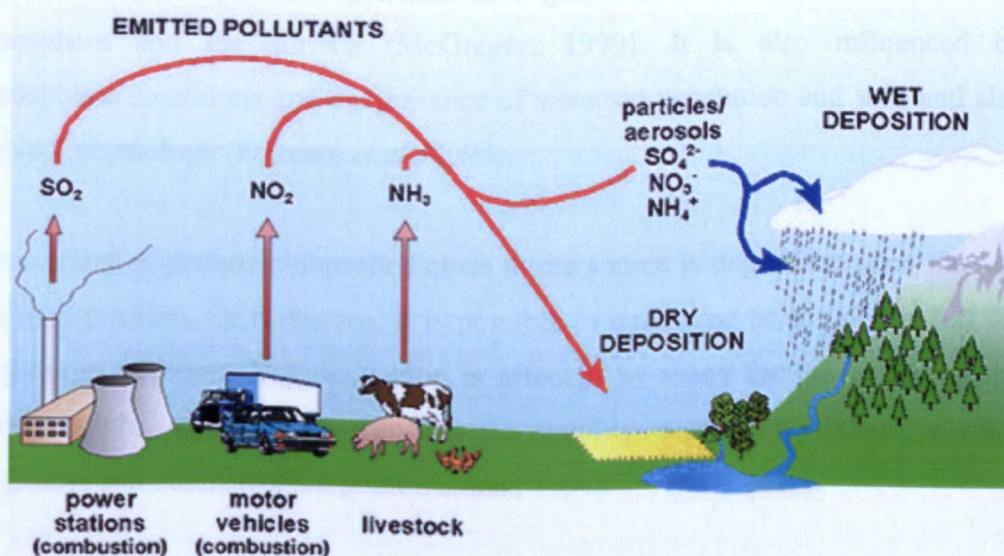


Figure 1.1: Mechanisms of transport and deposition of pollutants (ITE Edinburgh).

1.5.1 Plant-atmosphere exchange

A high proportion of the land mass upon which ammonia may be deposited is covered with vegetation. Studies of all types of surface (plant, land, water) have shown a dependence of ammonia emission upon the balance of the partial pressure of ammonia between the surface and the atmosphere. If the partial pressure is greater than the equilibrium value in the atmosphere, then the surface acts as a sink; if it is less, then the surface acts as a source (Galbally and Roy, 1983). For plants in particular, the equilibrium has been defined as the compensation point

for NH_3 concentrations in air, which is defined as the concentration at which NH_3 is neither emitted nor taken up. This is important in defining the direction of fluxes between plants and the atmosphere. When the ammonia concentration is greater in the atmosphere than in the plant, ammonia is taken up, when it is greater in the plant there is emission (Schjoerring *et al.*, 1998). Ammonium ions may also be absorbed by the plant canopy via the stomata or cuticle, or as deposited ions through macropores in the cuticle (Wilson and Tiley, 1998).

1.5.2 Dry deposition

Dry deposition is the transfer of pollutants to the surface from the atmosphere. The rate of deposition is not only dependent upon turbulence intensity and wind speed, but also upon the concentration gradient of ammonia between the atmosphere and the surface (McGregor, 1999). It is also influenced by atmospheric conditions and the presence of water on vegetation and soil, and also by plant physiology (Erisman *et al.*, 1993).

The amount of ammonia deposited close to the source is dependent upon the rate of dry deposition. Once known, it is possible to determine how much is left for long-range transport. Dry deposition is affected by many factors including the source height, wind speed, atmospheric stability, surface resistance, surface roughness and compensation point (Asman, 1998).

1.5.3 Precipitation scavenging

Precipitation scavenging refers to two different processes. Gaseous or particulate matter is either directly removed by collision with falling precipitation (e.g. rain, snow) or it is involved in an in-cloud scavenging process known as rainout or snowout. Particles carried up into the atmosphere often become condensation nuclei and grow into raindrops. Gases are often absorbed and suspended particles can be captured. This growth continues until the raindrop is no longer able to remain suspended in the cloud, the raindrop falls, carrying with it the original condensation nucleus, absorbed gases and any captured particulates (McGregor, 1999).

1.6 ENVIRONMENTAL IMPACT

1.6.1 Direct effects

1.6.1.1 Eutrophication

Nitrogen limits plant growth in nearly all natural and semi-natural ecosystems. Any nitrogen input from outside the system has the potential therefore to lead to changes in the species diversity of a community (Hovmand *et al.*, 1998). Deposition of nitrogen containing compounds, such as ammonia, can cause eutrophication, which is an increase in total nitrogen in an ecosystem.

The increase in nutrient availability in the soil through atmospheric deposition of ammonia has been linked to the change to grasslands at the expense of heathland (van Breemen and van Dijk, 1988; Hovmand *et al.*, 1998). Many plant species, particularly those found on heathlands, are adapted to low nutrient (oligotrophic) conditions and compete successfully in nitrogen deficient soils that are typical of most natural ecosystems (van Breemen and van Dijk, 1988; Sutton *et al.*, 1993; Mitchell *et al.*, 1997). An example of this is the replacement of *Calluna vulgaris* and *Erica tetralix* by grasses such as *Molinia caerulea*, *Deschampsia flexuosa* and *Festuca ovina*. As much as 35% of former Dutch heathland has been reported to have been replaced by grassland (Sutton *et al.*, 1993) and mass development of grasses has been found to occur at nitrogen inputs exceeding 20 kg ha⁻¹year⁻¹ (van Breemen and van Dijk, 1988). Plants with a higher sensitivity to nitrogen deposition decline first (Sutton *et al.*, 1993).

Direct effects of ammonia deposition on vegetation have only been found to occur in cold climates or in cold winters. Typical symptoms of ammonia damage are red or reddish-brown colouring of coniferous trees that is caused by the low ammonia detoxification capacity of plants at low temperatures (Roelofs and Houdijk 1991). Van der Eerden *et al.* (1998) also found defoliation and discoloration of the foliage of trees in Dutch forests, without a severe impact on tree growth. Uptake of NH₄⁺ by foliage leads to a loss of base cations, and assimilation into amino acids can cause acidosis in leaf cells (Wilson and Tiley, 1998). Resulting stresses,

discussed below, change the species composition of the undergrowth from lichen-dominated to grass-dominated vegetation (van der Eerden *et al.*, 1998).

1.6.2 Indirect effects

1.6.2.1 Acidification

A high deposition of ammonia leads to acidification of the soil, which can lead to plant damage and changes in species diversity (McGinn and Janzen, 1998). As a consequence, acid-resistant plant species become dominant and endangered plants found at intermediate pH values (6.5-4.5) disappear (Bobbink, 1998). Amongst acid-tolerant species, there will be competition between slow growing plant species and fast growing nitrophilous grass species. This process contributes to the observed change from heathland into grasslands (Roelofs and Houdijk, 1991).

Natural nutrient cycling within soil can contribute to acidification. However, there is no net increase in soil acidity as there is an equal amount of natural neutralisation (Binkley and Richter, 1987). Net soil acidification occurs following atmospheric deposition of ammonia which disrupts the natural cycle leading to an overall net input of hydrogen ions (Sutton *et al.*, 1993).

The cause of this is the nitrification of the ammonium to nitrate, producing two hydrogen ions for each ammonium ion oxidised, as shown in equation 1 (Binkley and Richter, 1987; Sutton *et al.*, 1993, Fangmeier *et al.*, 1994).



A possible effect of acidification is the leaching of cations such as potassium, calcium and magnesium which can lead to nutrient imbalances affecting plant growth and the release of metal ions such as Al_3^+ which is potentially toxic to plants (Fangmeier *et al.*, 1994).

The acidifying potential of nitrogen may be calculated by the change in hydrogen ions in the soil:

$$(\text{NH}_4^+\text{input} + \text{NO}_3^-\text{output}) - (\text{NH}_4^+\text{output} + \text{NO}_3^-\text{input})$$

or $(\text{NH}_4^+\text{input} - \text{NH}_4^+\text{output}) + (\text{NO}_3^-\text{output} - \text{NO}_3^-\text{input})$

Acidification occurs when this calculation yields values of hydrogen ions greater than zero (Fangmeier *et al.*, 1994).

The effects of eutrophication and acidification occur simultaneously and may be due to either process, or a complex interaction between them. Therefore, separating their effects is challenging but necessary to understand fully the impacts of ammonia deposition (Bobbink, 1998).

1.6.2.2 *Opening of the canopy*

Heathland species can successfully compete with grasses, even when the rate of nitrogen deposition is high, so long as the canopies are closed. This is because insufficient solar radiation is available for new seedlings to emerge. Once a gap is opened it is easily exploited by grass species which are more efficient at utilising high inputs of nitrogen and then gain a competitive advantage (Fangmeier *et al.*, 1994). A gap in the canopy can be caused by beetle attack, decrease in frost resistance and decrease in drought resistance.

An increase in foliar nitrogen can increase the likelihood of attack by the heather beetle, which feeds exclusively on the green parts of *Calluna vulgaris*. This can lead to the closed canopy of *C. vulgaris* being opened over large areas, increasing solar radiation below the canopy and leading to an enhanced growth of grasses (Bobbink, 1998).

A long-term experiment by Lee and Caporn (1998) quantified the responses to nitrogen deposition of different vegetation types, including heathland. Initially, the additions of nitrogen led to an increase in growth of heather, as it is usually

nitrogen-limited. For the first four years of nitrogen addition, frost tolerance increased during autumn, whilst at other times of the year, the results were not conclusive either way. After the first four years, however, the first signs of a negative effect were seen in the form of winter browning. This continued to reappear after every winter, most significantly in plots receiving the most nitrogen. They found this led to gaps in the canopy giving other species, such as underlying lichens and mosses, a chance to invade. Lee and Caporn (1998) stress the need for long term experiments, as their observations initially showed positive effects whilst later adverse effects occurred.

A study by Dueck *et al* (1998) into the influence of ammonia on a pine species found that drought stress was greatly enhanced. This was not only due to lower needle water potentials but also to an increase in the needle-to-root ratio. Pot experiments using herbaceous plants also showed an increase in shoot-to-root ratio suggesting that the area of water uptake surfaces (roots) had decreased compared with the transpiring surface area (leaves), which would lead to increased sensitivity to drought and a substantial reduction in growth (Bobbink, 1998).

1.6.2.3 Aerosol formation

Ammonia has been found to enhance atmospheric aerosol formation, particularly over agricultural areas, where urban emissions of nitrogen and sulphur oxides react with ammonia emissions forming ammonium nitrate and sulphate. Once in this form the light extinction characteristics of the aerosols are enhanced leading to higher fine mass concentrations and lower visibility in agricultural regions (Barthelmie and Pryor, 1998). The attenuation of light is particularly high when the aerosol diameter is comparable to the wavelength of light (0.3-0.7 μm). This regime is known as Mie Scattering (Heinsohn and Kabel, 1999).

1.7 MEASUREMENT OF EMISSIONS

Phillips *et al.* (2000b) have identified four different basic approaches to the measurement of ammonia emission rates from livestock:

- 1) nitrogen balance: where the difference between the amount of nitrogen excreted by an animal and the amount of nitrogen left in the manure after a period is used to determine the amount emitted from the manure;
- 2) summation of local ammonia sources, to provide an estimate of the emissions from the source of interest by measuring or modelling emissions from representative local components of the total source;
- 3) determination of ammonia fluxes, either directly or indirectly, which can be achieved by one of four methods: measuring or modelling the air velocities and ammonia concentrations at a downwind edge of the area of interest, or measuring or modelling the dilution of air within the source area; and
- 4) tracer ratio method. This involves the measurement of the overall, unknown, ammonia source strength directly, along with that of a tracer with similar properties in air. The ratio of measured concentrations is assumed to be equal to the ratio of the source strengths, hence the unknown ammonia source strength is determined.

Horizontal flux is the product of wind speed and ammonia concentration and can be calculated from simultaneous measurements of both, either in real time or using an average measure over a defined period. To simplify measurement, devices that measure flux directly have been developed (Ferm, 1986); these are based on passive sampling, which negates the need to measure wind speed. As this project focuses on measurements of emission rate, flux measurements are more appropriate than concentration measurements, and for this reason, passive flux samplers have been used. Other advantages of the passive flux sampler are discussed in the following section.

The ability to measure ammonia is central to the quantification of emission rates and a wide range of devices is available for its measurement. The devices can be classified into two main categories – active and passive samplers. Active samplers draw air into the sampling device at a known rate, whilst passive samplers rely on

either diffusion along a concentration gradient or wind-driven motion of the air with capture of the ammonia on a suitable substrate.

These two categories can be further divided into samplers that measure concentration and those that measure flux. Concentration measurements can be made in real-time, i.e. instruments, such as chemiluminescence analysers or continuous flow denuders return a value for the concentration within minutes or seconds. Other types of sampler, such as diffusion tubes, hollow tube denuders and acid bubblers, exploit the alkaline nature of ammonia by capturing it in some form of acidic substrate. Wet chemistry is then required to determine the amount of ammonia captured, giving an average concentration over the exposure period, typically from a few hours to a few days.

Each type of sampler varies in its sensitivity, selectivity, speed and cost and hence differs in its suitability for a particular project. Phillips *et al.* (2001) describe the main devices in some detail and also rate each for its suitability depending on a range of criteria. They conclude that passive flux samplers have advantages in their simplicity and low cost construction although the laboratory time required for sample analysis is quite substantial.

The following methods are available to measure ammonia emissions directly from small areas of land, and may be suitable for the second approach.

1.7.1 Ventilated volatilization chambers

A volatilization chamber consists of a cylinder pushed into the soil with a hinged lid, which is opened and closed periodically. A vacuum pump draws air, along with ammonia escaping from the soil surface, into the chamber and subsequently to a chemical trap (Kissel *et al.*, 1977). Ammonia volatilization is calculated from the increase of ammonia concentration in the flow of air passed through the chamber (Vandré and Kaupenjohann, 1998). It is assumed that the rate of ammonia release is the same during periods of lid closure as when the lid is open between measurements and the plot is exposed to normal environmental conditions (Ferguson *et al.*, 1988).

However, as ammonia volatilization is strongly influenced by air temperature and wind speed, the exclusion of ambient meteorological conditions from the surface for even the short time the lid is closed may potentially alter the microclimate (Schjoerring *et al.*, 1992; Vandré and Kaupenjohann, 1998) and lead to incorrect estimates of the ammonia emission (Ferm *et al.*, 1991). So, although this method is easily replicated and allows treatment comparisons, it may over- or underestimate the ammonia release rate depending on external conditions (Ferguson *et al.*, 1988). To achieve a better estimate, air flow rates through the chamber could be controlled to simulate the external natural wind speed (Sherlock and Goh, 1984).

1.7.2 Wind tunnels

Wind tunnels have been constructed which attempt to simulate the external wind environment and thus perturb the enclosed area as little as possible (Klarenbeek *et al.*, 1993). These consist of a canopy fixed into position over the experimental plot. A variable speed fan controls the speed of air through the canopy and an anemometer is used to measure the external wind speed that is to be simulated through the canopy. The ammonia concentration in air entering and leaving the tunnel is measured. The concentration measurements, together with the average wind speed through the tunnel, enable the ammonia emission from the experimental area (F ; $\mu\text{g m}^{-2} \text{s}^{-1}$) to be calculated using the following equation:

$$F = (\bar{C}_1 - \bar{C}_e) \times \bar{u} \quad (2)$$

where \bar{C}_e and \bar{C}_1 are the average concentrations of ammonia in air entering and leaving the wind tunnel, respectively ($\mu\text{g m}^{-3}$), and \bar{u} is the average wind speed (m s^{-1}) in the tunnel over the experimental period (Klarenbeek *et al.*, 1993).

The adjustment of air flow rate through the tunnel in this type of system allows a better correlation between internal and external conditions. An investigation by Lockyer (1984) found that differences in temperature, relative humidity and soil temperature internally and externally were negligible; hence the internal climate is not significantly altered. Consequently, measured ammonia release rates have

been shown to be in good agreement with those obtained by the integrated horizontal flux method or by the mass balance approach (Vandré and Kaupenjohann, 1998). Calm conditions and rain, however, cannot be simulated and under these conditions an overestimation of ammonia emissions is found (Vandré and Kaupenjohann, 1998). One disadvantage of wind tunnels is the high cost of air flow control equipment which can limit the number of wind tunnels used (Schjoerring *et al.*, 1992).

1.7.3 Recovery of ^{15}N

Recovery of ^{15}N from urea-containing fertilisers is another method used to estimate ammonia emission. Problems with this method include the expense of using ^{15}N -labelled fertiliser, which limits the size and/or number of the plots that can be treated, and the difficulty in separating ammonia losses from other nitrogen losses such as leaching and denitrification. Also, the equipment required to measure the ^{15}N content of materials, or the cost of laboratory analysis of samples is high (Fox *et al.*, 1996).

1.7.4 Micrometeorological methods

As mentioned in the introduction, ammonia emitted from soil is transported horizontally by wind and spread laterally and vertically by turbulent diffusion. If it is assumed that lateral diffusion is minimal, transportation may be considered to be two-dimensional (Wilson *et al.*, 1983), and for a steady wind direction, ammonia flux measurements can be made at various heights to determine the horizontal flux of ammonia at the downwind edge of the area of interest (Denmead *et al.*, 1977; Sherlock *et al.*, 1989). Reabsorption of the emitted ammonia is likely to be negligible and the horizontal flux of ammonia can be considered equal to the loss from the soil (Denmead *et al.*, 1977).

Various micrometeorological methods have been developed for measuring ammonia emission. They differ slightly in detail but use a similar basis for calculating the rate of transport, or flux, through a plane perpendicular to the wind direction at the downwind edge of an area source. The horizontal flux of ammonia

across a unit area of this plane at a particular height (z) due to emission from the soil can be calculated as the product of mean wind speed and mean concentration of ammonia in excess of background (Denmead *et al.*, 1977; Sherlock *et al.*, 1989; Sommer *et al.*, 1995). One such method for measuring the vertical ammonia flux from an experimental area is the mass balance method. This method assumes that the vertically integrated product of wind speed and ammonia concentration divided by the fetch is equal to the ammonia flux (Klarenbeek *et al.*, 1993):

$$F_v \equiv \frac{1}{x} \int_{z_0}^z ((\overline{C_d} - \overline{C_u}) \times \overline{u}) dz \quad (4)$$

where F_v is the vertical flux ($\mu\text{g m}^{-2} \text{s}^{-1}$), x is the distance (m) the wind travelled across the source area from the upwind to downwind side (i.e. the fetch), $\overline{C_d}$ and $\overline{C_u}$ are the mean ammonia concentrations ($\mu\text{g m}^{-3}$) over the exposure period downwind and upwind of the experimental plot, \overline{u} is the mean wind speed (m s^{-1}), z is the height (m) of the plume of ammonia and z_0 is the roughness length (m) (Sommer *et al.*, 1995).

Micrometeorological methods are preferable to those that enclose the emitting surface, which may influence ammonia volatilization (Ferm *et al.*, 1991), and allow continuous measurements to be undertaken. However, the methods can be labour intensive requiring large source areas and wet chemical sampling techniques or may use in-situ experimental equipment requiring a power source in the field, leading to high costs (Schjoerring *et al.*, 1992; Fox *et al.*, 1996). Large source areas makes replication and application of variable treatments difficult (Ferguson *et al.*, 1988).

An alternative to concentration and wind speed measurements at each sampling height could be to use passive sampling e.g. flux samplers which do not require a power source thus decreasing equipment costs (Sherlock *et al.*, 1989; Klarenbeek *et al.*, 1993). Conventional micrometeorological techniques also require uniform, plane, surface sources and fetches long enough to ensure that horizontal

concentration gradients are negligibly small (Denmead *et al.*, 1998). Extensive areas of uniform land are not, however, required for measurements based on mass balance and these methods are therefore suitable for measuring ammonia emissions from small plots (Schjoerring *et al.*, 1992).

For a given fetch and surface roughness there is a particular height above a field emitting ammonia where the vertical flux density of ammonia is directly proportional to the horizontal flux density of ammonia, over a wide range of atmospheric stability conditions. This height, Z_{inst} , can be determined empirically or from the use of a numerical model (Sherlock *et al.*, 1989) or determined once the roughness length is known (Wilson *et al.*, 1983). The Z_{inst} method could be an alternative to the mass balance method, where just one measurement height is required but the roughness length of the plot must be known reasonably well and the sources must be spatially uniform, which is not straightforward under field conditions. Thus, better precision may be obtained by using two measurement heights. The mass balance method can therefore be simplified by using only two measurement heights. This method was used assuming a zero ammonia concentration just above the field boundary layer and was found to satisfactorily estimate ammonia emissions (Genermont *et al.*, 1998).

Another particular use of a micrometeorological method is in the flux frame method: horizontal ammonia flux can be determined directly by using an array of ammonia flux samplers mounted on a downwind sampling frame to intercept the plume of ammonia from the source. A sampling mast is also required upwind of the source to allow the background ammonia flux to be measured. The flux frame measures the horizontal flux of ammonia through the vertical plane perpendicular to the wind direction downwind of an ammonia source and allows the ammonia source strength to be determined. However, there are limitations to the use of this method:

- i. the whole of the plume must be captured by the frame;
- ii. there must be a suitable fetch with minimum interference from obstacles;
- iii. the upwind and downwind fluxes must be measured simultaneously;
- iv. the weather conditions must be suitable e.g. wind direction; and

- v. the flux measurements must be sufficiently accurate to show the difference between upwind and downwind measurements of the source, whilst the emission upwind should be as low and uniform as possible (Michorius *et al.*, 1997).

Source strength is determined from the following relationship:

$$Q = \sum_{j=1}^m \left(\Delta z_j \times \sum_{i=1}^n d (F_{d_i} - F_{u_i}) \right) \quad (3)$$

where Q is the source strength ($\mu\text{g s}^{-1}$), Δz is the height over which the flux measurement is averaged (m), d is the distance between adjacent masts (m), F_d and F_u are the fluxes measured downwind and upwind of the source respectively ($\mu\text{g m}^{-2} \text{s}^{-1}$), n is the number of masts, i is the number of the mast, m is the number of sampling heights and j is the height. The net horizontal flux across the source ($F_d - F_u$) is multiplied by the distance between the masts and summed. This summation represents the source strength per height and is then multiplied by the height at which the flux measurement was taken (Michorius *et al.*, 1997).

Although this method enables the total source upwind to be sampled, there are disadvantages and determination of the best position for sampling is difficult. The erection of masts of sufficient height to capture the top of a plume from an extended source is essential to support the samplers. These must be permanent structures due to their height which makes it difficult to erect them in the correct position for the prevailing wind direction which, once determined, frequently changes. Masts must also not be positioned close to large obstructions such as buildings or trees, as these produce turbulence. If obstructions are unavoidable then the masts must be positioned around ten heights of the obstruction downwind and at this position the flux may have been reduced by dilution or the plume may be well above the mast height and accurate measurement will not be possible. A large structure also has the potential to interfere with the wind profile to some degree, can be cumbersome to use, and also poses problems related to changing wind directions (Phillips *et al.*, 1997; 2000b).

1.7.5 Tracer ratio method

The tracer ratio method can be used to determine an unknown ammonia source strength. The concentrations of ammonia and a tracer gas with a known source strength are measured directly. The most widely used tracer is sulphur hexafluoride due to low background levels in the northern hemisphere (Phillips *et al.*, 2001). The simplest calculation method available to find the unknown ammonia emission rate involves using the ratio of the observed maximum ammonia concentration, along with the sulphur hexafluoride flux and maximum concentration:

$$F_{\text{gas}} = F_{\text{SF}_6} \times \left(\frac{C_{\text{gas}}(\text{max})}{C_{\text{SF}_6}(\text{max})} \right) \quad (5)$$

where F_{gas} is the calculated ammonia flux ($\mu\text{g m}^{-2} \text{s}^{-1}$), F_{SF_6} is the measured tracer flux ($\mu\text{g m}^{-2} \text{s}^{-1}$), $C_{\text{gas}}(\text{max})$ is the maximum ammonia concentration and $C_{\text{SF}_6}(\text{max})$ is the maximum tracer concentration observed at the sampling line (Lamb *et al.*, 1986).

However, the tracer ratio method makes a major assumption that the tracer gas disperses in a similar way to the ammonia. To achieve this, especially when measuring the ammonia emission from a large area source, it is necessary to simulate the source distribution as accurately as possible, which may require a number of tracer release points and also by using a tracer with a similar density to ammonia. Several measurements of the concentration of both gases can then be taken downwind at various intervals and an average can then be taken. This further reduces uncertainty in the method (Phillips *et al.*, 2000*b*). The tracer approach does not perturb the environment nor does it rely upon precise gradient measurements. The tracer is released for a period of time at a known, constant rate, from appropriate release points within the source area at a representative height, whilst monitoring its concentration at appropriate points downwind (Lamb *et al.*, 1986).

1.7.6 Standard comparison method

The standard comparison method uses a direct comparison between unknown ammonia source strength (Q_E) from an experimental plot, with a measured concentration, C_A , whilst ammonia is released at known rates (Q_S) on standard plots (with measured concentration C_S). On each plot, the ammonia concentration is measured close to the ground whilst a measure of background concentration (C_B) is made at a distance from the plots. The standard plots are used to determine the transfer factor (T_F) of ammonia from the source to the sampler after correction for background:

$$T_F = Q_S / (C_S - C_B) \quad (6)$$

The value of T_F is a function of both microclimatic conditions and plot design, and the ammonia samplers used. T_F , however, is independent of the ammonia release rates. If all the conditions influencing T_F are equal, standard and experimental plots may be compared, and the unknown ammonia source strength from experimental plots, Q_E , can be estimated from T_F and measurements from the standard plots (after correction for background):

$$Q_E = T_F (C_A - C_B) \quad (7)$$

No absolute measure of ammonia concentration is needed for this method, as there is a simple relationship between ammonia release and sampler measurements. A problem with this method is keeping the ammonia release rate constant whilst temperatures vary, as the vapour pressure of ammonia varies significantly with temperature. It has been found that ammonia flow is difficult to maintain constant and must be readjusted regularly (Vandré and Kaupenjohann, 1998).

Due to the nature of the source to be measured in this project (a large field site with free-ranging pigs), it was not possible to use wind tunnels, volatilization chambers or the standard comparison method. A tracer ratio method would prove difficult due to the necessity of distributing the tracer in a similar pattern to the source. Thus a method which measures emissions from a site downwind of the

source is most suitable. The flux frame was chosen to allow a representative sample from the full length of the sow field, a source hundreds of metres wide.

The flux frame method is a relatively novel method of measuring ammonia emissions which does not perturb the environment, and is suitable for use with the recurved PAF samplers (see Chapter 2). The flux frame has been used elsewhere for example, by Jeschke (1996) to measure ammonia emissions from a slurry tank. However, it has not been validated using a source of known strength.

1.7.7 Modelling

The heterogeneous nature of ammonia sources and the subsequent deposition make it difficult to estimate the input of nitrogen to different ecosystems. Accurate quantification of the spatial variability of ammonia concentrations would require a large number of monitoring stations. This would be necessary to assess the impacts of acidification and eutrophication after deposition. Models are a useful tool for examining the spatial variability of deposition (Singles *et al.*, 1998). Such models include the TREND model (Asman, 2001; Asman and Vanjaarsveld, 1992) and the FRAME model (Fournier *et al.*, 2002; Singles *et al.*, 1998) both of which are capable of describing dispersion and deposition of ammonia.

Specific models relevant to ammonia abatement have been developed. The MANNER model (Chambers *et al.*, 2000) allows the management of manure to be investigated to enable increased fertilisation and decreased pollution. The MAST model (Ross *et al.*, 2002) also allows different abatement strategies for a dairy farm to be examined and the effect they have on ammonia emission to be determined. The strategy with the greatest reduction can then be implemented. This is also the purpose of the MARACCAS model (Cowell and ApSimon, 1998), mentioned in section 1.2.

Other more general models, such as Lagrangian or Eulerian plume models (Asman, 2001), or specific software such as the ADMS dispersion model (CERC, 1999), can be used to predict how ammonia may be dispersed from a particular

source. Another example is that of computational fluid dynamics (CFD) modelling which has been used to simulate air velocity and ammonia distributions within livestock buildings, and also to calculate ammonia concentration and emission rate from the building (Sun *et al.*, 2002).

1.8 PASSIVE AMMONIA FLUX SAMPLERS

A passive flux sampler is a simple and inexpensive device which provides a measurement of the average horizontal ammonia flux along the axis of the sampler over an exposure period (Phillips *et al.*, 2001). It is unlike other passive samplers, such as diffusion tubes and badge samplers, in that it gives a direct measure of flux rather than concentration.

1.8.1 Principle of operation

The principle of operation of the original passive flux sampler (more commonly known as a 'Ferm tube') is described in full by Ferm (1986), Ferm and Christensen (1987), Ferm *et al.* (1991) and Schjoerring *et al.* (1992), and is outlined below. The sampler comprises two pairs of glass tubes (100 mm long, 10 mm o.d. and 7 mm i.d.) joined in series (Figure 1.2), with a stainless steel orifice (1 mm diameter) at opposite ends of each pair (Ferm, 1986 *et seq.*) and an internal acid coating to capture the alkaline ammonia. One pair of tubes points towards the ammonia source of interest and the other pair points away (Sommer *et al.*, 1996).

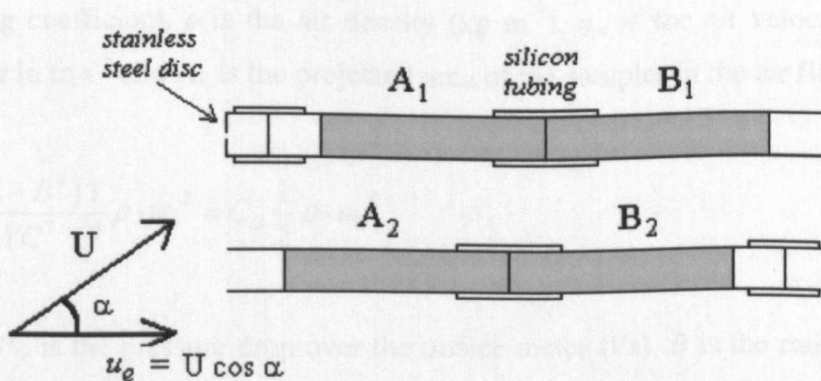


Figure 1.2: Passive ammonia flux sampler.

The flow of air through the sampler is completely wind driven. The purpose of the stainless steel orifice is to decrease the air speed through the tubes to achieve a high ammonia collection efficiency (Schjoerring *et al.*, 1992) and to allow only the collection of ammonia gas by greatly reducing the air flow through the tubes. Other alkaline gases, particularly amines, would be captured, although their flux was found to be <1% to that of ammonia from a cattle feedlot (Hutchinson *et al.*, 1982), so their contribution would be negligible. The air flow rate through the tubes is approximately proportional to the component of wind velocity parallel to the longitudinal axis of the tube, which is the wind velocity multiplied by the cosine of the angle between the wind direction and the axis. Therefore, the amount of ammonia collected in the sampler is in direct proportion to the external ammonia flux (Ferm *et al.*, 1991; Schjoerring *et al.*, 1992; Phillips *et al.*, 2001).

Scholtens *et al.* (2002) describe the basic principles upon which the proportionality of the passive flux sampler depends. By combining equations describing negative pressure downstream and pressure drop over the orifice (equations 8 and 9, respectively) an equation (10) describing the air velocity through the orifice is derived (assuming normal atmospheric conditions):

$$P_D = \frac{F_D}{A_p} = C_D \frac{1}{2} \rho \cdot u_m^2 \quad (8)$$

where P_D is the negative pressure (Pa), F_D is the drag force on the body (N), C_D is the drag coefficient, ρ is the air density (kg m^{-3}), u_m is the air velocity past the sampler in m s^{-1} and A_p is the projected area of the sampler in the air flow (m^2).

$$P_O = \frac{(1-B^4)}{YC^2} \frac{1}{2} \rho \cdot u_o^2 = C_o \frac{1}{2} \rho \cdot u_o^2 \quad (9)$$

where P_O is the pressure drop over the orifice meter (Pa), B is the ratio of orifice diameter D_O to tube diameter D_T , Y is the expansion factor (which is unity when pressures are near atmospheric), u_o is the air velocity through the orifice (m s^{-1}) and C_o is the orifice meter constant.

$$u_o = \sqrt{\frac{C_D}{C_o}} \cdot u_m = K \cdot u_m \quad (10)$$

where K is the sampler constant. This shows that the velocity through the orifice has a linear relationship with the external air velocity. The sampler constant K can be found experimentally, as follows. P_o equals P_D . Therefore, by plotting the relationship between air velocity past the sampler, u_m , and pressure drop, P_o , over the orifice meter over a range of velocities, C_D can be determined from a linear regression. Plotting the relationship between P_o and u_o over a range of pressure drops allows C_o to be determined from a linear regression. K is then determined using equation 10. K has been determined by Ferm and Christensen (1987) and Schjoerring *et al.* (1992), and ranges from 0.7 to 0.77 for the original Ferm tube design.

When wind direction and wind speed are represented by the vector U ($u_e = U \cos \alpha$, Figure 1.2), ammonia is collected in tubes A_1 and A_2 but not in B_1 and B_2 (unless saturation of the acid coating occurs). If α is 0° , tubes A_1 and A_2 collect the same amount of ammonia. It would be expected that as α increases, the amount of ammonia collected in tubes A_1 and A_2 would decrease following a cosine relationship since the velocity of the air impinging on the face of each tube is $U \cos \alpha$. Ferm (1986) found experimentally, however, that as α increases, the amount of ammonia collected by tube A_1 decreased more rapidly than would be expected if the cosine relationship was followed. Conversely, the amount of ammonia collected by tube A_2 decreased more slowly (i.e. tube A_1 underestimates, tube A_2 overestimates the amount of ammonia).

However, he also found that the average amount of ammonia collected in tubes A_1 and A_2 as a function of α resembles approximately the nominal $\cos \alpha$ relationship. Thus, the ammonia flux through a plane perpendicular to the axis of the samplers can be determined.

$$F_h \Delta t = \int_u^u U \cos \alpha \cdot C dt \approx \frac{(M_{A1} + M_{A2})}{2 \pi r^2 K} \quad (11)$$

where F_h is the horizontal flux density of ammonia, C is the atmospheric ammonia concentration, r is the radius of the stainless steel orifice, and t is time. M_{A1} and M_{A2} are the masses of ammonia captured on tubes A_1 and A_2 respectively (in μg) and K is the sampler constant. Ferm and Christensen (1987) determined the value of K to be 0.7 in wind tunnel experiments in which the air speed through the stainless steel orifice (u_o) was plotted as a function of ambient wind speed (U) for various orientations of the sampler to the wind.

The phenomenon of over- or under- estimation of ammonia flux in the different tubes A_1 and A_2 can be explained by the differing action of positive and negative pressure on the ends of the two tubes, as shown in Figure 1.3. When $\alpha = 0^\circ$, the resultant of the positive and negative pressures on the tubes is the same. However, for non-zero values of α , the positive and negative pressure profiles across the openings become 'skewed'. This influences the flow of air through the tubes. The resulting action of positive and negative pressure on the tube in which the orifice is positioned upwind (A_1) is more than that expected if there were no orifice at all, whilst when the orifice is downwind (A_2), the resultant is slightly less, leading to the over- and under- estimation of ammonia flux, respectively.

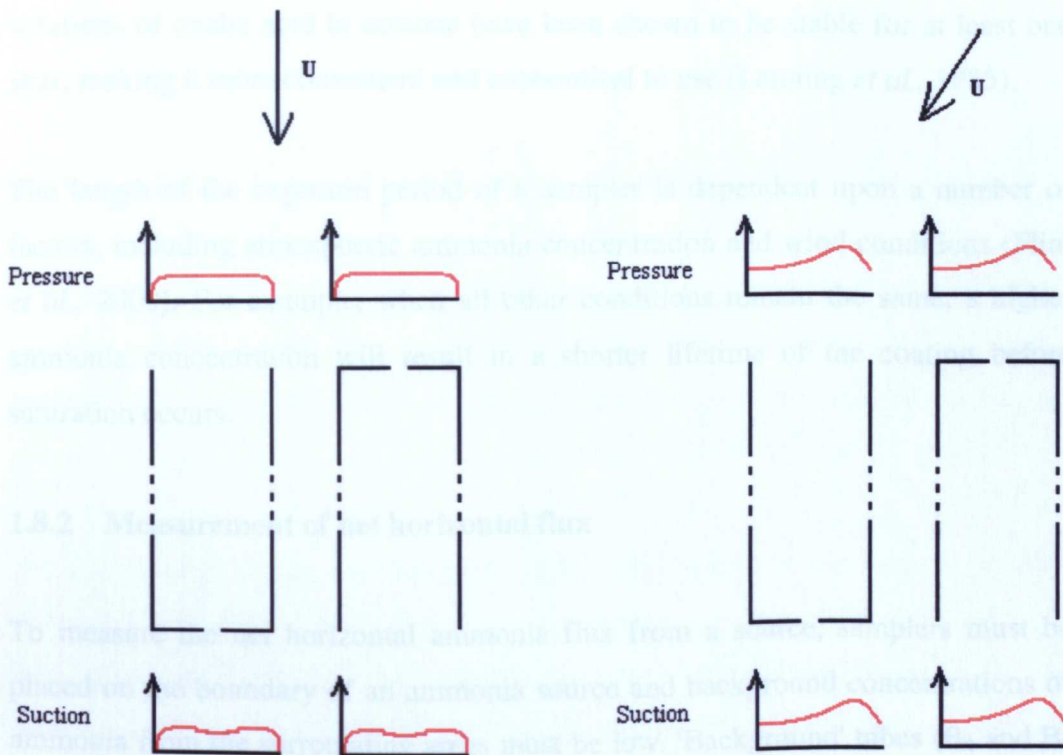


Figure 1.3: Sketch of the change in positive and negative pressure profiles over the ends of the tubes with an increased angle of incidence of the ambient wind.

1.8.1.1 Acid coating

The internal surfaces of both tubes are coated with an acid layer to capture the alkaline ammonia gas from the air as it passes through the sampler. A suitable coating for ammonia collection is oxalic acid, which can be applied by dissolving 4% oxalic acid in acetone or methanol and then drawing the solution into each glass tube using a pipette filler. The solution is then drained, and the tubes dried with ammonia-free air, leaving a deposit of oxalic acid. The tubes are capped immediately after drying (NEN method 6472, Appendix 1).

Using acetone as the solvent instead of methanol has been found to be preferable for a number of reasons. Acetone evaporates more quickly than methanol and provides a more even coating (Leuning *et al.*, 1985; Schjoerring *et al.*, 1992). When using a methanol solvent, the solution must be prepared immediately before use to avoid esterification of oxalic acid by methanol; otherwise its capacity to absorb ammonia is reduced by 10% within six hours and by 35% after 24 hours. Using an acetone solvent allows the solution to be prepared in advance, as

solutions of oxalic acid in acetone have been shown to be stable for at least one year, making it more convenient and economical to use (Leuning *et al.*, 1985).

The length of the exposure period of a sampler is dependent upon a number of factors, including atmospheric ammonia concentration and wind conditions (Flint *et al.*, 2000). For example, when all other conditions remain the same, a higher ammonia concentration will result in a shorter lifetime of the coating before saturation occurs.

1.8.2 Measurement of net horizontal flux

To measure the net horizontal ammonia flux from a source, samplers must be placed on the boundary of an ammonia source and background concentrations of ammonia from the surrounding areas must be low. 'Background' tubes (B_1 and B_2 in Figure 1.2) should collect very little ammonia unless the coating on the pair pointing towards the source become saturated. The net horizontal ammonia flux through a plane perpendicular to the sampler can then be calculated as in equation 11, replacing $(M_{A1} + M_{A2})$ with $((M_{A1} + M_{A2}) - (M_{B1} + M_{B2}))$ (Klarenbeek *et al.*, 1993).

1.8.3 Variations on the Ferm tube

Variations on the design of the original Ferm tube have been suggested though they continue to use an acid coating to collect the ammonia and orifices to restrict airflow through a sampler. One example is the addition of fins and pivots to the exterior of a metal tube with an internal coil of metal increasing the surface area for ammonia collection whilst enabling accurate tracking of changing wind direction. This sampler is then mounted in the field and exposed for a suitable sampling period (Sherlock *et al.*, 1989). This type of sampler is advantageous for use with plot experiments (Phillips *et al.*, 2001) and suitable for use with a micrometeorological technique. Provided the sampler remains pointed into the wind, the mean horizontal flux F_h is measured by the mass, M , of ammonia collected by the instrument during the sampling interval, t , since:

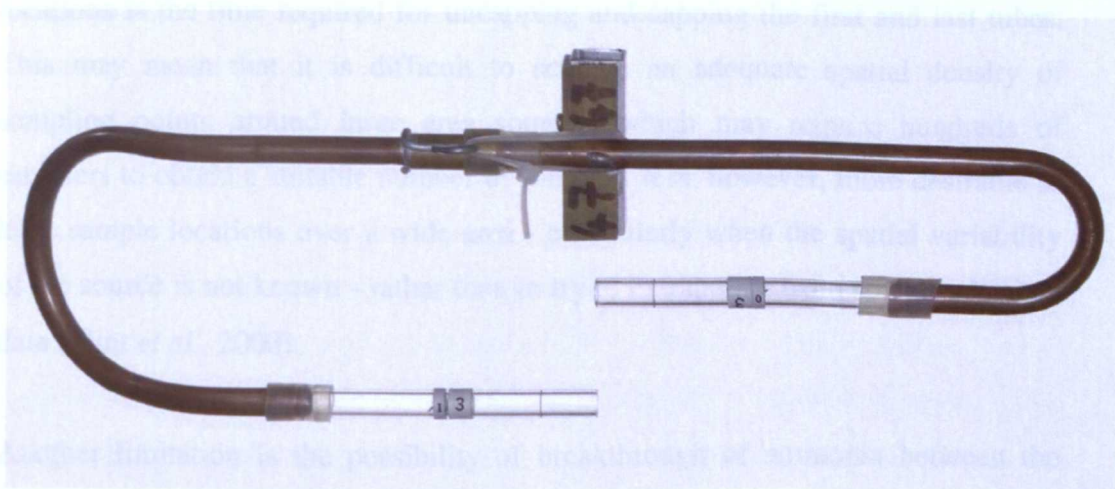
$$F_h = \frac{M}{At} \quad (12)$$

where A is the effective cross-sectional area of the sampler.

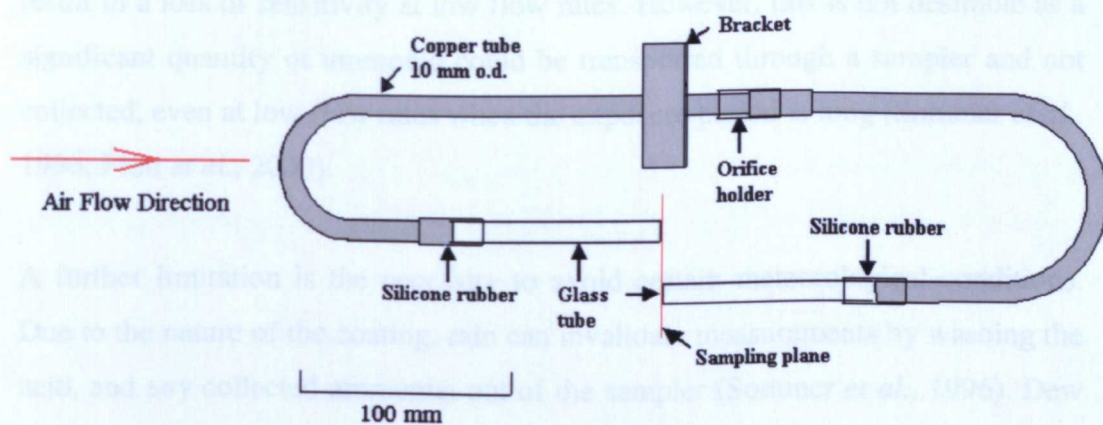
This type of sampler has an expected maximum exposure time of 5-70 days, making it very useful for long-term measurements (Leuning *et al.*, 1985). However, these samplers have a high cost (around £300 each) due to the internal coil of stainless steel sheet to increase the surface area (Phillips *et al.*, 2001).

A further simplification that has been made to the Ferm tube has been to position the orifice between the two glass tubes, eliminating the need for two sets of tubes with opposing orifices. This design has been further improved with the development of a 're-curved' version comprising two pieces of copper pipe, each with a 180° curve (Figure 1.4) (Phillips *et al.*, 2000a). The two glass sample tubes have their open ends in the same plane, approximately 60 mm apart, ensuring that any pressure build up is the same at both ends of the sampler. A single stainless steel orifice is located at the junction of the copper curves (Flint *et al.*, 2000). Phillips and Scholtens (1999) found that average ammonia recovery was 66% and that the recurved samplers were easy to use.

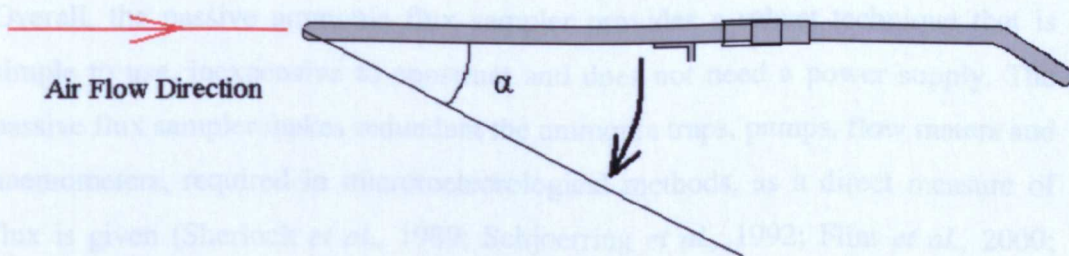
Whilst Ferm (1986) found a cosine dependence of flux collection efficiency with increasing α , Flint *et al.* (2000) found that there was a critical angle for the re-curved sampler of 80°, compared with 66° for the original Ferm tubes. At this angle, there was no flow through the sampler. A negative airflow regime was observed between the critical angle and 90°. Collection efficiency is calculated as the ratio of ammonia captured by the sampler to that released (and thus, expected to be captured by the sampler), expressed as a percentage. Whilst the data highlights the need for wind conditions to be known whenever an evaluation of the collection efficiency of the flux sampler is carried out (Flint *et al.*, 2000), Flint *et al.*'s (2000) work also highlights a difference between the original Ferm tubes and recurved samplers.



a)



b)



c)

Figure 1.4: a) Photograph of recurved passive ammonia flux sampler. b) Diagram of side view. c) Plan view.

1.8.4 Advantages and disadvantages of PAF samplers

As passive ammonia flux samplers are relatively cheap to construct, samples may be taken at many locations. One limitation on the maximum number of test

locations is the time required for uncapping and capping the first and last tubes. This may mean that it is difficult to achieve an adequate spatial density of sampling points around large area sources, which may require hundreds of samplers to obtain a suitable number of samples. It is, however, more desirable to have sample locations over a wide area - particularly when the spatial variability of the source is not known - rather than to try to extrapolate from spatially limited data (Flint *et al.*, 2000).

Another limitation is the possibility of breakthrough of ammonia between the tubes when wind speeds above 10 m s^{-1} occur (Ferm, 1986; Sommer *et al.*, 1996). The use of a smaller orifice to further restrict the flow through the sampler would result in a loss of sensitivity at low flow rates. However, this is not desirable as a significant quantity of ammonia could be transported through a sampler and not collected, even at low flow rates when the exposure period is long (Sommer *et al.*, 1996; Flint *et al.*, 2000).

A further limitation is the necessity to avoid certain meteorological conditions. Due to the nature of the coating, rain can invalidate measurements by washing the acid, and any collected ammonia, out of the sampler (Sommer *et al.*, 1996). Dew and fog can have a similar effect.

Overall, the passive ammonia flux sampler provides a robust technique that is simple to use, inexpensive to construct and does not need a power supply. The passive flux sampler makes redundant the ammonia traps, pumps, flow meters and anemometers, required in micrometeorological methods, as a direct measure of flux is given (Sherlock *et al.*, 1989; Schjoerring *et al.*, 1992; Flint *et al.*, 2000; Phillips *et al.*, 2001). However, the technique is extremely labour intensive with opportunity for human error during coating, extraction and analysis (Flint *et al.*, 2000).

Although validation experiments have taken place, these have been undertaken either with the original Ferm tubes (Ferm, 1986) or on recurved samplers in field conditions (Phillips and Scholtens, 1999). Also, Flint *et al.* (2000) have shown a different response with changing incident wind angle of recurved samplers

compared with original Ferm tubes. The ammonia collection efficiency of recurved PAF samplers in a highly controlled environment has not been measured.

1.9 CONCLUSIONS

Ammonia is the most abundant alkaline gas in the atmosphere and its main anthropogenic source is agriculture. It has the potential to acidify and add excess nutrients to soils and can thus lead to changes in species diversity. The contribution of outdoor pigs to the ammonia emissions estimate for the UK is not known accurately. Estimates have been made using emission factors for grazing cattle and there is only one study with outdoor pigs. As this source has increased over recent years it is important that its contribution to deposition of ammonia to susceptible habitats is determined.

Passive ammonia flux (PAF) samplers in a flux frame are a suitable method for measuring ammonia emissions at a free-range pig farm for a number of reasons. They measure flux directly, negating the need for wind speed measurements at each sampling height, and also require no power source. Being relatively cheap to construct, many samplers can be used at a large number of sampling locations. Their specificity to ammonia gas is high, with only a low possibility of interference from amines.

Whilst Ferm tubes have been validated under controlled conditions, the improved design of recurved PAF samplers has not, so it is necessary to validate these before they are used in the flux frame method.

1.10 THESIS OUTLINE

The aim of this study is to validate a method for the measurement of distributed agricultural sources of ammonia outdoors. Twenty five percent of the UK pig breeding herd are now kept outdoors on free-range sites, however, there are no accurate estimates of ammonia emissions from this source, as previously emission rates for grazing cattle were used. Now that this type of pig production represents such a large percentage of the total, it is desirable to quantify its contribution more

accurately by taking measurements. The overall aim of the project therefore is to validate recurved passive ammonia flux samplers and the flux frame method, and to then use this robust methodology to make accurate measurements of the ammonia emissions from a large distributed ammonia source.

The second chapter describes a validation experiment designed to determine the influence of ammonia concentration, wind speed and angle of orientation to the flow direction on the collection efficiency of the recurved passive ammonia flux sampler under laboratory conditions.

The third chapter presents the experiments undertaken in the Atmospheric Flow Laboratory (Hoxey *et al.*, 1999) to determine the collection efficiency of the flux frame method when validated samplers are used to collect the plume of ammonia from a known point source under controlled wind conditions. Modelled results are also presented to allow a comparison of measured results with those from a commercial atmospheric dispersion modelling package.

The fourth chapter presents the results from full-scale field experiments on the collection efficiency of a flux frame using controllable ammonia point and line sources at various distances upwind of the flux frame. Modelling of the conditions at the field site was performed to allow comparison.

The fifth chapter describes the measurements made at a commercial free-range farm using the fully validated method. A general discussion of the thesis findings is given in chapter six along with the final conclusions.

2. MEASUREMENT OF THE COLLECTION EFFICIENCY OF PASSIVE AMMONIA FLUX SAMPLERS

2.1 INTRODUCTION

Recurved passive ammonia flux samplers have been used to measure ammonia emissions from slurry tanks and other ammonia sources and have been validated in the field using controllable ammonia sources (e.g. Mahlcke, 1998; Kim *et al.*, 1999). However, they have not been validated using an ammonia source of known strength in controlled conditions. Intercomparisons of ammonia samplers have taken place. In many cases, however, this has been done by comparing results of field measurements rather than results obtained in controlled environments with known ammonia release rates (e.g. Appel *et al.*, 1988; Ferm *et al.*, 1988; Sickles *et al.*, 1988; Harrison and Kitto, 1990; Wiebe *et al.*, 1990; Kirchner and Braeutigam, 1998). One of the devices or techniques is assumed to provide an accurate measure of ammonia concentration and the other devices/techniques are then compared.

A more reliable method for determining the collection efficiency of a particular sampler is to expose it to constant source of ammonia at different concentrations/fluxes and to compare the measurement made by the sampler directly with the amount of ammonia released (Fox *et al.*, 1988 and Williams *et al.*, 1992).

The specific objectives of this set of experiments were to quantify the collection efficiency of recurved passive ammonia flux samplers in the laboratory under controlled environmental conditions and ammonia flux, and to determine the effect of orientation of the samplers to air flow direction.

2.2 MATERIALS AND METHODS

2.2.1 The fan test rig

The fan test rig (Moulsley *et al.*, 1987) at Silsoe Research Institute was used as an open circuit wind tunnel throughout this set of experiments (Figure 2.1). The fan test rig was designed to test the performance of fans whilst conforming to BS 848. The outlet was modified to enable six PAF samplers to be fixed downstream of the fan in a wooden and Perspex extension (800 mm high by 450 mm wide by 800 mm deep) without interference (Figure 2.2). The outlet cross-sectional area was small enough to achieve the desired concentrations and air speeds at low ammonia emission rates.

Figure 2.2: Sketch showing sampler position (1 of 6) in wind tunnel extension. Black lines represent the received PAF sampler held at an angle whilst the rest will accommodate the sampling plate. Direction of air flow is out of the plane of the page.



Figure 2.1: The fan test rig.

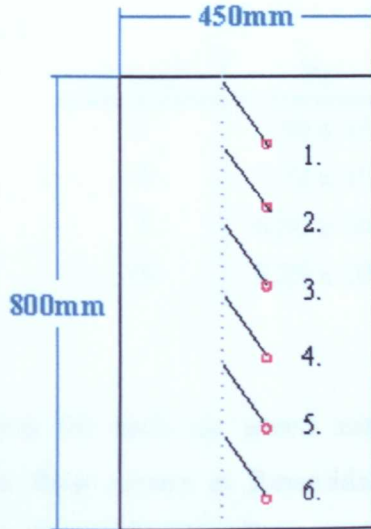


Figure 2.2: Sketch showing sampler position (1-6) in wind tunnel extension. Black lines represent the recurved PAF samplers held at an angle whilst the red circles represent the sampling plane. Direction of air flow is out of the plane of the page.

To reduce the possible effects of turbulence on the collection efficiency of the samplers, a honeycomb foil sheet was attached to the inside of the opening into the extension and the samplers were held around 400 mm into the extension where laminar flow was more likely. Smoke was released into the wind tunnel to allow a visual inspection of the flow through the Perspex side of the extension. The flow appeared to be laminar. The Reynolds number at each air speed was calculated, using:

$$Re = \frac{uE}{\nu} \quad (13)$$

where u is the air velocity in the extension, E is an appropriate dimension of the system (area of extension / perimeter of extension) and ν is the coefficient of kinematic viscosity of air ($15.5 \times 10^{-6} \text{ m}^2 \text{ s}^{-1}$ at 20°C) (Monteith and Unsworth, 1990).

Table 2.1: Reynolds numbers for air speeds to be used in experiments.

$u, \text{ m s}^{-1}$	Re
2	1.86×10^4
4	3.72×10^4
7	6.50×10^4
10	9.29×10^4

The Reynolds numbers for each air speed are presented in Table 2.1. The transition to turbulent flow occurs at Reynolds numbers of the order of 10^5 (Monteith and Unsworth, 1990), therefore at all speeds the free stream flow through the extension of the wind tunnel was laminar. However, at 10 m s^{-1} the Reynolds number is close to this transition.

2.2.2 Wind speed distribution

Measurements of wind speed were undertaken to quantify the variation in wind speed in the vertical sampling plane at the position of the inlets of the recurved PAF samplers (Figure 2.2). Six holes were drilled into the wooden side of the wind tunnel extension through which a hot-wire anemometer (Velocicalc 8345-M-GB, TSI Inc.) was inserted. Readings were taken continuously until a steady speed was measured over a five minute period. Thus the wind speed distribution was quantified and accounted for in ammonia flux measurements. This procedure was repeated at each location of the PAF samplers and at each of the three wind speeds to be used.

2.2.3 Ammonia supply system

An ammonia supply system was designed to create a constant ammonia concentration in the air supply to the fan test rig. Figure 2.3 shows a schematic diagram of the ammonia supply system and wind tunnel.

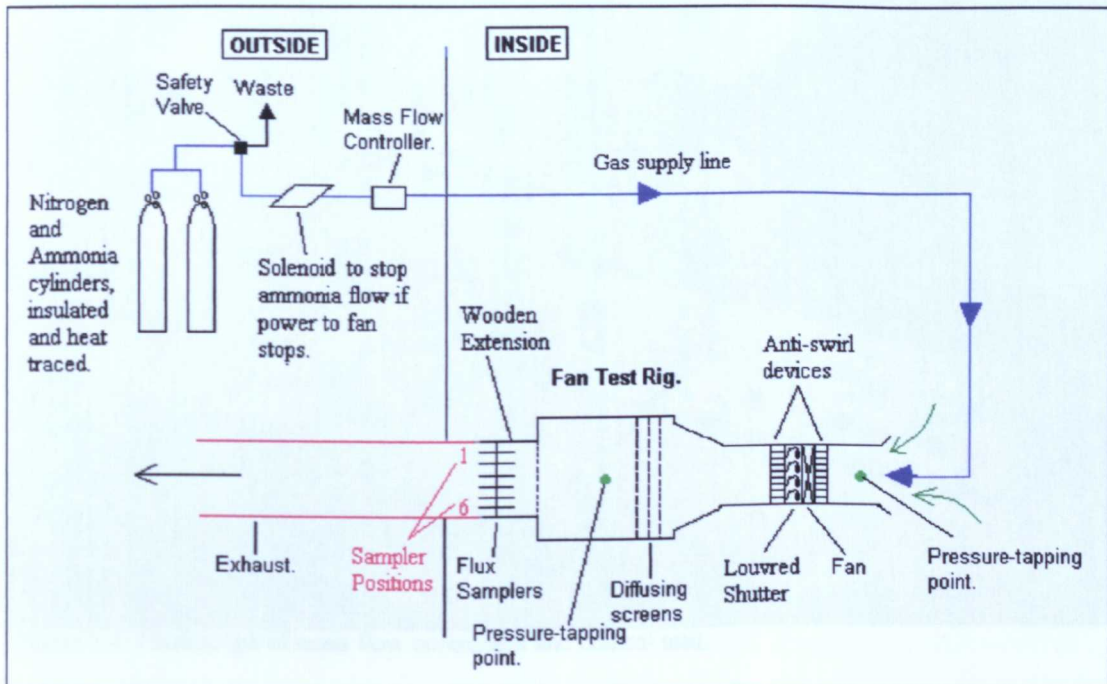


Figure 2.3: Ammonia supply system and wind tunnel.

Mass flow controllers (F-201D, Bronkhorst High-Tech) (Figure 2.4) were used to deliver the correct flow rate of ammonia gas to give the desired concentration, depending upon the air speed for each particular experiment. The desired flux was therefore introduced into the wind tunnel, taking into account air speed and ammonia concentration, and will be referred to as the 'nominal flux'. An ammonia cylinder and a nitrogen cylinder for flushing the gas lines were stored outside the building for safety reasons. Both cylinders were fitted with insulating jackets and all gas pipes were lagged with insulating material and heat trace cable to ensure the ammonia was kept at a constant temperature. A solenoid valve was fitted for safety reasons, which would stop the ammonia gas supply should the power supply to the fan fail. Ammonia was introduced upstream of the fan using a stainless steel tube supported at the rig inlet, thereby ensuring thorough mixing with minimum interference to the flow.

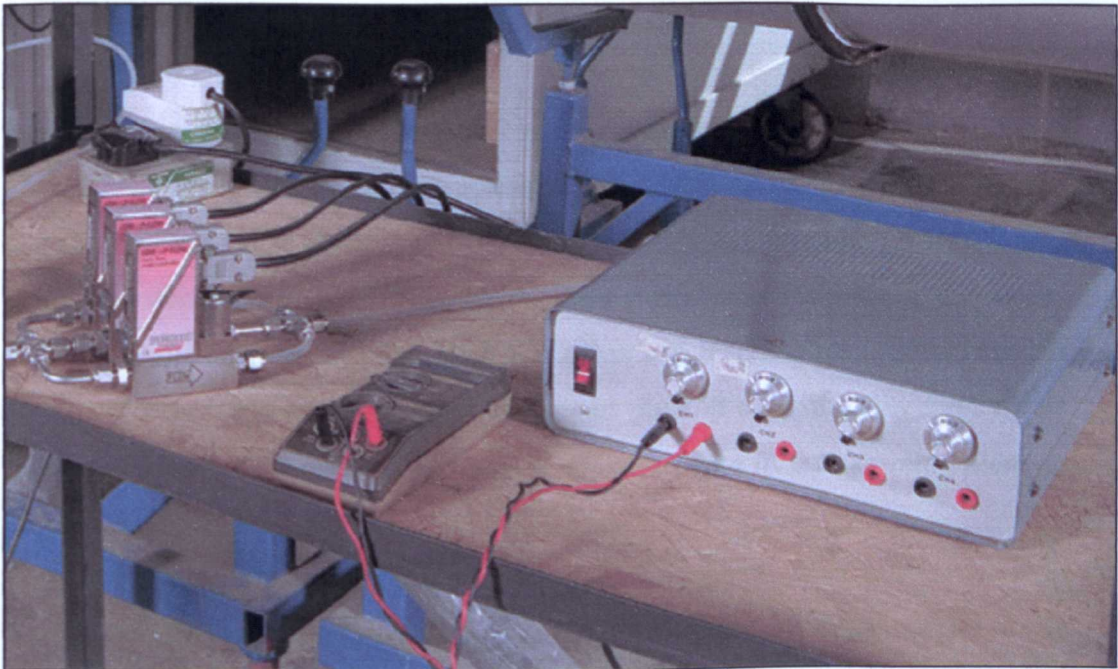


Figure 2.4: Photograph of mass flow controllers and control unit.

2.2.4 Preparation and analysis of recurved PAF samplers

Recurved PAF samplers were used (Figure 1.5), which differ from the traditional type of PAF sampler in that they sample in one plane (red line on figure 1.4) instead of two. Before coating, the glass tubes and end caps were washed well and then rinsed in ultra-high quality (UHQ) water. They were then oven-dried at around 50°C. A 4% oxalic acid in acetone solution was used to coat the tubes (4 g oxalic acid in 100 ml acetone). To reduce contamination, end caps were used to seal the tubes immediately after the acetone evaporated. Once coated the tubes were stored in a plastic bag and refrigerated at 5°C. Blank tubes were used to check for any ammonia contamination during coating, storage, handling and transport, during which time they remained capped and sealed in plastic bags.

After exposure, 6 ml of UHQ water was drawn up into the tubes twice using a pipette filler, and the extracted samples were stored in a refrigerator at 5°C until analysis. Analysis was performed using UV-visible spectrophotometry and followed the NEN (Nederlandse Eenheids Norm – Dutch Standard Method) method 6472 (Appendix I).

2.2.5 Experiment 1: Ammonia flux distribution

The sampling efficiency was measured at four different wind speeds (2.0, 4.0, 7.0 and 10.0 m s⁻¹) at each of three ammonia concentrations (0.5, 2.5 and 4.0 ppm) chosen to give a range of fluxes over which the efficiency would be tested, with a maximum exposure period of six hours. This period was reduced at the higher fluxes to avoid saturation of the tubes. Each flux was tested twice. Throughout the experiments, all six samplers were orientated parallel with the direction of air flow, i.e. $\alpha = 0^\circ$. This enabled variation in ammonia flux in the sampling plane to be examined.

Acid bubblers, set up as shown in Figure 2.5, were used throughout the experiment as a reference method, to measure the actual ammonia concentration in the fan test rig. Twenty millilitres of 0.025 M sulphuric acid (1.36 ml concentrated sulphuric acid per litre of water) was measured into each of two sintered glass bubblers connected in series. Two bubblers were used in series to ensure that all the ammonia was captured in the event of breakthrough or saturation of the acid. A third bubbler was used as a precaution to collect any liquid that evaporated from the second bubbler which would be transported to the pump. A bubble meter was also connected at the end of the system as another check on the volume of air passing through the acid solution.

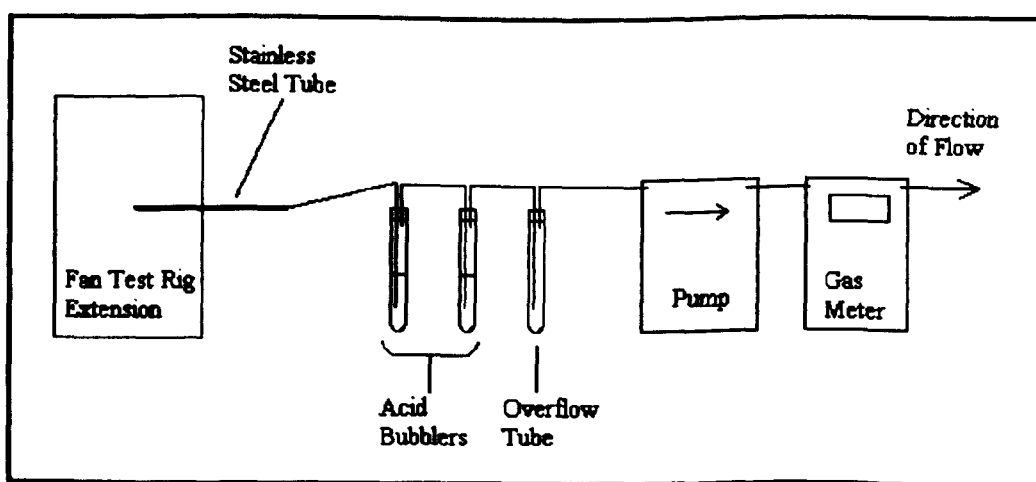


Figure 2.5: Bubbler system.

The bubblers were used three times in each session. Two of the sampling runs were performed with a stainless steel sampling rod inserted into the centre of the extension to measure the ammonia concentration. The third run was performed with the rod removed from the extension to measure the background ammonia concentration present near the inlet to the fan test rig. Before analysis, 2 ml of the bubbler solution was reacted with 2 ml of 0.04 M sodium hydroxide solution to raise the pH to between 6 and 12 and thus neutralise the acid and release the ammonia. The ammonia concentration was then determined using UV-VIS spectrophotometry as before (Appendix I).

Analysis gives the mass of ammonia on each tube. To determine the collection efficiency of recurved PAF samplers, the net horizontal flux for each sampler was determined from equation 11 with:

$$F_h = \frac{\Delta M}{\pi r^2 t} \quad (14)$$

The notation is as for equation 11, with ΔM equating to $(M_S - M_B)$, and M_S and M_B representing the masses of ammonia on the tubes pointing towards the source and background respectively. Note that a correction factor (K) is not included to enable the average collection efficiency of recurved PAF samplers to be found at a range of fluxes. Plotting the measured flux calculated with no correction factor against the nominal flux enables a correction factor specific to recurved PAF samplers to be determined from the slope of the line fitted to the data.

2.2.6 Experiment 2: Effect of orientation of sampler to air flow

A second experiment was undertaken to determine the effect of orientation of the sampler to the direction of the air flow on the sampler efficiency. Six angles to the direction of flow (0° , 30° , 60° , 70° , 80° and 90°) were randomly assigned to each of the six sampling positions. Three different air speeds (2.0 , 4.0 and 7.0 m s^{-1}) at each of three ammonia concentrations (0.5 , 2.5 and 4.0 ppm) were used. Each combination of air speed and ammonia concentration was repeated twice. When

high variability was found in the results (for example, at very low fluxes) repeats were performed for 24 hours.

Analysis was carried out using UV-visible spectrophotometry as described above and a reference measurement of ammonia concentration was again taken using acid bubblers.

2.3 RESULTS

2.3.1 Wind speed distribution

Accumulated analysis of variance tests were performed on the set of data for each wind speed to see which type of curve had the best fit. In all three cases, the addition of a quadratic term to produce a curvilinear fit had the highest statistical significance, and thus was fitted to the data.

The measured wind speed at each sampling position in the extension is plotted in Figure 2.6. Wind speed varied with vertical height in the extension. The curvilinear response can be seen with change in height down the extension and the curvature of the response was greatest at a wind speed of 10 m s^{-1} . Multiple regression analysis was performed on the results for each wind speed, and a summary of these analyses is presented in Table 2.2. The highly statistically significant t -value for all three parameters indicates that the polynomial trendline is a good fit to each set of measurements, along with small standard errors on each of the terms. The variation of wind speed with height is likely to be due to drag at the top and bottom enclosing surfaces; the increasingly curvilinear response with increasing wind speed shows that there is a higher level of drag at higher wind speeds.

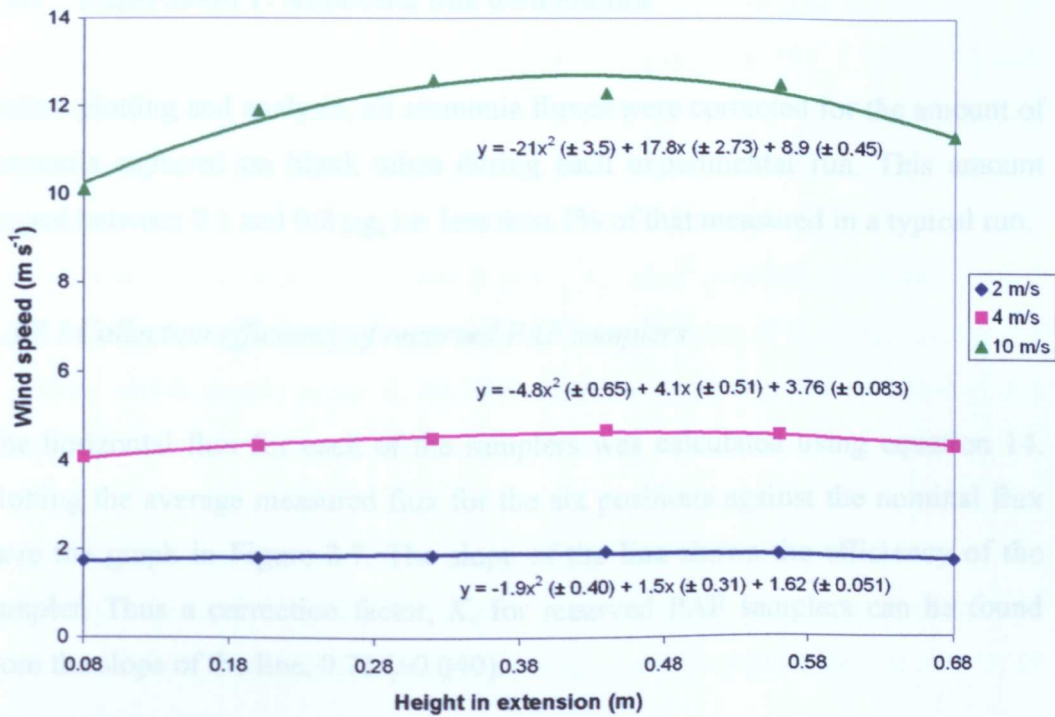


Figure 2.6: Wind speed distribution as a function of vertical position within the extension of the wind tunnel.

Table 2.2: Summary of multiple regression analysis results for wind speed distribution for each of the three wind speeds tested. Polynomial regressions were fitted to each data set; $y = a + bx + cx^2$ where y is the wind speed, x is the position and a , b and c are fitted parameters.

2 m s ⁻¹	Parameter estimate	s.e.	t	P
a	1.62	0.051	31.56	<.001
b	1.5	0.31	4.71	0.018
c	-1.9	0.40	-4.71	0.018

percentage variance accounted for 80.4

4 m s ⁻¹	Parameter estimate	s.e.	t	P
a	3.76	0.083	45.23	<.001
b	4.1	0.51	8.07	0.004
c	-4.8	0.65	-7.34	0.005

percentage variance accounted for 93.2

10 m s ⁻¹	Parameter estimate	s.e.	t	P
a	8.9	0.45	20.08	<.001
b	17.8	2.73	6.53	0.007
c	-21	3.5	-6.03	0.009

percentage variance accounted for 89.5

2.3.2 Experiment 1: Ammonia flux distribution

Before plotting and analysis, all ammonia fluxes were corrected for the amount of ammonia captured on blank tubes during each experimental run. This amount ranged between 0.1 and 0.2 μg , i.e. less than 1% of that measured in a typical run.

2.3.2.1 Collection efficiency of recurved PAF samplers

The horizontal flux for each of the samplers was calculated using equation 14. Plotting the average measured flux for the six positions against the nominal flux gave the graph in Figure 2.7. The slope of the line shows the efficiency of the sampler. Thus a correction factor, K , for recurved PAF samplers can be found from the slope of the line, 0.71 (± 0.040).

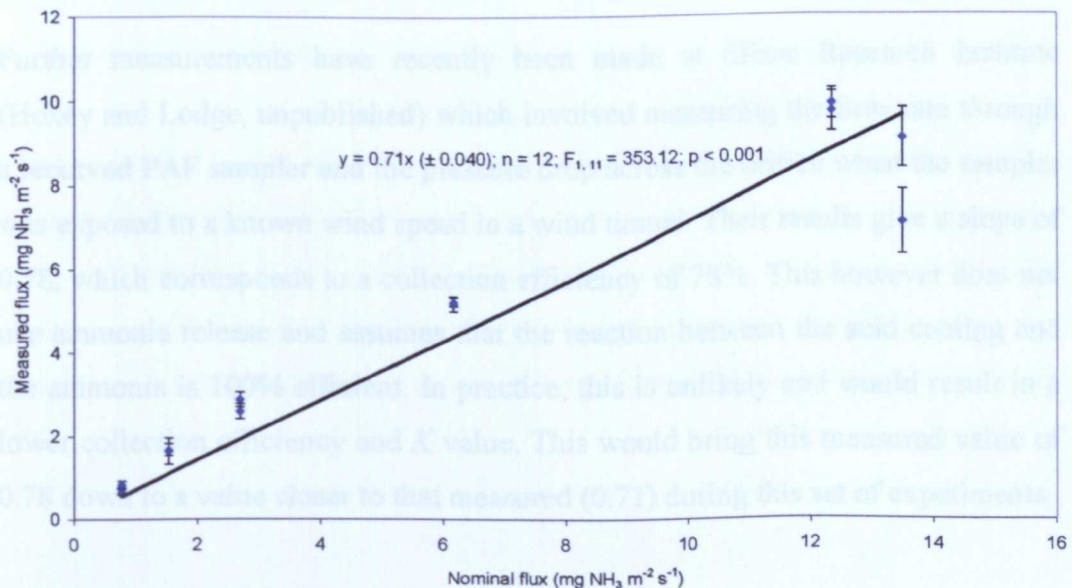


Figure 2.7: Collection efficiency of recurved PAF samplers.

However, despite the slope having a good fit ($p < 0.001$) and a small standard error (± 0.040), on closer inspection of the data points it is clear that the majority of the data lie above the regression line, with only data points at a nominal flux of 13.49 lying below. Fitting a linear regression to data points below a nominal flux of 12.5 gives a much better fit and a K value of 0.81, however there appears to be

no reason why data points above a nominal flux of 12.5 should be excluded. A wind speed effect can be disregarded as nominal fluxes of 0.771, 1.542 and 2.699 are produced using all three of the wind speeds (2 to 7 m s⁻¹). Concentration effects can also be disregarded as the nominal flux of 13.49 was produced using a concentration of 2.5 ppm, whilst lower nominal fluxes were produced with ammonia concentrations of 0.5 and 4 ppm. Another possible explanation, flux dependence, can also be discounted as there is no evidence of breakthrough in the raw data which would occur if the flux was too great and the reaction in the sample tube was not taking place fast, or efficiently, enough.

A non-linear fit, such as a polynomial, may fit the data better however for simplicity a linear fit is desirable. Further work would be necessary to determine the actual reason, perhaps using one ammonia concentration whilst varying wind speed, or *vice versa*.

Further measurements have recently been made at Silsoe Research Institute (Hoxey and Lodge, unpublished) which involved measuring the flow rate through a recurved PAF sampler and the pressure drop across the orifice when the sampler was exposed to a known wind speed in a wind tunnel. Their results give a slope of 0.78, which corresponds to a collection efficiency of 78%. This however does not use ammonia release and assumes that the reaction between the acid coating and the ammonia is 100% efficient. In practice, this is unlikely and would result in a lower collection efficiency and *K* value. This would bring this measured value of 0.78 down to a value closer to that measured (0.71) during this set of experiments.

2.3.2.1 Positional effect

Simple regression analysis was performed on the raw data for each set of conditions (i.e. no correction factor, *K*, used), with flux as the response variate and position as the explanatory variate. Three regressions were fitted to the data: $y = a_1$, $y = a_2 + b_2x$ and $y = a_3 + b_3x + c_3x^2$. In all cases, $y = a_1$ (a horizontal line with no slope) was found to have a highly statistically significant fit. A summary of the analysis is presented in Table 2.3. This shows that there was no positional effect in

the wind tunnel extension when recurved passive flux samplers were used to measure ammonia flux.

Table 2.3: Summary of simple regression analysis for positional effects on flux measurement.

Wind speed (m s ⁻¹)	Concentration (ppm)	Nominal flux (mg NH ₃ m ⁻² s ⁻¹)	Observed mean flux estimate (mg NH ₃ m ⁻² s ⁻¹)	s.e.	t	P
2.0	0.5	0.77	0.75	0.059	12.87	<.001
2.0	4.0	6.17	5.20	0.103	50.6	<.001
4.0	0.5	1.54	1.50	0.231	6.49	<.001
4.0	4.0	12.34	9.3	0.59	15.69	<.001
7.0	0.5	2.70	2.74	0.130	21.13	<.001
7.0	2.5	13.49	8.1	0.58	13.91	<.001

2.3.3 Experiment 2: Effect of orientation of sampler to air flow

Figure 2.8 shows the ratio of measured flux to nominal flux at all combinations of wind speed and ammonia concentration.

The results at 0.5 ppm, at all speeds, showed a large variability in measured flux. This variability was thought to be due to too short an exposure period, so repeats were undertaken at 2 m s⁻¹ and 0.5 ppm for 24 hours. The variability was greatly reduced, confirming that the short exposure period was the problem and it has therefore been assumed that this was the case for the other wind speeds at 0.5 ppm.

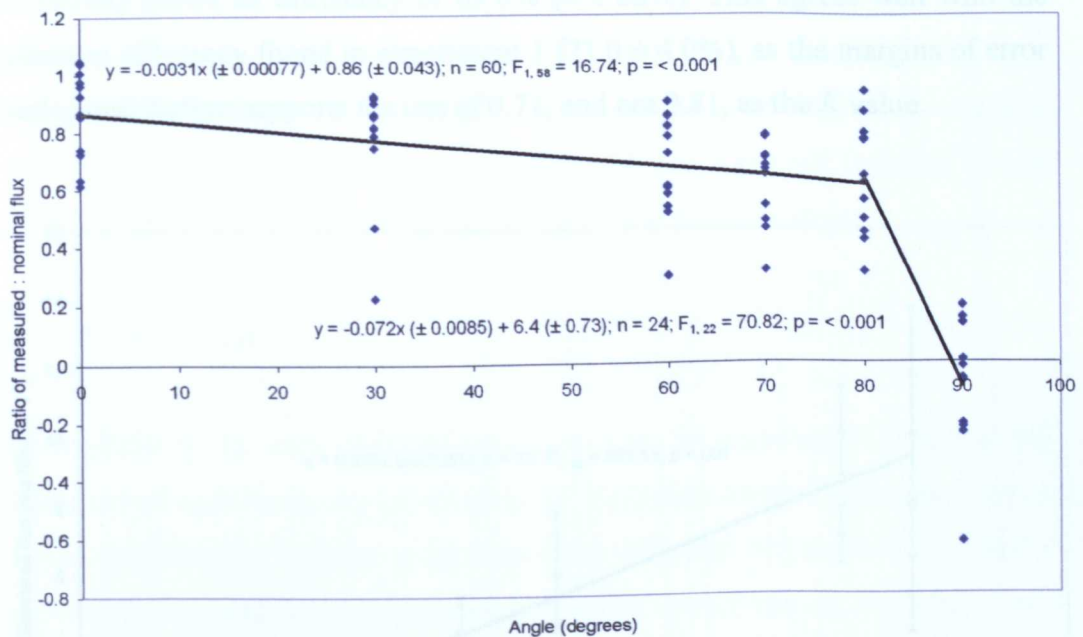


Figure 2.8: Variation of the ratio of measured to nominal fluxes with orientation of the flux sampler to the flow direction. Each symbol represents the net horizontal flux measured by a sampler.

Simple linear regression analysis was performed on two sections of the data set, between 0 and 80°, and 80 and 90°. The trendline fitted to data up to 80° has a small gradient of $-0.0031 (\pm 0.00077)$ which is significantly different from zero ($p < 0.001$). This shows that there was a small effect on measurement of ammonia flux up to an orientation of 80°. The trendline between 80 and 90° is also significantly different from zero ($p < 0.001$) but here the slope has a much steeper gradient of $-0.072 (\pm 0.0085)$, showing a greater dependence upon angle beyond 80°. Low, zero and negative fluxes were measured when the samplers were orientated at 90° to the air flow direction.

For each ammonia concentration and wind speed combination, the average measured horizontal flux over angles 0 to 80° was taken and plotted against the nominal flux (Figure 2.9). Due to the variability problem described previously, Figure 2.9 excludes the original 0.5 ppm data at all speeds and only includes 0.5 ppm data from the repeats at 2 m s^{-1} . As there was little variation between angles 0 and 80°, this enabled another estimate of collection efficiency to be made from the slope of the linear regression fitted to the resulting data. The slope of 0.696

(± 0.00288) shows an efficiency of 69.6% ($\pm 2.88\%$). This agrees well with the collection efficiency found in experiment 1 ($71.0 \pm 4.0\%$), as the margins of error overlap and further supports the use of 0.71, and not 0.81, as the K value.

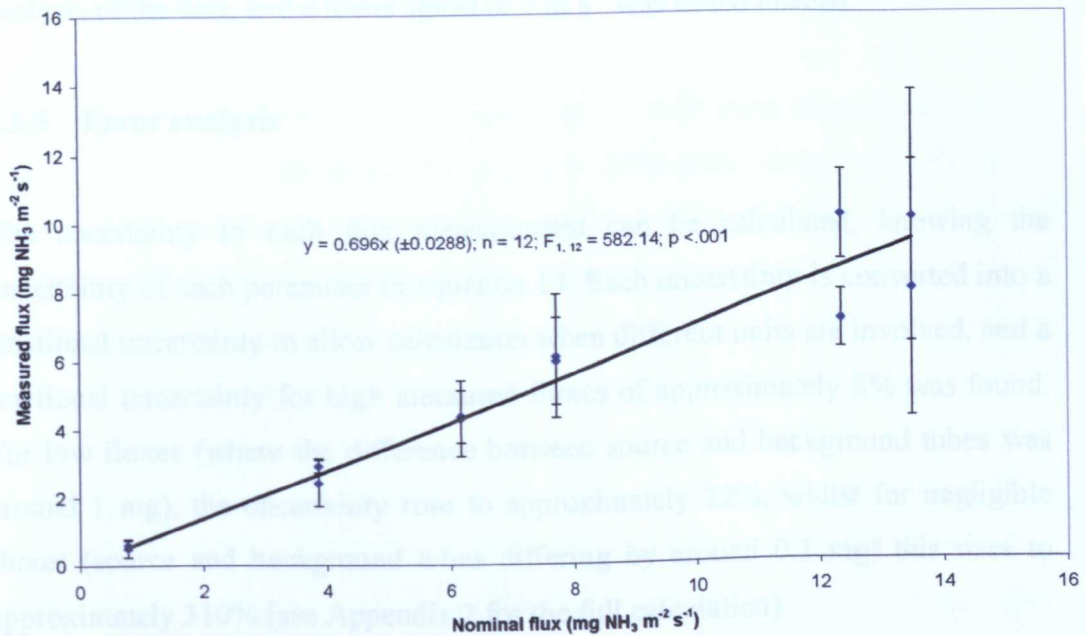


Figure 2.9: Average collection efficiency of recurved PAF samplers when orientated at angles 0 to 80°. Symbols represent the average measured flux for angles 0-80° for each of the 12 wind speed and ammonia concentration combinations.

2.3.4 Results at a wind speed of 10 m s^{-1}

Although a wind speed of 10 m s^{-1} was initially to be tested, ammonia flux measurements at this wind speed gave substantially lower values than the nominal flux at all angles of orientation to the air flow. No clear pattern was shown. The problem was attributed to breakthrough to the second tube.

2.4.1 Experiment 1: Ammonia flux distribution

Saturation could occur if the exposure period was too long; these measurements were repeated with exposure periods of just one hour and similar results were obtained. This suggested that bypass had occurred, whereby the wind speed through the sampler was too fast for the reaction between the absorbent coating and the ammonia in the air. Ammonia would then be carried through the sampler to the second tube or out of the sampler so that when a net horizontal flux was calculated a low, negative or zero flux would be observed. A solution to this

problem would be to decrease the size of the orifice to further reduce the flow through the sampler. However, this would result in the sampler being less sensitive at low wind speeds, which are more likely to occur. Therefore, results at 10 m s^{-1} were excluded from further experiments and were not included in any analysis of the data, and a lower speed of 7 m s^{-1} was tested instead.

2.3.5 Error analysis

The uncertainty in each flux measurement can be calculated, knowing the uncertainty of each parameter in equation 14. Each uncertainty is converted into a fractional uncertainty to allow calculation when different units are involved, and a fractional uncertainty for high measured fluxes of approximately 8% was found. For low fluxes (where the difference between source and background tubes was around 1 mg), the uncertainty rose to approximately 32%, whilst for negligible fluxes (source and background tubes differing by around 0.1 mg) this rises to approximately 310% (see Appendix 2 for the full calculation).

2.3.6 Reference ammonia flux

Ammonia concentrations determined using the reference method were used along with the wind speed measurements made for the wind speed distribution (section 2.2.2) to calculate an estimated ammonia flux. The mean estimated ammonia flux was $88.1\% \pm 9.4$ of the nominal flux.

2.3 DISCUSSION

2.4.1 Experiment 1: Ammonia flux distribution

Despite the curvilinear response of wind speed with position in the wind tunnel extension, no positional effects were found using the recurved PAF samplers to measure ammonia distribution in the wind tunnel extension. This is probably due to the averaging effect of the PAF samplers (average flux over hours) compared with the instant measurement of wind speed by the hot-wire anemometer. Also,

the curvilinear response was less pronounced at 2 and 4 m s⁻¹ compared with that at 10 m s⁻¹ and all measurements of horizontal flux at this high speed for all three ammonia concentrations were excluded. Wind speed measurements with the hot-wire anemometer were not repeated at 7 m s⁻¹, so the response of wind speed with position can not be considered further.

Ferm (1986) does not describe the details of his validation experiments, whilst Flint *et al.* (2000) monitored the pressure differential across the orifice to determine the wind speed through the sampler, without an actual release of ammonia and subsequent wet chemistry. Although the most realistic measure of ammonia collection efficiency is to produce a known ammonia flux by providing a known concentration of ammonia at a known wind speed and then to capture this with the samplers, a more efficient method may have been to emulate Flint *et al.* (2000). *Using pressure differences across the orifice to determine the airflow characteristics of the sampler allows quicker experiments to be undertaken, as it is not necessary to wait several hours for the samplers to collect a measurable amount of ammonia at low fluxes. It would also be less likely that errors would be introduced, as it would remove the need for coating and extraction where contamination is more likely to occur. Faster experiments would enable more experiments to be undertaken in the same time period. This would remove the need to expose a number of tubes at one time and thus enable a more uniform environment to be provided where there were no doubts about uniformity of ammonia flux distribution across the experimental area of the wind tunnel. Faster experiments would also have allowed the full set of conditions that had been decided upon to have been tested, providing a more uniform set of data with fewer assumptions.*

2.4.2 Critical angle of incidence

Figure 2.10 shows a comparison between three sets of data: that produced during experiment 2 in this study and those produced by Flint *et al.* (2000) and Ferm (1986). There are differences between the three sets of data. Ferm (1986 *et seq.*) reported for the original Ferm tube design a cosine dependency with increasing α

that enables a correction of the collection efficiency to be made so long as incident wind angle is known. Flint *et al.* (2000) reported a decrease in air speed through the recurved sampler, and thus collection of ammonia, after 30° that continued to decrease to an angle of 80° after which there was zero or negative flow through the samplers. The ‘critical’ angle found during the orientation experiment presented here was found to be 80°. Up to this angle, the net horizontal flux decreased slowly with increasing angle, whilst beyond 80° the flux fell off sharply.

However, differences are apparent between the conditions under which the three sets of data were obtained. Ferm (1986) validated the original Ferm tubes, which may have different pressure and suction profiles to the recurved samplers, whilst Flint *et al.* (2000) used pressure differentials across the orifice. Flint’s data would be supported by a recent paper by Scholtens *et al.* (submitted 2002), which described the principles by which PAF samplers work and the role of the orifice as a flow meter. The repositioning of the orifice between two tubes, rather than at opposing ends of two sets of tubes as in the original Ferm tube design, has been reported by Phillips and Scholtens (2001) to eliminate the wind direction effect. This would explain the difference between the results found by Ferm (1986 *et seq.*) and Flint *et al.* (2000), and agree to some extent with those presented by Flint *et al.* (2000) and found in this study.

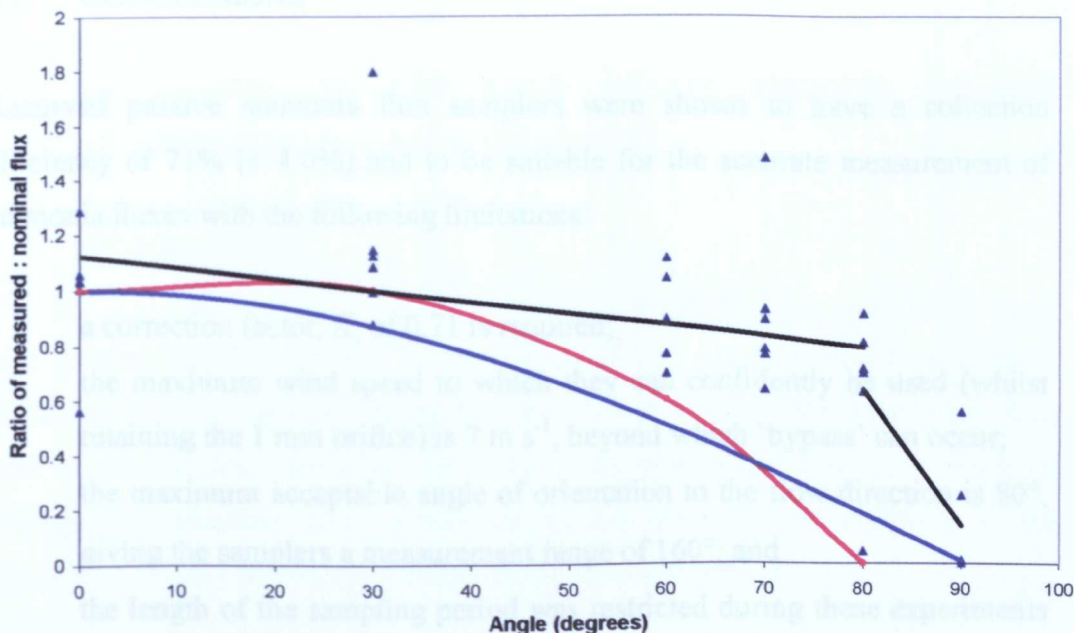


Figure 2.10: Comparison of experimental data from this study (black line), cosine curve, Fermi (1986) - blue line, and Flint *et al.* (2000) - red line.

2.4.3 Collection efficiency

Phillips and Scholtens (1999) found PAF samplers to have a capture efficiency of just 66% (s.e. = 3%, n = 5). However, these measurements were performed *in situ* in a naturally ventilated cattle house and not in the more controlled conditions found in a wind tunnel as in this study.

The collection efficiency was found to be 71% ($\pm 4.0\%$) for the recurved samplers in experiment 1, whilst in experiment 2 the average collection efficiency for angles 0 to 80° was 69.6% ($\pm 2.88\%$). As the error for experiment 1 is $\pm 4.0\%$, the range almost entirely includes the range of efficiencies found for experiment 2. Hence using a collection efficiency of 71% is suitable, particularly as experiment 2 includes a slightly larger underestimation due to the slight decrease in collection efficiency with increasing angle.

2.5 CONCLUSIONS

Recurved passive ammonia flux samplers were shown to have a collection efficiency of 71% ($\pm 4.0\%$) and to be suitable for the accurate measurement of ammonia fluxes with the following limitations:

- a correction factor, K , of 0.71 is required;
- the maximum wind speed to which they can confidently be used (whilst retaining the 1 mm orifice) is 7 m s^{-1} , beyond which 'bypass' can occur;
- the maximum acceptable angle of orientation to the flow direction is 80° , giving the samplers a measurement range of 160° ; and
- the length of the sampling period was restricted during these experiments due to saturation.

Measurements of distributed area sources would not be restricted by saturation, due to the low emission rate: Williams *et al.* (2000) used sampling periods of four weeks without any saturation apparent for measurements of free-range pigs.

This type of sampler negates the need for wind speed measurements at each sampling location as it measures horizontal flux directly. It is also suitable for use at remote sites, such as an outdoor pig farm, as it is passive and does not require a power source. The low cost of each sampler enables them to be used at many sampling locations; hence they are suitable for use in the flux frame method which requires over a hundred samplers to give a reliable estimate of the gaseous emission from a distributed source outdoors.

3. VALIDATION OF THE FLUX FRAME METHOD IN THE ATMOSPHERIC FLOW LABORATORY

3.1 INTRODUCTION

Natural wind has the potential to change speed and direction rapidly leading to difficulties in achieving high quality data for validation of the flux frame method. In order to control the variability associated with outdoor conditions, a series of validation experiments were carried out in the controlled environment of the Atmospheric Flow Laboratory (AFL) at Silsoe Research Institute.

The flux frame method captures the whole of the plume of emissions from a source (Michorius *et al.*, 1997). In other methods, difficulties arise in determining a sampling position that would enable a representative measurement to be made of the source strength. By capturing the whole of the plume, the uncertainty of sampling locations is removed and an accurate estimate of source strength can be determined.

A variation of the flux frame method, in which the framework of samplers is arranged around the source (in this case, a slurry tank) rather than in a single plane downwind of the source, was validated using a controllable ammonia area source of known release rate (Kim *et al.*, 1999). The collection efficiency of the flux frame was found to be 76% (s.e. 13). The variability in the collection efficiency was believed to be due to the samplers rather than the controllable ammonia source. Whilst the flux frame method has been used to measure emissions from a source by Michorius *et al.* (1997), there is no evidence of any validation of the method beforehand. Therefore, whilst the collection efficiency of a flux frame positioned around a source has been determined, the collection efficiency of a flux frame positioned in a single plane downwind of a source (as it is to be used in this project) has not, nor under the completely controlled conditions of a wind tunnel. The aim of this set of experiments was therefore to determine the collection efficiency of the flux frame method under controlled conditions of wind speed and direction, and of ammonia concentration.

3.2 MATERIALS AND METHODS

3.2.1 The Atmospheric Flow Laboratory

The AFL consists of a bank of 56 fans, a working section carpeted with Astroturf, and a return section. The 56 fans are arranged in an array of 8 wide (6 m wide) by 7 high (5 m high) with 28 individually addressable controllers, each controlling 2 fans. The AFL has the ability to produce a flow that has similar velocity and turbulence intensity profiles to those of the natural atmospheric boundary layer close to the surface. A maximum air speed of 5 m s^{-1} can be achieved with a velocity profile which would occur naturally with a ground roughness length of 0.01 m (Hoxey *et al.*, 1999).

The system can be run in two modes – circulating or non-circulating. For circulation, the doors of the AFL remain closed, whilst for non-circulation, the doors are opened and a curtain raised to prevent released pollutant tracers circulating around the AFL. For the experiments undertaken for this project, the non-circulation mode was used so that the pollutant (ammonia) was vented to the external air. This had a minor drawback in that external conditions, such as high wind speeds, could have an effect on the experiments taking place. Three background PAF samplers were deployed behind the fan bank during each experiment to check that no ammonia was being re-entrained into the air flow.

Figure 3.1 shows the working section of the AFL with the fan bank visible in the background. Figure 3.2 is a schematic diagram that shows in more detail the curtains (1 and 2) and mesh fitted to prevent recirculation of ammonia gas and to guide the contaminated air out of the open doorways (shown as gaps in the outline of the AFL).

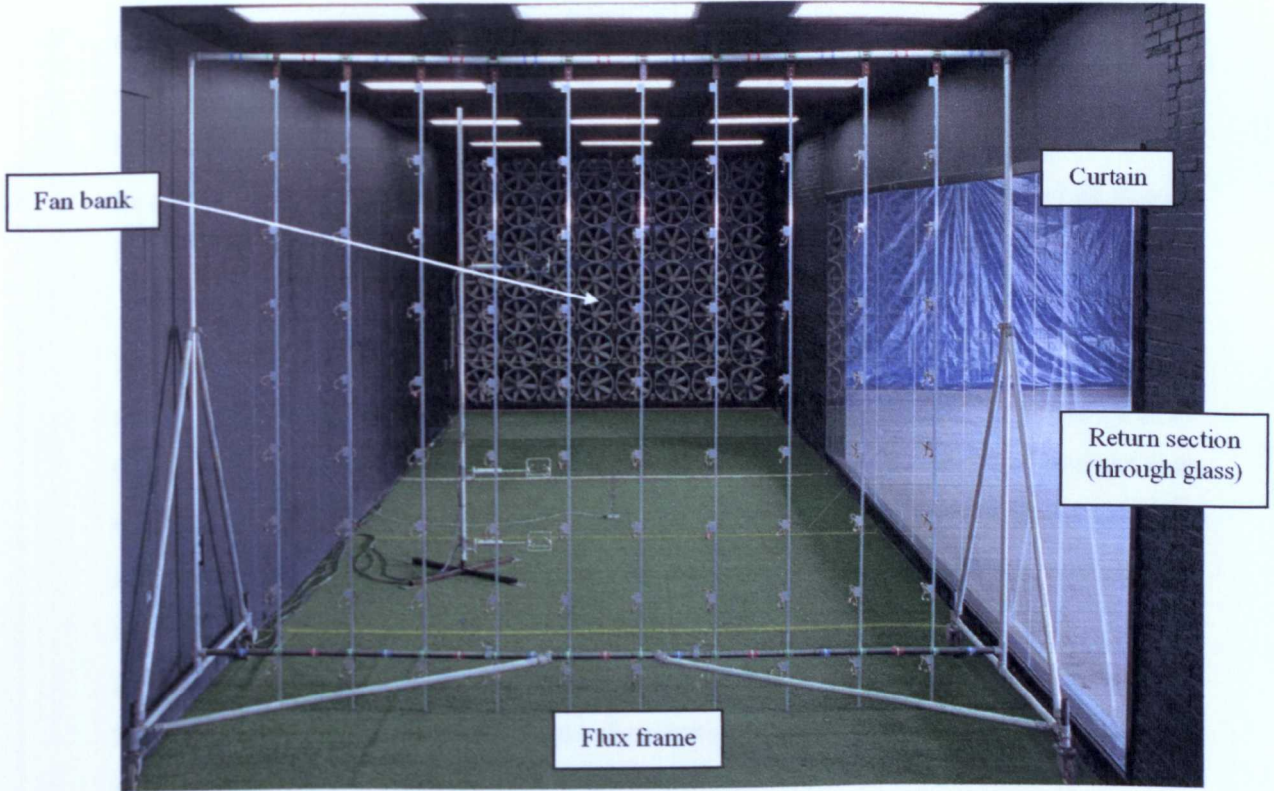


Figure 3.1: Working section of Atmospheric Flow Laboratory, viewed from downstream.

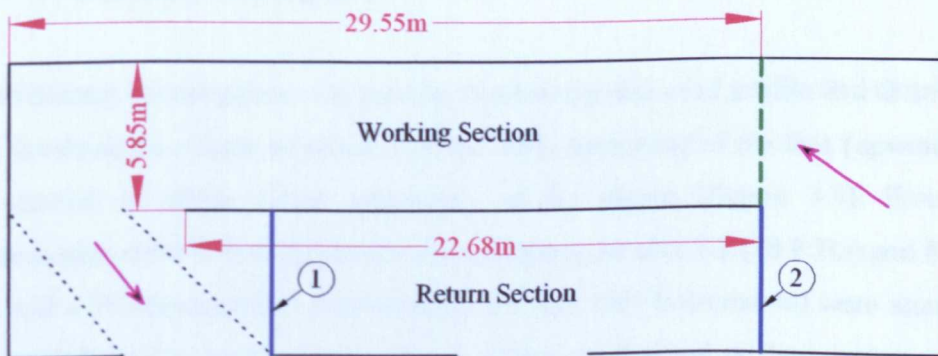


Figure 3.2: Schematic of AFL. Green dashed line represents the fan bank; blue lines show the positions of the curtain; dotted lines are mesh curtains; pink arrows show the direction of the air flow.

3.2.2 Flux frame

A scaffolding frame (5.5 m wide by 4.5 m high) on wheels was constructed enabling the frame to be easily positioned. Ten uprights were constructed from square-section

aluminium tubing, which hung from hooks on the scaffolding. Initially, the uprights were positioned at 0.5 m intervals with samplers attached at 0.5 m intervals starting at 0.3 m from the floor. This produced a regular array of 80 samplers, evenly distributed to a height of 3.8 m. This original flux frame is shown in the foreground of Figure 3.1.

The sampler distribution was modified after several runs to include an extra row of samplers at a height of 0.05 m (total of 90 samplers), which enabled the area close to the ground with highest horizontal fluxes to be sampled. Later, an extra upright was constructed for use with a centrally positioned ammonia source (1.8 m off the ground) and the positions of the five central uprights were adjusted to 0.25 m intervals. These modifications, together with extra samplers at 0.25 m spacing at the centre of the frame, increased the sampling density over the area where the highest horizontal fluxes would be expected. The exact distribution of samplers for a particular run is described for each set of runs as they are discussed.

3.2.3 Preliminary investigation

A preliminary investigation was used to characterise the wind profile and distribution. This involved the release of smoke into the AFL downwind of the fans (upwind of the flux frame) to allow visual inspection of the plume (Figure 3.3). Five sonic anemometers (four Solent Research Anemometers, models R2 (20.8 Hz) and R3 (100 Hz), and a Windmaster Pro Anemometer (10 Hz), Gill Instruments) were attached to a mast and used to make measurements of the wind speed at three points across a traverse of the AFL, from which calculations of turbulence intensity could be made (see equation 17). Measurements were made at heights 0.3, 1.0, 2.0, 3.0 and 4.0 m above the ground at the centre of the working section of the AFL and 1.53 m from each side, 17.6 m from the fans (Figure 3.4).

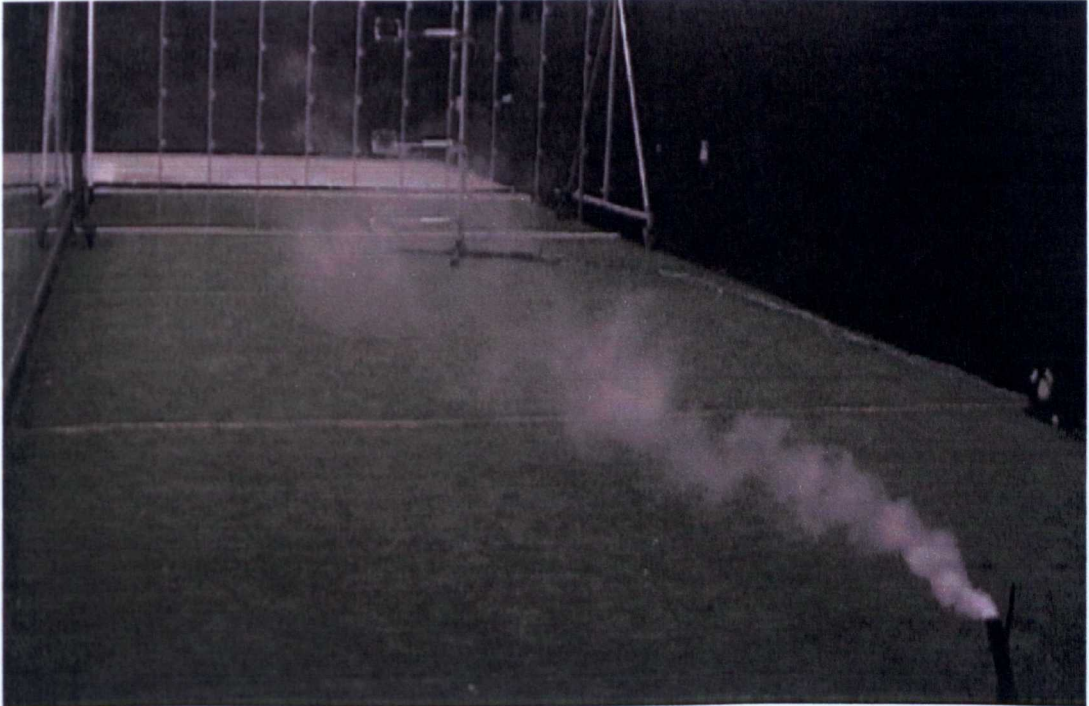


Figure 3.3: Smoke release in the AFL.

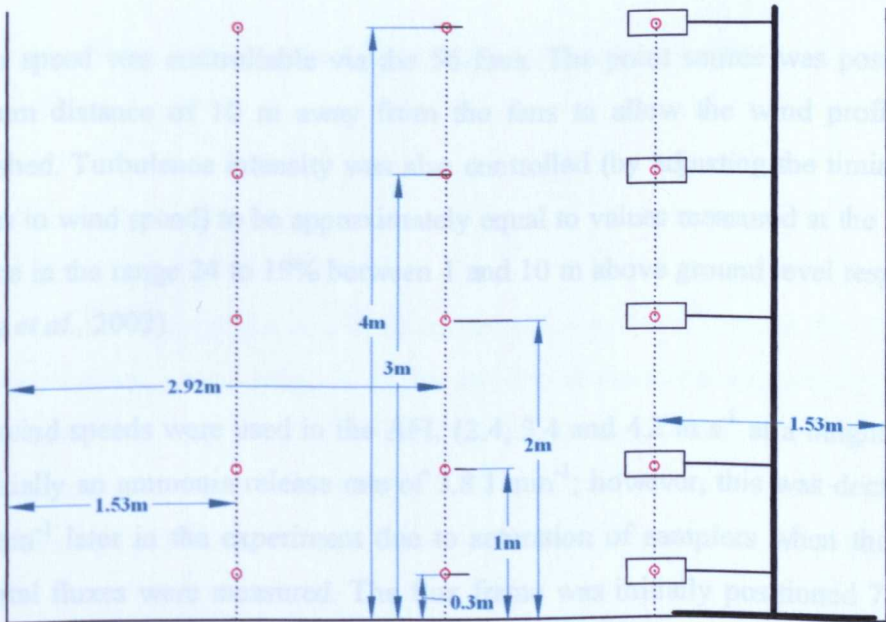


Figure 3.4: Cross-section of working section of AFL 17.6 m downwind of the fans. \circ indicate sampling locations, whilst the dashed lines indicate the three different sampling planes.

This preliminary investigation enabled the optimum distance of the point source from the frame to be determined. This is the distance at which the frame of samplers captures the whole width of the plume and no reflection at the walls occurs (which could affect the shape of the resulting plume).

3.2.4 Ammonia release experiments

A point source was used to deliver ammonia at a known rate. This was constructed using FEP tubing (o.d. 7 mm, i.d. 5 mm), which was held at either 0.3 or 1.8 m above ground level using a retort stand; this provided minimum interference with the flow of air through the AFL. A safety solenoid and flow meter (Roxspur Controls Direct, Basingstoke, Ammonia flow meter (1 - 10 l min⁻¹), model GTVS212 GTF2BHS) were included in the system and lagging and heat trace cable were added to the gas line from the cylinder situated in a cage outdoors. The ammonia cylinder was also weighed before and after release to measure the exact weight of ammonia released.

The air speed was controllable via the 56 fans. The point source was positioned a minimum distance of 10 m away from the fans to allow the wind profile to be established. Turbulence intensity was also controlled (by adjusting the timing of the changes in wind speed) to be approximately equal to values measured at the field site at Silsoe in the range 24 to 19% between 1 and 10 m above ground level respectively (Hoxey *et al.*, 2002).

Three wind speeds were used in the AFL (2.4, 3.4 and 4.2 m s⁻¹ at a height of 2 m) and initially an ammonia release rate of 3.8 l min⁻¹; however, this was decreased to 2.0 l min⁻¹ later in the experiment due to saturation of samplers when the highest horizontal fluxes were measured. The flux frame was initially positioned 7 m from the source (see smoke release results). However, it was found that, despite the use of smoke visualisation, the plume was off centre so that the whole width of the plume was not being captured in all cases. This distance was therefore decreased to 5 m with the flux frame being moved to a position 15.6 m from the fan bank. The flux frame

was moved towards the fans rather than the source nearer to the flux frame as it was possible that the off centre plume was being caused by the changing direction of the flow of air round the end of the central wall.

When the source was positioned centrally, 1.8 m above ground, only one wind speed was used (2.3 m s^{-1}) and the source was 3 m from the frame. Exposure periods were varied depending upon the wind speed used and the distance of the source from the frame and ranged between 1 and 6 hours.

Coating of the tubes and analysis of the solution resulting from their extraction after exposure was undertaken in the same manner as described in section 1.8.1.1, using 4% oxalic acid in acetone solution and analysis using NEN method 6472 and UV-visible spectrophotometry (Appendix 1). Net horizontal flux through the samplers was calculated using equation 14, with the correction factor K calculated in Chapter 2 included.

An estimate of the mass of ammonia passing through the flux frame was made using equation 15:

$$M_F = V \times t \quad (15)$$

where M_F is the mass of ammonia estimated to have passed through the flux frame over the exposure period (mg), V is the amount of ammonia captured by the flux frame per unit time (mg s^{-1}) (determined by plotting the net horizontal flux measured at each sampling position with a suitable 3D graphical software package (Surfer 7) and calculating the volume under the curve), and t is the exposure period (s).

This mass is directly comparable with the mass of ammonia released from the cylinder, calculated from the release rate (l min^{-1}) multiplied by the density of ammonia and the exposure period. A collection efficiency for the flux frame on each

particular run was calculated by dividing the amount of ammonia estimated to have passed through the flux frame by the amount of ammonia released.

$$\text{Collection Efficiency (\%)} = \frac{M_F}{M_R} \times 100 \quad (16)$$

where M_R is the amount of ammonia (mg) released throughout the exposure period. This assumes that the measurement of M_R is accurate.

3.2.5 Turbulence intensity

Turbulence intensity is calculated as the standard deviation of the wind speed divided by the mean wind speed. When wind speed is measured using a sonic anemometer, there are three components to the wind speed: streamwise, lateral and vertical. The turbulence intensities can be calculated for each component as:

$$I_{\text{stream}} = \frac{\text{s.d. } u_{\text{stream}}}{\overline{u_{\text{stream}}}} \times 100 \quad (17)$$

$$I_{\text{lat}} = \frac{\text{s.d. } u_{\text{lat}}}{\overline{u_{\text{stream}}}} \times 100 \quad (18)$$

$$I_{\text{vert}} = \frac{\text{s.d. } u_{\text{vert}}}{\overline{u_{\text{stream}}}} \times 100 \quad (19)$$

where I is the turbulence intensity and s.d. is the standard deviation in the streamwise (stream), lateral (lat) and vertical (vert) directions, and $\overline{u_{\text{stream}}}$ is the mean streamwise velocity (assuming that the mean velocity in the lateral and vertical directions is zero). Multiplying by 100 expresses the intensity as a percentage. Equation 17 is the most common calculation.

3.2.6 Total error

Each measurement using a recurved PAF sampler had an uncertainty associated with it, as described in section 2.3.5, ranging from a few percent to hundreds of percent. Therefore, the estimate of ammonia captured using the flux frame, calculated using a number of samplers, also had an associated error. A pragmatic calculation of error was made by plotting the error for each sampler in the same manner as each measurement was plotted, using Surfer 7, and then integrating to get the overall error for the flux frame.

3.2.7 Plume simulation

Atmospheric dispersion modelling of the dispersion of the plume of emissions from the point source was performed using a commercial modelling package, ADMS 3.0 (CERC, Cambridge). ADMS 3.0 is a short-range (up to 100 km) atmospheric dispersion model which models a wide range of buoyant and passive releases to the atmosphere either individually or in combination and has facilities to model the effect of buildings, terrain and coastlines on dispersion (CERC, 1999). Modelled gas concentrations are estimated over a regular grid of points and/or at particular points specified by the user. The parameters entered into ADMS 3.0 for each model run are described in Appendix 3.

Using a Cartesian grid and taking the point source as the origin, trigonometry was used to calculate the co-ordinates of the position of each sampler in the sampling plane. Concentrations of ammonia were then modelled at each of these points. The wind speed at each sampling height was calculated using the log law relationship (equations 20-23) (Duncan *et al.*, 1960) and the average wind speed measured using the sonic anemometers throughout the exposure period. The product of modelled concentration and wind speed at the correct height was the modelled flux estimate for each sampler position.

$$U_H = \frac{u_*}{\kappa} \ln\left(\frac{H + H_o}{H_o}\right) \quad (20)$$

where U_H is the wind speed at height H , H_o is the aerodynamic roughness of the site, and $\frac{u_*}{\kappa}$ is a constant found experimentally (u_* is a measure of the turbulent velocity

fluctuations and κ is the Von Kármán constant). $\frac{H + H_o}{H_o}$ can be approximated to

$$\frac{H}{H_o} \text{ when } H \gg H_o.$$

When H_{REF} is the height at which reference measurements are made (at the meteorological station):

$$U_{REF} = \frac{u_*}{\kappa} \ln\left(\frac{H_{REF}}{H_o}\right) \quad (21)$$

Which can be rearranged to:

$$\frac{u_*}{\kappa} = \frac{U_{REF}}{\ln\left(\frac{H_{REF}}{H_o}\right)} \quad (22)$$

Substituting equation 22 into equation 20 gives:

$$U_H = \frac{U_{REF} \ln\left(\frac{H}{H_o}\right)}{\ln\left(\frac{H_{REF}}{H_o}\right)} \quad (23)$$

This enables the wind speed at height H to be calculated whilst only knowing the wind speed at one height and the aerodynamic roughness length of the site. For the wind engineering site at Silsoe Research Institute, where full scale measurements

using the flux frame were to be made, the aerodynamic roughness length was determined to be 0.01 m (Hoxey and Richards, 1992; Hoxey *et al.*, 1998). An estimate of the aerodynamic roughness of the Astroturf in the AFL was found by plotting the change in wind speed with height on a logarithmic scale and finding the height where the intercept crosses the height axis. This is necessary to check that using an aerodynamic roughness height of 0.01 m is suitable during modelling, and for the correct determination of the wind speed in the AFL.

The total modelled amount of ammonia captured was then calculated in the same way as described earlier, after plotting using Surfer software. The modelled efficiency was then calculated using equation 16, replacing M_F with M_M :

$$\text{Modelled Collection Efficiency (\%)} = \frac{M_M}{M_R} \times 100 \quad (24)$$

where M_M and M_R are the amounts of ammonia (μg) predicted to have been collected by the frame and released throughout the exposure period respectively.

The measured and modelled collection efficiencies calculated by equations 16 and 24 respectively were then compared. The actual difference between the measured and modelled flux measurements at each sampling position was determined using:

$$\Delta F = F_A - F_M \quad (25)$$

where ΔF is the actual difference between the two fluxes ($\mu\text{g NH}_3 \text{ m}^{-2} \text{ s}^{-1}$), and F_A and F_M are the measured and modelled fluxes, respectively, at the sampling position. For each sampling position, ΔF could then be plotted using Surfer software and any trend identified visually.

The actual difference between the flux measurements made during two replicate runs was determined in the same manner as that for measured and modelled fluxes, using equation 25, replacing F_A and F_M with F_{run1} and F_{run2} :

$$\Delta F = F_{run1} - F_{run2} \tag{26}$$

where F_{run1} and F_{run2} were the fluxes measured at the same sampling position in two replicate runs. Once again, ΔF could be plotted and in this way, the repeatability of measurements in the AFL could be determined.

3.3 RESULTS

3.3.1 Preliminary investigation

3.3.1.1 Smoke release

The maximum distance the smoke nozzle could be positioned from the frame before the whole width of the smoke plume was not captured by the flux frame was dependent upon the wind speed. Table 3.1 shows the maximum distance at each of the three wind speeds.

Table 3.1: Maximum distance of smoke nozzle from frame at the three wind speeds.

Wind speed at 2 m (m s^{-1})	Maximum distance (m)
4.2	9.45
3.4	7.4
2.4	7.28

These results show that the source must be positioned within 7.28 m of the frame so that the whole width of the plume from the point source is captured by the frame of samplers, assuming that ammonia and smoke disperse in the same way. A distance of 7 m was chosen for all three speeds.

3.3.1.2 Variations in wind speed along a lateral traverse of the AFL

Figure 3.5 shows the wind speed measurements made using the sonic anemometers along the lateral traverse of the AFL. Measurements were made for 30 minutes at each of the three positions for each of the three wind speeds. There is little variation in wind speed at the three different positions up to 3 m above the ground, but measurements at 4 m show a larger variability and a decrease in speed at the left and centre positions. However, these measurements were made before the curtains and mesh shown in Figure 3.2 were fitted due to a time constraint on the availability of the AFL. It was also later found that measurements made with the anemometer positioned at the top of the profile were incorrect.

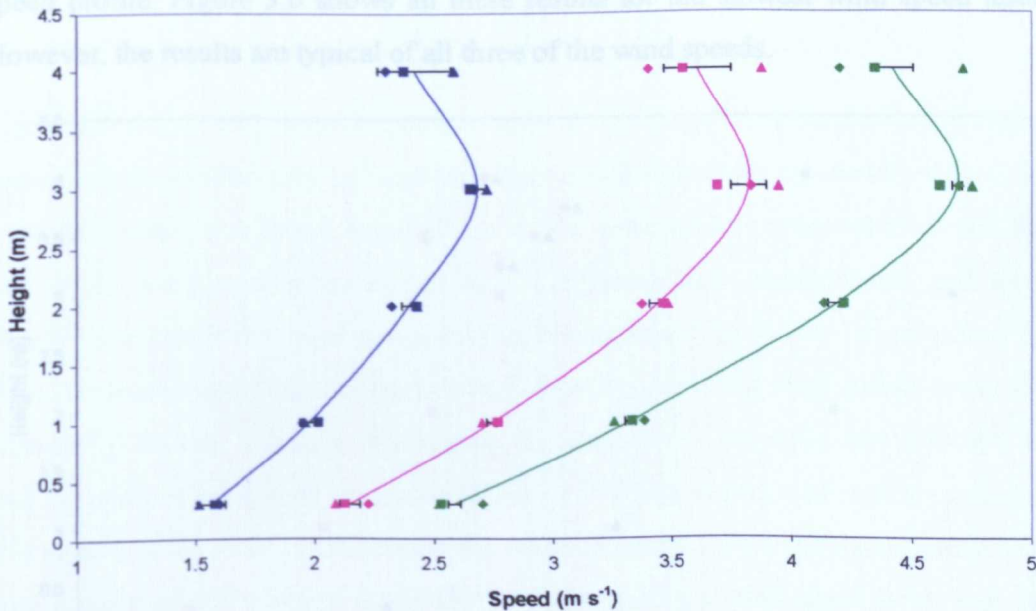


Figure 3.5: Variation in wind speed across a lateral traverse of the AFL. Blue lines and symbols represent the slowest nominal speed (2.4 m s^{-1}), pink the medium speed (3.4 m s^{-1}), and green the fastest (4.2 m s^{-1}). Diamonds represent measurements at the left side of the AFL, squares the centre and triangles the right. The lines represent the average profile and the error bars are one standard error of the mean.

It was assumed that the decrease in wind speed at a height of 4 m was due to an edge effect caused by the ceiling. As ammonia flux measurements were to be taken up to 3.8 m, it was necessary to determine exactly where the decrease in wind speed took

place, and measurements between 3 and 4 m at the centre position were undertaken. It was also thought that extractor fans fitted into the top of the centre wall of the AFL might help to reduce the ceiling effect by drawing air out at the top and increasing the wind speed near the ceiling. Measurements were made both with and without these extractor fans running to see if they had any effect on the resulting wind profile. Furthermore, in between the original set of measurements and these new measurements to determine where the ceiling started to affect the profile, the curtains and mesh (Figure 3.2) were added to the AFL and doors on the side of the AFL were opened to prevent the recirculation of the ammonia gas once ammonia release experiments began. Therefore, the wind profile was re-measured with the sonic anemometers at their original heights to see if the curtain had any effect on the wind speed profile. Figure 3.6 shows all these results for the slowest wind speed tested. However, the results are typical of all three of the wind speeds.

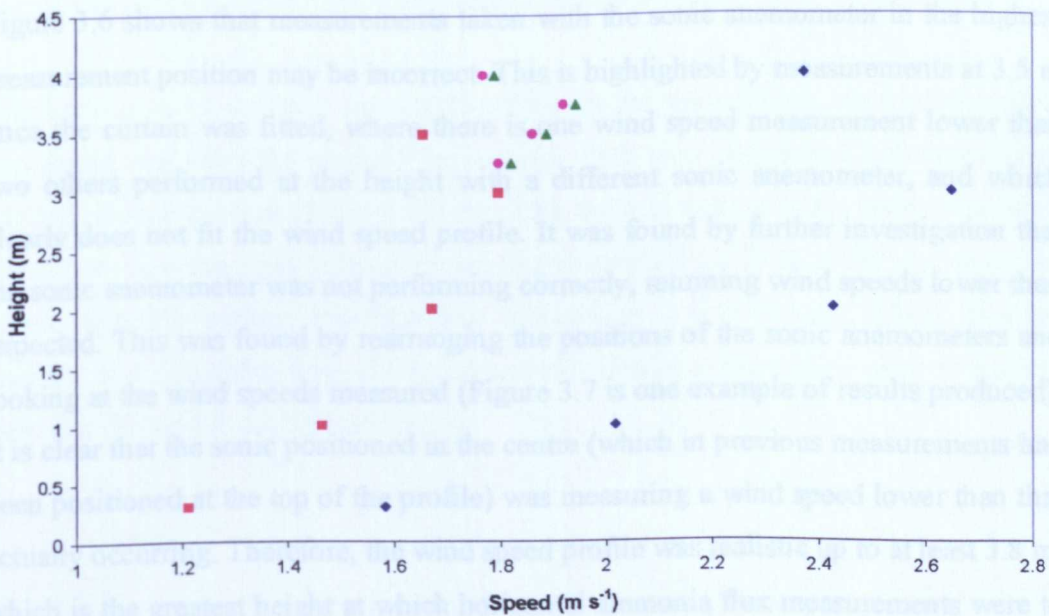


Figure 3.6: Wind speed profiles for the slowest wind speed (2.4 m s^{-1}) before the curtain was added (blue diamonds), with extractors on (green triangles) and off (pink circles), and repeat measurements at the original measurement heights with the curtain fitted and extractors off (red squares).

Figure 3.6 clearly shows that the addition of the curtains and mesh has a large effect on the wind speed profile, decreasing the wind speed at each measurement height.

The wind speed at a height of 2 m decreased as shown in Table 3.2. The use of extractors to draw out slower air at the top of the AFL in an attempt to increase the wind speed near to the ceiling had little or no effect. After examination of how the extractor fans worked, it was noted that even when the fans were switched off they did not stop turning, allowing air to move through the wall. Therefore it was decided that the extractor fans should remain off.

Table 3.2: Comparison of wind speed once curtain added to AFL.

Original speed at 2 m (m s^{-1})	Speed with curtain at 2 m (m s^{-1})
4.2	2.8
3.4	2.3
2.4	1.7

Figure 3.6 shows that measurements taken with the sonic anemometer in the highest measurement position may be incorrect. This is highlighted by measurements at 3.5 m once the curtain was fitted, where there is one wind speed measurement lower than two others performed at the height with a different sonic anemometer, and which clearly does not fit the wind speed profile. It was found by further investigation that the sonic anemometer was not performing correctly, returning wind speeds lower than expected. This was found by rearranging the positions of the sonic anemometers and looking at the wind speeds measured (Figure 3.7 is one example of results produced). It is clear that the sonic positioned in the centre (which in previous measurements had been positioned at the top of the profile) was measuring a wind speed lower than that actually occurring. Therefore, the wind speed profile was realistic up to at least 3.8 m, which is the greatest height at which horizontal ammonia flux measurements were to be taken.

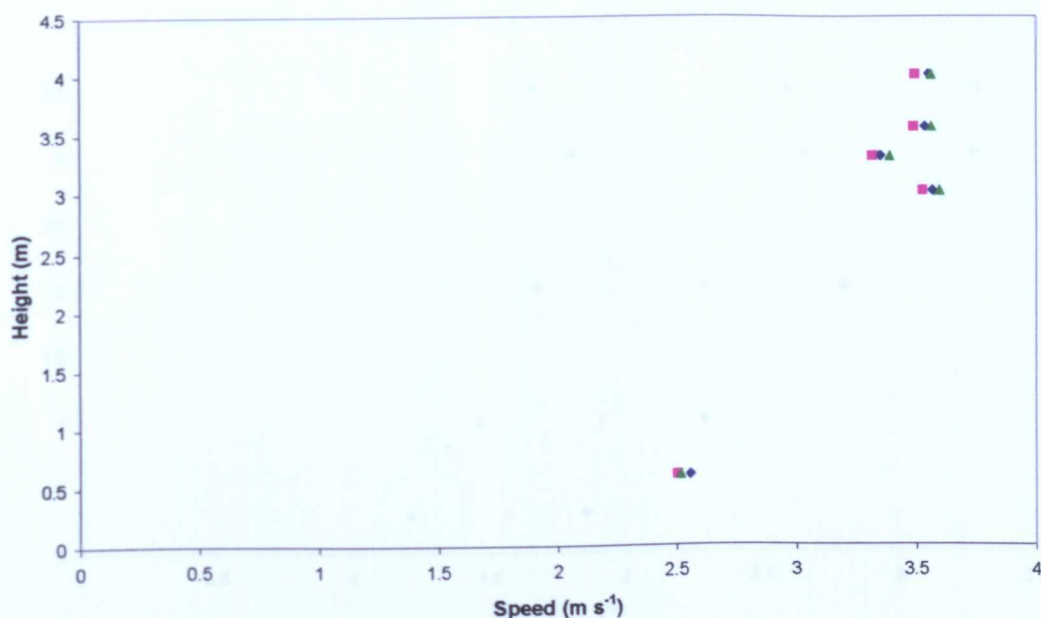


Figure 3.7: Wind speed profile when checking sonic anemometer. The three different symbols represent the results from three repeats at the same measurement heights.

Wind speed and turbulence intensity profiles for the three speeds were examined. It was found that, with the original fan settings, both wind speed and turbulence were too high below 2-2.5 m (Figures 3.8 and 3.9). By trial and error, the turbulence from the bottom four fans was reduced by varying amounts from 50 to 100%, and the wind speed from the bottom two fans was reduced by a few percent. These changes resulted in profiles that were similar to a profile produced from data taken at the SRI field site (Figures 3.10, 3.11 and 3.12).

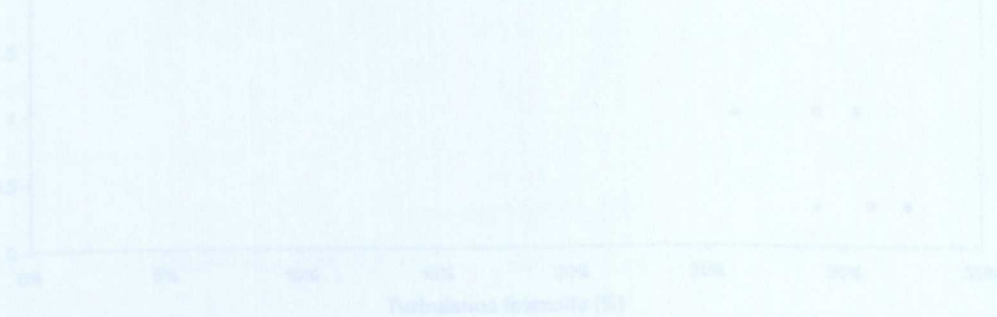


Figure 3.9: Turbulence intensity profiles with original fan settings. Legend as Figure 3.8.

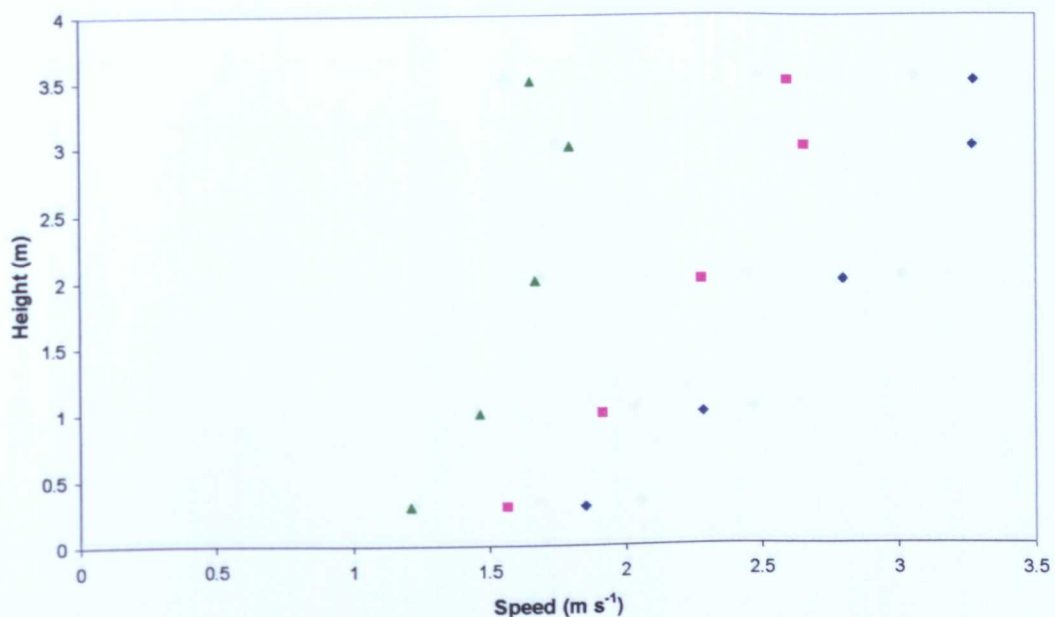


Figure 3.8: Wind speed profiles with original fan settings. Blue diamonds represent the fastest speed (2.8 m s^{-1} at a height of 2 m), pink squares the medium speed (2.3 m s^{-1} at 2 m) and green triangles the slowest (1.7 m s^{-1} at 2 m).

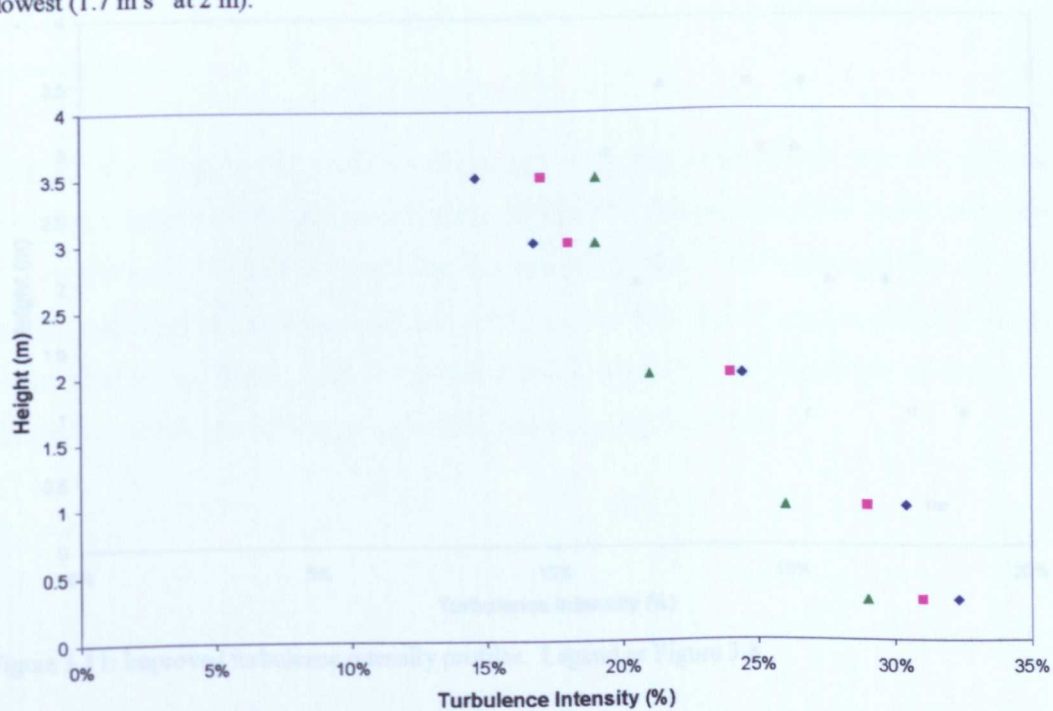


Figure 3.9: Turbulence intensity profiles with original fan settings. Legend as Figure 3.8. maximum of 19% at ground level, which is an improvement on the original settings that had turbulence intensities as high as 33%. The change in the wind speed profile is less

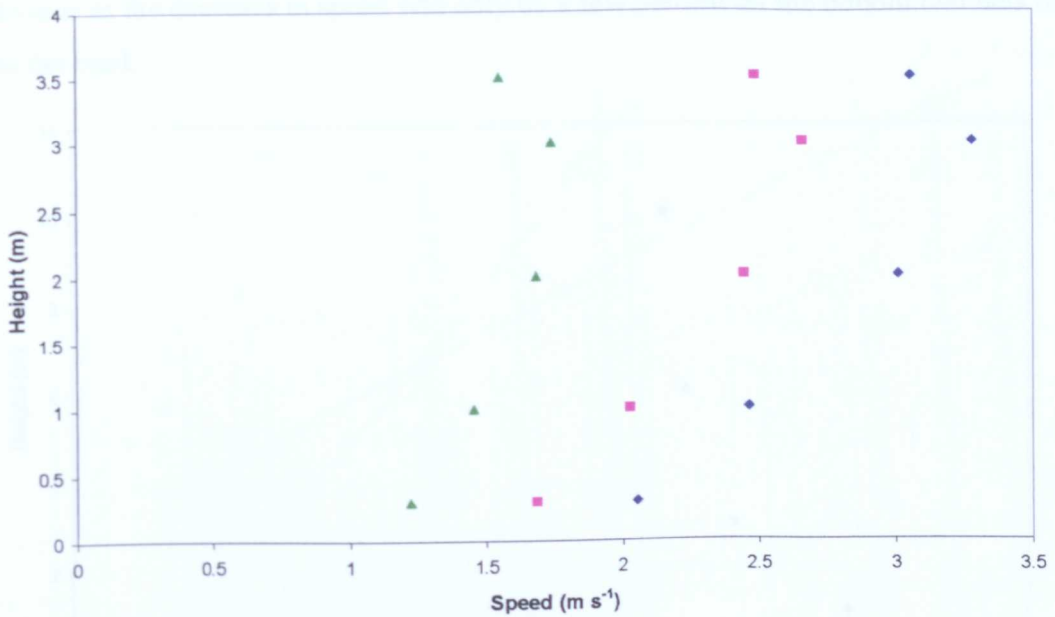


Figure 3.10: Improved wind speed profiles. Legend as Figure 3.8.

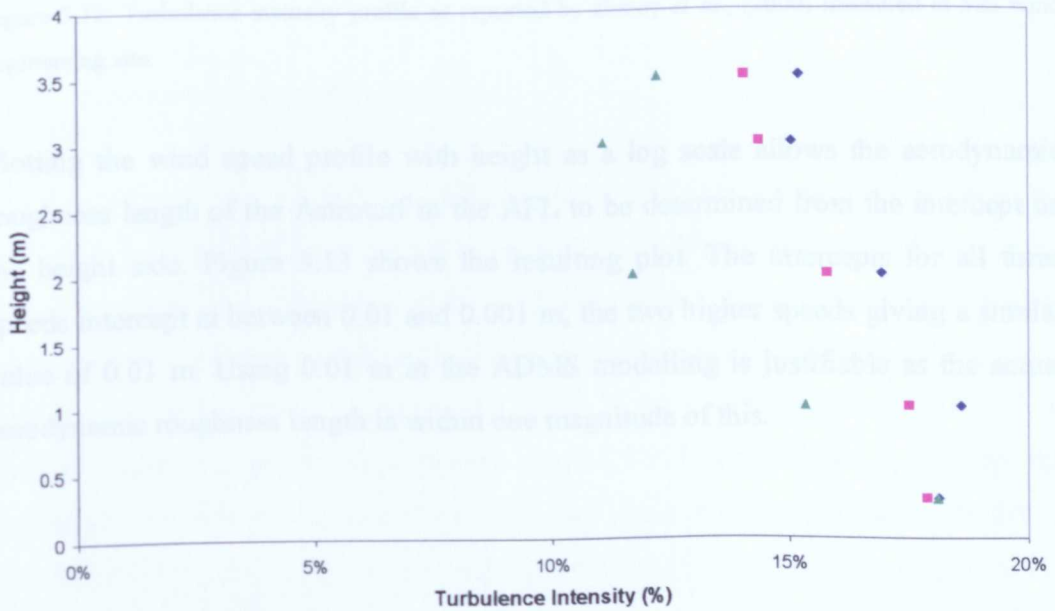


Figure 3.11: Improved turbulence intensity profiles. Legend as Figure 3.8.

The improved turbulence intensity profile has intensities not exceeding a maximum of 19% at ground level, which is an improvement on the original settings that had turbulence intensities as high as 33%. The change in the wind speed profile is less

obvious as the decrease in speed was only by a few percent on the bottom two fans of the fan bank.

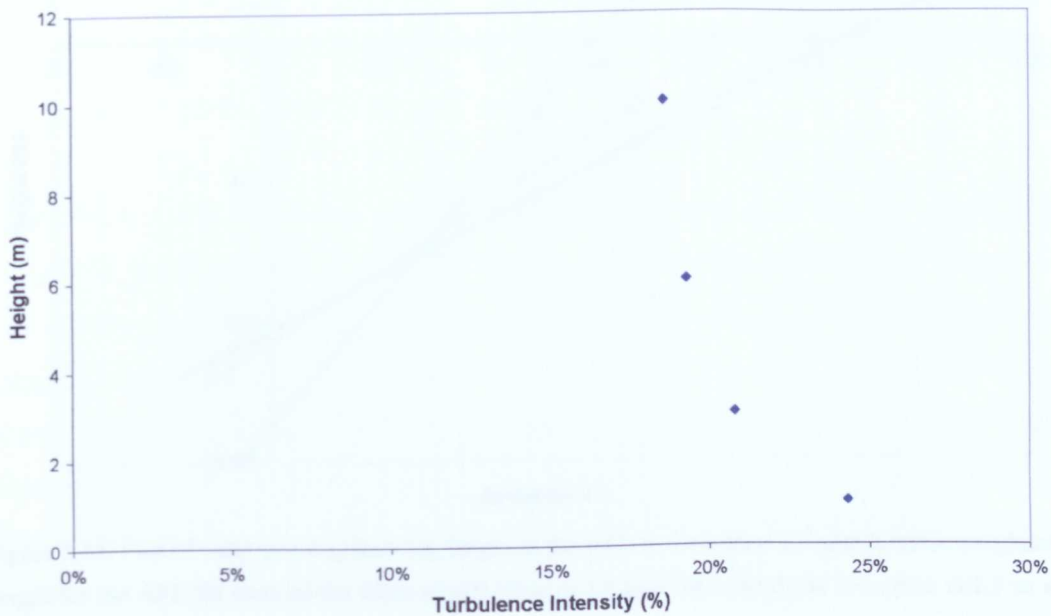


Figure 3.12: Turbulence intensity profile as reported by Hoxey *et al.*, (2000) measured at SRI wind engineering site.

Plotting the wind speed profile with height as a log scale allows the aerodynamic roughness length of the Astroturf in the AFL to be determined from the intercept on the height axis. Figure 3.13 shows the resulting plot. The intercepts for all three speeds intercept at between 0.01 and 0.001 m, the two higher speeds giving a similar value of 0.01 m. Using 0.01 m in the ADMS modelling is justifiable as the actual aerodynamic roughness length is within one magnitude of this.

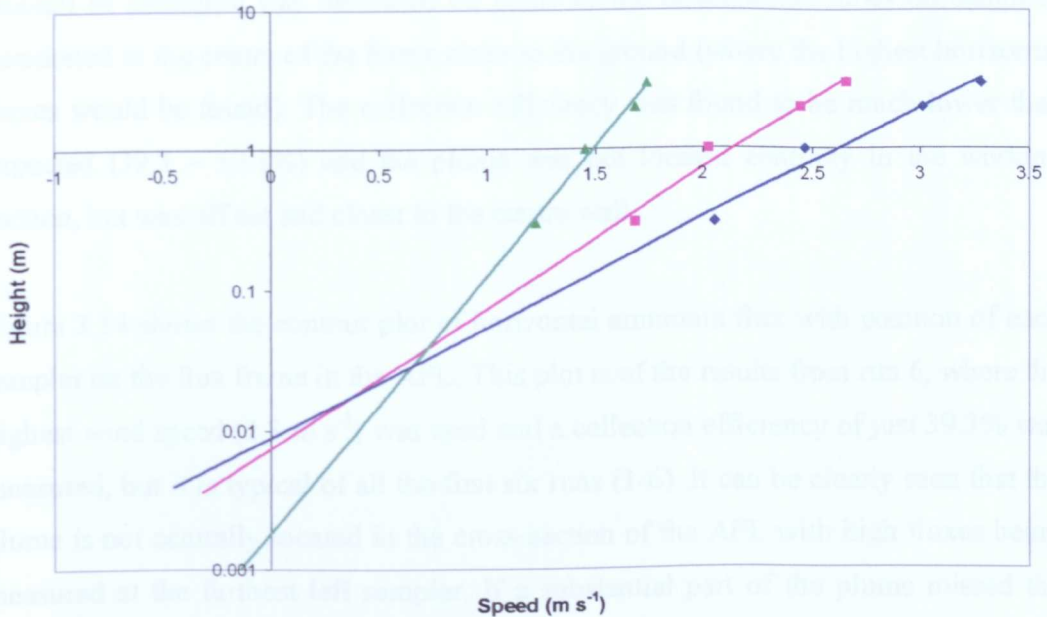


Figure 3.13: Plot of wind speed against log height in the AFL to determine the aerodynamic roughness length for the AFL for each of the three speeds (blue is 2.8 m s^{-1} at a height of 2 m , pink is 2.3 m s^{-1} and green 1.7 m s^{-1}).

3.3.2 Ammonia Release Experiments

A series of ammonia release experiments was undertaken using the improved fan settings to produce a realistic natural wind profile. An initial set of measurement runs took place with two experimental runs at each of the three wind speeds. Eighty samplers were mounted on the original regular framework described in section 3.2.1, with the source 7 m from the frame and 0.3 m above the ground, the frame 17.6 m from the fans and an ammonia release rate of 3.8 l min^{-1} . Table 3.3 shows the measured collection efficiencies for all the runs performed along with the modelled collection efficiencies where calculated. Descriptions of numbers of samplers used, mass of ammonia released, exposure periods and other parameters are also contained within the table.

After the first six runs (each of the three speeds repeated twice) it was noticed that at the fastest two speeds there was some saturation of the tubes taking place - a large

amount of ammonia was measured on some of the downstream tubes on samplers positioned in the centre of the frame close to the ground (where the highest horizontal fluxes would be found). The collection efficiency was found to be much lower than expected (39.3 – 59.1%) and the plume was not located centrally in the working section, but was off set and closer to the centre wall.

Figure 3.14 shows the contour plot of horizontal ammonia flux with position of each sampler on the flux frame in the AFL. This plot is of the results from run 6, where the highest wind speed (2.8 m s^{-1}) was used and a collection efficiency of just 39.3% was measured, but it is typical of all the first six runs (1-6). It can be clearly seen that the plume is not centrally located in the cross-section of the AFL with high fluxes being measured at the furthest left sampler. If a substantial part of the plume missed the edge of the sampling plane, this would account for the low collection efficiency. On this plot, it is also clear that the samplers at the centre of the plume have measured low fluxes. This is where the highest fluxes would be expected and is due to the fact that this is a net flux.

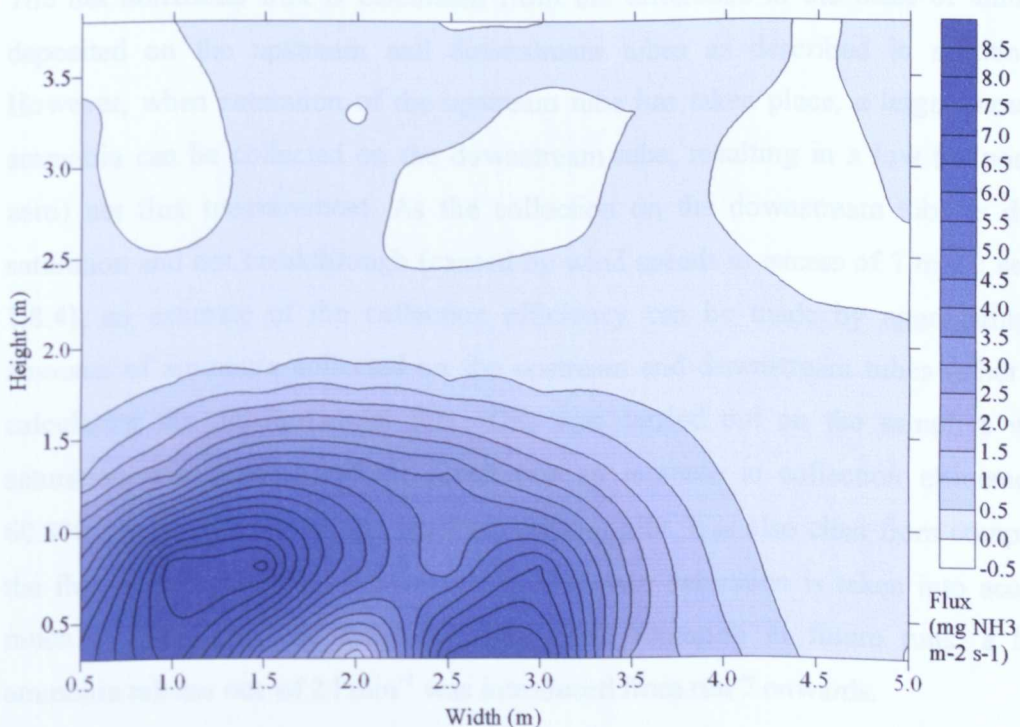


Figure 3.14: Contour plot of horizontal ammonia flux with position on flux frame using 80 recurved PAF samplers, Run 6.

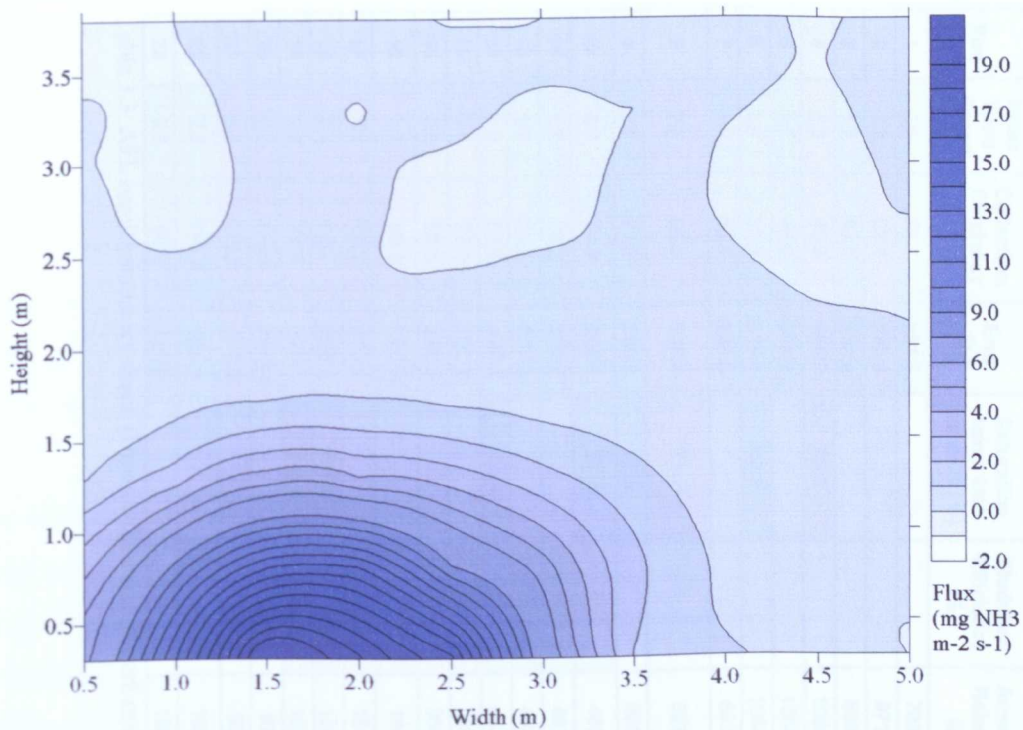


Figure 3.15: Contour plot of Run 6, with saturation taken into account.

The net horizontal flux is calculated from the difference in the mass of ammonia deposited on the upstream and downstream tubes as described in section 1.8. However, when saturation of the upstream tube has taken place, a large amount of ammonia can be collected on the downstream tube, resulting in a low (or possibly zero) net flux measurement. As the collection on the downstream tube is due to saturation and not breakthrough (caused by wind speeds in excess of 7 m s^{-1} ; section 1.8.4), an estimate of the collection efficiency can be made by aggregating the amounts of ammonia collected on the upstream and downstream tubes rather than calculating the net horizontal flux. This was carried out on the samplers where saturation was evident and the result was an increase in collection efficiency to 60.3%. Figure 3.15 shows the resulting contour plot. It is also clear from comparing the flux scales of Figures 3.14 and 3.15 that once saturation is taken into account, much higher fluxes are measured. To avoid saturation in future runs, a lower ammonia release rate of 2 l min^{-1} was introduced from run 7 onwards.

Run	Mean Wind Speed (m/s)	Collection Efficiency (%)	Error (%)	Saturation taken into account (%)	Modelled Efficiency (%)	Ammonia Released (g)	Exposure Period (s)	Number of Samplers	Source to Frame Distance (m)	Source Height (m)	Notes
1	2.8	59.1	±51.1			798.00	18000	80	7	0.3	
2	2.3	52.1	±33.3			971.46	21600	80	7	0.3	
3	1.7	42.0	±48.6			839.62	19800	80	7	0.3	
4	2.3	46.8	±65.3	58.8		1054.73	21600	80	7	0.3	
5	1.7	46.2	±34.7			1054.73	21600	80	7	0.3	
6	2.8	39.3	±19.5	60.3		1054.73	21600	80	7	0.3	
7	1.7	55.5	±38.5			693.90	21600	80	7	0.3	
8	2.3	66.9	±19.6	71.7		693.90	21600	90	5	0.3	Frame moved nearer to source to centralise plume, extra samplers to capture highest fluxes
9	2.8	73.2	±90.2	89.5		693.90	21600	90	5	0.3	
10	2.8	74.3	±55.9	87.5	85.2	462.60	18000	90	5	0.3	Exposure period decreased to 5 hrs due to saturation
11	1.7	73.2	±32.4		77.1	462.60	18000	90	5	0.3	Exposure period - 5 hrs
12	1.7	76.8	±50.0		76.8	462.60	18000	90	5	0.3	Exposure period - 5 hrs
13	2.8	81.5	±47.4	84.1	85.8	462.60	18000	90	5	0.3	Exposure period - 5 hrs
14	2.3	77.5	±37.9		82.6	369.60	14400	90	5	0.3	Exposure period - 4 hrs
15	2.3	86.8	±46.9		83.2	369.60	14400	90	5	0.3	Exposure period - 4 hrs
16	2.3	88.5	±112.5		99.1	184.80	7200	90	3	1.8	Source centrally located, exposure period - 2 hrs
17	2.3	88.2	±93.8		98.0	184.80	7200	90	3	1.8	Repeat of run 16
18	2.3	83.7	±53.3	105.9	101.2	184.80	7200	87	3	1.8	Sampler density at centre of plume increased
19	2.3	84.4	±75.0	134.6	101.2	184.80	7200	87	3	1.8	Repeat of run 18
20	2.3	135.5	±153.8			92.52	3600	87	3	1.8	Repeat of runs 18 and 19, performed for 1 hr
21	2.3	133.2	±75.0			92.52	3600	87	3	1.8	Repeat of run 20, due to fog
22	2.8	119.4	±50.0			185.00	7200	88	5	0.3	Repeat of runs 10 + 13, higher sampler density at ground level, 2 hrs to avoid saturation
23	2.8	90.8	±88.2			185.00	7200	88	5	0.3	Repeat of run 22

Table 3.3: AFL results summary sheet. (Green cells are runs performed at 1.7 m/s; orange 2.3 m/s; blue 2.8 m/s and pink with the source centrally located).

The following modifications to the experimental protocol were made in subsequent runs. The frame was moved closer to the source to enable the plume to be captured before reaching the central wall of the AFL, and an extra row of samplers at 0.05 m above the ground was added to capture the highest horizontal fluxes. These conditions were used for three runs before it was noted that saturation was still occurring at the two highest wind speeds where the plume is less dispersed. Therefore shorter exposure periods (5 hours or less) were used. Once again, two repeats of each speed were performed. Modelling of the results began with run 10, which was the first successful run.

The capture efficiency of the frame when the plume of emissions was completely captured by the frame was investigated by positioning the source centrally at a height of 1.8 m above the ground, 3 m from the frame. Just one wind speed, 2.3 m s^{-1} , was investigated. Figures 3.16 and 3.17 show the resultant contour plots for Run 16 where the horizontal fluxes were measured and modelled at 90 sampling locations over the frame area. The measured collection efficiency was 88.5% whilst the modelled collection efficiency was 99.1%. One explanation for the low measured collection efficiency was thought to be to the highly concentrated plume and the possibility that the highest fluxes at the very centre of the plume were not being sampled adequately. Thus repeats were performed with a higher sampler density at the centre of the plume.

Figures 3.18 and 3.19 show contour plots for the horizontal fluxes measured and modelled at 87 sampling positions within the frame area, in Run 19. The collection efficiencies were 84.4% and 101.2% respectively. It is clear from Figure 3.18, however, that saturation of the samplers at the centre of the plume has occurred, with low measured horizontal fluxes where the highest fluxes are expected. Figure 3.20 shows the contour plot when saturation is taken into account by adding the deposition to the upstream and downstream tubes as described earlier. Here the collection efficiency is 134.6%, which compares well with the collection efficiencies measured during Runs 20 and 21 performed under the same conditions and with no saturation of the tubes due to shorter exposure periods. Note that Figure 3.20 has a much larger scale than Figures 3.18 and 3.19 due to the very high fluxes found at the centre of the plume.

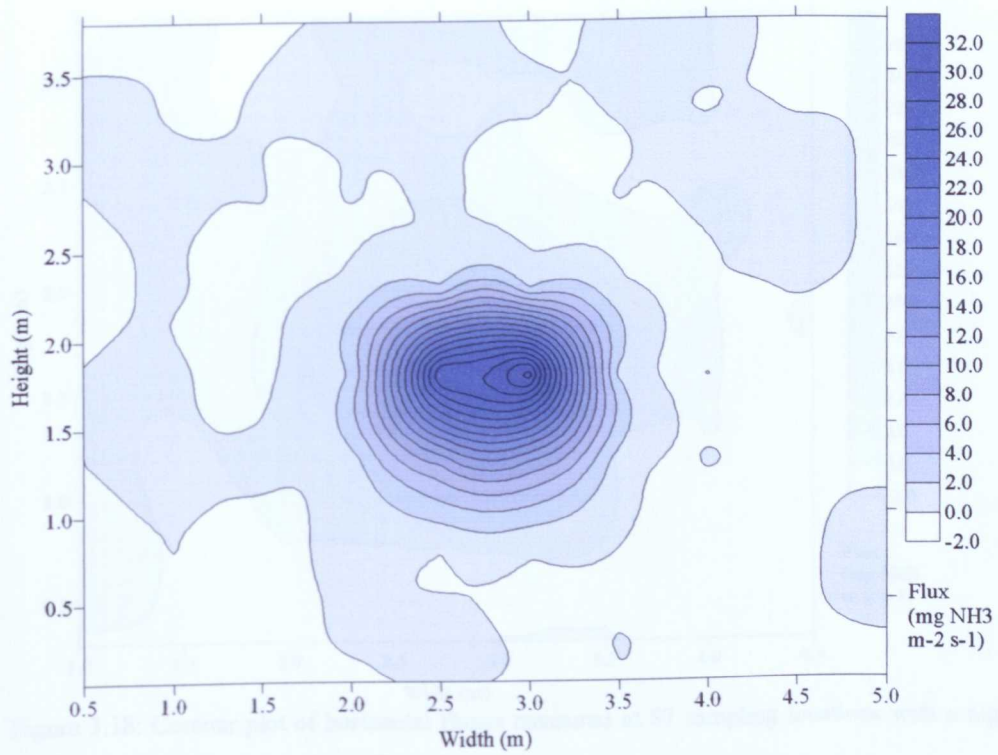


Figure 3.16: Contour plot of horizontal fluxes measured at 90 sampling locations, Run 16.

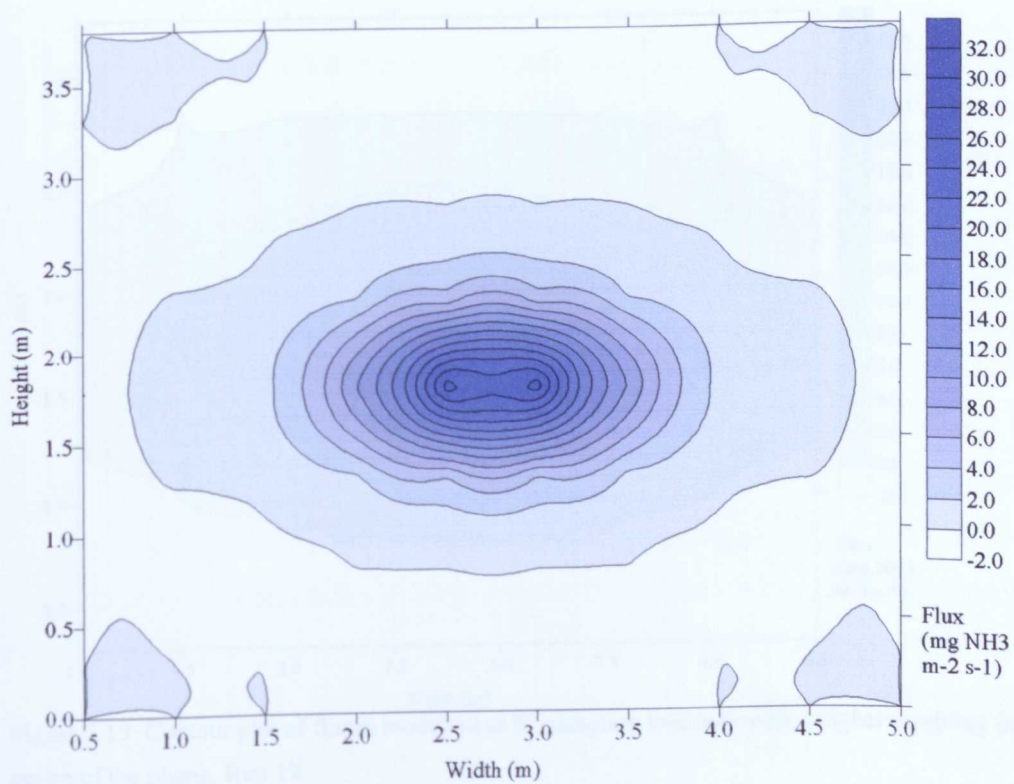


Figure 3.17: Contour plot of fluxes modelled at 90 sampling locations, Run 16.

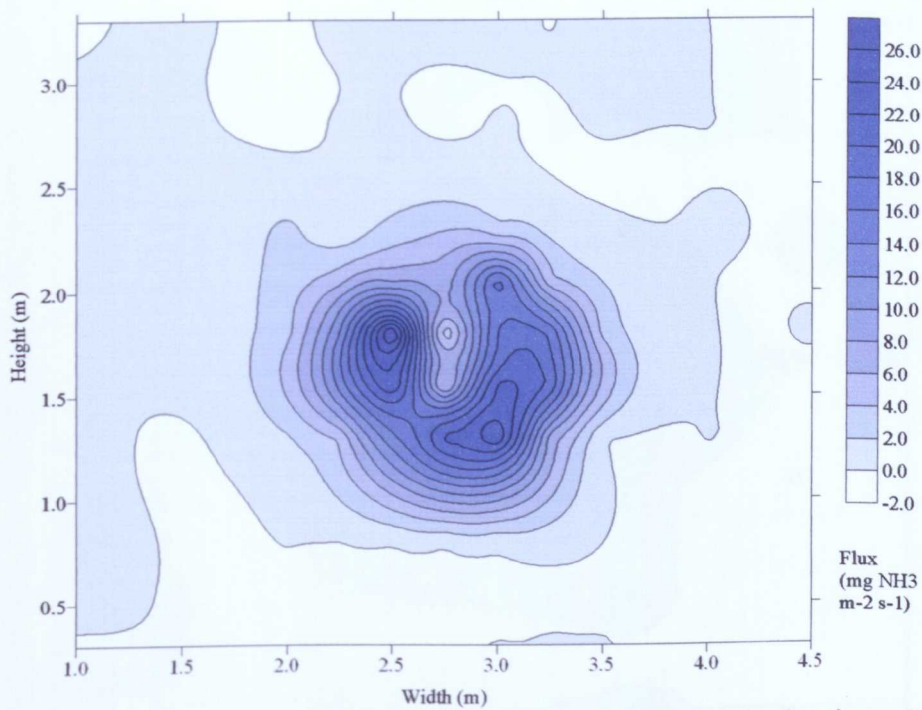


Figure 3.18: Contour plot of horizontal fluxes measured at 87 sampling locations with a higher sampling density at the centre of the plume, Run 19.

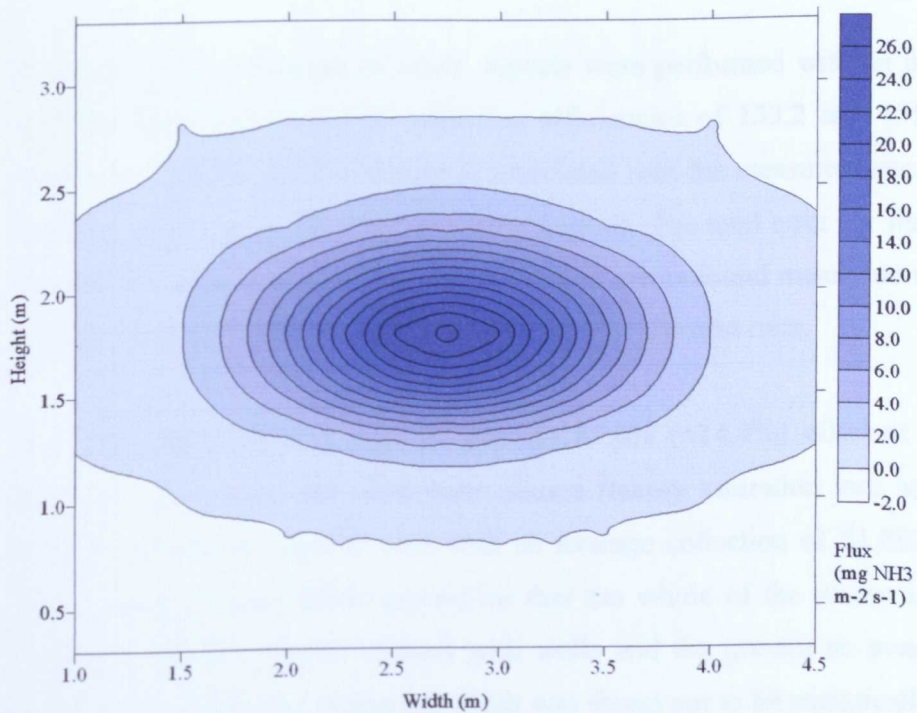


Figure 3.19: Contour plot of fluxes modelled at 87 sampling locations with a higher sampling density at the centre of the plume, Run 19.

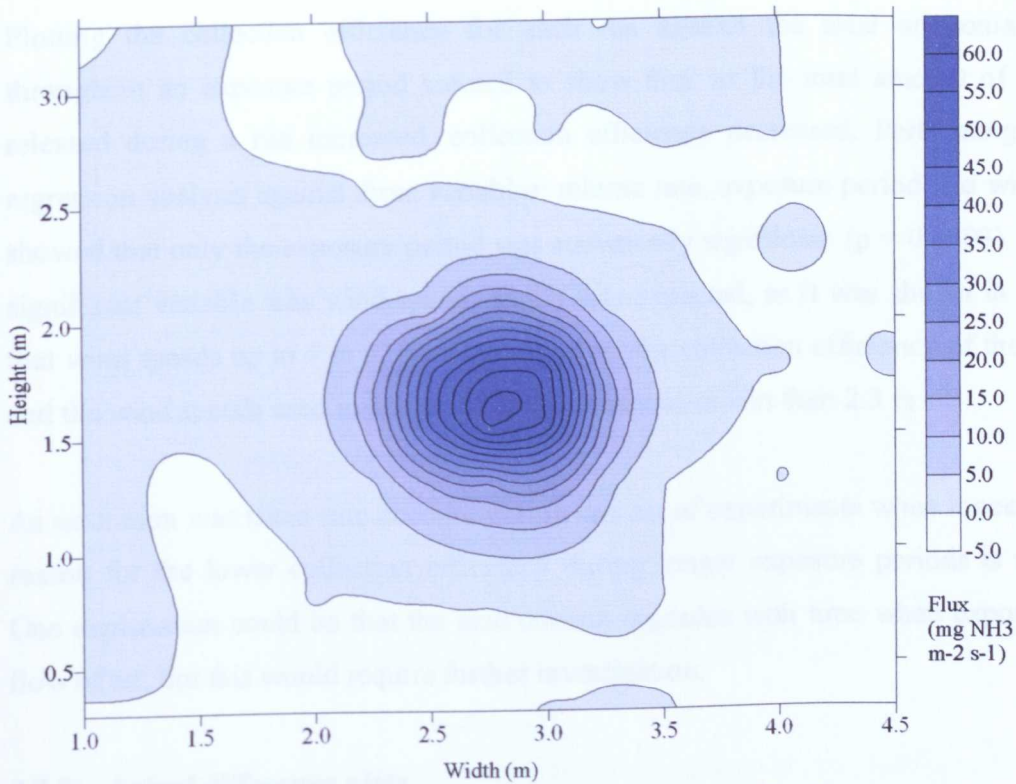


Figure 3.20: Contour plot when saturation has been taken into account, Run 19.

Because of the saturation of tubes, repeats were performed with an exposure period of just one hour and measured collection efficiencies of 133.2 and 135.5% were found. However, a higher degree of error is associated with the measurements (Table 3.3) which is likely to be due to the short exposure periods. The total error for flux frame estimates ranged from ± 19.5 to 153.8%, with the largest errors found mainly on the runs where the plume was centrally located, which were also the shortest runs.

The flux frame method was on average 87.0% ($\pm 14.4\%$) efficient in its capture of ammonia from a ground level point source (taking saturation into account). Modelled capture efficiencies agreed well with an average collection of 81.8% ($\pm 3.93\%$). For a point source located above ground so that the whole of the plume is captured by the frame of samplers before contact with walls and the ground an average efficiency of 114.3% ($\pm 23.0\%$) was measured, which was found not to be statistically significant from 100% ($p > 0.05$). Modelled collection efficiencies ranged between 98.0 and 101.2%, with an average of 99.9% ($\pm 1.6\%$).

Plotting the collection efficiency for each run against the total ammonia released throughout an exposure period seemed to show that, as the total amount of ammonia released during a run increased, collection efficiency decreased. Performing multiple regression analysis against three variables: release rate, exposure period and wind speed, showed that only the exposure period was statistically significant ($p = 0.0003$). The least significant variable was wind speed, which was expected, as it was shown in chapter 2 that wind speeds up to 7 m s^{-1} have no effect on the collection efficiency of the sampler, and the wind speeds used in this set of experiments were less than 2.3 m s^{-1} .

As saturation was taken into account during this set of experiments when it occurred, the reason for the lower collection efficiency during longer exposure periods is unknown. One explanation could be that the acid coating degrades with time when exposed to the flow of air, but this would require further investigation.

3.3.3 Actual difference plots

The actual difference between the measured and modelled fluxes for each sampling position in a particular run were determined using equation 25. When saturation of samplers had occurred, the flux where saturation had been taken into account was used. The actual difference for each sampling position was then plotted using Surfer software.

Figure 3.21 shows the actual difference plot for Run 10. However, the trend in the plots for Runs 11 to 15 is almost identical, with just the magnitude of the difference varying. The model underestimates the flux on the left of the plot whilst overestimating on the right side of the plot. Figure 3.22 shows the actual difference plot for Run 17, but once again, Runs 16, 18 and 19 show a similar trend, only differing in the magnitude of the difference. The model underestimates the peak of the flux in the centre of the plume and due to its spread being greater laterally, an overestimation is shown to each side of the centre of the plume.

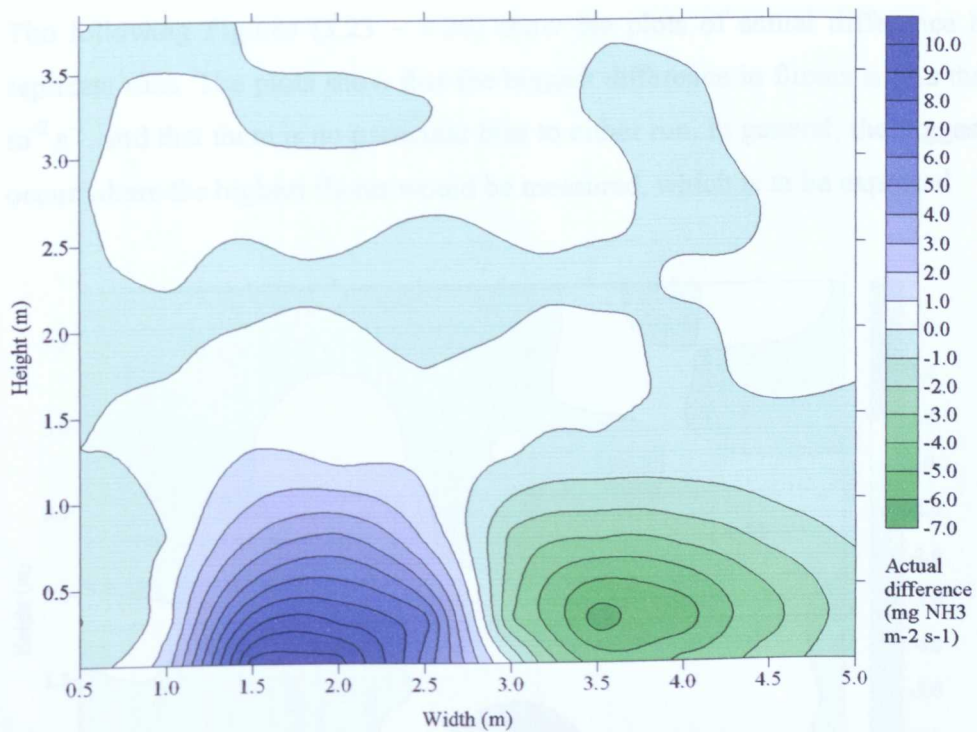


Figure 3.21: Actual differences between measured and modelled fluxes for each sampling position, plotted on flux frame area. Run 10 – ground level source, wind speed at 2 m = 2.8 m s^{-1} .

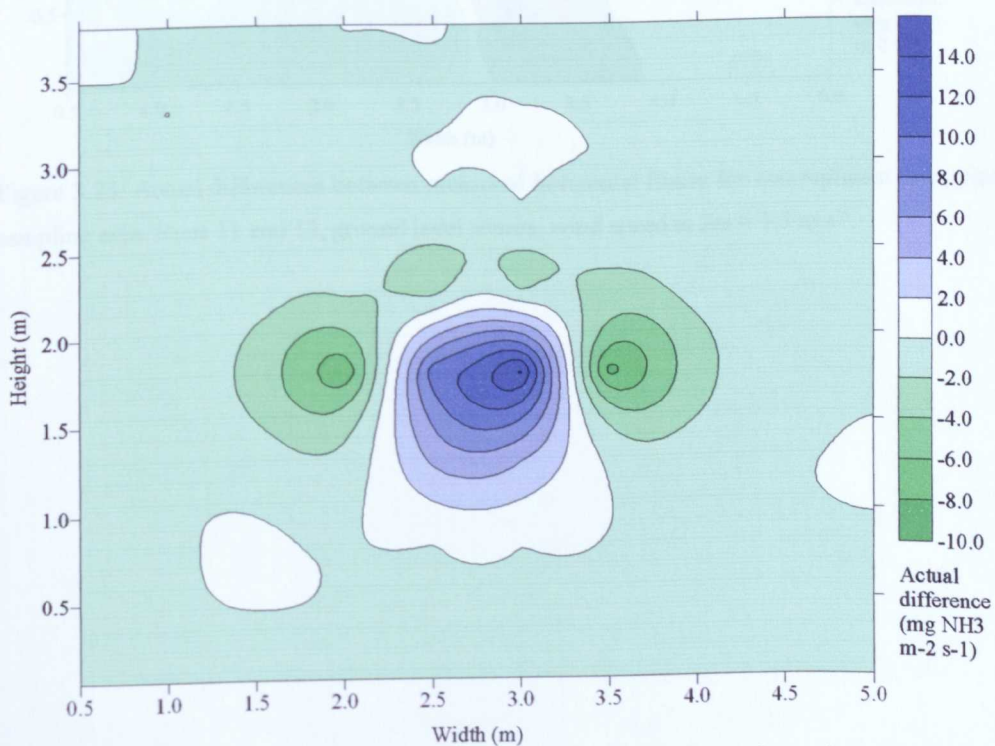


Figure 3.22: Actual differences between measured and modelled fluxes for each sampling position, plotted on flux frame area. Run 17 – source positioned centrally, wind speed at 2 m = 2.3 m s^{-1} .

The following Figures (3.23 – 3.26) show the plots of actual difference between two replicate runs. The plots show that the biggest difference in fluxes is less than $7 \mu\text{g NH}_3 \text{ m}^{-2} \text{ s}^{-1}$, and that there is no particular bias to either run. In general, the biggest differences occur where the highest fluxes would be measured, which is to be expected

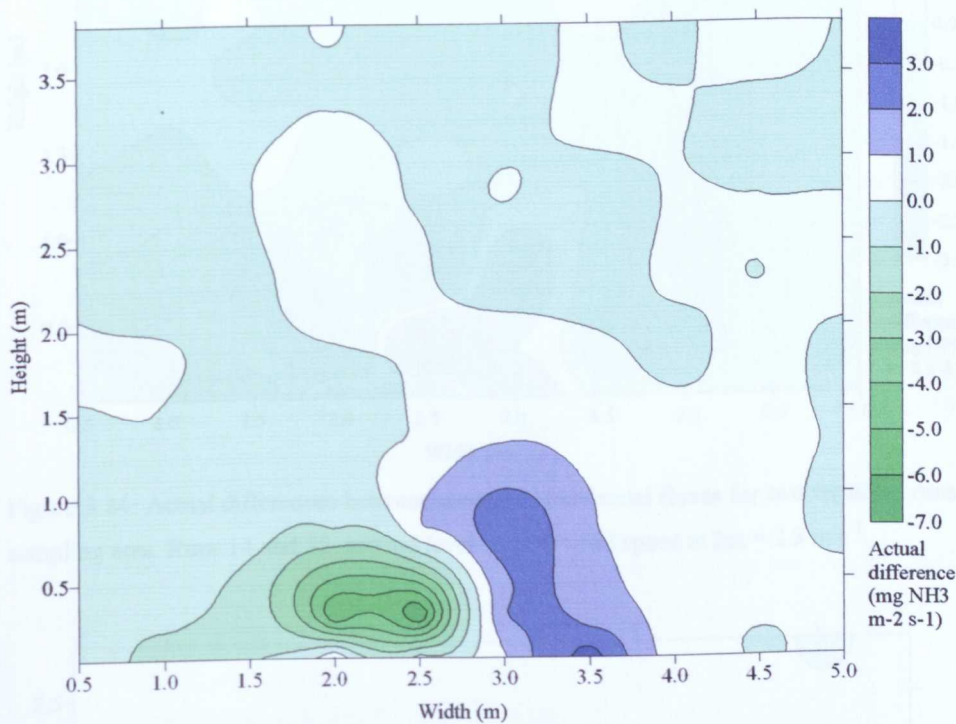


Figure 3.23: Actual differences between measured horizontal fluxes for two replicate runs, plotted over the sampling area. Runs 11 and 12, ground level source, wind speed at 2m = 1.7 m s^{-1} .

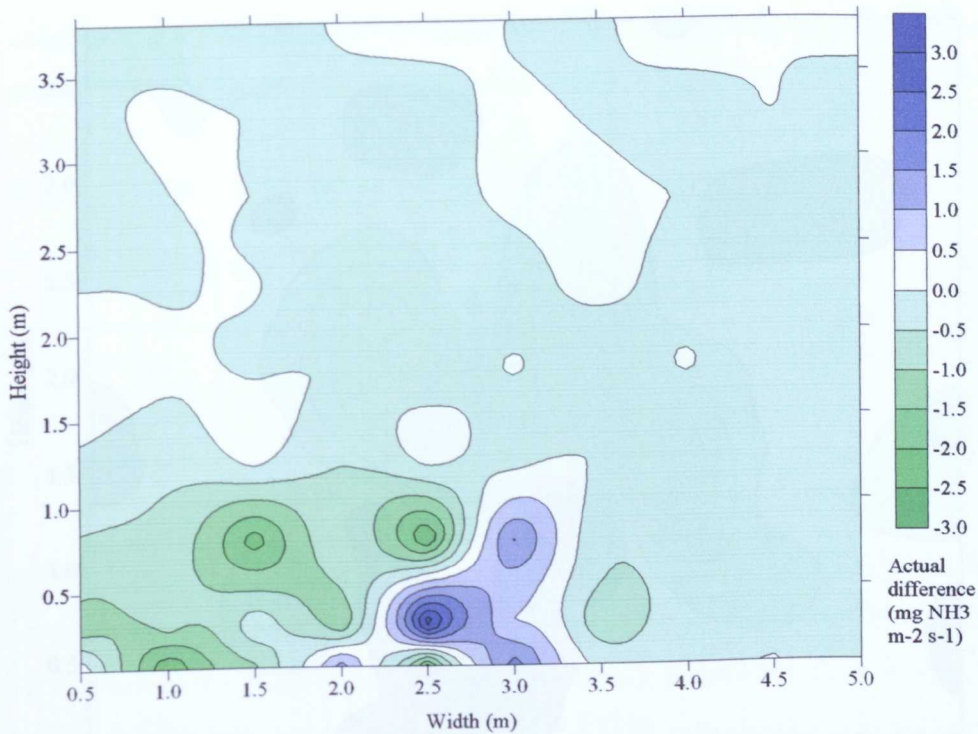


Figure 3.24: Actual differences between measured horizontal fluxes for two replicate runs, plotted over the sampling area. Runs 14 and 15, ground level source, wind speed at 2m = 2.3 m s^{-1} .

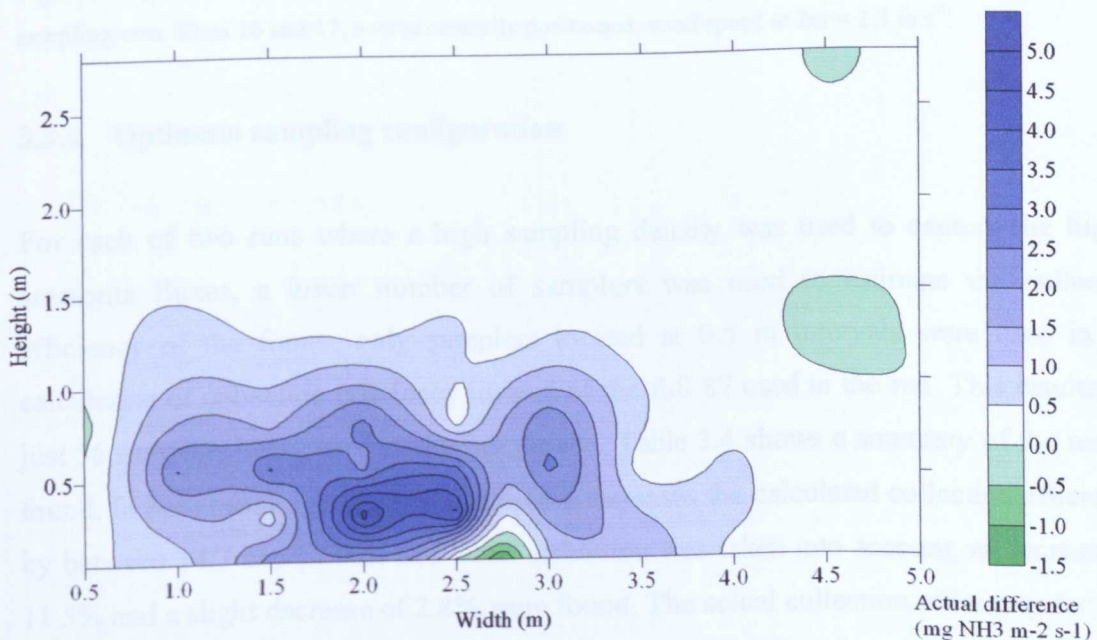


Figure 3.25: Actual differences between measured horizontal fluxes for two replicate runs, plotted over the sampling area. Runs 22 and 23, ground level source, wind speed at 2m = 2.8 m s^{-1} .

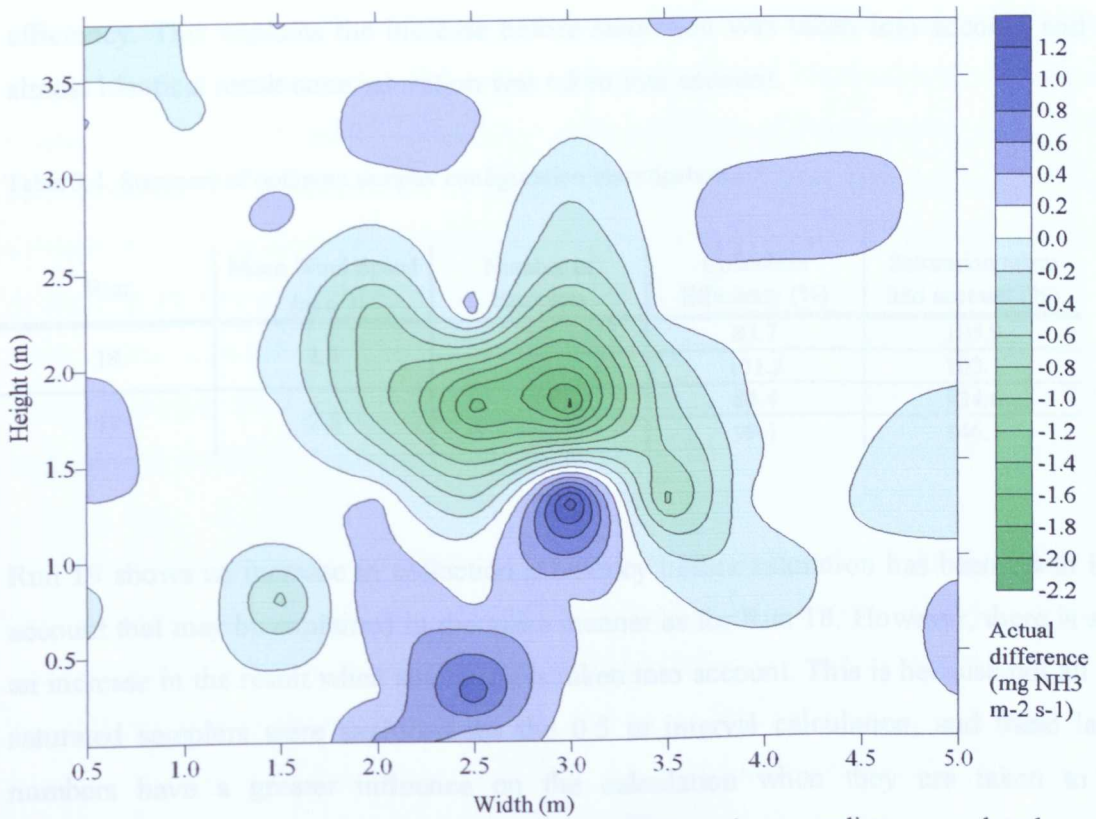


Figure 3.26: Actual differences between measured horizontal fluxes for two replicate runs, plotted over the sampling area. Runs 16 and 17, source centrally positioned, wind speed at 2m = 2.3 m s^{-1} .

3.3.4 Optimum sampling configuration

For each of two runs where a high sampling density was used to capture the higher ammonia fluxes, a lower number of samplers was used to estimate the collection efficiency of the frame: only samplers located at 0.5 m intervals were used in the calculation of collection efficiency instead of the full 87 used in the run. This resulted in just 56 samplers being used in the calculation. Table 3.4 shows a summary of the results found. In both cases, using just 56 samplers increases the calculated collection efficiency by between 14.7 and 17.5%, and when saturation was taken into account, an increase of 11.5% and a slight decrease of 2.8% were found. The actual collection efficiency for Run 18, with no correction for saturation, improves by 17.5%. When the data for this run were examined further, it was found that most of the samplers where saturation occurred were excluded when the 56 samplers at 0.5 m intervals were used to calculate the collection

efficiency. This explains the increase before saturation was taken into account and the almost identical result once saturation was taken into account.

Table 3.4: Summary of optimum sampler configuration investigation.

Run	Mean Wind Speed (m s ⁻¹)	Number of Samplers	Collection Efficiency (%)	Saturation taken into account (%)
18	2.3	87	83.7	105.9
		56	101.2	103.1
19	2.3	87	84.4	134.6
		56	99.1	146.1

Run 19 shows an increase in collection efficiency before saturation has been taken into account that may be explained in the same manner as for Run 18. However, there is also an increase in the result when saturation is taken into account. This is because not all the saturated samplers were excluded for the 0.5 m interval calculation, and these large numbers have a greater influence on the calculation when they are taken to be representative of a larger area than when a higher sampling density was used.

3.4 DISCUSSION

3.4.1 The use of the AFL

The AFL is a unique facility which enables a realistic wind profile to be established. The ability to control wind speed, turbulence levels and (obviously) wind direction whilst preventing rain from disrupting experiments makes the AFL almost ideal for validation experiments of this nature, particularly where an absence of rain and a constant wind direction are necessary to get accurate results. The realistic wind and turbulence intensity profiles (Figures 3.10 and 3.11) compare well with data measured at full scale on the wind engineering site at SRI, (Figure 3.12; Hoxey *et al.*, 2002) where subsequent field experiments were due to take place (Chapter 4).

One limitation of the AFL is that it is only possible to test a point source due to the constraining walls and ceiling that would affect the lateral dispersion of an extended source and give rise to mirror effects. A further limitation of the enclosing surfaces was their potential for collection of ammonia. Hence, the frame had to be positioned sufficiently close to the source for the plume not to have dispersed to the walls or ceiling. A distance of 7 m upwind of the frame was found to be the maximum distance for the point source. The effect of the enclosing surfaces is seen by comparing measured and modelled results. The lateral spread (the standard deviation of the wind direction) is much higher in the modelled results, which do not take the effect of the walls into account.

One other minor limitation encountered was due to the open doors. Strong winds could enter the AFL through the doors, which were open to allow the ammonia to be exhausted and not recirculated. This could affect the wind profile and be one of the factors causing the difference in plots between two runs shown in Figures 3.23-3.26. Also, on one occasion in very cold conditions (Run 20), the metal components of the frame and samplers froze with water vapour from the air. The glass tubes also gathered a layer of ice, which may affect the collection of ammonia by the sampler as water is a sink for ammonia.

3.4.2 Loss of ammonia

The average collection efficiency for ground level releases, once the plume was positioned more centrally (Runs 10-15, and 22-23), was 87.0% (when saturation was accounted for). This is despite minimising the potential of ammonia to be lost to surfaces before reaching the frame of samplers by ensuring that the whole width (and height) of the plume of emission from the source was captured by the width of the frame. This was done using the smoke release, and also by analysis of the results found during the first few experimental runs in the AFL. This meant that the plume did not reach the walls (or ceiling) and thus there was no possibility of loss there.

The only place where the source contacted a surface before reaching the frame of samplers was the ground, which was covered with AstroTurf. Taking a deposition velocity value of 1.6 cm s^{-1} , which is a high value reported in the literature (Yamulki *et al.*, 1996), a deposition rate of $1.06 \times 10^{-6} \text{ kg s}^{-1}$ was found. This equates to a 4.4% loss of the amount of ammonia released (see Appendix 4 for full calculation), and contributed to the approximately 13% loss found during ground level release runs.

The remaining loss could be due to a reaction between the AstroTurf and ammonia gas. This is unlikely, since it is simply a dry plastic surface, but has not been tested. One possible way of doing this would be to look at the difference in collection efficiencies between ground level and centrally located sources. Whilst this may give some indication, losses could be due to the plume being slightly wider than the frame near ground level and the highest horizontal fluxes being found at ground level – despite the addition of samplers at 0.05 m above ground level.

3.4.3 Optimum sampling configuration

A high sampling density was used to capture the highest horizontal fluxes at the centre of the plume. However, this was shown to be unnecessary as using just 56 of the samplers to calculate the collection efficiency of the flux frame gave a similar (2.8%), or greater (11.5%), result. When saturation was not taken into account for both Runs, the use of the lower sampling density showed less saturation and a better estimate was obtained than when originally calculated using all 87 samplers (increases of 14.7 and 17.5%).

At the higher sampling densities, the flux measured by a sampler was representative of a smaller area than when the lower sampling density was used. Therefore, the horizontal flux measured had less of an effect on the overall flux through the frame. The larger the interval between samplers, the greater the effect one sampling position has on the overall result.

3.4.4 Agreement between ammonia release experiments

The highest differences between fluxes measured over two different runs were found at the positions where the highest fluxes were measured, which would be expected. This variability could be due to slight variations in wind speed, turbulence and lateral spread due to the open doors and external wind conditions affecting flow through the AFL, even though the exact same wind regime was used in both runs. Due to time constraints, it was not always possible to use the AFL when external wind conditions were calm. However, the two most important factors affecting validation experiments in the field are the wind direction (due to the cumbersome nature of the flux frame and its fixed position (Phillips *et al.*, 1997; 2000)) and rain (which would remove the acidic coating from the samplers (Mahlcke, 1998)). Neither of these factors affects the use of the AFL for validation experiments, except in very strong winds.

3.4.5 Agreement between measured and modelled plots

Figures 3.21 and 3.22 show the agreement between measured and modelled fluxes for each sampling position. The position of the observed over- and under-estimation of the measured plot by the model when the source was positioned at ground level is due to the symmetrical nature of the modelled plot compared to the slightly off centre measured plot. The position of the observed over- and under-estimation of the measured plot by the model when the source was positioned centrally in the AFL is due to the restrictions imposed by the walls. The plume of emissions can not spread laterally as much as would occur in the field, and thus is over predicted by the model at the edges and under predicted in the centre. For ground level release sources, all modelled and measured efficiencies were within 5.2%. For centrally located sources, most efficiencies were within 10.6%, however, the maximum difference was 33.4%. There was no bias for either under- or over- prediction by the model. Hanna *et al.* (2001), however, found that, on average, ADMS underpredicted by 20% when comparing modelled data to actual measured field data. Hanna (1993) also found that when several air quality models were evaluated using several different scenarios, at distances between 0.1 and 1 km downwind,

uncertainties in ground-level concentration predictions lead to biases of around ± 20 to 40%. Also, for the same model and an identical application, over-prediction at one site could be as great as 50% and at another site under-prediction could be of the same magnitude. Therefore, a difference of 33.4% between modelled and measured values is not unlikely.

3.4.6 The use of ADMS 3.0 in the AFL

ADMS models have been validated substantially against measured data sets and have been compared with other dispersion models. One particular comparison by Hanna *et al.* (2001) compares the UK ADMS, US AERMOD (AMS/EPA Regulatory MODEL) and the US EPA regulatory model, ISC3 developed in the 1960's (Industrial Source Complex Model Version 3). Of the three models, ADMS performed the best with an underprediction of around 20%, whilst AERMOD underpredicted by around 40%. ISC3 had about 33% of its predictions within a factor of two of the observations, whilst ADMS and AERMOD had about 53% and 46% of their predictions within this limit, respectively. In a previous study, Carruthers *et al.* (1997) compared the ability of ADMS, R-91 and ISC to predict measurements taken using LIDAR. This was performed to decide whether to move to the new generation model ADMS instead of using the existing model, R-91. They also found ADMS provided a more reliable prediction than either of the other two models.

Certain assumptions had to be made to use ADMS inside a building, which provides less than ideal conditions for its use. Parameters must be entered into the software and where there was no obvious input, a close approximation was entered. For example, cloud cover, which affects solar radiation, which in turn impacts air and surface temperatures and thus buoyancy of gases, was entered as total cloud cover (8 oktas). This assumes no impact of solar radiation on the turbulent dispersion from the source in the closed environment of the AFL. Despite the non-ideal conditions of use, modelled collection efficiencies generally agreed well with those measured, with most differences less than 11%, a maximum difference of 33% and an average difference of just 7.5%.

3.4.7 Saturation of samplers

Although a correction for saturation was used to allow an estimate of collection efficiency to be made when saturation had occurred, this is not ideal. There is the possibility that the background tube may also have become saturated and ammonia may have been lost completely from the sampler. This could be determined by looking at the amount of ammonia captured on each tube, however, saturation would not occur during farm measurements due to the low ammonia emission expected and so no correction for saturation would be necessary.

3.4.8 Improvements and possibilities for future work

The emission of ammonia was controlled using a flow meter ($1 - 10 \text{ l min}^{-1}$) as originally a high flow rate was to be used. Once saturation occurred it was necessary to reduce the flow rate to a low level and it would have been more accurate to use a method more suited to low emission rates, one such example being mass flow controllers.

Further improvements to the experiments undertaken in the AFL (with unlimited time and access) would have been to look at the effect of humidity on the capture efficiency, or the effect of damp or dewy grass, which may affect capture by increasing the deposition of ammonia. It is however unlikely that it would be possible to detect any change over such a short distance, being limited to 7 m due to reflection at walls.

3.4 CONCLUSIONS

The flux frame method is a suitable method for measuring ammonia emissions from ground level point sources with an average collection efficiency of 87.0%. Thus, a small correction factor of 1.15 is required.

Measured and modelled efficiencies agreed well, despite using ADMS for predictions in a non-ideal environment. Most measured and modelled efficiencies agreed to within 10.6%.

The ability to create realistic wind speed and turbulence profiles means that the AFL is a suitable facility for the validation of the flux frame - and other - methods for releases from a point source so long as the limitations are known, which include the effects of the enclosing walls and ceiling.

The sampler configuration and sampling interval are important when sampling the plume. However, at this scale a minimum interval of 0.5 m is adequate to allow a reasonable collection of the plume. At a larger scale, e.g. full scale in the field, this can be scaled up appropriately.

4. VALIDATION OF THE FLUX FRAME METHOD IN THE FIELD

4.1 INTRODUCTION

Whilst the collection efficiency of the flux frame method was being measured under controlled conditions in the AFL, field experiments using a full size flux frame began. The aim of this set of experiments was to determine the efficiency of the flux frame method under conditions more like those to be found in the field, whilst still enabling the source strength to be controlled.

Various factors, including the distance of the frame from the source, the source geometry and meteorological conditions, (particularly wind speed and direction) were investigated. The distance of the frame from the source is critical as the plume must be sampled over its whole height (Michorius *et al.*, 1997); as the distance from the source increases, it is increasingly likely that the plume would pass over the top of the frame. As the height of the masts to be erected was limited to 12 m, the effect this had on the capture of the plume with increasing distance of the source from the frame was investigated. Both point and line sources were tested, because different source geometries produce different shaped plumes.

It has already been shown in Chapter 2 that the maximum air speed at which the samplers can be used with the existing orifice size and without breakthrough is 7 m s^{-1} . A minimum speed was not determined due to limitations of the fan test rig. However, it is logical to assume that an air speed greater than zero is required to drive the ammonia through the sampler for collection. During calm conditions, with a wind speed approaching 0 m s^{-1} , ammonia would be released from the surface of a field by vertical diffusion; however, the majority of this would pass the sampler without collection, as there would be no horizontal component of flux through the sampler. A small amount might diffuse into the sampler. However, this is likely to be identical for both tubes and would cancel out in the calculation of net flux. It was also determined in Chapter 2 that incident wind directions up to 80° from parallel to the

length of the sampler were acceptable with little loss of collection efficiency. Both these conclusions limit the range of conditions under which experiments in the field could take place. Therefore it was desired to run experiments on days when a wind speed of around 2 - 5 m s⁻¹ and a direction of south-westerly was forecast, along with dry conditions. Forecasts were obtained from www.bbc.co.uk/weather.

Field runs took place between August 2000 and November 2001, and the exposure period for each run lasted between 4.5 and 8 h. The duration of the exposure period was limited by the time it took to put up and take down a full set of samplers and the need to expose tubes only during daylight hours to avoid both the possibility of condensation in the ammonia release pipe and early morning dew. Twelve runs were performed in total, which satisfied the requirements for suitable wind conditions and the absence of rain during and before the trial.

4.2 MATERIALS AND METHODS

4.2.1 Flux frame

A flux frame was erected on the wind engineering field site at Silsoe Research Institute. It was orientated perpendicular to the prevailing wind direction (South Westerly) to maximise the possible number of measurement days (Figure 4.1). The frame consisted of nine, 12 m high masts at 6.9 m spacing (total length of 55.2 m), giving a flux frame area of 662.4 m². Aluminium frames were attached to ropes, and pulleys on each side of the masts allowed each frame to be hoisted between adjacent masts. Each aluminium frame supported three columns of samplers, with four samplers on each end frame and six on the six central frames. This resulted in sampling positions 2.3 m apart at heights of 1.47, 4.37, 7.27 and 10.17 m or 0.99, 2.92, 4.85, 6.78, 8.71 and 10.64 m, respectively.



Figure 4.1: The flux frame viewed from upwind of the prevailing wind direction.

4.2.2 Field site

The field site was an area of land with a homogeneous upwind cut-grass sward and an upwind fetch of several hundred metres clear of trees and other obstructions. Downwind obstructions (visible in the background of Figure 4.1) were at a distance of over 50 m from the flux frame. Meteorological variables such as wind speed and direction were measured over the sampling period using a meteorological station, described in section 4.2.6. A 2 m high mast was erected upwind of the source allowing three measurements of background ammonia flux to be taken. The field site, known as the wind engineering site at Silsoe Research Institute, has been well documented due to its use in field measurements (e.g. Hoxey *et al.*, 2002).

4.2.3 Ammonia point source

A moveable ammonia point source was constructed using FEP tubing (o.d. 7 mm, i.d. 5 mm) mounted at 0.3 m above ground level and positioned either 15, 25, or 50 m from the frame, allowing capture of the whole plume under variable wind directions. The 15 m position was chosen initially to ensure that the whole plume was captured. Once it had been established that the plume was easily captured at this distance, the two greater distances were chosen. A known mass of ammonia was delivered via a flow meter (Roxspur Controls Direct, Basingstoke, Ammonia flow meter, model

GTVS212 GTF2BHS) from a cylinder wrapped with heat trace cable to prevent it freezing due to the evaporative heat loss during high ammonia release rates. The cylinder was placed on a balance to allow the weight of the cylinder to be measured at the beginning and end of each experiment. The flow rate depended upon the cylinder temperature, and despite the heat trace cable, a pressure drop was experienced due to the low temperature. Thus, the maximum flow rate achieved on a particular day was used and noted, along with the weight change of the cylinder.

The maximum flow rate achievable was used to ensure that conditions throughout the experimental run remained as consistent as possible. Emission rates typical of those from an area source of pigs were not used as this would have required the samplers to be exposed for about 7 days. During this period, the meteorological conditions would be unlikely to remain the same. Therefore, to ensure optimal, narrowly defined conditions it was necessary to use a short exposure period.

Coating of the tubes and analysis of the solution resulting from their extraction after exposure were undertaken in the same manner as described in section 1.13.1.1, using 4% oxalic acid in acetone solution and analysis using the NEN method 6472 and UV-visible spectrophotometry (Appendix 1). The net horizontal flux through the samplers was once again calculated using equation 14, with the correction factor found in Chapter 2 included. (Reference to 'measured flux' refers to the net horizontal flux calculated using equation 14).

A comparison was then made between the amount of ammonia released from the source and the amount captured by the flux frame. The amount of ammonia captured by the flux frame was determined as described in section 3.2.4 using equation 15.

4.2.3 Ammonia line source

An investigation into the capture of the plume from a line source (80 m long and 25 m from the frame, at a height of 0.3 m above ground) was also made. In order to

deliver a uniform flow rate over the 80 m distance, ammonia was released under pressure from 21 stainless steel orifices (0.85 mm diameter) spaced at 4 m intervals using specially adapted Swagelok T-joints. The supply pressure was sufficient to operate all orifices in critical orifice mode, which ensured that the flow rate through each of the orifices along the line source was the same. The length of the line source could be varied (80, 40 and 20 m) by positioning the T-joints at appropriate intervals (of 4, 2 and 1 m).

The source was initially designed to be used at its full length of 80 m, which was approximately one and a half times the length of the flux frame. This length was used so that when the wind was perpendicular to the flux frame, edge effects of the plume were not recorded on the frame. However, this made it difficult to determine the overall collection efficiency of the frame. Using shorter lengths of 40 and 20 m allowed the total collection efficiency to be determined. The amount of ammonia released over a sampling period was determined by weighing the ammonia gas bottle at the beginning and end of the sampling period and at intervals throughout to confirm a constant emission. The instantaneous ammonia flow rate varied with temperature. Thus, the cylinder weight change for a particular run was noted to determine the average release rate.

As with the point source, the ammonia delivered by the source was compared with that sampled by the flux frame. The amount of ammonia sampled by the flux frame was determined as described in section 3.2.4 using equation 15.

4.2.4 Modifications to the flux frame

After five measurement runs, an extra row of samplers was added to each column of samplers at 0.3 m above ground to enable the highest fluxes to be captured by the flux frame and thus to obtain a higher collection efficiency. This was decided after modelling was performed on the bottom metre of the flux frame. Results of this modelling are shown in section 4.3.4.

4.2.5 ADMS modelling

Atmospheric dispersion modelling was carried out with ADMS 3.0 using meteorological data collected at the site throughout the exposure period of the samplers. Taking the point source or centre of the line source as the origin, trigonometry was used to calculate the co-ordinates of the position of each sampler on the flux frame to enable concentrations of ammonia to be modelled at each of the sampling positions. The wind speed at each sampling height was calculated using the log law relationship (equations 17-20) and the average wind speed measured at a particular height throughout the exposure period. The product of these two measurements was the modelled flux estimate. The total modelled amount of ammonia captured could then be calculated as described previously and a modelled efficiency was calculated using equation 24. The actual and modelled collection efficiencies calculated could then be compared. A full list of parameters used in the model is given in Appendix 3.

4.2.6 Meteorological station

Meteorological measurements were taken throughout the experimental period at a meteorological station erected 50 m to the North West of the flux frame. This enabled the changing environmental conditions to be logged throughout the exposure period, and provided accurate data for dispersion modelling. Measurements of wind speed and direction were made with a cup anemometer (Porton anemometer, type A100, Vector instruments, Rhyl) and wind vane (Potentiometer wind vane, type W200P, Vector instruments, Rhyl). Rainfall measurements were made using a rain gauge (Tipping bucket, product ARG 100/EC, Campbell Scientific Ltd., Shepshed). One-minute averages were collected every minute during the exposure period using a data logger (21X Micrologger, Campbell Scientific Ltd., Shepshed), powered by a 12V car battery.

4.3 RESULTS

Table 4.1 shows a summary of all the results during successful field experiments with five point sources and six line sources. Run 9 is not included as, whilst the run was completed successfully, contamination of the sample bottles into which the samples were extracted meant that no meaningful results were found. Two other runs are not presented in the table because they were abandoned due to rain during the run, which washed the coating off the tubes. Runs 6 and 7 show apparent rather than actual measured collection efficiencies, due to the length of the line source being longer than the flux frame (described in section 4.3.9). Using a correction factor of 80/55.2, apparent measured efficiencies of 23.0 and 49.6% respectively can be calculated.

4.3.1 Run 1: Point source at 15 m

In Run 1, the point source was positioned at a distance at which the whole height of the plume was certain to be captured. Figure 4.2 is a schematic scale diagram of the site for run 1. The positions of the flux frame (pink line) and point source (circle) are shown relative to each other and to North. The blue line represents the location of the source relative to the flux frame given the mean wind direction. Dashed black lines indicate the lateral spread of the plume (the standard deviation of the wind direction throughout the exposure period). Figure 4.3a is the plot produced when the fluxes from each of the 132 samplers are plotted using 3D graphical software, Surfer 7.

Run	Date	Source Type	Source Distance (m)	Line Source Length (m)	Exposure Period (s)	Release Rate (g s ⁻¹ or g m ⁻¹ s ⁻¹)	Mean Wind Speed (m s ⁻¹)	Maximum Wind Speed (m s ⁻¹)	Mean Wind Direction (deg)	Lateral Spread (deg)**	Measured Collection Efficiency (%)	Error (%)	Modelled Collection Efficiency (%)	Modelled Collection Efficiency (%)**
1	17/8/00	point	15		28800	0.35	4.98	6.95	287.0	12.5	63.5	±10.5	52.0	48.1
2	5/9/00	point	25		25740	0.35	2.93	5.43	201.4	12.9	47.6	±8.9	30.0	38.9
3	12/9/00	point	25		25200	0.29	5.45	6.65	258.0	12.9	60.6	±8.9	59.7	81.9
4	4/10/00	point	50		22440	0.41	4.38	7.35	243.1	16.1	63.5	±7.6	56.0	64.8
5	28/10/00	point	50		21360	0.42	6.80	12.24	254.4	12.2	46.7	±9.5	57.8	68.9
6	20/8/01	line	25	80	21600	0.0020	2.99	6.91	288.7	23.8	15.9	±77.8	48.6	
7	7/9/01	line	25	80	21600	0.0025	5.47	9.48	266.7	18.1	34.2	±34.7	62.6	
8	3/10/01	line	25	40	21600	0.0024	6.91	12.61	238.4	12.6	45.3	±42.1	82.6	
10	29/10/01	line	25	20	18000	0.0053	5.30	7.91	245.7	9.5	81.2	±36.7	82.6	
11	30/10/01	line	25	20	18000	0.0069	6.61	10.19	219.3	9.3	113.9	±19.3	88.0	
12	21/11/01	line	25	20	16200	0.0096	8.19	11.22	234.8	5.1	97.8	±17.2	86.3	

* Lateral spread: the standard deviation of the wind direction throughout the exposure period

** Collection efficiency modelled with an extra row of samplers at a height of 0.3 m.

Table 4.1: Summary of results for all experimental runs successfully performed and analysed.

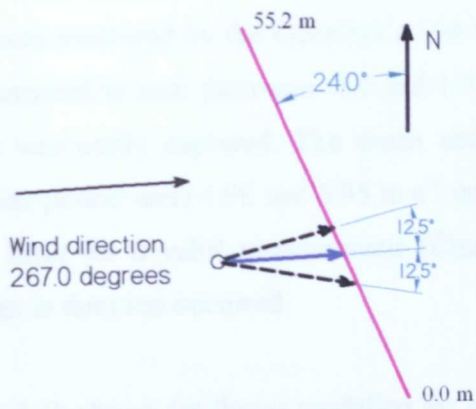


Figure 4.2: Run 1: scale diagram.

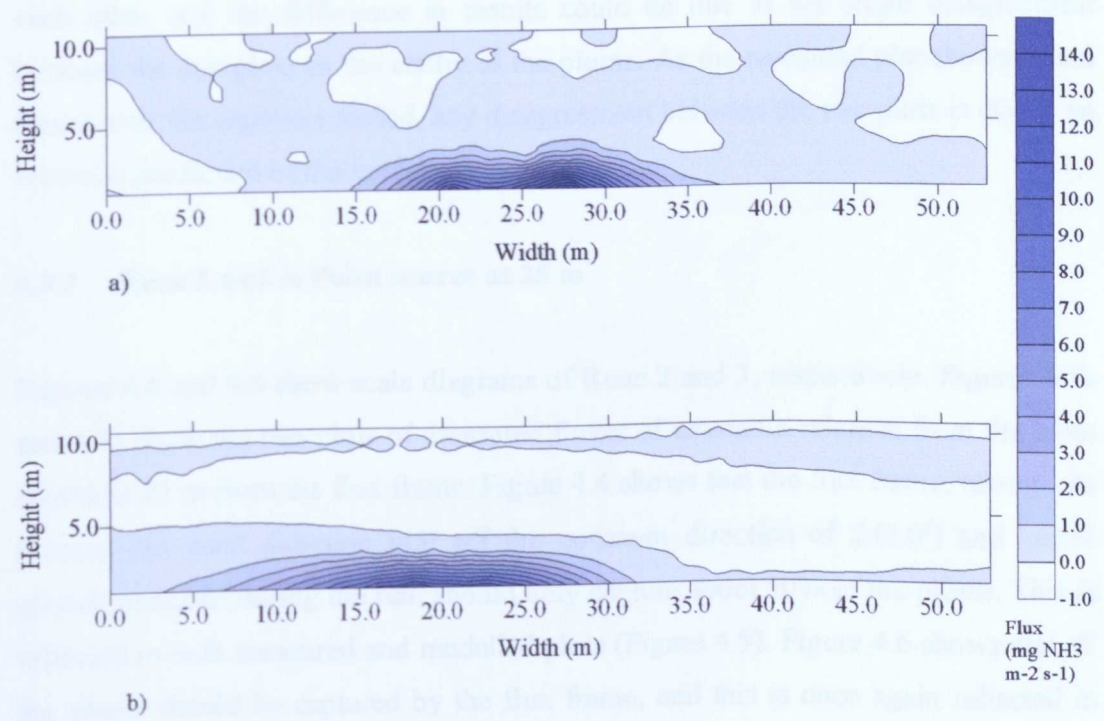


Figure 4.3: Run 1: point source at 15 m from the flux frame: a) Fluxes measured at 132 sampling locations (Collection efficiency = 63.5%); b) fluxes modelled for the same sampling locations (C.E.=52.0%).

The average wind direction throughout the exposure period was 267.0° (246.0° being perpendicular to the flux frame) with a lateral spread of 12.5°. The plot reflects this with a compact plume that is positioned almost centrally, as shown in Figure 4.2. As the fluxes measured by the samplers at the top of the flux frame (above around 5 m) have returned to zero (between -1.0 and 1.0 mg NH₃ m⁻² s⁻¹), the whole height of the plume was easily captured. The mean and maximum wind speeds throughout the exposure period were 4.98 and 6.95 m s⁻¹ respectively (Table 4.1), which is below the upper limit for a valid measurement (Chapter 2) and a light shower, less than 5 minutes in duration occurred.

Figure 4.3b shows the fluxes modelled for each of the 132 sampling positions plotted in the same manner as the measured fluxes. The plume is not located in exactly the same position, but the majority of the plume's width is still captured. The measured and modelled collection efficiencies (63.5 and 52.0% respectively) are within 12% of each other and the difference in results could be due to the slight disagreement between the two plots on the centre of the plume. As the measured plot shows actual fluxes over the exposure period, any disagreement between the two plots is due to an incorrect prediction of the model.

4.3.2 Runs 2 and 3: Point source at 25 m

Figures 4.4 and 4.6 show scale diagrams of Runs 2 and 3, respectively. Figures 4.5a and 4.7a show the two plots of measured fluxes of ammonia released from the point source at 25 m from the flux frame. Figure 4.4 shows that the flux frame, taking into account the wind direction (45° off the optimum direction of 246.0°) and lateral spread measured during the run, should only capture about 50% of the plume. This is reflected in both measured and modelled plots (Figure 4.5). Figure 4.6 shows that all the plume should be captured by the flux frame, and this is once again reflected in both measured and modelled plots (Figure 4.7). In this run, the collection efficiency was within 1% of the measured efficiency.

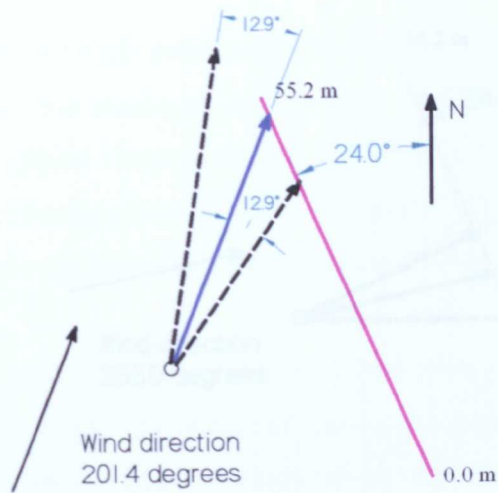


Figure 4.4: Run 2: scale diagram.

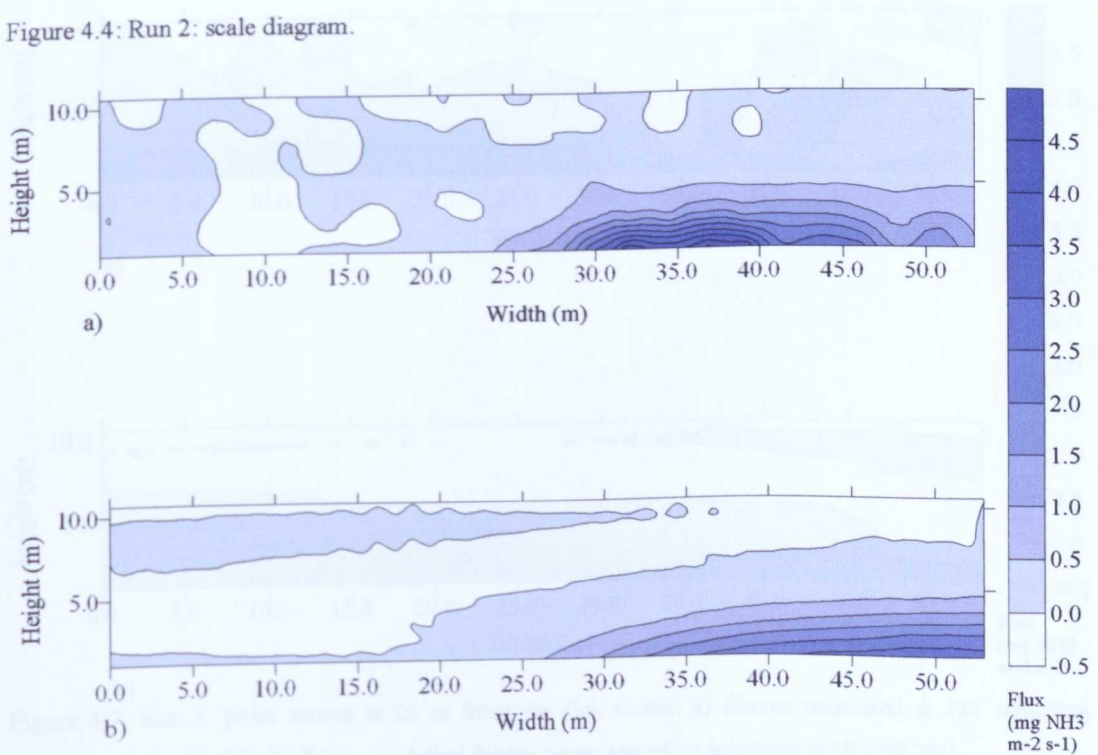


Figure 4.5: Run 2: point source at 25 m from the flux frame: a) Fluxes measured at 132 sampling locations (C.E.=47.6%); b) fluxes modelled for the same sampling locations (C.E.=30.0%).

4.3.3 Run 3 and 2: Point source at 25 m

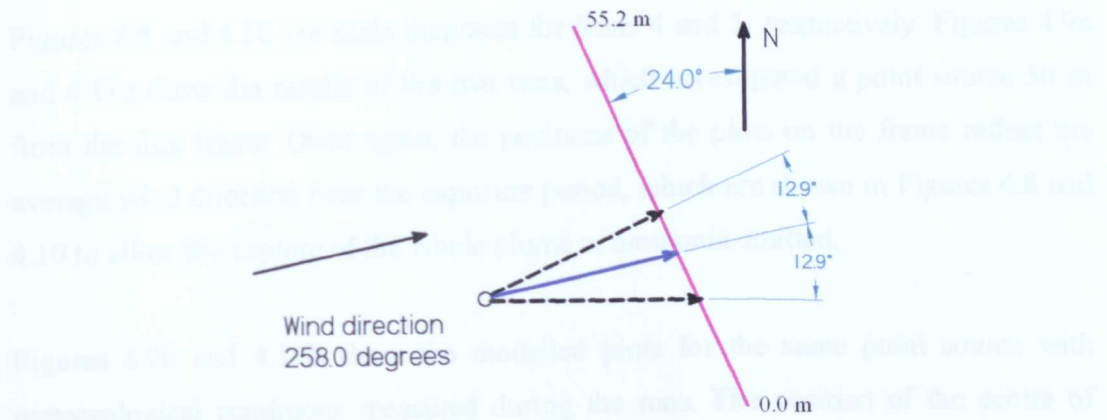


Figure 4.6: Run 3: scale diagram.

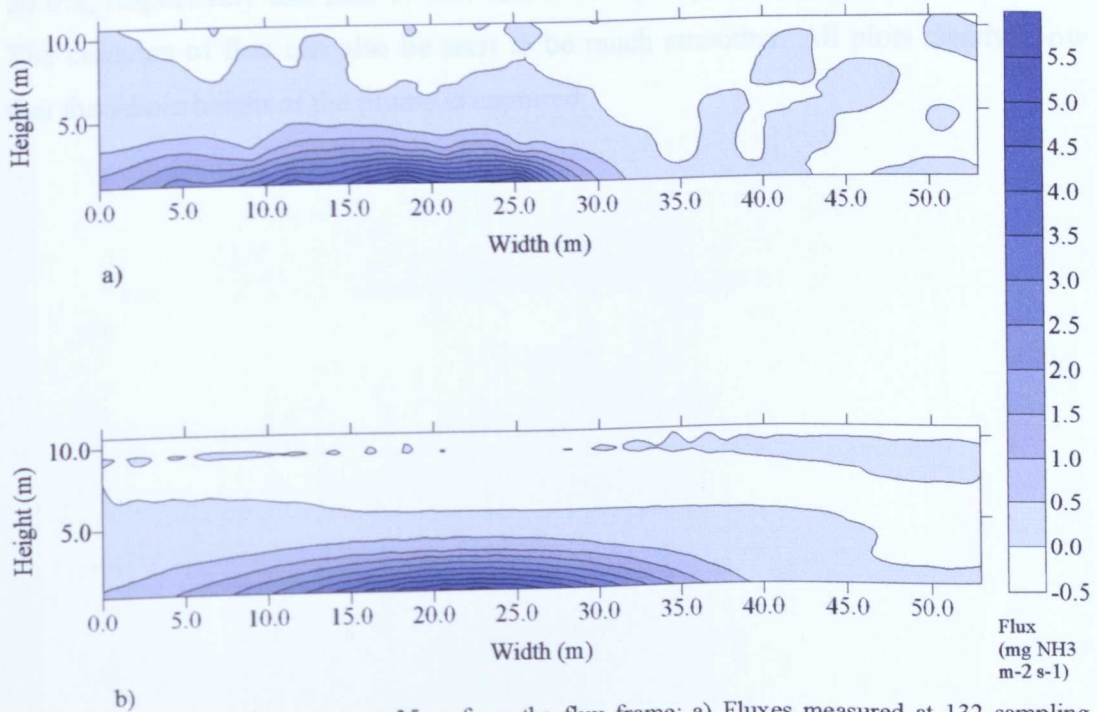


Figure 4.7: Run 3: point source at 25 m from the flux frame: a) Fluxes measured at 132 sampling locations (C.E.=60.6%); b) fluxes modelled for the same sampling locations (C.E.=59.7%).

4.3.3 Runs 4 and 5: Point source at 50 m

Figures 4.8 and 4.10 are scale diagrams for Runs 4 and 5, respectively. Figures 4.9a and 4.11a show the results of the two runs, which investigated a point source 50 m from the flux frame. Once again, the positions of the plots on the frame reflect the average wind direction over the exposure period, which are shown in Figures 4.8 and 4.10 to allow the capture of the whole plume of ammonia emitted.

Figures 4.9b and 4.11b show the modelled plots for the same point source with meteorological conditions measured during the runs. The position of the centre of each plume (measured and modelled) agrees well. However, the modelled plumes are clearly much wider, despite a lateral spread parameter being entered into the model (see Table 4.1). Measured and modelled collection efficiencies (Run 4: 63.5 and 56.0%, respectively and Run 5: 46.7 and 57.8% , respectively) agree within 11.1%. The contours of flux can also be seen to be much smoother. All plots clearly show that the whole height of the plume is captured.

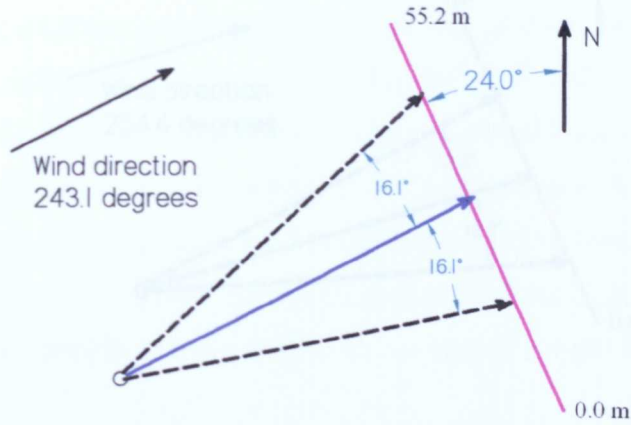


Figure 4.8: Run 4: scale diagram.

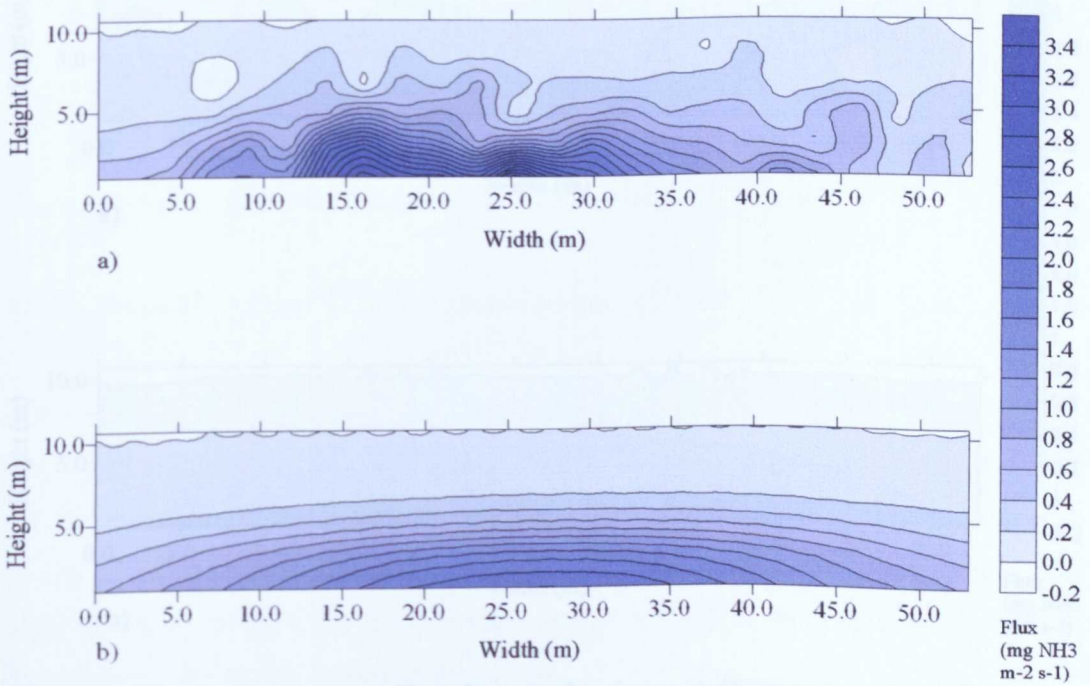


Figure 4.9: Run 4: point source at 50 m from the flux frame: a) Fluxes measured at 132 sampling locations (C.E.=63.5%); b) fluxes modelled for 132 sampling positions (C.E.=56.0%).

4.3.3 Flux Direction in the Flux Frame

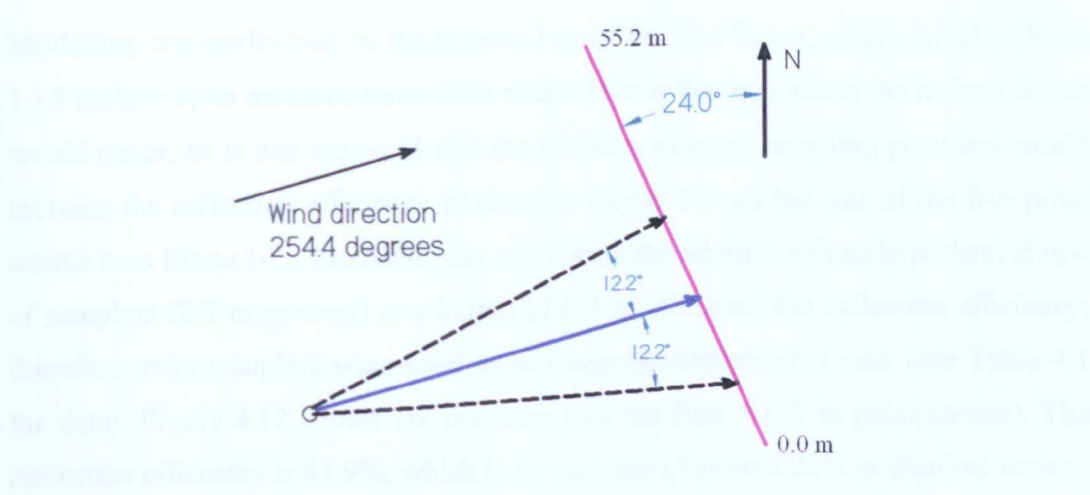


Figure 4.10: Run 5: scale diagram.

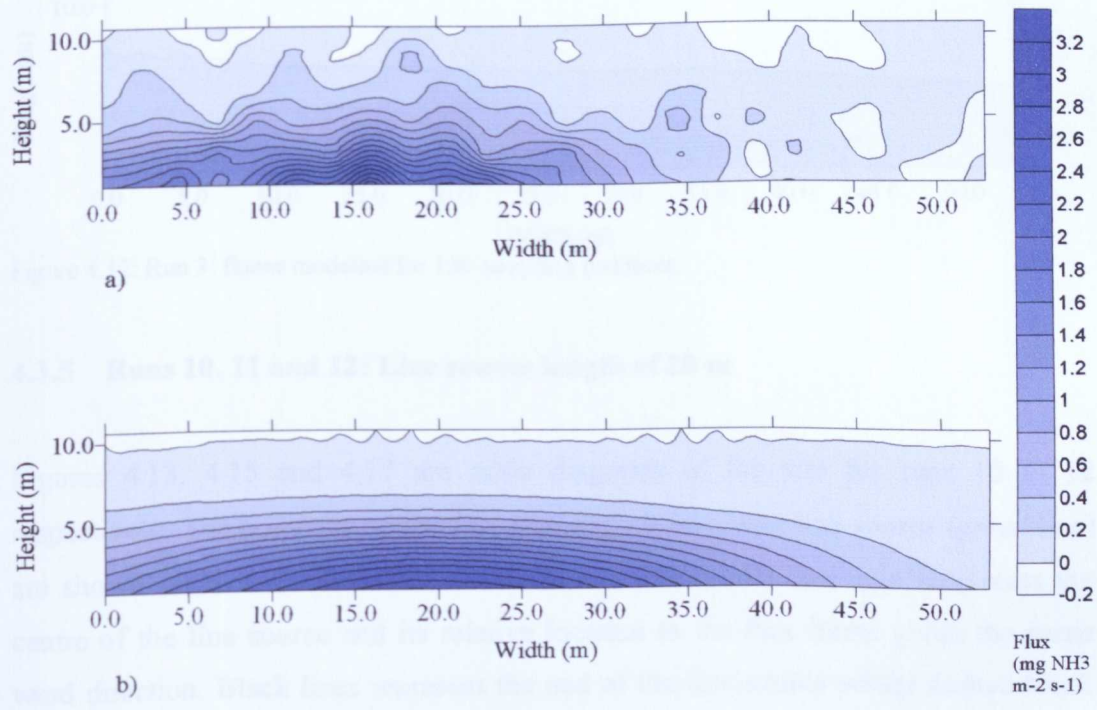


Figure 4.11: Run 5: point source at 50 m from the flux frame: a) Fluxes measured at 132 sampling locations (C.E.=46.7%); b) fluxes modelled for the same sampling positions (C.E.=57.8%).

4.3.4 Modifications to the flux frame

Modelling was performed on the bottom 1 m of the flux frame, where initially (Runs 1 - 5 inclusive) no measurements were made. This is the area where the highest fluxes would occur, so it was expected that the addition of extra sampling positions would increase the collection efficiency of the flux frame. For all but one of the five point source runs (Runs 1-5), modelling the result with the addition of one hypothetical row of samplers (2.3 m spacing) at a height of 0.3 m increased the collection efficiency: therefore extra samplers were used in subsequent measurement runs (see Table 4.1 for data). Figure 4.12 shows the resulting plot for Run 3 (25 m point source). The collection efficiency is 81.9%, which is an increase of around 22% in absolute terms.

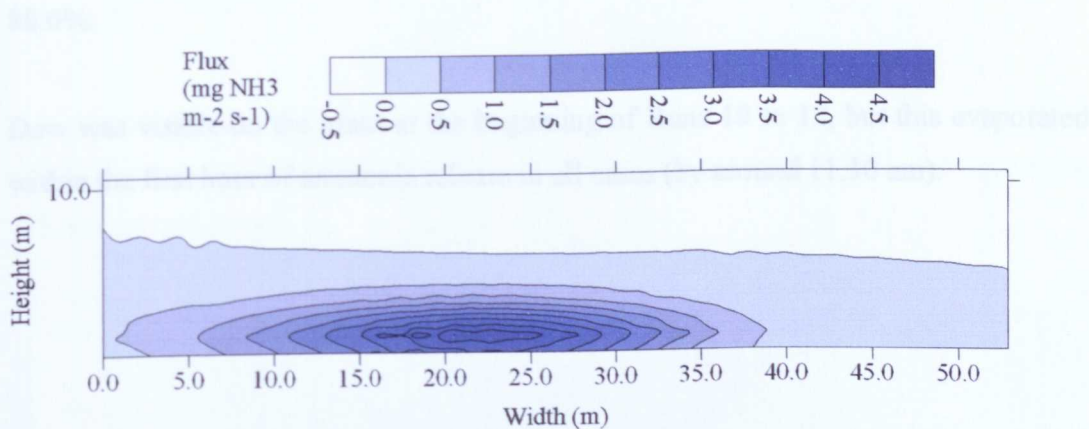


Figure 4.12: Run 3: fluxes modelled for 156 sampling positions.

4.3.5 Runs 10, 11 and 12: Line source length of 20 m

Figures 4.13, 4.15 and 4.17 are scale diagrams of the site for runs 10 to 12 respectively. The positions of the flux frame (pink line) and line source (green line) are shown relative to each other and to North. The centre blue line represents the centre of the line source and its relative location to the flux frame given the mean wind direction. Black lines represent the end of the line source whilst dashed black lines indicate the lateral spread of the plume.

Figures 4.14a, 4.16a and 4.18a show the three plots for the three runs (10-12) successfully completed using a 20 m long line source. It can be seen that, even with the lateral spread of the plume, the whole width of the plume should be captured by the flux frame in runs 10 and 12, whilst in Run 11 the majority of the plume should be captured. This is supported by Figures 4.14a, 4.16a and 4.18a which show the whole of the plume of ammonia being captured in Runs 10 and 12, and the majority in Run 11. Figures 4.14b, 4.16b and 4.18b show the equivalent modelled plots. The shape and position of the measured and modelled plots agree very well. However, the fluxes at the centre of the modelled plume are not as high as those of the measured plume. Measured runs had collection efficiencies above 80% (range 81.2% - 113.9%), whilst the modelled plots had collection efficiencies in the range 82.6% to 88.0%.

Dew was visible on the grass at the beginning of Runs 10 to 12, but this evaporated within the first hour of ammonia release in all cases (by around 11.30 am).

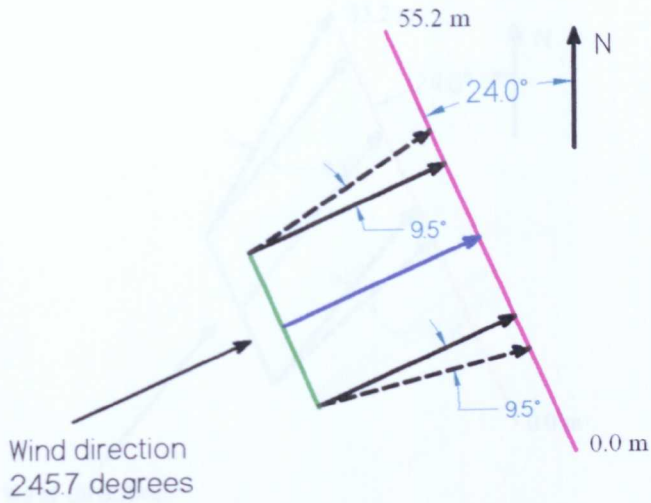


Figure 4.13: Run 10: scale diagram showing source position (green line) and wind conditions relative to flux frame (pink line).

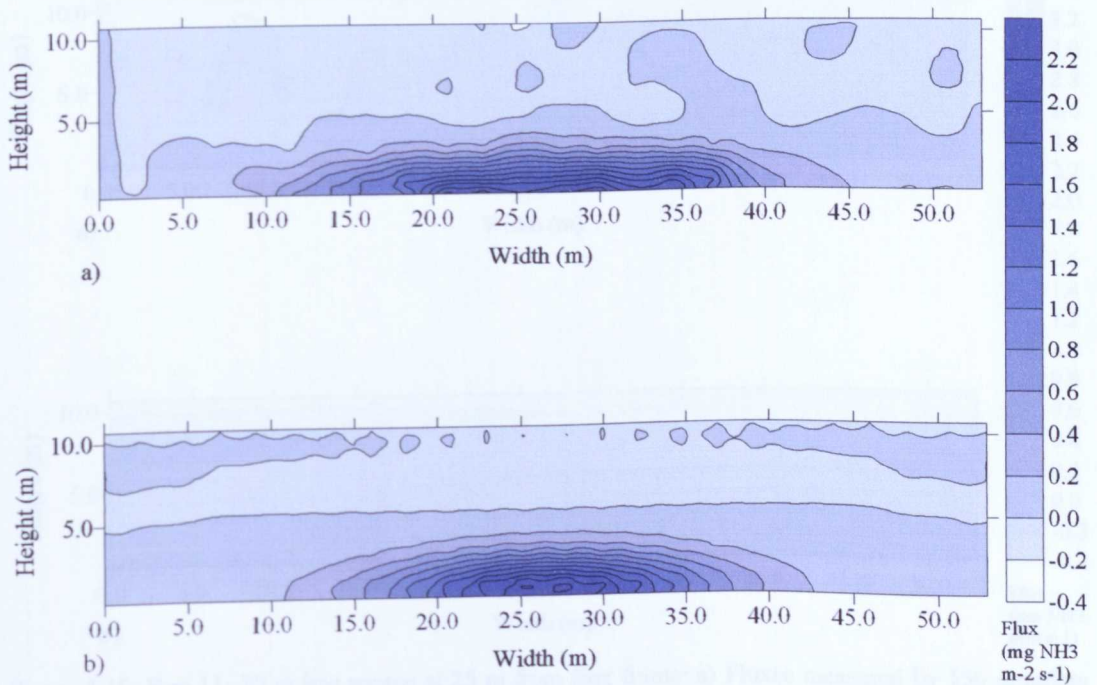


Figure 4.14: Run 10: 20 m line source at 25 m from flux frame: a) Fluxes measured by 156 samplers (C.E.=81.2%); b) fluxes modelled for the same sampling locations (C.E.=82.6%).

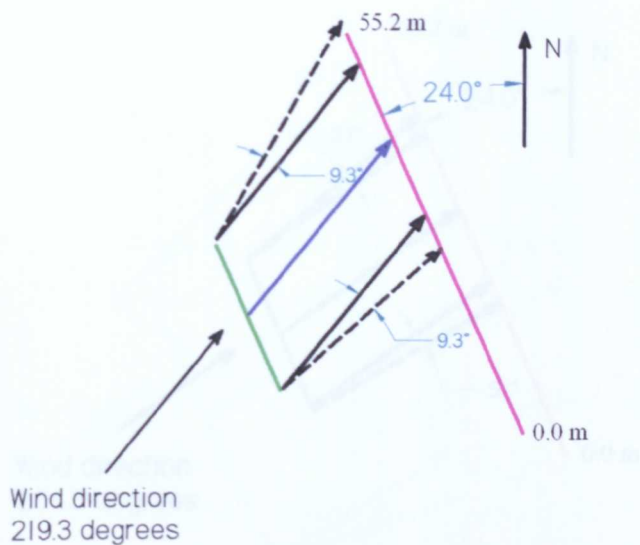


Figure 4.17: Run 11: scale diagram.

Figure 4.15: Run 11: scale diagram.

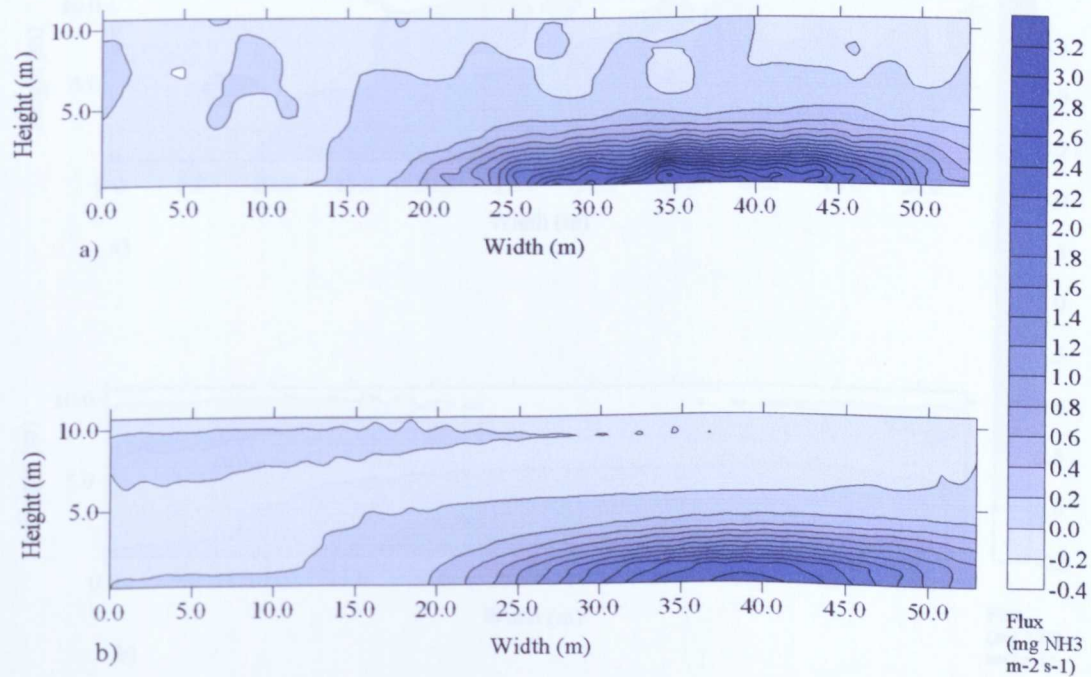


Figure 4.16: Run 11: 20 m line source at 25 m from flux frame: a) Fluxes measured by 156 samplers (C.E.=113.9%); b) fluxes modelled for the same sampling locations (C.E.=88.0%).

4.1.8 Run 12: Line source length of 40 m

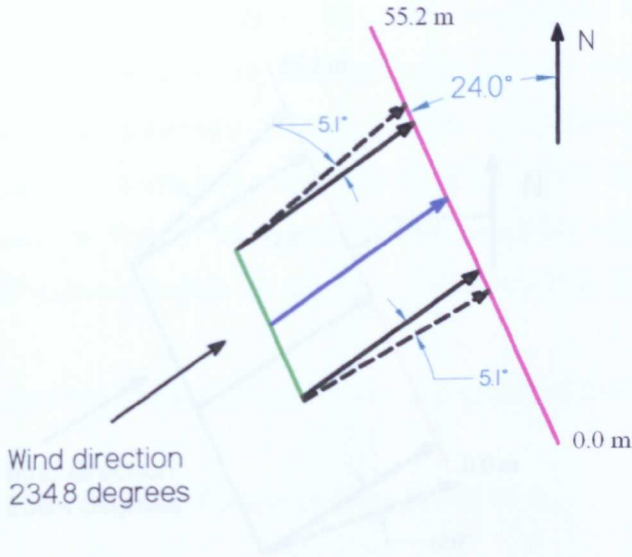


Figure 4.17: Run 12: scale diagram.

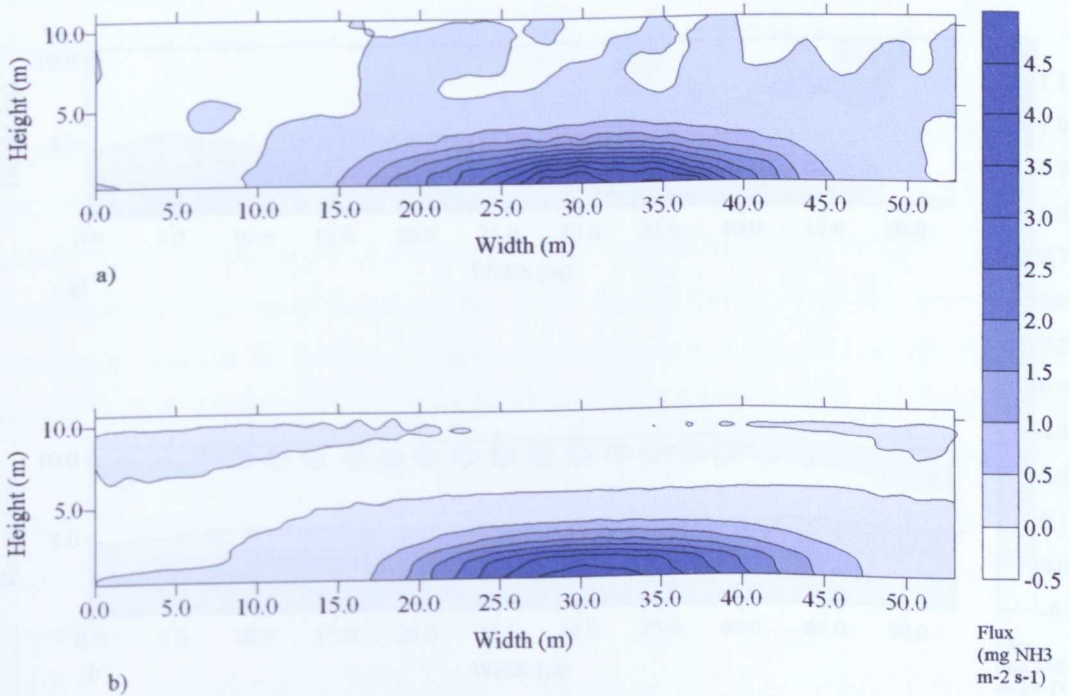


Figure 4.18: Run 12: 20 m line source at 25 m from flux frame: a) Fluxes measured by 156 samplers (C.E.=97.8%); b) fluxes modelled for the same sampling locations (C.E.=86.3%).

4.3.6 Run 8: Line source length of 40 m

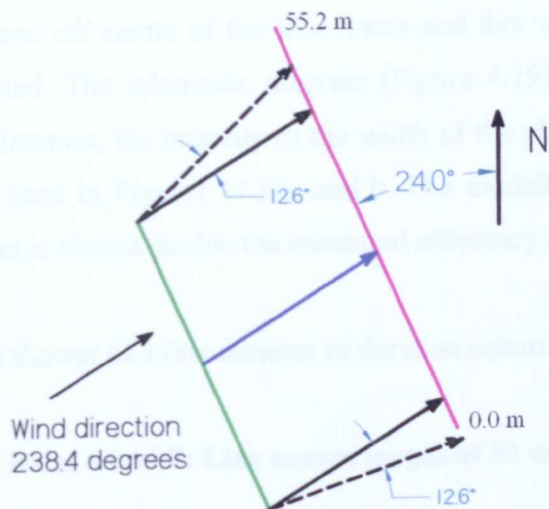


Figure 4.19: Run 8: scale diagram.

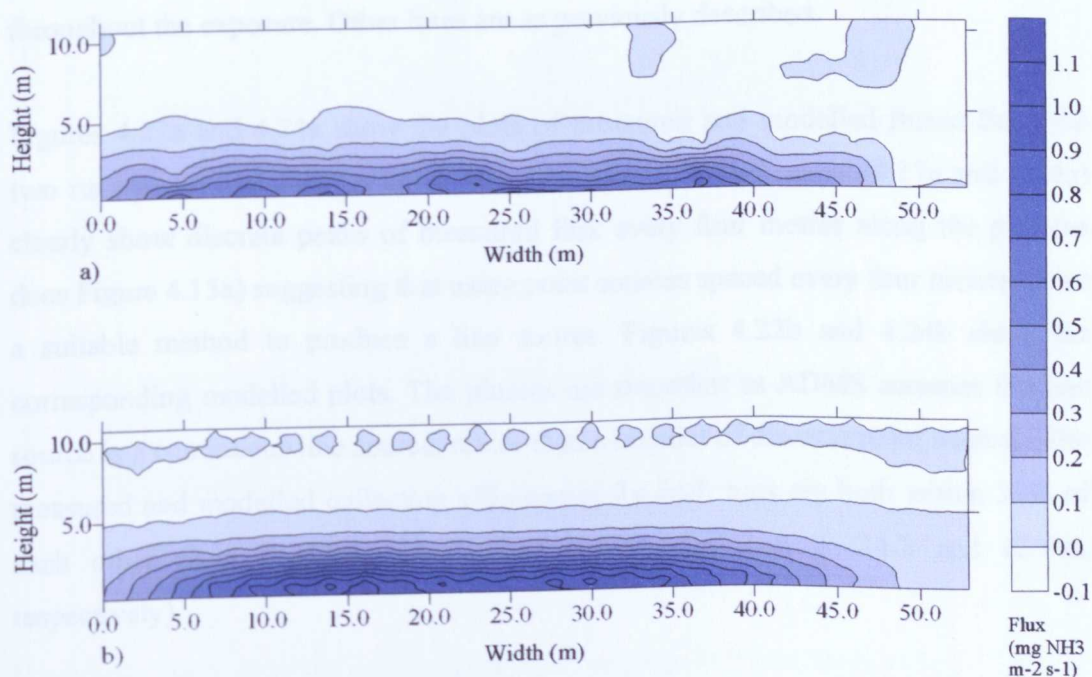


Figure 4.20: Run 8: 40 m line source at 25 m from flux frame: a) Fluxes measured by 156 samplers (C.E.=45.3%); b) fluxes modelled for the same sampling locations (C.E.=82.6%).

Whilst two runs were performed using a 40 m long line source, results are only available for one of the runs due to contamination of the bottles into which the samples were extracted (Run 9). Also, the source for Run 8 was mistakenly positioned off centre of the flux frame and this was only realised after the run was completed. The schematic diagram (Figure 4.19) shows, however, that due to the wind direction, the majority of the width of the plume would be captured, and this is clearly seen in Figures 14.20a and b. The modelled collection efficiency for Run 8 however is almost double the measured efficiency (82.6% and 45.3%, respectively).

A light shower of a few minutes in duration occurred during Run 8.

4.3.7 Runs 6 and 7: Line source length of 80 m

Figures 4.21 and 4.23 are scale diagrams of the site during runs 6 and 7 using an 80 m long line source. The blue lines represent the portion of the source that could potentially pass through the frame, taking into account the average wind direction throughout the exposure. Other lines are as previously described.

Figures 4.22a and 4.24a show the plots of measured and modelled fluxes from the two runs performed with an 80 m long line source. Both Figures (4.17a and 4.19a) clearly show discrete peaks of measured flux every four metres along the plot (as does Figure 4.15a) suggesting that using point sources spaced every four metres is not a suitable method to produce a line source. Figures 4.22b and 4.24b show the corresponding modelled plots. The plumes are smoother as ADMS assumes the line source is a continuous line source, rather than a number of discrete point sources. The measured and modelled collection efficiencies for both runs are both within 33% of each other (Run 6: 15.9 and 48.6%, respectively, Run 7: 34.2 and 62.6%, respectively).

A short shower occurred fifteen minutes before Run 6 began.

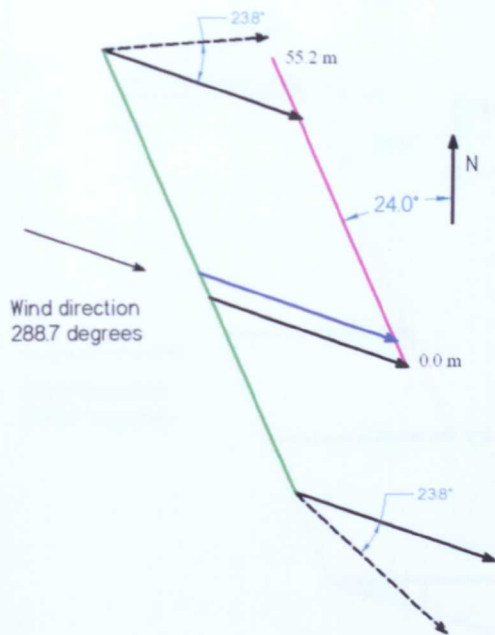


Figure 4.21: Run 6: scale diagram.

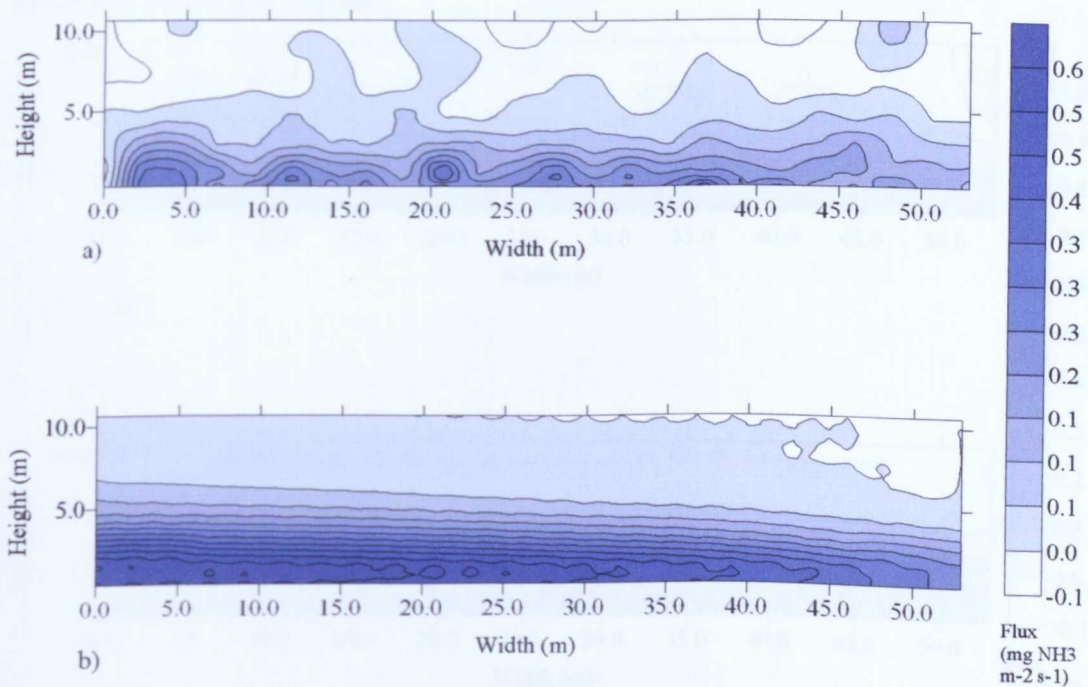


Figure 4.22: Run 6: 80 m line source at 25 m from flux frame: a) Fluxes measured by 156 samplers (C.E.=15.9%); b) fluxes modelled for the same sampling locations (C.E.=48.6%).

4.3.8 Test cases

The 2000 test cases for the flux estimator was calculated as described in section 4.2.5. The width for each test case is given in Table 4.1 and it can be seen that the larger the width the higher the R^2 value. Flux estimates have errors less than 10.5% with the largest error source being $\pm 7.7\%$ and $\pm 4.7\%$.

4.3.9 Measurement

The measured and modelled fluxes for each position in each experimental run are plotted in Figure 4.23. The linear correlation coefficient, R^2 values, for each of the runs is given in Table 4.2. Figure 4.23(a) shows the same graph as Figure 4.23(b) however fluxes greater than 1.0 $\text{mg NH}_3 \text{ m}^{-2} \text{ s}^{-1}$ have been omitted (all 8 data points included) see from Run 1), as they were considered to be outliers when compared with the other 1500 data points. Data plotted in Figure 4.26 have a higher R^2 value

Figure 4.23: Run 7: scale diagram.

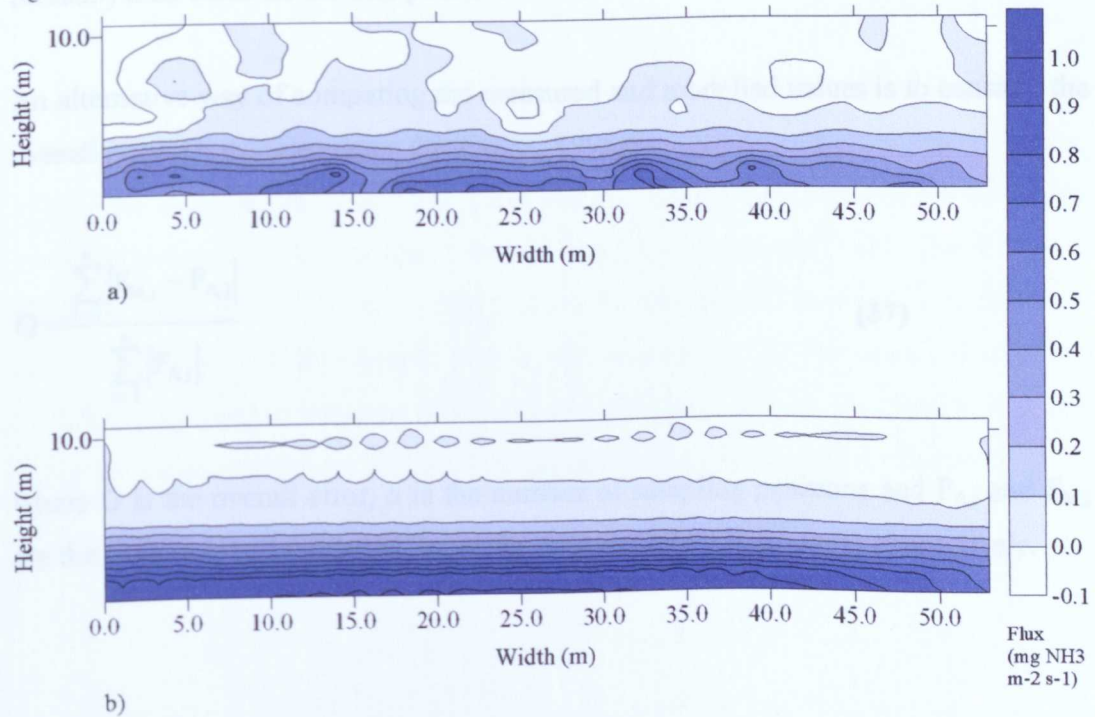


Figure 4.24: Run 7: 80 m line source at 25 m from flux frame: a) Fluxes measured by 156 samplers (C.E.=34.2%); b) fluxes modelled for the same sampling locations (C.E.=62.6%).

4.3.8 Total error

The total error for each flux frame estimate was calculated as described in section 3.2.5. The errors for each run are presented in Table 4.1 and it can be seen that the longer the source, the higher the error. Point sources have errors less than 10.5%, whilst the longest line source has errors of 77.8 and 34.7%.

4.3.9 Measured vs. modelled fluxes

The measured and modelled fluxes for each position in each experimental run are plotted in Figure 4.25. The linear correlation coefficient, R^2 values, for each of the runs is given in Table 4.2. Figure 4.26 shows the same graph as Figure 4.25(i), however fluxes greater than $5 \text{ mg NH}_3 \text{ m}^{-2} \text{ s}^{-1}$ have been omitted (all 8 data points excluded are from Run 1), as they were considered to be outliers when compared with the other 1588 data points. Data plotted in Figure 4.26 have a higher R^2 value (0.7653) than when all the data points are used.

An alternative way of comparing the measured and modelled values is to consider the overall error, O , using equation 27 (Quinn, 1996):

$$O = \frac{\sum_{i=1}^n |F_{M,j} - F_{A,j}|}{\sum_{i=1}^n |F_{A,j}|} \quad (27)$$

where O is the overall error, n is the number of sampling positions and $F_{A,j}$ and $F_{M,j}$ are the measured and modelled fluxes for each sampling position (j), respectively.

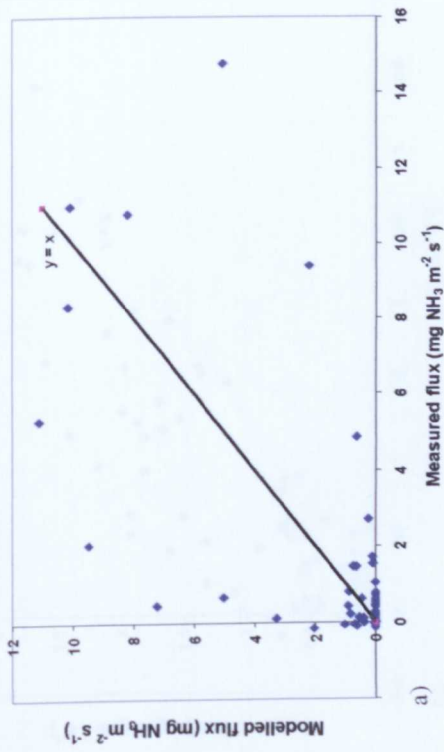
Table 4.2: R^2 and O values for each experimental run.

Run	Source Type	R^2	p	O
1	Point	0.4869	<0.01	0.88
2		0.7028	<0.01	0.50
3		0.8440	<0.01	0.44
4		0.7365	<0.01	0.41
5		0.7689	<0.01	0.58
6	Line	0.7110	<0.01	1.32
7		0.9044	<0.01	0.61
8		0.8847	<0.01	0.62
10		0.8998	<0.01	0.34
11		0.9593	<0.01	0.31
12		0.9643	<0.01	0.25
All Data			0.6691	<0.01

The R^2 values for each plot are highly statistically significant, all having p values <0.01. When all the data are plotted together as in Figure 4.20(1), the R^2 value shows that 67% of the variation can be accounted for by the linear association between the measured and modelled fluxes, whilst 33% cannot.

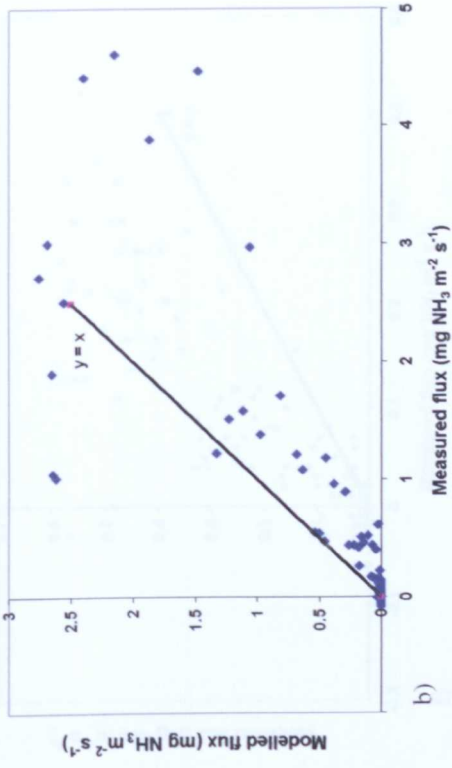
Overall error values, O, give the absolute error as a fraction of the total absolute sum of the measured values. This produces an unbiased measure of absolute error (Quinn, 1996). The O values show that Run 6 has the worst agreement between measured and modelled values (1.32), with Run 1 also having poor agreement (0.88). The R^2 values show the worst agreement is for Run 1 (0.4869) with Runs 2 and 6 also having poor agreement ($R^2 < 0.7110$). Overall, both R^2 and O values show that Runs 3-5 and 7-12 have good agreement between measured and modelled values. The data points that cause this large differences in Runs 1 and 6 can be seen on Figures 4.25a and f.

Run 1



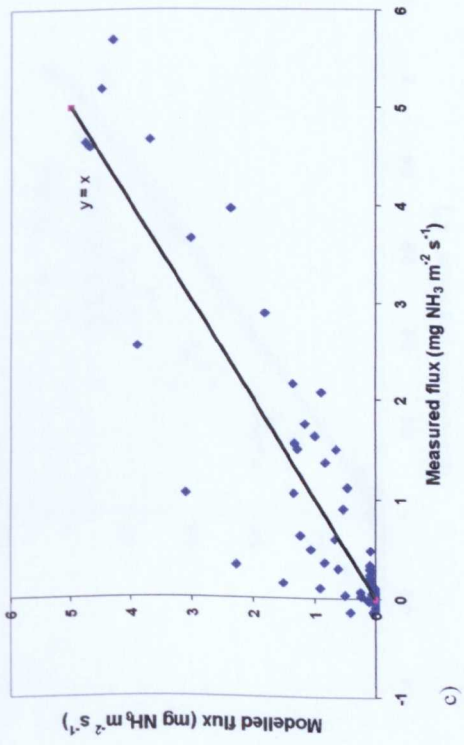
a)

Run 2



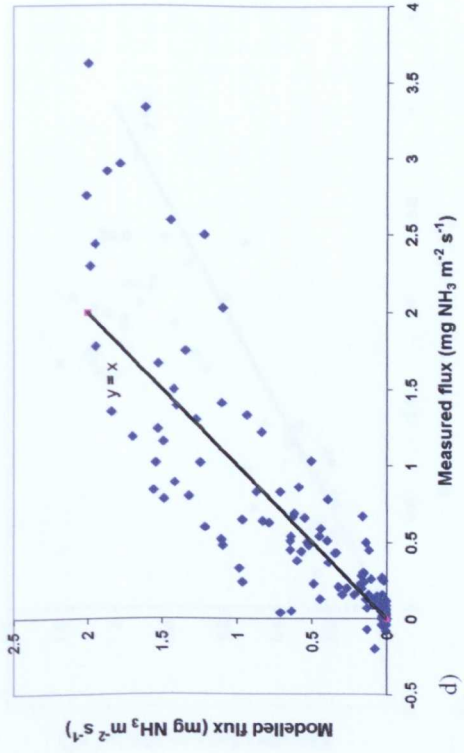
b)

Run 3



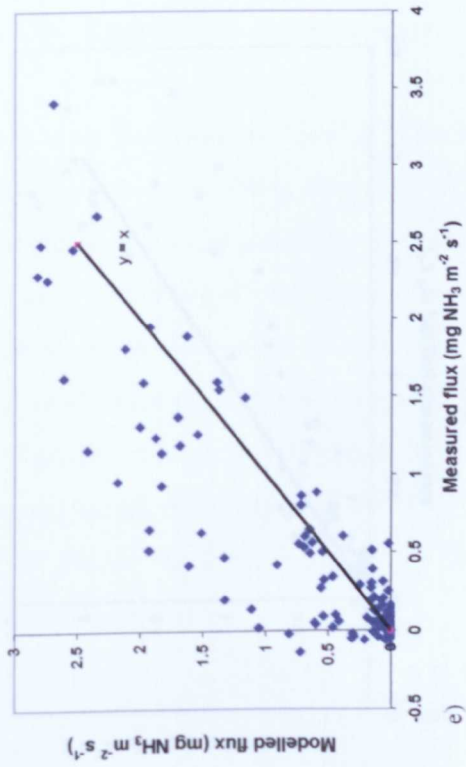
c)

Run 4

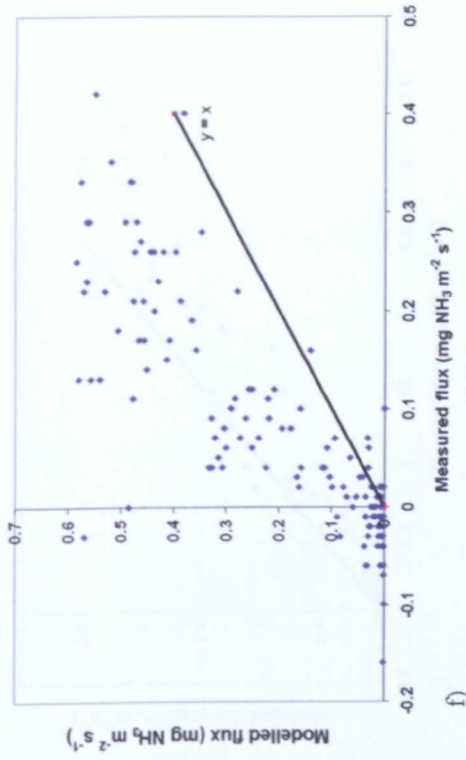


d)

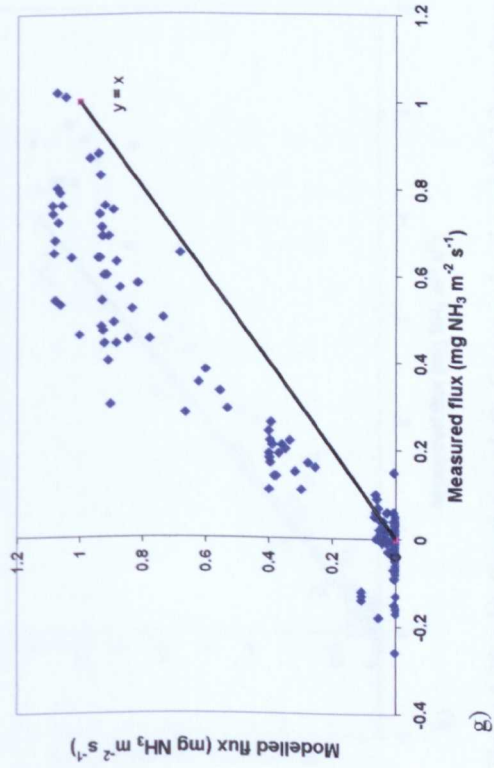
Run 5



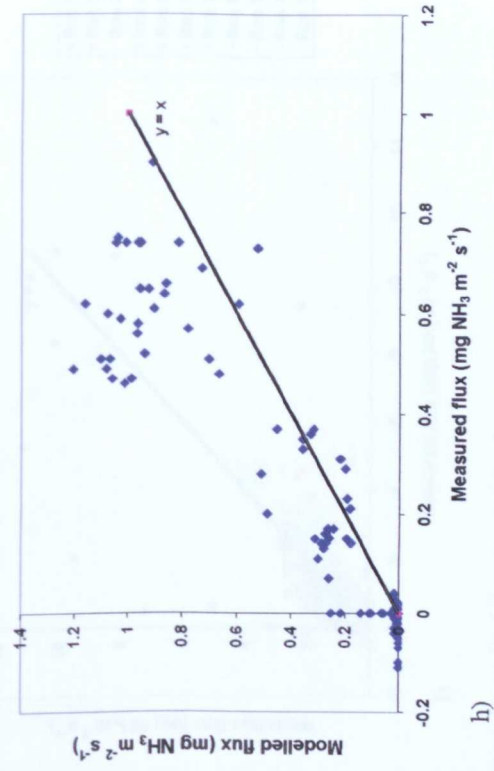
Run 6



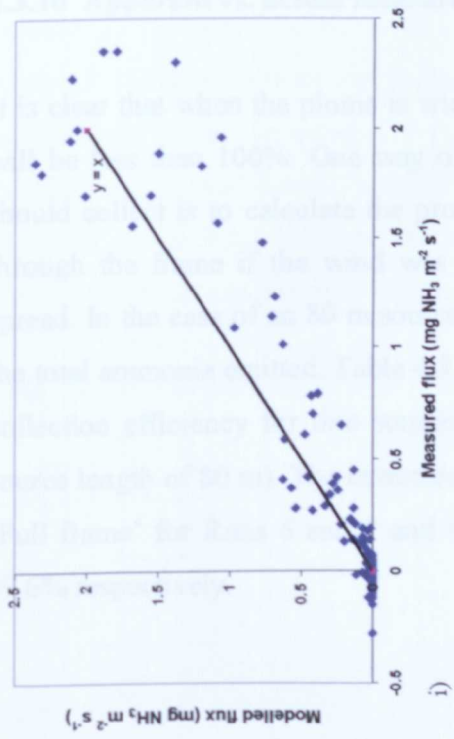
Run 7



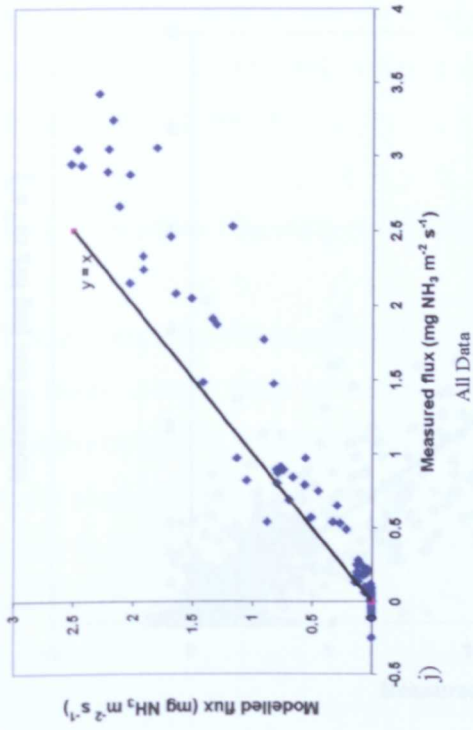
Run 8



Run 10



Run 11



Run 12

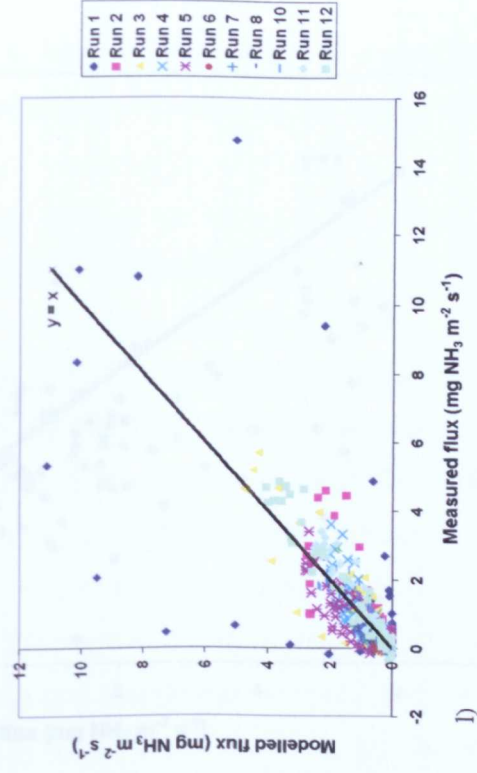
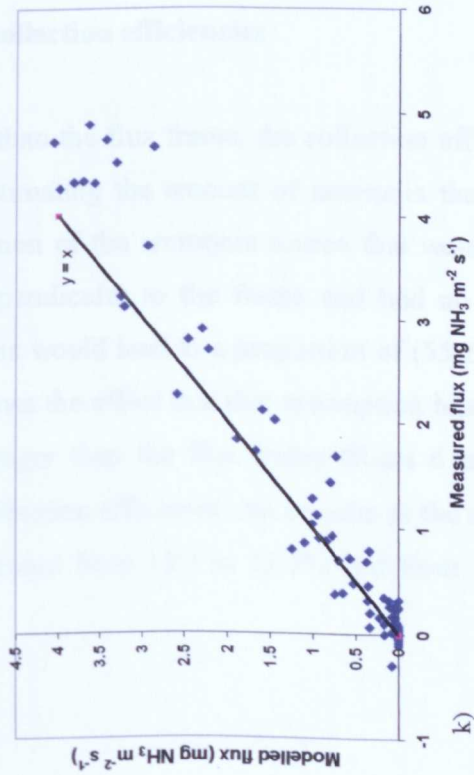


Figure 4.25: a-k): Correlation plots of measured and modelled fluxes for each experimental run; l): All runs combined.

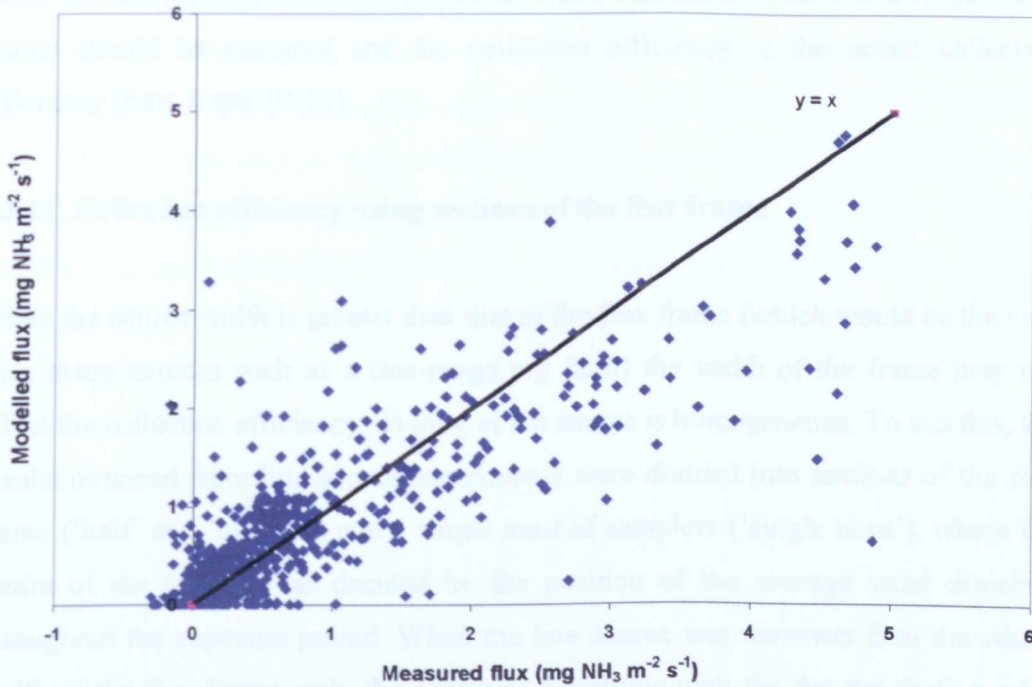


Figure 4.26: Correlation plot of all measured and modelled flux data, restricted to fluxes below 5 mg $\text{NH}_3 \text{ m}^{-2} \text{ s}^{-1}$.

4.3.10 Apparent vs. actual measured collection efficiencies

It is clear that when the plume is wider than the flux frame, the collection efficiency will be less than 100%. One way of estimating the amount of ammonia the frame should collect is to calculate the proportion of the ammonia source that would pass through the frame if the wind was perpendicular to the frame and had no lateral spread. In the case of an 80 m source, this would lead to a proportion of $(55.2/80)$ of the total ammonia emitted. Table 4.3 shows the effect that this assumption has on the collection efficiency for line sources longer than the flux frame (Runs 6 and 7 – source length of 80 m). The corrected collection efficiency can be seen in the column ‘Full frame’ for Runs 6 and 7 and increased from 15.9 to 23.0% and from 34.2 to 49.6% respectively.

When the source width is narrower than the frame and lateral spread is low, the whole plume should be captured and the collection efficiency is the actual collection efficiency (runs 8 and 10-12).

4.3.11 Collection efficiency using sections of the flux frame

When the source width is greater than that of the flux frame (which would be the case with many sources such as a free-range pig farm) the width of the frame may not affect the collection efficiency, so long as the source is homogeneous. To test this, the results obtained from line source experiments were divided into sections of the flux frame ('half' and 'quarter') and a single mast of samplers ('single mast'), where the centre of the section was decided by the position of the average wind direction throughout the exposure period. When the line source was narrower than the whole width of the flux frame, only the centre of the plume with the flat top (before edge effects were seen) was used to determine the effect on the collection efficiency. The amount expected to be captured was the actual amount of ammonia released multiplied by the section of the flux frame – for example for half a flux frame, the amount of ammonia expected to be captured was half the amount of ammonia released. Table 4.3 shows the apparent collection efficiencies calculated for shorter sections of the flux frame, with 'Full frame' referring to the full 55.2 m, 'Half frame' to 27.6 m, 'Quarter frame' to 13.8 m and 'Single mast' being the single mast of samplers determined to be at the centre of the plume, extrapolated using Surfer software to a one-metre wide collection area.

Table 4.3: Apparent collection efficiencies of sections of the flux frame.

Run	Apparent collection efficiency \pm error (%) for:			
	Full frame	Half frame	Quarter frame	Single mast
6	23.0 \pm 77.8	21.9 \pm 53.7	21.4 \pm 38.9	39.4 \pm 10.7
7	49.6 \pm 34.7	53.4 \pm 23.1	50.6 \pm 15.6	48.8 \pm 4.6
8	45.3 \pm 42.1	41.4 \pm 29.5	41.4 \pm 21.1	39.4 \pm 5.9
10	81.2 \pm 35.7	58.7 \pm 24.0	61.3 \pm 17.5	73.4 \pm 5.1
11	113.9 \pm 19.3	55.1 \pm 13.3	83.4 \pm 9.8	88.3 \pm 2.7
12	97.8 \pm 17.2	74.7 \pm 11.6	85.8 \pm 8.6	97.8 \pm 2.3

In 4 of the 6 cases, the apparent collection efficiency when using just one mast of samplers and extrapolating to a 1 m wide plume using Surfer agrees with the collection efficiency for the full flux frame to within 8%. In the worst case (Run 11), this difference is as high as 26%, although the estimate using the full size flux frame is over 100%. Figure 4.27a is the plot of the plume using half of the frame of samplers for run 7, whilst 4.27b is the plot of the centre mast of samplers extrapolated to a 1 m wide plume. The profile of decreasing flux with height can be seen to follow a very similar trend.

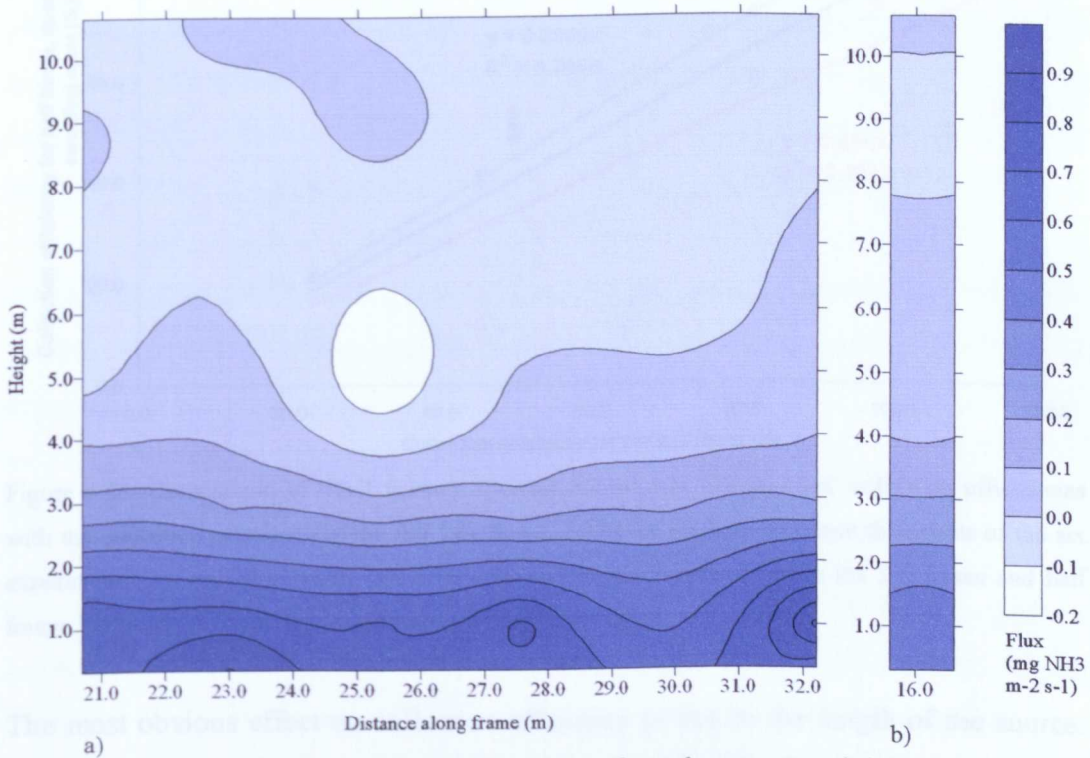


Figure 4.27: a) Run 7: Half frame; b) Run 7: Single mast of samplers at centre of plume.

The collection efficiency measured using the full flux frame was compared to each of the apparent collection efficiencies calculated for half the flux frame, a quarter of the flux frame and for a single sampling mast. This is plotted in Figure 4.28, with the y intercept forced through zero. The linear regressions show that the collection efficiency of a single sampling mast compares best with that of the full flux frame, with a collection efficiency 90% of that measured using the full flux frame. However,

only the p value for a quarter frame vs. a full frame is significant ($p < 0.05$) and the high errors associated with each of the four different sampling configurations means that the margins of error overlap and that any configuration would produce an equally accurate result (Table 4.3).

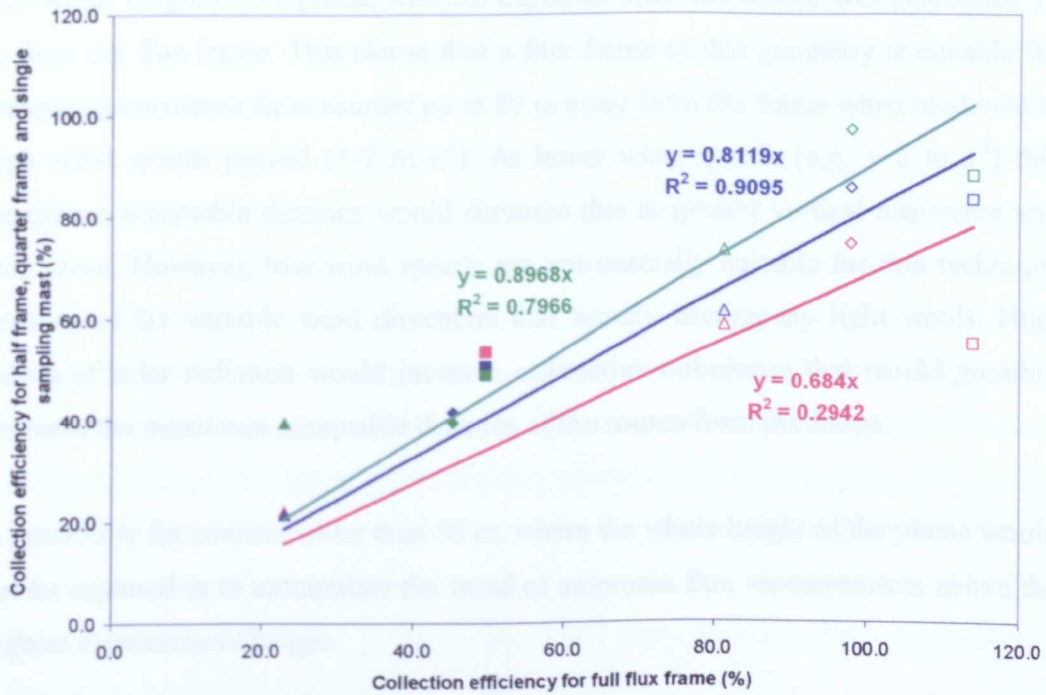


Figure 4.28: Comparison of ‘Half frame’, ‘Quarter frame’ and ‘Single mast’ collection efficiencies with the collection efficiency of the full flux frame. Different symbols represent the results of the six experimental runs; Red symbols and lines refer to the relationship between the full frame and half frame, blue – full and quarter, and green – full and single mast.

The most obvious effect on collection efficiency is due to the length of the source. Looking at the collection efficiencies for the 1 m wide plume, it can be seen that for runs 6, 7 and 8, for which the source is longer than the frame (or almost as long as, in the case of Run 8), the collection efficiency is around 40-50%. In runs 10, 11 and 12, for which the source is shorter than the flux frame, the collection efficiency is around 70-100%.

4.4 DISCUSSION

4.4.1 Capture of the height of the plume

The whole height of the plume was just captured when the source was positioned 50 m from the flux frame. This shows that a flux frame of this geometry is suitable for measuring emissions from sources up to 50 m away from the frame when moderate to high wind speeds prevail (4-7 m s⁻¹). At lower wind speeds (e.g. < 2 m s⁻¹) this maximum acceptable distance would decrease due to greater vertical dispersion and *vice versa*. However, low wind speeds are not normally suitable for this technique because of the variable wind directions that usually accompany light winds. High values of solar radiation would increase convective turbulence that would possibly decrease the maximum acceptable distance of the source from the frame.

A possibility for sources wider than 50 m, where the whole height of the plume would not be captured is to extrapolate the trend of ammonia flux measurements above the highest measurement height.

4.4.2 Agreement between ammonia release experiments

The agreement between two runs with nominally similar conditions (i.e. a point source at 25 m) is complicated by the other factors which varied, for example, release rates with temperature, and different wind speeds and directions. Therefore they are not true repeats and must be looked at individually. For example, Runs 2 and 3 have the same ammonia release conditions (point source at a distance of 25 m from the flux frame). However (most obviously), the wind direction is almost 60° different and the plume of emissions for Run 2 is not completely captured by the flux frame. This explains, in part, the 13% difference in their measured collection efficiencies.

4.4.3 Agreement between measured and modelled plots

The agreement between measured and modelled results was generally good with six of the eleven measured and modelled efficiencies being within 11.5%, and the maximum difference being 37.3%. The average difference for all 11 Runs was 16.9%, once again, with no bias for over- or under- prediction. However, Hanna *et al.* (2001) found that ADMS had an average underprediction of 20%. The poorest agreement was found using long line sources, where the whole plume was not captured. Point sources generally had the best agreement, and this is likely to be due to the whole, or at least the majority, of the plume being captured by the flux frame.

O values (Table 4.2) show that the agreement between measured and modelled values is no better for either point or line sources. In contrast, R^2 values suggest that overall the model predicts the flux at each sampling position better when using line sources than when using point sources. If line sources were predicted better, this could have been due to variations in wind direction (i.e. turbulence and lateral spread) being less important when a line source is used, particularly when the source is longer than the width of the flux frame and edge effects are not visible.

One explanation for the disagreement between measured and modelled collection efficiencies in Runs 5, 8, 11 and 12 could be the high average wind speed measured throughout the exposure period, shown in Table 4.1. In three of these runs the average wind speed was close to 7 m s^{-1} . In Run 8, where the highest difference was found, a maximum wind speed of 12.61 m s^{-1} was measured which is much higher than the maximum wind speed recommended for the sampler to perform optimally (Chapter 2). Breakthrough may have occurred which would reduce the measured collection efficiency. However, even in Run 12 where the highest wind speeds were measured, there was no evidence of breakthrough in the data, with the average amount of ammonia captured on the background tubes being less than 1% of that captured on the source tubes.

Hanna (1993) report that, despite the large number of air quality models available, the uncertainties are not well known due to the lack of comprehensive studies using independent data sets. During his study, using several different models and data sets, he found differences between modelled and measured values to be typically ± 20 to 40%, and as high as 50% in certain cases. He reports that, as good as the model may be, there are always uncertainties due to data input errors and turbulent processes.

4.4.4 Collection efficiency using sections of the flux frame

Figure 4.28 shows that measurements made with half a flux frame, quarter of a flux frame and a single sampling mast agree with the collection efficiency of the full flux frame within 68, 81 and 90% respectively. Each configuration has a high error associated with the flux estimate and the error margins overlap in each case. Therefore, one single mast of samplers extrapolated to one-metre wide gives an estimate of collection efficiency to within 10% of that given by a full size flux frame (55.2 m wide, supporting 156 samplers) with the smallest error margins.

4.4.5 Potential for loss of ammonia

For 8 out of the 11 successful measurement runs, the collection efficiency of ammonia was less than 80% of the amount released. Potential areas of loss were therefore identified.

As water is a sink for ammonia, this introduces a number of potential areas for loss, including dew and light rain. Early morning dew, which may absorb the ammonia, evaporates as solar radiation and temperature increase during the day. A light shower would have the same effect but if it occurred early in the day the ammonia would possibly be re-emitted as the water evaporates. If rain occurred towards the end of the run, the amount of ammonia captured would be very small and have little effect on the overall collection efficiency. This assumes that the shower is very light, otherwise the acid coating would be washed off the sampler. Light showers occurred during two

of the runs (1 and 8) and before Run 6, however these were very short in duration (a few minutes). Dew was present at the beginning of Runs 10 to 12 which took place at the end of October and the beginning of November 2001. As dew would have evaporated during the first few hours of the experiments, and the showers were very short and light, any ammonia captured would have been re-emitted.

Another possible area of loss could be to the grass itself, despite the low deposition rate calculated (Appendix 4). The grass on which the experimental runs took place was unfertilised, so the amount of ammonia in the grass was likely to be low. Therefore, the concentration of ammonia in the air during ammonia release would have been high enough for the partial pressure to be greater than the equilibrium (compensation point) of ammonia emission and uptake for the grass. Thus, ammonia is likely to be taken up and the grass would act as a sink (Galbally and Roy, 1983; Schjoerring *et al.*, 1998).

4.4.6 Usefulness of flux frame method

Twelve successful runs were performed in the 16 months that the flux frame was erected at the field site. This questions the practicality of the method because the time required to prepare the sampling tubes, assemble, deploy and remove the samples from the flux frame and analyse the samples was two weeks for each run. However, so long as there is a plentiful supply of sampling tubes - which in the case of this project was a minor limitation - experimental runs can be set up whilst conditions are suitable and the samples can be stored and analysed later, when external conditions are not suitable for runs. Due to the nature of British weather, suitable conditions for external runs tended to be either a single day every now and then or many days in a row. Hot summer weather when no rain fell was often accompanied by calm wind conditions which leads to variable wind direction, both of which are unsuitable for using flux samplers and the flux frame method. The permanent position of the flux frame further limited its use to a particular wind direction, as during dry conditions throughout the summer periods of both years, the correct wind direction either did not

occur or calm conditions prevailed. Thus, most runs were performed in the months of September to November.

Despite the ability to control or monitor conditions at the field site, this set of measurements does not represent what would occur at a large farm. The farm to be used during the field campaign (Chapter 5) is a very large heterogeneous area source, whilst these measurements used a relatively small, homogeneous point or line source.

4.4.7 Future work

Whilst the line source was used to represent the far edge of an area source, the resulting plume of emissions is not the same as that from an area source. The maximum distance the furthest edge of an area source can be from the flux frame is the same, but the cumulative effect of the source closer to the flux frame is not shown. This however is a minor limitation to the validation. An improvement or possibility for future work would be to validate the flux frame using a controllable ammonia area source.

For the flux frame to estimate the source strength accurately the source must be homogeneously distributed, but the spatial variability of the ammonia emission from the farm is not known. Future work could include a study of the spatial variability of excretory behaviour in free-range sows to increase knowledge of this area.

4.5 CONCLUSIONS

The flux frame method has been validated at full scale for ammonia emission from line and point sources. Sources up to 50 m from the flux frame were measured using the flux frame at wind speeds down to around 4 m s^{-1} . For sources deeper than 50 m and wind speeds less than 4 m s^{-1} , extrapolation of the measurements above the height of the sampling frame would allow an estimate of emission to be made.

The average measured efficiency of a point source was 56.4%, whilst the average measured efficiency of a line source was 68.5%. Therefore, a flux frame would be suitable for measurements of ammonia emissions from source areas with clearly defined boundaries (such as slurry lagoons or livestock buildings), with an appropriate correction factor.

A full size flux frame was shown to be unnecessary to measure ammonia emissions from an area source. One column of samplers estimates the collection efficiency of the source to within 10% of that estimated by the whole frame. Therefore single masts of samplers may be erected at different sites around an area source, alleviating the problem positioning the flux frame to maximise the number of sampling days. This would also ease the setting up of samplers in a farm environment.

ADMS modelling of the collection efficiency agreed on average to within 16.9% (s.d. 12.5) of the measured collection efficiency of the flux frame.

Limitations are the necessity of a suitable wind direction depending upon the orientation of the flux frame and dry conditions before and during the measurement run.

5. MEASUREMENT OF AMMONIA EMISSIONS AT A FREE-RANGE SOW FARM

5.1 INTRODUCTION

Ammonia volatilisation from outdoor pig farming systems has been measured by Williams *et al.* (2000) during a two-year field study, along with nitrate leaching and nitrous oxide emissions. Losses of ammonia from outdoor dry sows were found to be in the region of $11 \text{ g NH}_3 \text{ sow}^{-1} \text{ day}^{-1}$. Ferm tubes coated with 3% oxalic acid in acetone solution were exposed for periods of 4 weeks at heights of 0.2, 0.4, 0.8, 1.1, 2.2, 3.3, 4 and 5 m above ground level, 40 m from the south western edge of each paddock. Wind speed and direction measurements were taken throughout the sampling period. Ammonia losses were reported to be similar to those measured by Misselbrook *et al.* (2000) for grazing dairy and beef cattle. It is known that Ferm tubes are rendered useless when rain is experienced due to the acid coating being washed out of the tube, however, only the season total is presented, with no indication of rainfall during each measurement period. This limitation may cast doubt on the validity of the emission estimate.

Another study performed by Sommer *et al.* (2001) used passive ammonia flux samplers in a mass balance technique along with measurements of spatial variability using dynamic chambers to estimate the annual ammonia volatilization from sows with piglets on organic farms. They found that ammonia volatilization was spatially very variable, with greatest volatilization nearest the feeding area and the pig huts, which corresponded with their urination behaviour. Using their measurements and a model, which takes account of all parameters affecting ammonia volatilization, an annual ammonia volatilization rate was calculated as $4.8 \text{ kg NH}_3 \text{ sow}^{-1}$ (with piglets).

Other ammonia emission rates reported in literature are for intensively housed pigs. For example, estimated ammonia emission rates from livestock buildings, measured using thermal converters with chemiluminescence NO_x-analysers, were found to be

46.9 kg lu⁻¹ yr⁻¹ for a fattening pig unit (lu = livestock unit, 500 kg – which allows for comparison between different types of livestock) (Demmers *et al.*, 1999). Another study on slurry-based sow units in Europe monitored over 24 hours in wintertime gave an internal ammonia concentration in the range of 5.3-17.4 ppm (Phillips *et al.*, 1998b). In a similar study ammonia concentrations were found to be between 5 and 18 ppm in pig houses, while emission rates varied between 22 and 1298 mg NH₃ hr⁻¹ animal⁻¹ (0.022 and 1.298 g hr⁻¹ animal⁻¹). There were, however, large variations between countries and the season (Groot Koerkamp *et al.*, 1998).

If a sow is taken to be 190 kg in weight, a comparison can be made between the four emissions rates, Table 5.1.

Table 5.1: Comparison of reported ammonia emission rates.

Reported emission rate	Emission rate g NH ₃ kg ⁻¹ (of sow) day ⁻¹	Reference
11 g NH ₃ sow ⁻¹ day ⁻¹	0.06	Williams <i>et al.</i> , 2000
4.8 kg NH ₃ sow ⁻¹ yr ⁻¹	0.07	Sommer <i>et al.</i> , 2001
46.9 kg NH ₃ lu ⁻¹ yr ⁻¹	0.26	Demmers <i>et al.</i> , 1999
22-1298 mg NH ₃ hr ⁻¹ animal ⁻¹	0.003 - 0.16	Groot Koerkamp <i>et al.</i> , 1998

Whilst the emission rates reported by Williams *et al.* (2000) and Sommer *et al.* (2001) for outdoor sows are within the range reported by Groot Koerkamp *et al.* (1998) for housed pigs, the emission rate for housed pigs reported by Demmers *et al.* (1999) is four times that measured for outdoor sows. This agrees with Jarvis (1991), who found that ammonia losses associated with housed animals can be between 3.5 to 11.4 times greater per animal than for grazing cattle and sheep.

Although there have been two estimates of ammonia emissions from free-range sows, the Williams *et al.* (2000) study lacks rainfall data, which makes it difficult to assess the reliability of the results, and Sommer *et al.*'s (2001) measurements were taken for a small number of sows (6-11). Therefore, this type of source, whilst increasing in popularity, requires further quantification. The aim of this set of measurements was to

use a variation of the fully validated flux frame method to make reliable full-scale measurements of ammonia emission from free-range sows.

Preliminary measurements were made at a free-range sow farm using recurved passive ammonia flux samplers on two occasions, at heights of 0.3 and 0.99 m, for exposure periods of 7 and 72 hours. Subsequently, six sampling masts were erected at the farm around the perimeter of the paddocks and three measurement runs lasting 2-4 days were undertaken.

5.2 MATERIALS AND METHODS

5.2.1 Farm

Figure 5.1 shows an aerial photograph taken of the farm (www.multimap.co.uk), which is situated next to the A507 near Steppingley, Bedfordshire (coordinates 501600, 238000). Figure 5.2 shows typical conditions found at the farm. Approximate dimensions of the area under investigation are 435 m x 330 m x 525 m x 362.5 m. The area is approximately 0.158 km². The pigs are all Landrace x Duroc x Large White hybrids.



Figure 5.1: Aerial photograph of farm (www.multimap.co.uk).



Figure 5.2: Typical conditions at farm.

5.2.2 Preliminary Investigation

Thirteen posts were positioned at 8 locations around the perimeter of the free-range sows and 5 locations within the area under investigation. Samplers were attached at heights of 0.3 and 0.99 m above ground – these were assumed to be the heights where most ammonia would be captured, as during validation experiments (Chapters 3 and 4) this was shown to be the case. Exposure periods of 7 and 72 hours were used. Meteorological conditions were monitored throughout the exposure period.

5.2.3 Flux sampling

A simplified version of the flux frame was used at the farm. Individual masts were erected at six positions around the outside of the main sow confinement area that houses breeding sows and boars (Figure 5.3). The six positions were chosen to allow sampling to take place no matter what the wind direction during the measurement period, with two masts on each of the longest sides of the paddock. Farrowing sows are housed to the South and East of this area. A permanent structure can be seen to be positioned in the south-west corner of the farm in Figure 5.3. This is not visible on the aerial photograph as the structure was erected around a month before sampling began at the farm. Each of the six masts (Figure 5.5) had a pulley system, which allowed the seven samplers to be raised and lowered vertically to the desired height. Metal guide wires were attached from the top to the bottom of the sampling mast and pulled taught, thereby maintaining the correct orientation of the samplers. The pulley arrangement avoided the need for frames to be lowered into the pig paddock, which would have increased the risk of contamination due to the close proximity of the source whilst the samplers were being attached. This would also have caused technical difficulties, e.g. having to fence off an area of paddock to keep the pigs away from the frame whilst attaching the samplers and the chance of dropping the frame into the mud after wet weather. Figure 5.4 shows a scale diagram of the measurement positions and their respective heights. Figure 5.5 shows a sampling mast in use, and the pulley system using ropes to hoist the samplers up to each

sampling height. In total, 42 samplers were deployed around the farm. Coating of the tubes and analysis of the samples was undertaken as described in section 1.13.1.1 and Appendix 1.

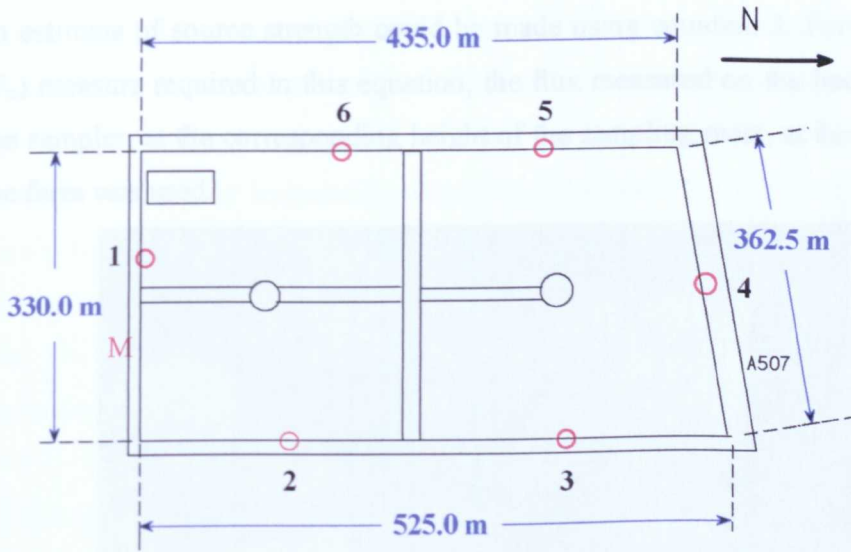


Figure 5.3: Positions of sampling masts around farm perimeter on simplified plan of the site.

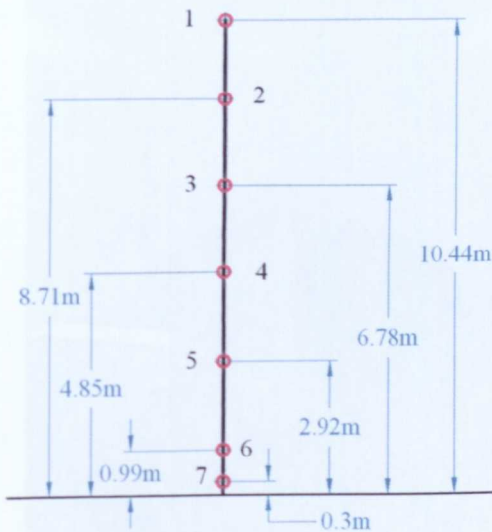


Figure 5.4: Schematic of sampling mast.

Three successful measurement periods were achieved out of five undertaken (rain rendered two runs useless) during the period May – July 2002, and ranged in length from 2 to 4 days depending on the weather forecast (if rain was forecast, the samplers were removed). If a measurable amount of ammonia was measured at the farm, then an estimate of source strength could be made using equation 3. For the upwind flux (F_u) measure required in this equation, the flux measured on the background tube of the sampler, at the corresponding height of the sampling mast, at the opposite side of the farm was used.

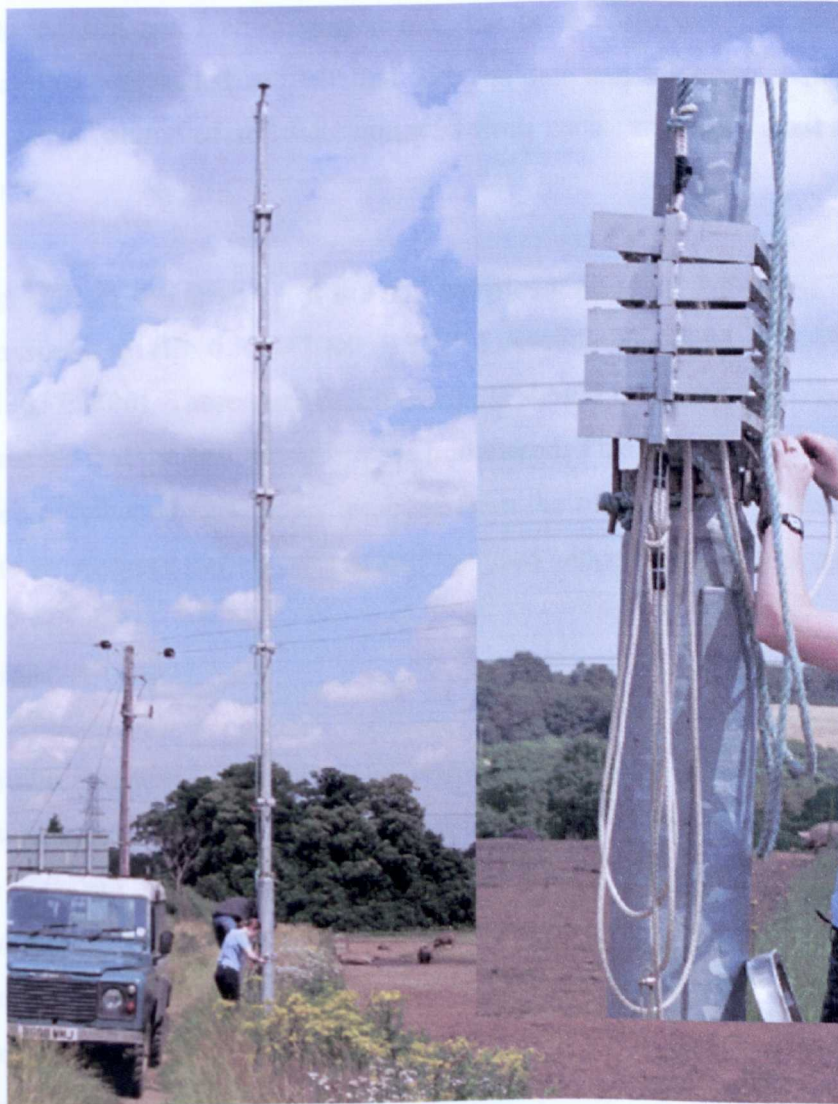


Figure 5.5: Sampling mast in use at farm. (position 4 on Figure 5.3). Inset: Close-up of sampler holders lowered to enable samplers to be attached.

5.2.4 Soil Sampling

As soil moisture content and pH are important factors involved in ammonia volatilization (Freney *et al.*, 1983), measurements of these properties were taken during the field campaign. Twenty locations were chosen at random across the farm to determine the variability of the soil properties across the farm, from which three soil cores were taken. In later runs just six sampling positions were chosen. The three cores were taken by hammering a stainless steel cylinder of 80 mm i.d. and 50 mm depth into the soil and then digging it out. The three cores were transferred into a plastic bag that was sealed and labelled with the date and sampling position. In this way, the same volume of soil was removed from each sampling location from the same depth.

Sampling, storage and analysis of the soil samples took place following British and European Standards (EN 13040:2000; BS 7755: Section 3.1: 1994; ISO 11465:1993; BS EN 13037:2000). These state that the sample should be transported and stored in such a manner that the soil properties are not altered. This means storing the sample in a closed polythene bag with air removed from the bag at 1 – 5 °C (not freezing). The soil to be analysed must be sieved and analysed within two weeks of collection.

5.2.4.1 Moisture content

To determine moisture content, the collected soil was mixed well and large objects, such as stones (greater than 2 mm), were removed. A suitable container was dried at 105°C ± 5°C and then cooled in a desiccator for 45 minutes. The mass of the container was then determined to an accuracy of 10 mg. The soil sample was transferred to the container and the mass of the container and the soil was determined to the same accuracy. The sample was then dried at 105 °C ± 5 °C for 16 to 24 hours (until constant mass was reached), and was then cooled. The mass was once again determined to an accuracy of 10 mg. The moisture content was then determined using equation 28:

$$W_m = \frac{(M_w - M_D)}{(M_w - M_T)} \times 100 \quad (28)$$

where W_m is the moisture content (%), M_w is the mass of the wet sample plus the container (g), M_D is the mass of the dried sample plus the container (g) and M_T is the mass of the empty dry container (g).

5.2.4.2 pH

60 ml of sample soil was sieved through a 20 mm sieve and transferred to a container with a lid. 300 ml of UHQ water were added, the lid was secured and the container was shaken for 1 h on a shaking machine at $22^\circ\text{C} \pm 3^\circ\text{C}$. The pH meter was calibrated using pH 4 and 7 buffer solutions. The sample was agitated just before measurement and the pH was measured in the settling suspension. The pH was recorded after allowing the reading to stabilise for 15 s.

5.2.5 Additional information

The area from which the measurements were being taken housed the breeding sows and boars (ratio 6:1), whilst farrowing sows and piglets were housed to the South and East of this area. It was necessary to know the number of pigs housed on the area from which the ammonia emissions were being measured along with their approximate live weight during the exposure period. The stockman provided this information after each measurement run was completed.

5.2.6 Meteorological station

Meteorological measurements were taken throughout the experimental period at a meteorological station erected at the farm. This enabled the changing environmental conditions to be logged throughout the measurement period, and provided accurate

data for dispersion modelling, if required. The measurements comprised wind speed and direction from a cup anemometer (Porton anemometer, type A100, Vector instruments, Rhyl) and wind vane (Potentiometer wind vane, type W200P, Vector instruments, Rhyl), and rainfall measurements using a rain gauge (Tipping bucket, product ARG 100/EC, Campbell Scientific Ltd., Shepshed). Five-minute averages were collected every five minutes during the measurement period using a data logger (21X Micrologger, Campbell Scientific Ltd., Shepshed) powered using a 12V car battery. The position of the meteorological station is labelled as 'M' on Figure 5.3.

5.3 RESULTS

5.3.1 Preliminary results

The maximum measured horizontal flux during the first preliminary run was $0.06 \text{ mg NH}_3 \text{ m}^{-2} \text{ s}^{-1}$. However, there was no distinguishable difference between the amounts of ammonia captured on each tube (that capturing ammonia from the source, and that capturing it from the background). The maximum horizontal flux measured during the second preliminary run was $0.03 \text{ mg NH}_3 \text{ m}^{-2} \text{ s}^{-1}$. However, larger amounts of ammonia were captured on each tube, particularly the source tube, and a determinable difference was seen. This was due to the longer exposure period allowing a better estimate of ammonia mass to be found. For example, $4.78 \text{ } \mu\text{g}$ of ammonia were captured on the source tube whilst $0.62 \text{ } \mu\text{g}$ of ammonia were captured on the background tube. This highlighted the need for long sampling periods to minimise errors.

5.3.2 Flux sampling

The horizontal fluxes measured at each sampling position for each of the three successful runs are presented below.

5.3.2.1 Run 1

The net horizontal flux at each sampling height was calculated using equation 14 (including a correction factor calculated in Chapter 2), and Table 5.2 shows the resulting fluxes.

Table 5.2: Net fluxes measured at each sampling position, Run 1.

	Net Flux ($\mu\text{g NH}_3 \text{ m}^{-2} \text{ s}^{-1}$)					
Mast						
Sampling height (m)	1	2	3	4	5	6
10.44	-1.96	1.30	-5.93	7.23	29.21	4.55
8.71	2.13	-0.13	-5.74	4.62	4.65	-1.77
6.78	-4.47	-6.76	-1.92	7.71	-8.00	-9.73
4.85	-3.81	7.74	-4.41	12.96	-2.13	5.08
2.92	4.59	-22.49	-6.35	7.64	7.40	2.43
0.99	-2.60	-49.59	-1.63	28.36	10.11	-2.86
0.30	-1.43	-41.21	-5.82	8.03	3.80	-8.38

Figure 5.6 shows the change in net horizontal flux with height for each of the six sampling masts. Only mast 4 has positive values for all seven of the flux measurements, and only mast 3 has all negative values. There appears to be no clear trend in horizontal ammonia flux with increase in height, and certainly no similar trend between different sampling masts. Table 5.3 shows the measured fluxes on each individual tube of the flux sampler. S is the tube pointing towards the source which captures the ammonia when the wind blows across the source ($\pm 80^\circ$), whilst B was the amount of ammonia captured on the tube pointing away from the source (background tube). The fluxes on both the S and B tubes are similar, and it would be difficult to decide which tube is facing the source and which is facing the background.

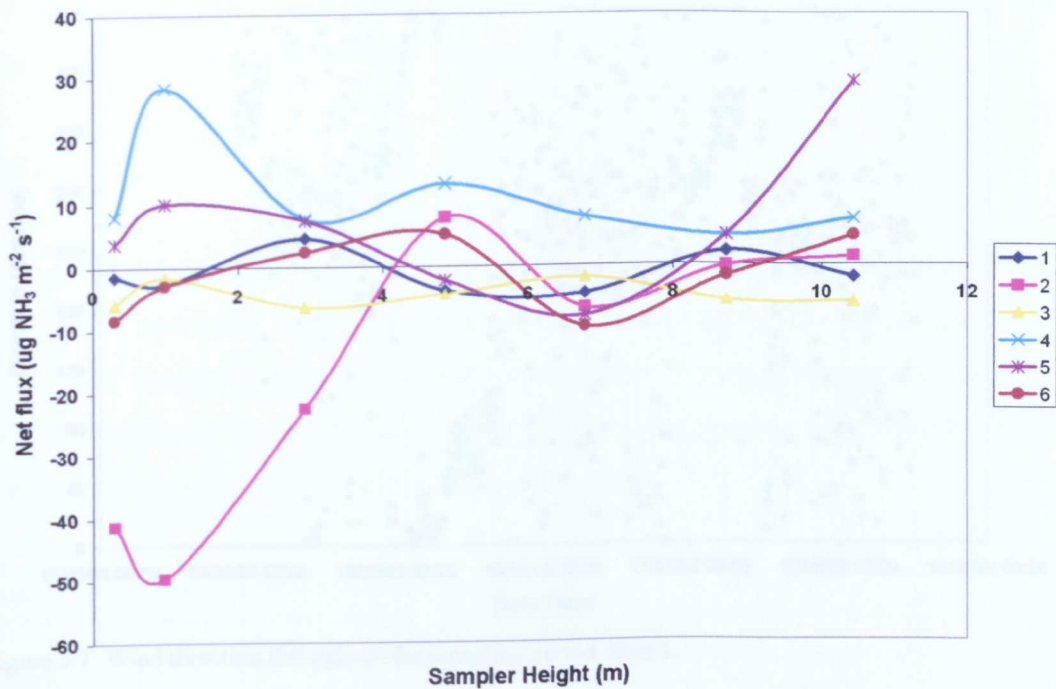


Figure 5.6: Change in net flux with height for each sampling mast (1-6), Run 1.

It is not clear whether the whole height of the plume of emission is captured by the sampler at 10.44 m, as net horizontal fluxes at least as high as those measured at lower heights are found at the top sampling position.

Table 5.3: Fluxes measured on individual tubes of the sampler, Run 1.

Mast	Flux (ug NH ₃ m ⁻² s ⁻¹)											
	1		2		3		4		5		6	
Sampling height (m)	S	B	S	B	S	B	S	B	S	B	S	B
10.44	2.56	4.75	5.02	3.65	1.28	7.67	19.64	11.78	43.47	11.87	13.79	8.95
8.71	8.40	6.03	4.75	4.84	1.92	8.13	14.61	9.59	11.78	6.76	12.79	14.70
6.78	3.11	7.95	6.48	13.88	7.95	9.95	13.33	4.93	15.34	24.02	5.30	15.80
4.85	6.76	10.96	20.91	12.42	5.21	9.95	21.46	7.40	17.44	19.73	10.78	5.30
2.92	18.63	13.61	11.23	35.71	5.48	12.33	21.37	13.06	21.37	13.33	16.07	13.52
0.99	6.03	8.95	6.94	60.91	12.33	14.16	34.52	3.74	26.48	15.53	17.35	20.37
0.30	2.47	4.11	2.37	47.22	5.57	11.87	15.89	7.12	15.34	11.23	13.52	22.56

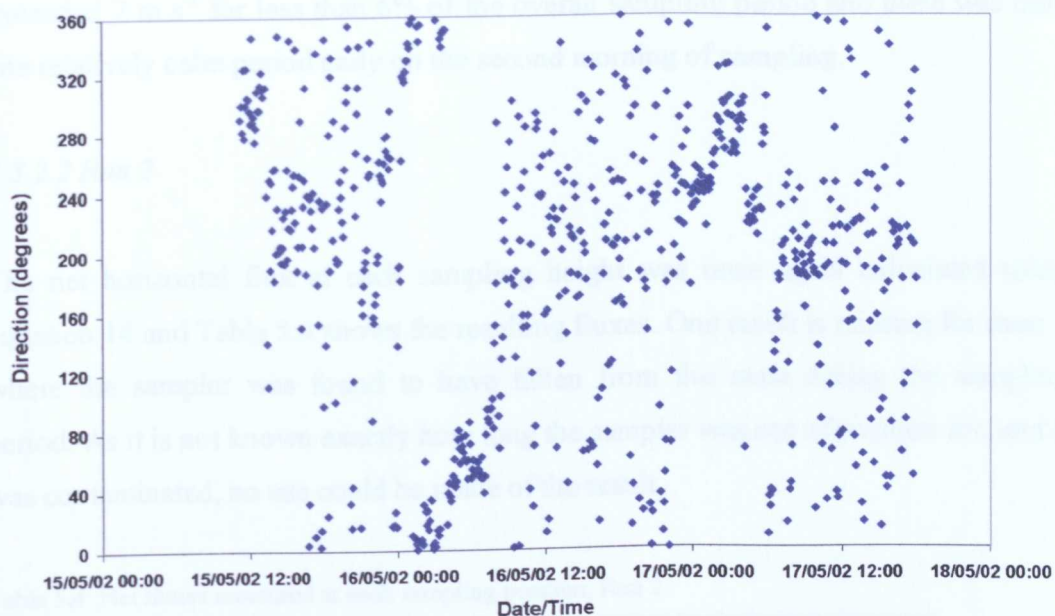


Figure 5.7: Wind direction throughout the sampling period, Run 1.

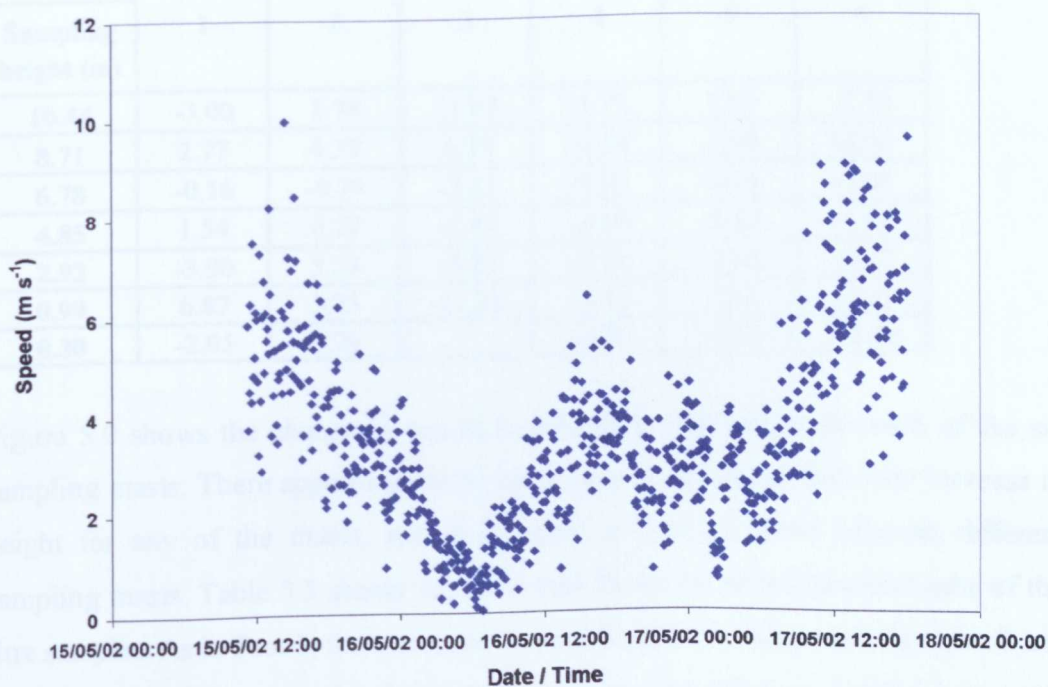


Figure 5.8: Wind speed throughout the sampling period, Run 1.

Figures 5.7 and 5.8 show the wind data collected throughout Run 1. The wind direction was variable throughout the whole sampling period. The wind speed

exceeded 7 m s^{-1} for less than 6% of the overall sampling period and there was only one relatively calm period early on the second morning of sampling.

5.3.2.2 Run 2

The net horizontal flux at each sampling height was once again calculated using equation 14 and Table 5.4 shows the resulting fluxes. One result is missing for mast 3 where the sampler was found to have fallen from the mast during the sampling period. As it is not known exactly how long the sampler was out of position for, and it was contaminated, no use could be made of the result.

Table 5.4: Net fluxes measured at each sampling position, Run 2.

	Net Flux ($\mu\text{g NH}_3 \text{ m}^{-2} \text{ s}^{-1}$)					
Mast						
Sampling height (m)	1	2	3	4	5	6
10.44	-3.00	1.78	-3.97	-1.71	3.49	-2.58
8.71	2.77	4.37	6.39	-0.50	-1.98	12.02
6.78	-0.16	-0.74	-7.63	-3.01	-7.34	-0.03
4.85	1.54	0.27	-1.42	-4.48	-2.60	-1.47
2.92	-3.90	3.23	-5.23	-2.38	-1.64	-0.77
0.99	6.87	5.33	-11.21	-1.66	2.22	-3.45
0.30	-2.05	0.76		-9.76	-2.43	-12.52

Figure 5.9 shows the change in net horizontal flux with height for each of the six sampling masts. There appears to be no clear trend in ammonia flux with increase in height for any of the masts, and once again no similar trend between different sampling masts. Table 5.5 shows the measured fluxes on each individual tube of the flux sampler. As in Run 1, there is no obvious difference in most cases between S and B tubes and both have similar fluxes (which is why the values in Table 5.3 alternate between positive and negative values).

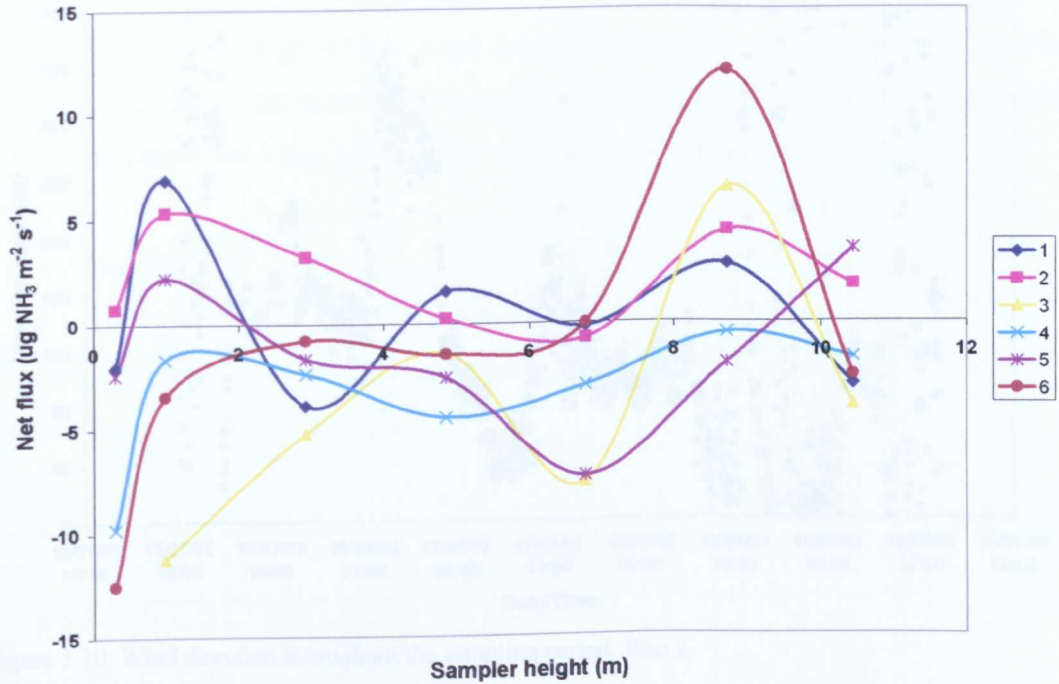


Figure 5.9: Change in net flux with height for each sampling mast (1-6), Run 2.

Figure 5.9 suggests that the whole height of the plume was not captured during Run 2.

Table 5.5: Fluxes measured on individual tubes of the sampler, Run 2.

Mast	Flux ($\mu\text{g NH}_3 \text{ m}^{-2} \text{ s}^{-1}$)											
	1		2		3		4		5		6	
Sampling height (m)	S	B	S	B	S	B	S	B	S	B	S	B
10.44	9.12	12.17	8.26	6.49	1.93	5.88	11.10	12.83	13.74	10.29	3.50	6.08
8.71	10.59	7.86	14.14	9.78	16.98	10.59	9.73	10.24	7.50	9.48	19.77	7.76
6.78	10.95	11.10	9.94	10.65	1.27	8.92	5.68	8.67	6.18	13.53	3.14	3.14
4.85	11.15	9.63	9.63	9.38	7.15	8.57	3.40	7.86	9.73	12.32	5.27	6.74
2.92	12.88	16.27	13.08	9.89	2.69	7.91	2.23	4.61	8.72	10.34	1.62	2.38
0.99	17.34	10.44	14.30	8.97	3.70	14.90	4.26	5.93	11.76	9.53	2.53	5.98
0.30	8.62	10.65	6.18	5.42			9.18	18.96	10.90	13.28	2.33	14.85

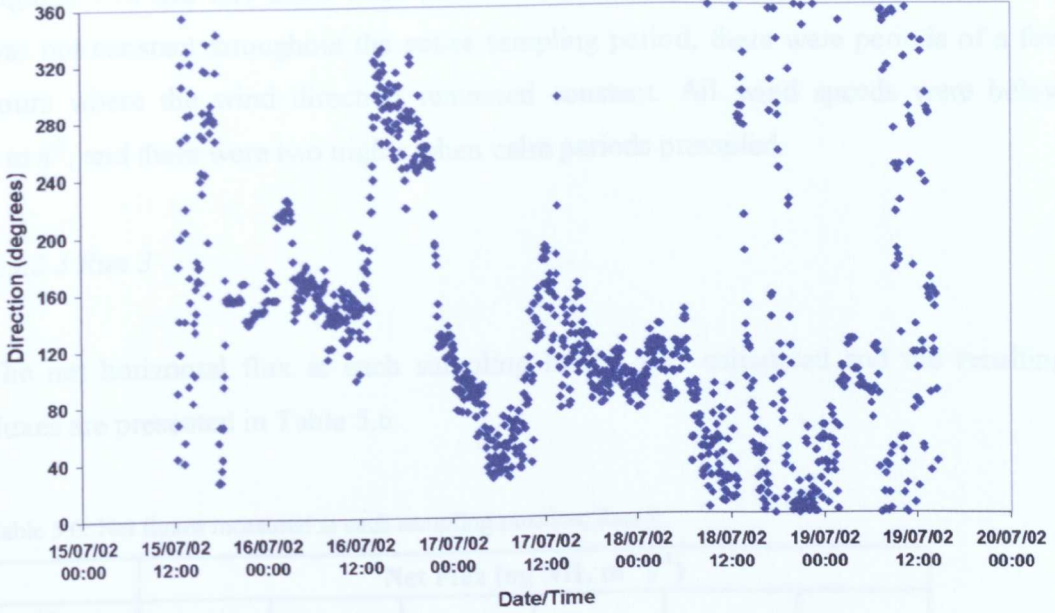


Figure 5.10: Wind direction throughout the sampling period, Run 2.

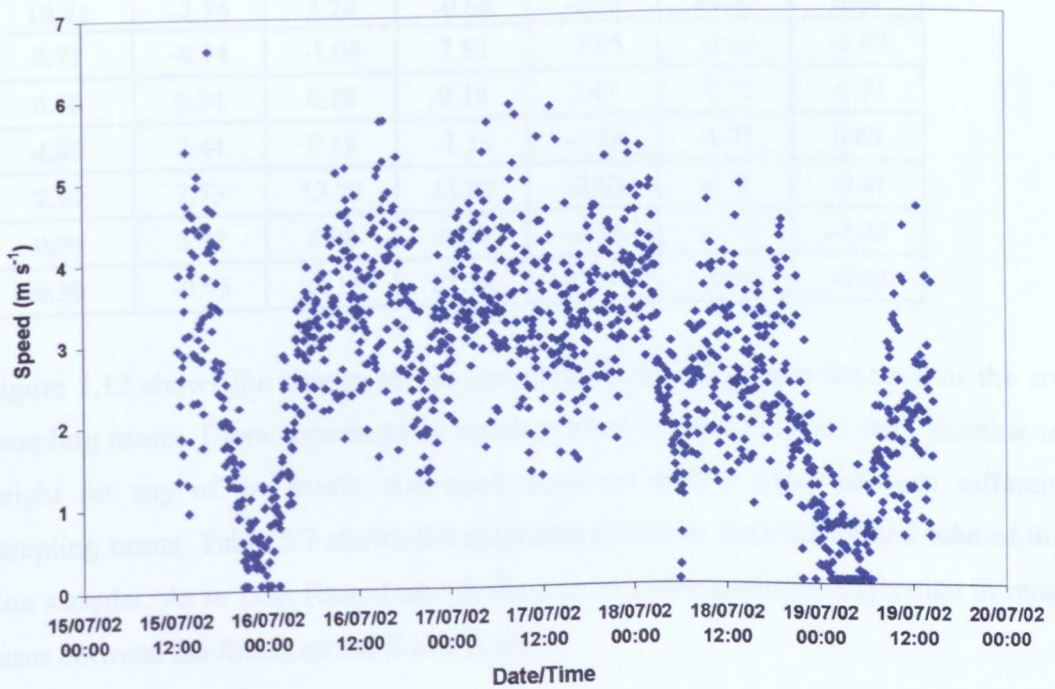


Figure 5.11: Wind speed throughout the sampling period, Run 2.

Figures 5.10 and 5.11 show wind data collected during Run 2. Whilst wind direction was not constant throughout the entire sampling period, there were periods of a few hours where the wind direction remained constant. All wind speeds were below 7 m s^{-1} , and there were two nights when calm periods prevailed.

5.3.2.3 Run 3

The net horizontal flux at each sampling height was calculated and the resulting fluxes are presented in Table 5.6.

Table 5.6: Net fluxes measured at each sampling position, Run 3.

	Net Flux ($\mu\text{g NH}_3 \text{ m}^{-2} \text{ s}^{-1}$)					
Mast						
Sampling height (m)	1	2	3	4	5	6
10.44	-2.76	3.28	-0.68	-3.83	10.43	0.01
8.71	-0.34	-1.00	7.52	-2.05	-0.60	-3.89
6.78	6.54	0.78	9.18	3.47	-1.75	-0.91
4.85	2.44	9.18	-1.16	-1.78	-2.71	0.69
2.92	2.73	13.25	11.03	-2.63	0.51	-0.81
0.99	3.32	6.98	6.60	-2.44	-1.19	-1.25
0.30	-0.95	-2.17	21.74	-13.44	-3.64	-0.63

Figure 5.12 shows the change in net horizontal flux with height for each of the six sampling masts. There appears to be no clear trend in ammonia flux with increase in height for any of the masts, and once again no similar trend between different sampling masts. Table 5.7 shows the measured fluxes on each individual tube of the flux sampler. As in both Runs 1 and 2, there is no distinguishable difference in most cases between the fluxes on the S and B tubes.

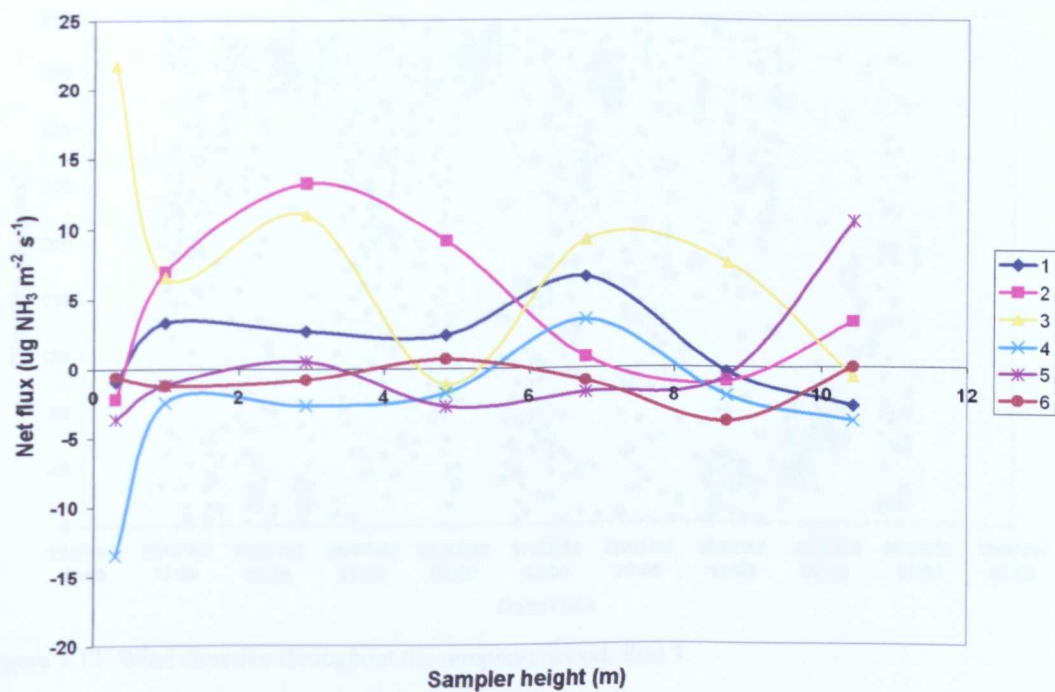


Figure 5.12: Change in net flux with height for each sampling mast (1-6), Run 3.

Table 5.7: Fluxes measured on individual tubes of the sampler, Run 3.

Mast	Flux ($\mu\text{g NH}_3 \text{ m}^{-2} \text{ s}^{-1}$)											
	1		2		3		4		5		6	
Sampling height (m)	S	B	S	B	S	B	S	B	S	B	S	B
10.44	8.84	11.60	8.12	4.85	3.27	3.99	3.42	7.26	14.56	4.14	5.72	5.72
8.71	3.99	4.34	11.55	12.52	11.24	3.73	4.70	6.80	5.88	6.49	0.97	4.85
6.78	12.42	5.88	8.02	7.21	13.85	4.65	8.94	5.47	5.62	7.41	2.61	3.53
4.85	6.03	3.58	15.59	6.44	5.88	7.05	3.27	5.06	4.19	6.90	6.13	5.47
2.92	8.02	5.26	15.74	2.50	28.87	17.83	4.39	7.00	6.64	6.13	2.20	3.01
0.99	9.40	6.08	15.89	8.89	15.74	9.10	1.02	3.47	0.72	1.89	2.15	3.42
0.30	7.77	8.74	5.31	7.46	31.99	10.22	4.14	17.58	14.36	17.99	4.45	5.11

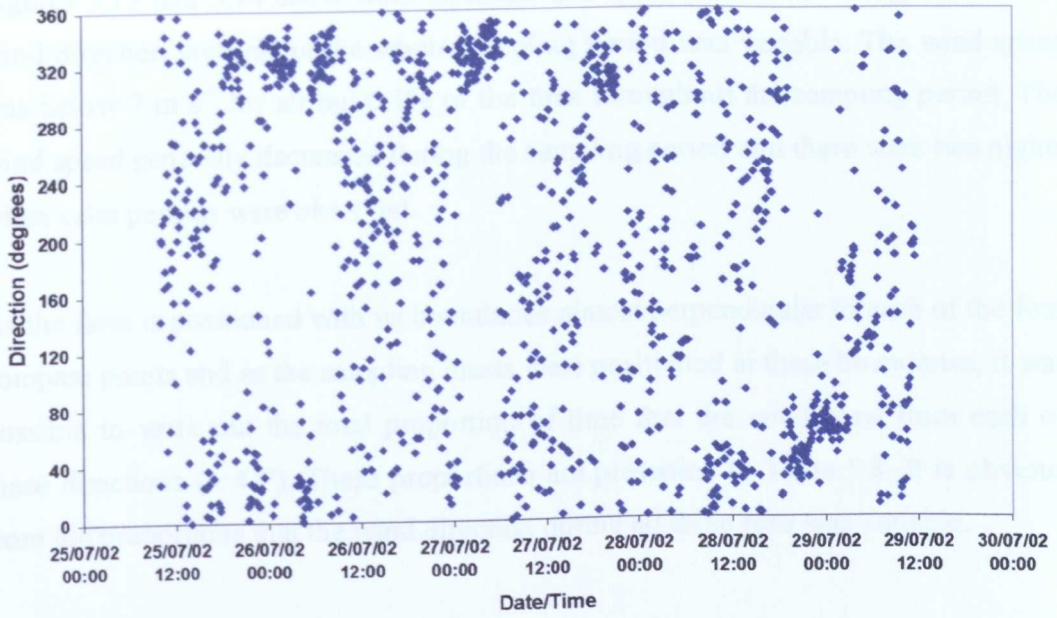


Figure 5.13: Wind direction throughout the sampling period, Run 3.

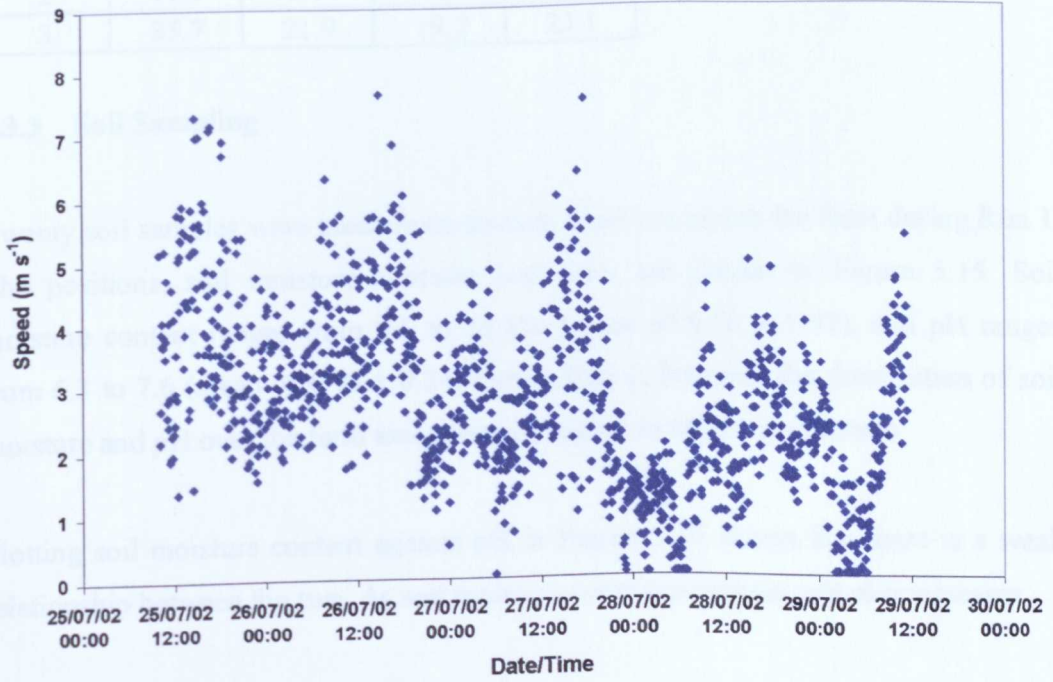


Figure 5.14: Wind speed throughout the sampling period, Run 3.

Figures 5.13 and 5.14 show wind direction and speed measured during Run 3. The wind direction throughout the whole sampling period was variable. The wind speed was below 7 m s^{-1} for all but 0.1% of the time throughout the sampling period. The wind speed generally decreased during the sampling period and there were two nights when calm periods were observed.

As the farm is positioned with its boundaries almost perpendicular to each of the four compass points and as the sampling masts were positioned at these boundaries, it was possible to work out the total proportion of time that the wind blew from each of these directions ($\pm 45^\circ$). These proportions are presented in Table 5.8. It is obvious from the proportions that the wind direction during all three runs was variable.

Table 5.8: Wind direction proportions, all Runs.

Run	Proportion (%) of wind from:			
	N	E	S	W
1	20.9	14.9	30	34.1
2	17.3	43.9	26.4	12.5
3	35.7	21.9	19.2	23.1

5.3.3 Soil Sampling

Twenty soil samples were taken from random locations across the farm during Run 1. The positions, soil moisture contents and pH's are shown in Figure 5.15. Soil moisture content ranges from 6.6 to 13.3% (mean of 9.16 ± 1.97), and pH ranges from 6.3 to 7.6 (mean of 6.95 ± 0.24) during Run 1, however the distribution of soil moisture and pH over the farm area does not appear to follow any pattern.

Plotting soil moisture content against pH in Figure 5.16 shows that there is a weak relationship between the two. As soil moisture content increases, pH also increases.



Figure 5.15: Soil sampling positions, Run 1. Soil moisture content is marked for each position in dark blue, whilst pH is yellow.

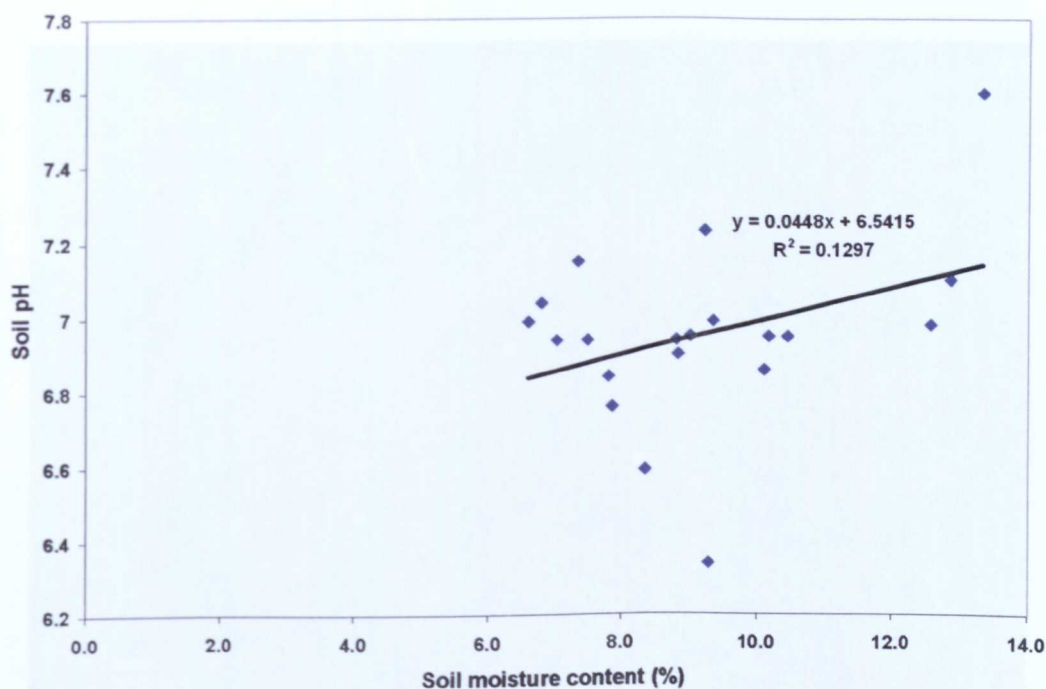


Figure 5.16: Soil moisture content vs. Soil pH, Run 1.

In future runs, only six samples were taken to indicate the soil moisture content and pH, rather than the larger survey of twenty samples which showed no clear trend with sampling position.

Figures 5.17 and 5.18 show the sampling positions for Runs 2 and 3, and the soil moisture contents and pH's for each position. Soil moisture content and pH ranged from 4.2 to 6.1% (mean of 5.38 ± 0.77), and from 6.6 to 7.2 (mean of 6.82 ± 0.25), respectively during Run 2. During Run 3, soil moisture content and pH ranged from 5.0 to 5.9% (mean 5.52 ± 0.41), and 6.6 to 7.1 (mean of 6.88 ± 0.19), respectively.

Once again, there was no clear pattern and the soil samples can be said to be homogeneous. For both Runs 2 and 3 there was a period of two days before the measurement period when there was no rain. Also, the maximum and minimum temperatures recorded were of the order Run 3 > Run 2 > Run 1. The soil moistures and pH's were lower than in Run 1.



Figure 5.17: Soil sampling positions, Run 2. Soil moisture content: dark blue; pH: yellow.

Figure 5.18: Soil sampling positions, Run 3. Soil temperature: dark red; soil depth: yellow.

5.3.4 Additional information

While the exact numbers of pigs housed on the site varied throughout the study, the average number of pigs housed on the site was approximately 100. The average live weight of the pigs housed on the site was approximately 100 kg.



Figure 5.18: Soil sampling positions, Run 3. Soil moisture content: dark blue; pH: yellow.

5.3.4 Additional information

Whilst the exact numbers of pigs housed on the area under investigation changed from run to run due to movement to other areas (whilst farrowing, for example), the average approximate live weight of the pigs remained the same.

Table 5.9: Summary of pig numbers and live weights.

Run	Date	Total pig numbers	Approx. live weight (kg)
1	15-17 May 02	457	190
2	15-19 July 02	432	190
3	25-29 July 02	450	190

5.3.5 Source strength calculation

Whilst there appears to be no trend of net horizontal ammonia flux with height for any of the sampling masts, and no consistency between different Runs, a crude estimate of the maximum ammonia emission rate could be made for the farm using the highest flux measured during the three Runs performed. This can be done using Equation (3) and making assumptions about the inputs to the equation as follows: the background net flux (F_u) was $0.0 \mu\text{g NH}_3 \text{ m}^{-2} \text{ s}^{-1}$; the height over which this flux is representative (Δz) is the total height of the sampling mast (10.44 m to highest sampling position); the distance between sampling masts (d) is the length of the farm (525.0 m); the highest net flux (measured during Run 1 on mast 4 at a height of 0.99 m) was $28.36 \mu\text{g NH}_3 \text{ m}^{-2} \text{ s}^{-1}$. From this an estimate of Q can be made of 0.156 g s^{-1} . This is equivalent to a source strength of $0.16 \text{ g NH}_3 (\text{kg of sow})^{-1} \text{ day}^{-1}$.

5.4 DISCUSSION

5.4.1 Limitations

As long dry periods are required for the measurement of the low ammonia emissions expected from a free-range sow farm, a compromise on suitable wind conditions must be made. Suitable wind speeds and directions are rare over long periods of time, particularly with diurnal variations and calm conditions throughout the night. Similarly in the U.K. long periods without rain are also sparse and the combination of dry weather with a constant wind direction and wind speed is infrequent. It may, however, be possible to take calm periods into account once meteorological data have

been collected. The period when calm conditions prevailed can be deducted from the total measurement period to improve the estimate of flux. However, calm periods may also mean that ammonia diffuses into both ends of the sampler. If the same amount of ammonia diffused into both sides of the sampler, the amount would cancel out. Until further work takes place and the effect is quantified, however, an adjustment to the ammonia fluxes should not be made, particularly when calm periods are short.

These findings suggest that the recurved passive ammonia flux sampler is not suitable for measurement of the very low ammonia emissions evident at the pig farm ($\mu\text{g m}^{-2}\text{s}^{-1}$ rather than $\text{mg m}^{-2}\text{s}^{-1}$), particularly when the wind direction is variable. Low emissions may be successfully measured if a constant wind direction and a wind speed greater than, say, 1.5 m s^{-1} are prevalent. Otherwise, the time scale for a minimum amount of ammonia to be captured is too great, (in the order of weeks) particularly as dry weather is required so as not to render the samplers useless without their acid coating. The error on measurements where the difference between the source and background tubes is small (1 mg NH_3) is also much higher than when there is a large difference (say 10 mg NH_3) (see section 2.3.5, and Appendix 2).

Williams *et al.* (2000) exposed their ammonia flux samplers for periods of four weeks, which would allow enough ammonia to be captured from such a diffuse source. However, wind direction and speed data are not presented, and rainfall is presented as a total over a whole season (1st Oct – 31st March). It is unlikely that any four week period would be dry for the whole period, and as no wind direction data are presented the length of time the wind blew from each direction can only be assumed. Sommer *et al.* (2001) report that 10% of the measurements using PAF samplers were rejected because of wind direction difficulties (wind not passing over site before reaching sampling mast) and one whole run was excluded due to high background fluxes, so high that no ammonia enrichment occurred on the source tubes. This was seen to occur during Run 1 in particular, where high negative fluxes were measured. This could possibly be due to high emissions from the farrowing sows and piglets to

the East of the measurement site. A possible cause of this is described by Sommer *et al.* (2001). They report how ammonia volatilization increases with the amount of feed given to the pigs, especially sows suckling piglets.

A further limitation arises from obstacles surrounding the measurement area. The use of these samplers around farms is compromised by the presence of hedges bordering the perimeter. The use of the flux frame has been described by Michorius *et al.* (1997) to be necessarily 10x any obstruction height downwind as the wind profile is incorrect due to the effects of turbulence. Therefore the use of recurved PAF samplers is less advisable in three of the six sampling positions (4, 5 and 6) around the farm due to turbulent effects, which may result in the background tube collecting more ammonia than it should if the obstruction was not there. This effect, however, is not distinguishable in graphs 5.6, 5.9 and 5.12 due to the low flux measurements with height and lack of a visible trend at any of the six sampling masts.

5.4.2 pH vs. ammonia emission

It is known that higher pH values lead to higher ammonia emissions (Freney *et al.*, 1983; Sherlock and Goh, 1984), so it would be expected that higher ammonia emissions would be measured for Run 1, where the highest mean soil pH of 6.95 was measured. Hoff *et al.* (1981) found that 65% of ammoniacal-N was emitted when the soil/manure pH was >7, but was just 14% over the same time period when the pH was 6.4. For Runs 2 and 3 the mean soil pH was 5.38 and 5.52 respectively, which may explain the difficulties in measuring ammonia emissions from the farm throughout the measurement runs.

5.4.3 Moisture vs. ammonia emission

As urea hydrolysis has been found to increase with increasing water content (Freney *et al.*, 1983; Black *et al.*, 1985; Ferguson *et al.*, 1988) (and a lack of water was assumed to be the cause of restricted volatilisation (Vallis *et al.*, 1982; Harper *et al.*,

1983)), a higher volatilisation would be expected in Run 1 where moisture contents were, on the whole, higher.

5.4.4 Variability of wind direction

The high variability of the wind direction during Runs 1 and 3 could be due to an averaging error. As five minute averages were taken of measurements made every second, when wind direction were from the North, the average wind direction could be around 180°, rather than the actual direction of 0 or 360°. As the fluxes measured were negligible, this has little importance, but if measurements were to be made in future, an alternative averaging method would have to be undertaken, or periods with Northerly winds avoided.

5.4.5 Nitrogen losses

A large nitrogen surplus exists between inputs from feed and outputs in meat (Williams *et al.*, 2000). Whilst ammonia losses appear to be negligible from free-range sows, this surplus nitrogen deposited to the soil must go somewhere. Another major form of nitrogen produced, by nitrification and mineralisation, is nitrate-N and this is available for uptake by plants (of which there were none at the farm studied) and leaching, and also conversion to N₂ and N₂O through nitrification and denitrification. A future study of free-range pigs may examine all forms of nitrogen present in the soil to determine the losses of ammonia, nitrate and nitrous oxide from the system and the amount immobilised or mineralised (Jarvis *et al.*, 1996).

Delgado (2002) reviews the different methods for quantifying nitrogen losses including ammonia volatilization, emissions of nitrous oxide, oxides of nitrogen and dinitrogen gases, leaching of nitrates, transport due to wind and water erosion of organic matter containing nitrogen and also the inorganic nitrate and ammonium components. He also describes variability in soil properties, including both chemical and physical, as the main difficulty in enabling nitrogen use efficiency to be

maximised. One example given is that of coarse textured soil, where losses of N are mainly due to nitrate leaching, whilst losses in areas with clay soil are dominated by denitrification from pools of water on the soil surface. As the best site for a free-range pig farm is on free-draining soil (Thomton, 1988), this suggests that this could be the largest pathway of loss, rather than ammonia emission.

5.4.6 Source strength comparison

The estimate of ammonia source strength made for this farm ($0.16 \text{ g NH}_3 \text{ (kg of sow)}^{-1} \text{ day}^{-1}$) compares well with those of Williams *et al.* (2000) and Sommer *et al.* (2001) for outdoor pigs, and Demmers *et al.* (1999) and Groot Koerkamp *et al.* (1998) for housed pigs (see Table 5.1). However, this very crude calculation uses the highest horizontal ammonia flux measured and assumes that this is constant for the whole length of the farm and for the whole height of the sampling mast.

5.4.7 Uses of flux samplers

Whilst the samplers are not completely suitable for the low emissions from grazing animals, they are useful for larger emissions. It has been shown in this study that, if the emission is high enough, both individual samplers and the flux frame method are suitable for measuring ammonia emissions from point sources. PAF samplers were originally designed to measure ammonia emissions from naturally ventilated cattle houses (e.g. Kim *et al.*, 1999), where they sample in one plane between the Yorkshire boarding. In this situation, not only are the emissions high enough that a large enough amount of ammonia is captured in a short time period (< 24 hours), but the position of the samplers between Yorkshire boarding and at the boundaries of buildings means that they are protected from rain in all but the strongest of winds and harshest of conditions.

The use of passive ammonia flux samplers is suitable also for area sources such as slurry lagoons and tanks where emissions are high and a frame work of samplers is easily erected (e.g. Kim *et al.*, 1999; Michorius *et al.*, 1997).

5.4.8 Other possible methods

Other possible methods for measuring ammonia emissions from free-range sows that could be considered in future are:

5.4.8.1 Micrometeorological methods

Micrometeorological methods have been described in section 1.7.5 (e.g. Denmead *et al.*, 1977; Sherlock *et al.*, 1989; Sommer *et al.*, 1995), and are suitable for measuring ammonia emissions from large area sources. It would be necessary to use active samplers, however, to avoid the same problem encountered in this study of ensuring adequate exposure periods with passive samplers. The use of an active sampler would increase the costs involved with making the measurements and a power source would be required in the field, most likely leading to a reduction in the number of measurement positions used.

5.4.8.2 Tracer techniques

The tracer ratio method (described in section 1.7.6; e.g. Lamb *et al.*, 1986) is suitable for large area sources, assuming that the tracer is distributed in such a way that the source is adequately simulated. This would be difficult to achieve for a pig farm however, due to the heterogeneous distribution of the source and the difficulty that would be experienced in installing a tracer system in a field full of inquisitive pigs.

5.4.8.3 Measurements from other grazing animals

Measurements of methane emissions from grazing sheep and cattle have been made. Lockyer and Jarvis (1995) used wind tunnels attached to both ends of a large polythene tunnel erected over an area of grass, along with gas chromatography to measure the concentration of methane in the air entering and leaving the tunnel. Sheep were then housed under the polythene canopy and the methane emission measured. Leuning *et al.* (1999) used a micrometeorological mass balance method (described in detail in Denmead *et al.*, 1998) to measure the methane emissions from sheep fenced within a 24 m x 24 m enclosure. The air flowing across the enclosed animals was enriched with methane, and this increase in concentration was measured using an active sampling method, FTIR. This method compared well to a tracer ratio method of measurement (measuring the ratio of methane and SF₆ released directly from the rumen of the sheep). This method may not be suitable for ammonia emission measurements, however, as the microclimate under the polythene may differ from that externally and a true estimate of ammonia emission may not be measured.

Harper *et al.* (1999) also used the micrometeorological mass balance method described by Denmead *et al.* (1998) to measure methane emissions from four heifers in two systems: grazing on pasture (22m x 22m square field) and in a feedlot. Measurements were made at four heights on each boundary of the field using infrared gas analysis and gas chromatography. This method was chosen because not only was it a field technique, but it was virtually non-intrusive, permitted a large sample size and could be run automatically over several days. The active sampling techniques used, however, make this an expensive method when compared to the use of passive flux samplers.

Whilst the same micrometeorological method and a variation on the wind tunnel method used for measuring ammonia emissions have been used for measuring methane emissions from grazing sheep and cattle, the measurements were made over a much smaller area than the free-range sow farm investigated as part of this study.

There appears to have been no measurements made of any atmospheric pollutant from grazing livestock over large areas of land. This suggests that the most suitable way to measure emissions from a large area source would be to measure the emissions from a smaller area with the same stocking density, and then to scale up to the farm scale. The flux frame method could be used for this, so long as the area of land upon which the pigs were kept was around half the width of the flux frame, thus ensuring that the whole width and height of the resulting plume of emissions was captured.

5.5 CONCLUSIONS

Recurved passive ammonia flux samplers in a flux frame are not suitable for the measurement of ammonia emissions from free-range sows due to the low emissions and the extensive period of sampling required to capture adequate ammonia for analysis. During long exposure periods, the likelihood of samplers being ruined by rain and the change in wind direction lead to further difficulties in their use.

However, it is still necessary to measure emissions from this type of source. Active samplers would be required to measure at a number of measurement locations to enable the low emissions to be measured accurately in a short time period though these would increase the cost of the measurement campaign.

6. GENERAL DISCUSSION AND CONCLUSIONS

6.1 INTRODUCTION

The objective of this study was to validate a method for the measurement of ammonia emissions from a distributed source, and to then use it to measure ammonia emissions from free-range sows. There is very little information about this type of source apart from studies by Williams *et al.* (2000) and Sommer *et al.* (2001) though an increasing proportion of the UK pig-breeding herd are now kept under this system of husbandry (25%). The increase is, in part, due to an increased awareness by consumers of animal welfare issues and also to this type of extensive farming being favourable to farmers in the recent economic climate.

Whilst recurved PAF samplers had been used previously in field experiments (e.g. Kim *et al.*, 1999), the particular design used in this study had not been validated in a controlled environment. The flux frame method of sampling also required validation using full-scale measurements and controllable ammonia sources. The flux frame method had also been used previously (Jeschke, 1996), but full-scale validation had not been undertaken.

6.2 VALIDATION OF RECURVED PASSIVE AMMONIA FLUX SAMPLERS

The collection efficiency of Ferm tubes and recurved PAF samplers has been tested under various conditions by Ferm (1986), Ferm *et al.* (1991), Schjoerring *et al.* (1992), Ferm and Christensen (1987) and Phillips and Scholtens (1999). The studies reported collection efficiencies ranging between 66 and 77% depending upon the design of sampler and the conditions under which they were tested. It was therefore necessary to determine the efficiency of the recurved PAF sampler, used in the flux frame method, under controlled conditions of wind speed and ammonia concentration. Over a wind speed range of 2 to 7 m s⁻¹ and ammonia concentration range of 0.5 to 4 ppm, which are equivalent to an ammonia flux range of 0.771 to 13.493 mg m⁻² s⁻¹, the samplers had a measured collection efficiency of 71% (±4.0%)

and a correction factor of 0.71 was used in subsequent experiments, which agrees well with that given in the literature.

Various studies have found different effects of angle of wind incidence on sampler performance. Ferm (1986) found a cosine dependency of flux with increasing angle for original Ferm tubes and his findings have recently been reinforced in a theoretical study by Scholtens *et al.* (2002). Flint *et al.* (2000), however, found critical angles of 66° and 80° for the original Ferm tube and the re-curved PAF sampler respectively, after which zero or negative flow through the sampler was reported. A critical angle of 80° was found in this study, in closer agreement with Flint *et al.* (2000), though this is specific to this design of sampler.

There is a need to investigate further the effects of wind speed on sampler collection efficiency to determine the wind speed at which breakthrough occurs more accurately. Results from Chapter 2 show that breakthrough does not occur at 7 m s⁻¹, however, at 10 m s⁻¹ breakthrough does occur. This leaves a range of wind speeds unaccounted for, and an uncertainty when using the samplers in the field as to the proportion of time the samplers were experiencing breakthrough (if the wind speed exceeds 7 m s⁻¹).

Since this study began, further developments to PAF samplers have taken place, mainly in their physical appearance, but also in the use of filter papers impregnated with acid to capture the ammonia. The paper not only gives the samplers a longer life, by increasing the amount of ammonia they can capture before saturation (no risk of saturation up to 500 µg of ammonia, however, this is not essential for this study), but also reduces the effect a shower of rain may have on the coating by not allowing the acid to be washed off. The value of the sampler constant, *K*, was found to be 0.81, which indicates a greater collection efficiency when using acid impregnated filter papers (Scholtens *et al.*, 2002).

There is also the possibility of passive flux samplers being used to collect other gaseous pollutants, providing a capture medium coated or impregnated with a suitable chemical, specific to the pollutant of interest, is found. For example, Mahlcke (1998) describes samplers using a molecular sieve to collect nitrous oxide (once water vapour and carbon dioxide were removed) and activated charcoal cloth (similar to activated carbon granules) to collect methane. Both types of sampler are still under development.

6.3 VALIDATION OF THE FLUX FRAME METHOD

A flux frame is a suitable method to measure emissions from an area source, so long as the whole height of the plume is captured (Michorius *et al.*, 1997) and the dispersion of the plume is predictable. For this to be true, the source must be homogeneous or at least have defined plume characteristics. Flux frames have been used by Kim *et al.* (1999) to measure controlled emissions of ammonia from slurry tanks and by Michorius *et al.* (1997) to measure emissions from a force ventilated pig house with a covered cattle slurry store. The method has advantages and disadvantages. For example, the whole height of the plume is captured. Its limitations include the necessity to presuppose a prevalent wind direction to enable the frame to be erected in a position to maximise the number of sampling days possible, with the additional requirement of wind conditions greater than calm conditions but less than 7 m s^{-1} . The best estimates of emission are made under favourable conditions – moderate wind, high emission and low background concentration (Michorius *et al.*, 1997).

Whilst Chapter 4 concludes that the flux frame is suitable for measuring point sources up to 50 m from the flux frame, the farm where measurements were made was greater than 330 m deep. The source was therefore too wide for the ammonia emissions to be sampled within the available measurement height – a prerequisite described by Michorius *et al.* (1997). This, however, could be overcome, if the trend of horizontal flux with height is clear, using extrapolation of the curve above the height to which

samplers were deployed. Also, the distance over which ammonia was transported before it reached the flux frame was so great that dilution of the ammonia concentration with air would take place. Therefore, the flux frame would be suitable, so long as a trend of horizontal ammonia flux with height was apparent.

The ammonia emissions from the free-range sow farm in this study were below the minimum horizontal flux that could be detected accurately using recurved PAF samplers over the sampling periods of 2 to 4 days. For example, referring to Appendix 2, with a ΔM (which equals $M_S - M_B$, where M_S and M_B represent the mass of ammonia collected on the source tube and background tube respectively; equation 14) of 10 mg NH_3 , there is an error of 3.1%. For a ΔM equal to just 0.1 mg NH_3 (which was quite often the case during farm measurements), there is an error of 310%. This period was short enough to minimise the possibility of rain disrupting the ammonia capture in the samplers or violent wind shifts but not long enough to detect a horizontal flux greater than negligible. Williams *et al.* (2000) used sampling periods of one month but did not state the actual rainfall (only that it was similar to the long-term average) or wind speed and direction during each period. Since it is unlikely that no rain fell, then the results of their study must be in doubt due to the failure of PAF samplers to work in wet weather. Sommer *et al.* (2001) used passive flux samplers for periods of 24, 48 and 72 hours at heights up to 3 m above ground level. No quantitative measure of rainfall is presented, although it is stated that rainfall was 15% higher than the average between measuring periods. They also report that on one occasion ammonia volatilization was not measured due to slurry spreading producing a high background concentration that could have affected the flux calculation. During the measurement periods of 72 hours, Sommer *et al.* (2001) appear to have measured sufficient ammonia to allow an accurate measure of emission to be made. This could be due to the smaller area from which ammonia emissions were being measured, and a low background ammonia concentration. Wind direction data are not presented, although it is reported that a tenth of the measurements were discarded due to an incorrect direction (not passing over the source before reaching the samplers).

Recurved PAF samplers require a period of stable weather without rainfall and with a wind speed of at least 2 m s^{-1} , preferably with a spread of direction of no more than 160° . Although such conditions do occur in the UK, this limitation of PAF samplers affects their suitability for use on a free-range sow farm. Active measurements of ammonia concentration, along with wind speed measurements, over short time periods with low detection limits would be necessary for measurements at a free-range sow farm.

The original decision to use a flux frame was based on the experience of Williams *et al.* (2000) and Michorius *et al.* (1997). In practice, the flux frame had significant limitations which restricted its use for measuring ammonia emissions from a free-range sow farm. Recurved PAF samplers do not need a power source and are low cost to construct. They were considered suitable since many could be used around the farm. However, the logistics of erecting a framework of flux samplers in a single location which would sample the emissions from the farm accurately was very difficult – Phillips *et al.* (2000b) describe the use of stationary masts, which are not only difficult to erect but must presuppose a particular wind direction, both of which are serious drawbacks to the method.

Measurements of emission rates of ammonia and other forms of nitrogen were made using a Lindvall Hood at several locations around the farm studied in this project. The bag samples taken were analysed using chemiluminescence. The measurements were taken for another project (unpublished) and ammonia emissions were found to be less than $0.66 \mu\text{g NH}_3 \text{ m}^{-2} \text{ s}^{-1}$ at all but one of the sampling locations, where an emission rate of $14.5 \mu\text{g NH}_3 \text{ m}^{-2} \text{ s}^{-1}$ was measured. It is likely that this location coincided with a fresh urine patch. This corresponds to an emission rate of $0.015 \text{ mg NH}_3 (\text{kg of sow})^{-1} \text{ day}^{-1}$, which is in the order of a thousand times less than the emission rates presented in Table 5.1, where the units are $\text{g NH}_3 (\text{kg of sow})^{-1} \text{ day}^{-1}$.

The flux frame was originally devised to measure the plume of emission from a strong ammonia source such as a slurry lagoon or tank. The flux frame has proved

useful for large emissions, especially point sources. For example, ammonia emissions from housed pigs (Michorius *et al.*, 1997) and area sources such as slurry lagoons and tanks (e.g. Kim *et al.*, 1999) have been measured.

If the source strength was high and the depth of the source was < 50 m, the flux frame would be suitable for the measurement of any pollutant provided a sampler suitable for the pollutant of interest was attached to the flux frame. Discrete sources with definable boundaries (such as animal houses) would be particularly suited to the use of the flux frame. However, a large source strength would be required due to the necessity of erecting the flux frame 10 heights of any obstruction downwind to ensure the wind profile is set up (Michorius *et al.*, 1997). Using a flux frame downwind of an animal house would avoid the determination of all the inlets and outlets of the building from which pollutants could escape, and which would be the most suitable for measurement of the emission. Other methods do exist, however, which simplify this procedure, such as a tracer gas release method (Demmers *et al.*, 2001). Recurved PAF samplers are particularly suitable for measurement of horizontal ammonia fluxes from buildings as the ventilation rate does not need to be determined for each opening, removing the problem of accurate measurement of ventilation rates of buildings.

Micrometeorological methods are particularly suited to sources from large areas (see section 1.7.5 for descriptions of these methods and their advantages and disadvantages). However, when the emission is low the problem of sensitivity of the sampler still arises, which clearly depend upon the kind of sampler employed. The use of active samplers either in a micrometeorological method or in an adaptation of the flux frame method would prevent any problems encountered by long exposure periods. However, active samplers are much more expensive, so the use of many would be unfeasible, and they require a power source, which at a pig farm might be difficult.

Michorius *et al.* (1997) report that the flux frame method is suitable if the whole of the plume of emissions from a source is captured. However, it was decided that the flux frame would be useful for line sources longer than the flux frame and this was investigated. It was concluded (Chapter 4), however, that a single sampling mast was almost as efficient for calculating the source strength as a full flux frame when the whole width was not sampled, which reduces the flux frame method to a simple micrometeorological method.

Modelled flux frame collection efficiencies agreed with measured collection efficiencies to within 37.3% in all experimental runs for which modelling took place. For AFL experiments, measured and modelled efficiencies for all ground level releases agreed to within 5.2%, whilst for field experiments, agreement between measured and modelled efficiencies was, on average, 16.9% (s.d. 12.5). Hanna (1993) found uncertainties in ground-level concentration predictions from several air quality models of around ± 20 to 40%. Therefore, the differences found in this study between modelled and measured values are in line with those found during several other model simulations.

6.4 AMMONIA EMISSIONS FROM FREE-RANGE SOWS

During farm measurements, the amount of ammonia captured was very low ($< 30 \mu\text{g NH}_3 \text{ m}^{-2} \text{ s}^{-1}$), and despite the whole height of the plume not being captured, the horizontal fluxes measured at the highest sampling position were less than $11 \mu\text{g NH}_3 \text{ m}^{-2} \text{ s}^{-1}$ in all but one case. One possibility to allow the flux frame to be used for sources greater than 50 m deep was to extrapolate the estimate of the horizontal flux above the top of the flux frame. However, to do this the source strength must be high enough, and meteorological conditions stable enough, that the amount of ammonia captured on the samplers show a noticeable trend with height, which was not the case. Alternatively, taller single sampling masts could be used to attempt to capture the whole height of the plume, as done by Michorius *et al.* (1997) (at 15 and 19 m above ground level).

The very low horizontal fluxes measured also lead to the conclusion that ammonia emissions from free-range sows are very low (although, a worst case source strength calculation compares well with other emission rates in literature). This has been confirmed by another study using Lindvall Hoods, which took measurements from random locations over the site.

More likely, nitrate leaching would be the main pathway of loss. Williams *et al.* (2000) found nitrate leaching losses to be three times greater than those from conventional arable production and that leaching losses increased as the grass cover was destroyed by the pigs. At the farm where measurements were taken in this project, there was no grass cover and the pigs were not part of an arable rotation. There was no possibility of uptake of nitrogen into crops or grass as a fertiliser. This would mean that free-range sows, for which nitrate leaching is thought to be very high, (whilst ammonia emissions are low), would not be suitable for areas where pollution of water may occur, particularly Nitrate Sensitive Areas and Nitrate Vulnerable Zones (NVZs) as set out in the EC Nitrate Directive (91/676/EEC) (MAFF, 1998).

Whilst this study has gone some way to validating the flux frame method, there have been no measurements when the ground is wet and a sink for ammonia. However, as water is a sink, it is unlikely that under these conditions there would be a measurable amount of ammonia, particularly as the emissions measured during dry conditions were so low. During wet conditions, the most probable pathway for nitrogen loss would be as nitrate in leachate.

Pain *et al.* (1998) assumed that 20% of pigs were kept outdoors in the UK inventory of ammonia emissions. As no emission factor for outdoor pigs was available, the emission factor for grazing cows was used once differences in live weight and N content of excreta had been taken into account. They found that whilst the animal numbers equalled 20% of the total number of pigs in the UK, the emission of

ammonia from them was only 1% of the total emissions from pigs, with housed pigs emitting by far the most (64%) (Table 6.1). Of the total ammonia emissions from agriculture, pig production accounts for only 12% with cattle the main offender, contributing 50% (Table 6.2). This means that outdoor pig production accounts for only 0.12% of the total ammonia emissions from agriculture – a relatively insignificant source of ammonia.

Table 6.1: Total ammonia emission from pig production (from Pain *et al.*, 1998).

Farm management source	Amount of NH ₃ -N lost (kt NH ₃ -N yr ⁻¹)	Percentage of total
Housing	15.0	64
Storage	1.0	4
Land spreading	7.4	31
Outdoors	0.2	1
Total	23.6	100

Table 6.2: Total ammonia emission from UK agriculture (from Pain *et al.*, 1998).

Source	Amount of NH ₃ -N lost (kt NH ₃ -N yr ⁻¹)	Percentage of total
Cattle	98.7	50
Sheep	12.7	7
Pigs	23.6	12
Poultry	30.2	15
Deer	0.02	<0.01
Fertiliser	32.1	16
Total	197.3	100

Whilst Williams *et al.* (2000) measured ammonia emissions from free-range sows which are comparable with those from housed sows (Table 5.1), the length of time for which their samplers were exposed could have led to significant errors. The shorter time periods used during this project allowed less chance of contamination or erroneous results after the samplers had been exposed during wet weather. The measurements were all taken during the summer/autumn months when temperatures were at their highest and ammonia emissions would also be expected to be at their

highest. The low capture of ammonia suggests that nitrogen loss from free-range sow farms is not primarily through ammonia volatilisation.

6.5 FURTHER WORK

To achieve an accurate emission rate over a short time period, active samplers could be used in a meteorological method, as they would have a lower detection level. LIDAR measurements (e.g. Zhao *et al.*, 2002; Zhao, 2000) could be made across the farm, which would enable not only a quick response with a low detection level, but also the emission from the whole width of the farm to be integrated. This would go some way to overcoming the problem of the measurement location that is inherent in most methods and was potentially overcome by the flux frame method.

Whilst the same methods used for measuring ammonia emissions (e.g. Leuning *et al.*, 1999) are used for measuring methane emissions from grazing sheep and cattle (e.g. micrometeorological methods), the source area is much smaller than a free-range sow farm. Future work on ammonia emissions from free-range pigs could use a purpose built area containing the correct stocking density which is, however, completely isolated from other sources of ammonia, so that a micrometeorological method using active samplers could be used to provide an estimate of ammonia emission. Alternatively, in this case, the full flux frame could be used (along with active samplers) to capture the whole plume of emissions from the pigs, particularly if a smaller area, e.g. 24 by 24 m, was used (narrower than the full width of the flux frame). Future work could include a study of the spatial variability of excretory behaviour in free-range sows to identify the exact source of ammonia emissions.

Ammonia emissions originate from soil and excreta. However, the effects of various soil properties such as moisture, pH and temperature, amongst others, as reported in literature are contradictory or inconclusive. Further work into the effect of physical, chemical and microbiological properties of soil is required to enable estimates of

emissions from sources under different conditions (i.e. geographical locations) to be made more accurately.

Improving the utilisation of nitrogen from animal feed (section 1.2), seems the most promising method to abate nitrogenous losses from agriculture. If there is less nitrogen in the excreta in the first place there is less to be potentially lost. Other methods, which decrease loss of ammonia, such as the use of additives, still lead to losses of other forms of nitrogen, which are just as harmful to the environment - they just have a different pathway. Obviously, whilst animals are kept intensively for the food industry the potential for pollution of the environment with anthropogenic sources of particulate and gaseous pollutants is high. Perhaps with the rise in vegetarianism - along with the increase in awareness of animal welfare issues - a corresponding decrease in livestock numbers, and thus pollution, may be found?

A recent review of research funded by Defra relating to air pollution from ammonia from agriculture (Dämmgen and Avon, 2002) concluded that further work should be carried out in a number of areas where measurements are lacking or as yet inconclusive, including:

- the temperature dependence of ammonia emissions;
- the influence of organic farming on ammonia loss;
- the variation with time of ammonia compensation points; and
- the relationship between the emission of ammonia and other nitrogen containing species, particularly nitrates.

The last area, suggesting whole system analysis of emissions from livestock is an important new approach where abatement is being performed: there is little point abating one pollutant only to find that another increases. For example, reducing ammonia emissions from slurry lagoons means that more nitrogen is present in the slurry when it is spread. Without a crop to take up the nitrogen as a fertiliser, it is likely to be lost through other routes, and as rain is highly likely, nitrate leaching is

probable. The MANNER model (Chambers *et al.*, 2000) is one way in which the abatement of pollution from one nitrogen species can be investigated to examine the impact on the environment of another form of pollution which may arise. A suitable compromise may then be reached. A holistic approach to measuring nitrogen losses from agriculture would be most appropriate for any future measurement campaign, particularly if abatement techniques have been employed.

6.6 CONCLUSIONS

Recurved passive ammonia flux samplers have been shown to be suitable for the accurate measurement of horizontal ammonia fluxes with the following limitations: a correction factor must be applied to the measured flux, the wind speed during sampling must not exceed 7 m s^{-1} , and the wind direction must not exceed an angle of 80° parallel to the sampler axis.

The flux frame method is a suitable method for measuring ammonia emissions from ground level point sources, requiring a small correction factor due to an underestimation (average capture efficiency in the AFL of 87.4%, and in field trials, 56.4%). This is limited however to 'strong' ($\text{mg NH}_3 \text{ m}^{-2} \text{ s}^{-1}$) sources which would require no longer than 24-48 hours for a minimum amount of ammonia to be captured on the sampler, avoiding problems caused by changing wind direction and rain fall.

The flux frame method is suitable for the measurement of line sources, although assumptions must be made about the homogeneity of the source and dispersion of the plume of emissions.

A full size flux frame is not necessary to measure ammonia emissions from large area sources as one column of samplers produces a very similar estimate of horizontal flux to that of the whole frame. Therefore single masts of samplers may be erected at different sites around an area source, enabling the problem of wind direction to be

alleviated, so long as obstructions such as hedges are not in close proximity to the masts.

Measured and modelled collection efficiencies for the flux frame method agreed to within 37.3%. This agrees well with other studies looking at the agreement between measured and predicted values from air quality models.

This study has shown that whilst the flux frame method may not be entirely suitable for measuring ammonia emissions from free-range sows, the amount of ammonia emitted from this source is very low. Although the method is not ideal, the samplers were still capable of measuring strong ammonia sources, and the fact that the amount of ammonia collected is so low over exposure periods of days shows that free-range sow farms have a negligible contribution to ammonia emissions from agriculture.

BIBLIOGRAPHY

- Amberger, A. (1991) Ammonia emissions during and after land spreading of slurry. In: *Odour and Ammonia Emissions from Livestock Farming* (Eds: Nielsen, V.C., Voorburg, J.H. and L'Hermite, P.) Elsevier Science Publishers Ltd., Essex. pp 126-131.
- Appel, B.R., Tokiwa, Y., Kothny, E.L., Wu, R. and Povard, V. (1988) Evaluation of procedures for measuring atmospheric nitric acid and ammonia. *Atmospheric Environment* **22**(8): 1565-1573.
- ApSimon, H.M. and Kruse-Plass, M. (1991) The Role of Ammonia as an Atmospheric Pollutant, In: *Odour and Ammonia Emissions from Livestock Farming* (eds. Nielsen, V.C., Voorburg, J.H. and L'Hermite, P.) Elsevier Science Publishers Ltd., Essex. pp 17-20.
- Asman, W.A.H. (1998) Factors influencing local dry deposition of gases with special reference to ammonia. *Atmospheric Environment* **32**(3): 415-421.
- Asman, W.A.H. (2001) Modelling the atmospheric transport and deposition of ammonia and ammonium: an overview with special reference to Denmark. *Atmospheric Environment* **35**(11): 1969-1983.
- Asman, W.A.H. and Vanjaarsveld, H.A. (1992) A variable-resolution transport model applied for NH_x in Europe. *Atmospheric Environment Part A – General Topics* **26**(3): 445-464.
- Barthelmie, R.J. and Pryor, S.C. (1998) Implications of ammonia emissions for fine aerosol formation and visibility impairment – a case study from the Lower Fraser Valley, British Columbia. *Atmospheric Environment* **32**(3): 345-352.
- Black, A.S., Sherlock, R.R., Cameron, K.C., Smith, N.P. and Goh, K.M. (1985) Comparison of three field methods for measuring volatilisation from urea granules broadcast on to pasture. *Journal of Soil Science* **36**:271-280.
- Binkley, D. and Richter, D (1987) Nutrient cycles and H⁺ budgets of forest ecosystems. *Advances in Ecological Research* **16**:1-51.
- Bobbink, R. (1998) Impacts of tropospheric ozone and airborne nitrogenous pollutants on natural and semi-natural ecosystems: a commentary. *New Phytologist* **139**(1): 161-168.
- BS 7755: Section 3.1 : 1994; ISO 11465 : 1993. *Soil quality. Part 3. Chemical methods. Section 3.1. Determination of dry matter and water content on a mass basis by a gravimetric method.* British Standard. London: BSI.
- BS EN 13037:2000. *Soil improvers and growing media – determination of pH.* British Standard. London: BSI.

BS EN 13040:2000. *Soil improvers and growing media. Sample preparation for chemical and physical tests, determination of dry matter content, moisture content and laboratory compacted bulk density*. British Standard. London: BSI

Canh, T.T., Aarnink, A.J.A., Mroz, Z., Jongbloed, A.W., Schrama, J.W. and Verstegen, M.W.A. (1998) Influence of electrolyte balance and acidifying calcium salts in the diet of growing-finishing pigs on urinary pH, slurry pH and ammonia volatilization from the slurry. *Livestock Production Science* **56**(1): 1-13.

Carruthers, D.J., Edmunds, H.A., Bennett, M., Woods, P.T., Milton, M.J.T., Robinson, R., Underwood, B.Y., Franklin, C.J. and Timmis, R. (1997) Validation of the ADMS dispersion model and assessment of its performance relative to R-91 and ASC using archived LIDAR data. *International Journal of the Environment and Pollution* **8**(3-6): 264-278.

CERC (1999) *ADMS 3: User guide*. CERC, Cambridge.

Chambers, B.J. (1998) Sustainable systems of outdoor pig production. Final Project Report to MAFF NT1814.

Chambers, B.J., Smith K.A. and Pain B.F. (2000) Strategies to encourage better use of nitrogen in animal manures. *Soil Use and Management* **16**(S1): 157-161.

Cole, J.A. (1988) Assimilatory and dissimilatory reduction of nitrate to ammonia, In: *The Nitrogen and Sulphur Cycles* (eds. Cole, J.A. and Ferguson, S.J.) Cambridge University Press, Cambridge. pp 281-329.

Colls, J. (1997) *Air Pollution: An Introduction*. Chapman & Hall, London. pp 128-143.

Cowell, D.A. and Apsimon, H.M. (1998) Cost-effective strategies for the abatement of ammonia emissions from European agriculture. *Atmospheric Environment* **32**(3):573-580.

Dämmgen, U. and Avon, B. (2002) In-depth review of the outputs of DEFRA's programme of research on the measurement and control of ammonia emissions from agriculture (1998-2002). *DEFRA project AM 0119, Final report*.

Delgado, J.A. (2002) Quantifying the loss mechanisms of nitrogen. *Journal of Soil and Water Conservation* **57** (6): 389-398.

Demmers, T.G.M, Burgess, L.R, Short, J.L, Phillips, V.R., Clark, J.A. and Wathes, C.M. (1999) Ammonia emissions from two mechanically ventilated UK livestock buildings. *Atmospheric Environment* **33**(2): 217-227.

Demmers, T.G.M., Phillips, V.R., Short, L.S., Burgess, L.R., Hoxey, R.P. and Wathes, C.M. (2001) Validation of ventilation rate measurement methods and the ammonia emission from naturally ventilated dairy and beef buildings in the United Kingdom. *Journal of Agricultural Engineering Research* **79**(1): 107-116.

Denmead, O.T., Harper, L.A., Freney, J.R., Griffith, D.W.T., Leuning, R. and Sharpe, R.R. (1998) A mass balance method for non-intrusive measurements of surface-air trace gas exchange. *Atmospheric Environment* **32**(21): 3679-3688.

Denmead, O.T., Simpson, J.R. and Freney, J.R. (1977) A direct field measurement of ammonia emission after injection of anhydrous ammonia. *Soil Science Society of America Journal* **41**: 1001-1004.

Doak, B.W. (1952) Some chemical changes in the nitrogenous constituents of urine when voided on pasture. *Journal of Agricultural Science* **42**: 162-171.

Döhler, H. (1991) Laboratory and field experiments for estimating ammonia losses from pig and cattle slurry following application. In: *Odour and Ammonia Emissions from Livestock Farming* (Eds: Nielsen, V.C., Voorburg, J.H. and L'Hermite, P.) Elsevier Science Publishers Ltd., Essex. pp 132-140.

Dourmad, J.Y., Guingand, N., Latimier, P. and Sève, B. (1999) Nitrogen and phosphorus consumption, utilisation and losses in pig production: France. *Livestock Production Science* **58**(3): 199-211.

Dueck, Th.A., Zuin, A. and Elderson, J. (1998) Influence of ammonia and ozone on growth and drought sensitivity of *Pinus sylvestris*. *Atmospheric Environment* **32**(3): 545-550.

Duncan, W.J., Thom, A.S. and Young, A.D. (1960) *An elementary treatise on the mechanics of fluids*. Edward Arnold (Publishers) Ltd., London.

ECETOC, (1994) *Ammonia Emissions to Air in Western Europe*, ECETOC, Brussels.

Erismann, J.W., Versluis, A.H., Verplanke, T.A.J.W., De Haan, D., Anink, D., Van Elzakker, B.G., Mennen, M.G. and Van Aalst, R.M. (1993) Monitoring the dry deposition of SO₂ in The Netherlands: results for grassland and heather vegetation. *Atmospheric Environment* **27A**(7): 1153-1161.

Fangmeier, A., Hadwiger-Fangmeier, A., Van der Eerden, L. and Jager, H.J (1994) Effects of atmospheric ammonia on vegetation - a review. *Environmental Pollution* **86**: 43-82.

Ferguson, R.B., McInnes, K.J., Kissel, D.E. and Kanemasu, E.T. (1988) A comparison of methods of estimating ammonia volatilization in the field. *Fertilizer Research* **15**: 55-69.

Ferm, M. (1986) Concentration measurements and equilibrium studies of ammonium, nitrate and sulphur species in air and precipitation. PhD thesis, Department of Inorganic Chemistry, Göteborg, Sweden.

Ferm, M., Areskoug, H., Hanssen, J.-E., Hilbert, G. and Lättilä, H. (1988) Field intercomparison of measurement techniques for total NH₄⁺ and total NO₃⁻ in ambient air. *Atmospheric Environment* **22**(10): 2275-2281.

Ferm, M. and Christensen, B. (1987) Determination of the NH₃ volatilization from surface-applied cattle slurry using flux samplers. In: *Ammonia and Acidification* (Eds: Asman WAH and Diederer HSMA), proceedings of the EURASAP Symposium, Bilthoven, 13-15 April 1987, RIVM, The Netherlands.

Ferm, M., Schjørring, J.K., Sommer, S.G. and Nielsen, S.B. (1991) Field investigation of methods to measure ammonia volatilization. In: *Odour and Ammonia Emissions from Livestock Farming* (Eds: Nielsen, V.C., Voorburg, J.H. and L'Hermite, P.) Elsevier Science Publishers Ltd., Essex. pp 148-155.

Flint, T.A., Persaud, K.C. and Sneath, R.W. (2000) Automated indirect method of ammonia flux measurement for agriculture: effect of incident wind angle on airflow measurements. *Sensors and Actuators B* **69**: 389-396.

Fox, R.H., Piekielek, W.P. and Macneal, K.E. (1996) Estimating ammonia volatilisation losses using a simplified micrometeorological sampler. *Soil Science Society of America Journal* **60**: 596-601.

Fox, D.L., Stockburger, L., Weathers, W., Spicer, C.W., Mackay, G.I., Schiff, H.I., Eatough, D.J., Mortensen, F., Hansen, L.D., Shepson, P.B., Kleindienst, T.E. and Edney, E.O. (1988) Intercomparison of nitric acid diffusion denuder methods with tunable diode laser absorption spectroscopy. *Atmospheric Environment* **22**(3): 575-585.

Freney, J.R., Simpson, J.R. and Denmead, O.T. (1983) Volatilization of ammonia. In: *Gaseous Loss of Ammonia from Plant-Soil Systems* (Eds: Freney, J.R. and Simpson, J.R.) Kluwer Academic Publishers Group, Dordrecht. pp 1-32.

Galbally, I.E. and Roy, C.R. (1983) The fate of nitrogen compounds in the atmosphere. In: *Gaseous Loss of Ammonia from Plant-Soil Systems* (Eds: Freney, J.R. and Simpson, J.R.) Kluwer Academic Publishers Group, Dordrecht. pp 265-284.

Galperin, M.V. and Sofiev, M.A. (1998) The long-range transport of ammonia and ammonium in the northern hemisphere. *Atmospheric Environment* **32**(3): 373-380.

Genermont, S., Cellier, P., Flura, D., Morvan, T. and Laville, P. (1998) Measuring ammonia fluxes after slurry spreading under actual field conditions. *Atmospheric Environment* **32**(3): 279-284.

Groot Koerkamp, P.W.G., Metz, J.H.M., Uenk, G.H., Phillips, V.R., Holden, M.R., Sneath, R.W., Short, J.L., White, R.P., Hartung, J., Seedorf, J., Schroder, M., Linkert, K.H., Pederson, S., Takai, H., Johnsen, J.O. and Wathes, C.M. (1998) Concentrations and emissions of ammonia in livestock buildings in Northern Europe. *Journal of Agricultural Engineering Research* **70**(1): 79-95.

Gustavsson, J. (1998) Swedish measures to reduce ammonia emissions. *Nutrient Cycling in Agroecosystems* **51**(1): 81-83.

Hanna, S.R. (1993) Uncertainties in air quality model predictions. *Boundary-Layer Meteorology* **62**: 3-20.

Hanna, S.R., Egan, B.A., Purdum, J. and Wagler, J. (2001) Evaluation of the ADMS, AERMOD, and ISC3 dispersion models with the OPTEX, Duke Forest, Kincaid, Indianapolis and Lovett field datasets. *International Journal of Environment and Pollution* **16**(1-6): 301-314.

Harper, L.A., Catchpole, V.R. and Vallis, I. (1983) Ammonia loss from fertilizer applied to tropical pastures. In: *Gaseous Loss of Ammonia from Plant-Soil Systems* (Eds: Freney, J.R. and Simpson, J.R.) Kluwer Academic Publishers Group, Dordrecht. pp 195-214.

Harper, L.A., Denmead, O.T., Freney, J.R. and Byers, F.M. (1999) Direct measurements of methane emissions from grazing and feedlot cattle. *Journal of Animal Science* **77**: 1392-1401.

Harrison, R.M. and Kitto, A.-M.N. (1990) Field intercomparison of filter pack and denuder sampling methods for reactive gaseous and particulate pollutants. *Atmospheric Environment* **24A**(10): 2633-2640.

Hartung, J. (1991) Influence of Housing and Livestock on Ammonia Release from Buildings, In: *Odour and Ammonia Emissions from Livestock Farming* (eds. Nielsen, V.C., Voorburg, J.H. and L'Hermite, P.) Elsevier Science Publishers Ltd., Essex. pp 22-30.

Heinsohn, R.J. and Kabel, R.L. (1999) *Sources and Control of Air Pollution*. Prentice-Hall Inc., New Jersey.

Hoff, J.D., Nelson, D.W. and Sutton, A.L. (1981) Ammonia volatilization from liquid swine manure applied to cropland. *Journal of Environmental Quality* **10**(1): 90-95.

Holman, C. (1999) Sources of air pollution. In: *Air Pollution and Health* (Eds: Holgate, S.T., Samet, J.M., Koren, H.S. and Maynard, R.L.) pp 115-148. Academic Press, London.

Hovmand, M.F., Andersen, H.V., Løfstrøm, P., Ahleson, H. and Jensen, N.O. (1998) Measurements of the horizontal gradient of ammonia over a conifer forest in Denmark. *Atmospheric Environment* **32**(3): 423-429.

Hoxey, R.P., Reynolds, A.M., Richardson, G.M., Robertson, A.P. and Short, J.L. (1998) Observations of Reynolds number sensitivity in the separated flow region on a bluff body. *Journal of Wind Engineering and Industrial Aerodynamics* **73**: 231-249.

Hoxey, R.P. and Richards, P.J. (1992) Structure of the Atmospheric Boundary Layer below 25 m and implications to wind loading on low-rise buildings. *Journal of Wind Engineering and Industrial Aerodynamics* **41-44**: 317-327.

- Hoxey, R.P., Richards, P.J. and Short, J.L. (2002) A 6m cube in an atmospheric boundary layer flow Part 1. Full-scale and wind-tunnel results. *Wind and Structures* 5(2-4): 165-176.
- Hoxey, R., Short, L. and Quinn, A. (1999) *Atmospheric Flow Laboratory – A report on the performance of the completed first phase of the atmospheric flow laboratory*. Silsoe Research Institute, Bedfordshire.
- Hutchinson, G.L., Mosier, A.R. and Andre, C.E (1982) Ammonia and amine emissions from a large cattle feedlot. *Journal of Environmental Quality* 11(2): 288-293.
- ITE Edinburgh, (now CEH, Edinburgh) web site at:
<http://www.nmw.ac.uk/ite/edin/pollut.html> (accessed Jan 2000).
- Jarvis, S.C. (1991) Grazed pastures as sources of ammonia. In: *Odour and Ammonia Emissions from Livestock Farming* (Eds: Nielsen, V.C., Voorburg, J.H. and L'Hermite, P.) Elsevier Science Publishers Ltd., Essex. pp 184-191.
- Jarvis, S.C., Stockdale, E.A., Shepherd, M.A. and Powlson, D.S. (1996) Nitrogen mineralization in temperate agricultural soils: processes and measurement. *Advances in Agronomy* 57: 187-235.
- Jeschke, Ch. (1996) Measuring gaseous emissions from an above-ground steel slurry store. *Report on an industrial training period at Silsoe Research Institute, UK, October 1995-February 1996*. Silsoe Research Institute, Bedford.
- Kim, J.H., Williams, A.G. and Phillips, V.R. (1999) A simple, controllable, non-point source of gaseous ammonia, for use in field experiments. *Environmental Technology* 20: 239-247.
- Kirchmann, H. and Lundvall, A. (1998) Treatment of solid animal manures: identification of low NH₃ emission practices. *Nutrient Cycling in Agroecosystems* 51(1): 65-71.
- Kirchner, M. and Braeutigam, S. (1998) Active and passive measurements of ammonia in Upper Bavaria. *Fresenius Environmental Bulletin* 7(3A-4A): 231-237.
- Kissel, D.E., Brewer, H.L. and Arkin, G.F. (1977) Design and test of a field sampler for ammonia volatilization. *Soil Science Society of America Journal* 41: 1133-1138.
- Klarenbeek, J.V. and Bruins, M.A. (1991) Ammonia Emissions after Land Spreading of Animal Slurries, In: *Odour and Ammonia Emissions from Livestock Farming* (eds. Nielsen, V.C., Voorburg, J.H. and L'Hermite, P.) Elsevier Science Publishers Ltd., Essex. pp 107-115.
- Klarenbeek, J.V., Pain, B.F., Phillips, V.R. and Lockyer, D.R. (1993) A comparison of methods for use in the measurement of ammonia emissions following the application of livestock waste to land. *International Journal of Environmental Analytical Chemistry* 53: 205-218.

- Lamb, B., Westberg, H. and Allwine, G. (1986) Isoprene emission fluxes determined by an atmospheric tracer technique. *Atmospheric Environment* **20**(1): 1-8.
- Lee, J.A. and Caporn, S.J.M (1998) Ecological effects of atmospheric reactive nitrogen deposition on semi-natural terrestrial ecosystems. *New Phytologist* **139**: 127-134.
- Lekkerkerk, L.J.A. (1998) Implications of Dutch ammonia policy on the livestock sector. *Atmospheric Environment* **32**(3): 581-587.
- Leuning, R., Baker, S.K., Jamie, I.M., Hsu, C.H., Klein, L., Denmead, O.T. and Griffith, D.W.T. (1999) Methane emission from free-ranging sheep: a comparison of two measurement methods. *Atmospheric Environment* **33**: 1357-1365.
- Leuning, R., Freney, J.R., Denmead, O.T. and Simpson, J.R. (1985) A sampler for measuring atmospheric ammonia flux. *Atmospheric Environment* **19**(7): 1117-1124.
- Lockyer, D.R. (1984) A system for the measurement in the field of losses of ammonia through volatilisation. *Journal of the Science of Food and Agriculture* **35**: 837-848.
- Lockyer, D.R. and Jarvis, S.C. (1995) The measurement of methane losses from grazing animals. *Environmental Pollution* **90**(3): 383-390.
- MAFF (1998) *Code of good agricultural practice for the protection of water*. MAFF, London.
- Mahlcke, M. (1998) The use of passive flux samplers in environmental atmospheric monitoring. *Report on an industrial training period at Silsoe Research Institute, UK, March 1998 – July 1998*. Silsoe Research Institute, Bedfordshire.
- Malgeryd, J. (1998) Technical measures to reduce ammonia losses after spreading of animal manure. *Nutrient Cycling in Agroecosystems* **51**(1): 51-57.
- McGinn, S.M. and Janzen, H.H. (1998) Ammonia sources in agriculture and their measurement. *Canadian Journal of Soil Science* **78**(1): 139-148.
- McGregor, G.R. (1999) Basic Meteorology. In: *Air Pollution and Health* (Eds: Holgate, S.T., Samet, J.M., Koren, H.S. and Maynard, R.L.) Academic Press, London.
- Michorius, J.A.T., Hartog, K.D., Scholtens, R. and Harssema, H. (1997) Measuring ammonia emissions from building complexes using the flux frame method and the Gaussian plume model: a feasibility study. (Translation of 'Ammoniakemissiemeting aan stalcomplexen met de fluxraammethode en het Gaussisch pluimmodel: een haalbaarheidsstudie', IMAG-DLO rapport 95-11 by Jones, S.H., Information Services, Silsoe Research Institute).
- Misselbrook, T.H., van der Weerden, T.J., Pain, B.F., Jarvis, S.C., Chambers B.J., Smith, K.A., Phillips, V.R. and Demmers, T.G.M. (2000) Ammonia emission factors for UK agriculture. *Atmospheric Environment* **34**: 871-880.

- Mitchell, R.J., Marrs, R.H., Le Duc, M.G. and Auld, M.H.D (1997) A study of succession on lowland heaths in Dorset, southern England: changes in vegetation and soil chemical properties. *Journal of Applied Ecology* **34**: 1426-1444.
- Monteith, J.L. and Unsworth, M.H. (1990) *Principles of environmental physics*. Edward Arnold, London.
- Moulsley, L.J., Randall, J.M., Hartshorn, R.L., Houghton, C.J. and Randle, D.G. (1987) *Facilities for measuring fan performance*. Divisional Note DN 1408, Bedford, UK: Silsoe Research Institute.
- Pain, B.F., Van der Weerden, T.J., Chambers, B.J., Phillips, V.R. and Jarvis, S.C. (1998) A new inventory for ammonia emissions from UK agriculture. *Atmospheric Environment* **32**(3): 309-313.
- Pearson, J. and Stewart, G.R., (1993) Tansley Review No. 56: The deposition of atmospheric ammonia and its effects on plants. *New Phytologist* **125**: 283-305.
- Peterson, S.O., Sommer, S.G., Aaes, O. and Søegaard, K. (1998) Ammonia losses from urine and dung of grazing cattle: effect of N intake. *Atmospheric Environment* **32**(3): 295-300.
- Phillips, V.R., Bishop, S.J., Price, J.S. and You, S. (1998a) Summer emissions of ammonia from a slurry-based, UK, dairy cow house. *Bioresource Technology* **65**(3): 213-219.
- Phillips, V.R., Holden, M.R., Sneath, R.W., Short, J.L., White, R.P., Hartung, J., Seedorf, J., Schroder, M., Linkert, K.H., Pederson, S., Takai, H., Johnsen, J.O., Koerkamp, P.W.G.G., Uenk, G.H., Scholtens, R., Metz, J.H.M. and Wathes, C.M. (1998b) The development of robust methods for measuring concentrations and emission rates of gaseous and particulate air pollutants in livestock buildings. *Journal of Agricultural Engineering Research* **70**(1): 11-24.
- Phillips, V.R., Lane, S.J. and Burgess, L.R. (2000a) A technique for measuring ammonia emissions from the individual parts of a livestock building. *Air pollution from agricultural operations*. Proceedings of the 2nd International Conference, Des Moines, Iowa, USA, 9-11 October 2000, St Joseph, USA: ASAE. pp: 84-91.
- Phillips, V.R., Lee, D.S., Scholtens, R., Garland, J.A. and Sneath R.W. (2001) A review of methods for measuring emission rates of ammonia from livestock buildings and slurry or manure stores, Part 2: Monitoring flux rates, concentrations and airflow rates. *Journal of Agricultural Engineering Research* **78**(1): 1-14.
- Phillips, V.R., Pain, B.F. and Klarenbeek, J.V. (1991) Factors Influencing the Odour and Ammonia Emissions During and After the Land Spreading of Animal Slurries, In: *Odour and Ammonia Emissions from Livestock Farming* (eds. Nielsen, V.C., Voorburg, J.H. and L'Hermite, P.) Elsevier Science Publishers Ltd., Essex. pp 98-106.

Phillips, V.R. and Scholtens, R. (1999) Improvements to the use of passive flux samplers for monitoring gaseous emissions from livestock buildings and manure stores. In: *Regulation of Animal Production in Europe*, International Congress in Wiesbaden, May 9-12, 1999. KTBL, Darmstadt, Germany pp. 375-376.

Phillips, V.R., Scholtens, R., Lee, D.S., Garland, J.A. and Sneath R.W. (2000) A review of methods for measuring emission rates of ammonia from livestock buildings and slurry or manure stores, Part 1: Assessment of basic approaches. *Journal of Agricultural Engineering Research* 77(4): 355-364.

Phillips, V.R. and Scholtens, R. (2001) Robust methods for measuring ammonia emission rates from livestock buildings and manure stores. Part 4. Development and validation of a method based on passive flux sampling. *Submitted to Atmospheric Environment*.

Phillips, V.R., Sneath, R.W., Williams, A.G., Welch, S.K., Burgess, L. R., Demmers, T.G.M. and Short, J.L. (1997) Measuring emission rates of ammonia, methane and nitrous oxide from full-sized slurry and manure stores. In: Voermans, J.A.M. and Monteny (Eds). Proceedings of the international conference "Ammonia and Odour Emissions from Animal Production Facilities" Vinkeloord, the Netherlands, October 6-10, 1997.

Quinn, A. (1996) The ventilation of a chick transport vehicle. PhD thesis, University of Nottingham.

Riley, J.E. (1990) In: *Outdoor Pigs: Principles and Practice*. Eds: Stark, B.A, Maclin, D.H. and Wilkinson, J.M. Chalcombe Publications, Buckinghamshire.

Roelofs, J.G.M. and Houdijk, A.L.F.M., (1991) Ecological Effects of Ammonia, In: *Odour and Ammonia Emissions from Livestock Farming* (eds. Nielsen, V.C., Voorburg, J.H. and L'Hermite, P.) Elsevier Science Publishers Ltd., Essex. pp 10-16.

Ross, C.A., Scholefield, D. and Jarvis, S.C. (2002) A model of ammonia volatilisation from a dairy farm: an examination of abatement strategies. *Nutrient Cycling in Agroecosystems* 64(3): 273-281.

Schjoerring, J.K., Sommer, S.G. and Ferm, M. (1992) A simple passive sampler for measuring ammonia emission in the field. *Water, Air and Soil Pollution* 62: 13-24.

Schjoerring, J.K., Husted, S. and Mattsson, M. (1998) Physiological parameters controlling plant-atmosphere ammonia exchange. *Atmospheric Environment* 32(3): 491-498.

Scholtens, R., Hol, J.M.G., Wagemans, M.J.M. and Phillips, V.R. (2002) Improved passive flux samplers for measuring ammonia emissions from animal houses, Part 1: Basic principles. *Submitted to Biosystems Engineering*.

Sherlock, R.R., Freney, J.R., Smith, N.P. and Cameron, K.C. (1989) Evaluation of a sampler for assessing ammonia losses from fertilized fields. *Fertilizer Research* 21: 61-66.

Sherlock, R.R. and Goh, K.M. (1984) Dynamics of ammonia volatilization from simulated urine patches and aqueous urea applied to pasture. I. Field experiments. *Fertilizer Research* **5**: 181-195.

Sickles, J.E., Perrino, C., Allegrini, I., Febo, A., Possanzini, M. and Paur, R.J. (1988) Sampling and analysis of ambient air near Los Angeles using an annular denuder system. *Atmospheric Environment* **22**(8): 1619-1625.

Simpson, J.R. and Steele, K.W. (1983) Gaseous nitrogen exchanges in grazed pastures. In: *Gaseous Loss of Ammonia from Plant-Soil Systems* (Eds: Freney, J.R. and Simpson, J.R.) Kluwer Academic Publishers Group, Dordrecht. pp 215-236.

Singles, R., Sutton, M.A. and Weston, K.J. (1998) A multi-layer model to describe the atmospheric transport and deposition of ammonia in Great Britain. *Atmospheric Environment* **32**(3): 393-399.

Sommer, S.G., Mikkelsen, H. and Mellqvist, J. (1995) Evaluation of measurement techniques for measurements of ammonia loss from pig slurry. *Agricultural and Forest Meteorology* **74**: 169-179.

Sommer, S.G., Olesen, J.E. and Christensen, B.T. (1991) Effects of temperature, wind speed and air humidity on ammonia volatilization from surface applied cattle slurry. *Journal of Agricultural Science* **117**: 91-100.

Sommer, S.G., Sibbesen, E., Nielsen, T., Schjoerring, J.K. and Olesen, J.E. (1996) A passive flux sampler for measuring ammonia volatilization from manure storage facilities. *Journal of Environmental Quality* **25**: 241-247.

Sommer, S.G., Søgaard, H.T., Møller, H.B. and Morsing, S. (2001) Ammonia volatilization from sows on grassland. *Atmospheric Environment* **35**: 2023-2032.

Sun, H., Stowell, R.R., Keener, H.M. and Michel, F.C. (2002) Two-dimensional fluid dynamics (CFD) modelling of air velocity and ammonia distribution in a High-Rise™ hog building. *Transactions of the ASAE* **45**(5): 1559-1568.

Sutton, M.A., Pitcairn, C.E.R. and Fowler, D. (1993) The exchange of ammonia between the atmosphere and plant communities. *Advances in Ecological Research* **24**: 301-390.

Sutton, M.A., Place, C.J., Eager, M., Fowler, D. and Smith, R.I. (1995) Assessment of the magnitude of ammonia emissions in the United Kingdom. *Atmospheric Environment* **29**(12): 1393-1411.

Sutton, M.A., Lee, D.S., Dollard, G.J. and Fowler, D. (1998) Introduction: Atmospheric ammonia: emission, deposition and environmental impacts. *Atmospheric Environment* **32**(3): 269-271.

Sutton, M.A., Dragosits, U., Tang, Y.S. and Fowler, D. (2000) Ammonia emissions from non-agricultural sources in the U.K. *Atmospheric Environment* **34**(6): 855-869.

Taylor, J.R. (1997) *An introduction to error analysis*. 2nd Edition. University Science Books, California.

Thornton, K (1988) *Outdoor Pig Production*. Butler and Tanner, Somerset.

Vallis, I., Harper, L.A., Catchpoole, V.R. and Weier, K.L. (1982) Volatilization of ammonia from urine patches in a subtropical pasture. *Australian Journal of Agricultural Research* **33**: 97-107.

van Breemen, N. and van Dijk, H.F.G (1988) Atmospheric deposition of N in The Netherlands. *Environmental Pollution* **54**:249-274.

van der Eerden, L., de Vries, W. and Van Dobben, H. (1998) Effects of ammonia deposition on forests in The Netherlands. *Atmospheric Environment* **32**(3): 525-532.

van der Peet-Schwering, C.M.C., Aarnink, A.J.A., Rom, H.B. and Dourmad, J.Y. (1999) Ammonia emissions from pig houses in The Netherlands, Denmark and France. *Livestock Production Science* **58**(3): 265-269.

Vandré, R. and Kaupenjohann, M. (1998) In situ measurement of ammonia emissions from organic fertilizers in plot experiments. *Soil Science Society of America Journal* **62**: 467-473.

Vertregt, N. and Rutgers, B. (1991) Ammonia emissions from grazing. In: *Odour and Ammonia Emissions from Livestock Farming* (Eds: Nielsen, V.C., Voorburg, J.H. and L'Hermite, P.) Elsevier Science Publishers Ltd., Essex. pp 177-183.

Vlassak, K., Bomans, H. and Van den Abbeel, R. (1991) Ammonia Emission and Control after Spreading Livestock Waste, In: *Odour and Ammonia Emissions from Livestock Farming* (eds. Nielsen, V.C., Voorburg, J.H. and L'Hermite, P.) Elsevier Science Publishers Ltd., Essex. pp 116-125.

Webb, J., Henderson, D. and Anthony, S.G. (2001) Optimizing livestock manure applications to reduce nitrate and ammonia pollution: scenario analysis using the MANNER model. *Soil Use and Management* **17**(3): 188-194.

Wiebe, H.A., Anlauf, K.G., Tuazon, E.C., Winer, A.M., Biermann, H.W., Appel, B.R., Solomon, P.A., Cass, G.R., Ellestad, T.G., Knapp, K.T., Peake, E., Spicer, C.W. and Lawson, D.R. (1990) A comparison of measurements of atmospheric ammonia by filter packs, Transition-flow reactors, Simple and Annular Denuders and Fourier Transform Infrared Spectroscopy. *Atmospheric Environment* **24A**(5): 1019-1028.

Williams, E.J., Sandholm, S.T., Bradshaw, J.D., Schendel, J.S., Langford, A.O., Quinn, P.K., LeBel, P.J., Vay, S.A., Roberts, P.D., Norton, R.B., Watkins, B.A., Buhr, M.P., Parrish, D.D., Calvert J.G. and Fehsenfeld, F.C. (1992) An intercomparison of five ammonia measurement techniques. *Journal of Geophysical Research* **97**(D11): 11591-11611.

Williams, J.R., Chambers, B.J., Hartley, A.R., Ellis, S. and Guise, H.J. (2000) Nitrogen losses from outdoor pig farming systems. *Soil Use and Management* **16**: 237-243.

Wilson, E.J. and Tiley, C. (1998) Foliar uptake of wet-deposited nitrogen by Norway spruce: an experiment using ^{15}N . *Atmospheric Environment* **32**(3): 513-518.

Wilson, J.D., Catchpole, V.R., Denmead, O.T. and Thurtell, G.W. (1983) Verification of a simple micrometeorological method for estimating the rate of gaseous mass transfer from the ground to the atmosphere. *Agricultural Meteorology* **29**: 183-189.

Yamulki, S., Harrison, R.M. and Goulding, K.W.T. (1996) Ammonia surface-exchange above an agricultural field in Southeast England. *Atmospheric Environment* **30**(1): 109-118.

Zhao, Y.Z. (2000) Line-pair selections for remote sensing of atmospheric ammonia by use of a coherent CO₂ differential absorption lidar system. *Applied Optics* **39** (6): 997-1007.

Zhao, Y.Z., Brewer, W.A., Eberhard, W.L. and Alvarez, R.J. (2002) Lidar measurement of ammonia concentrations and fluxes in a plume from a point source. *Journal of Atmospheric and Oceanic Technology* **19** (12): 1928-1938.

APPENDIX 1: CHEMICAL ANALYSIS OF SAMPLERS

NEN method 6472:

Standards and reagents were prepared for analysis:

- 1000 ppm NH₃ Standard (3.819 g ammonium chloride, predried at 105°C for 2 hours, dissolved in 1 litre of deionised water, stored at 4°C).
- 0.4-0.01 M NaOH
- Ultra high quality (UHQ) water
- Reagent A: Dichloroisocyanurate Reagent
Dissolve 32.0 g sodium hydroxide in 500 ml UHQ water. Cool to room temperature and add 2.0 g of sodium dichloroisocyanurate (NaC₃N₃O₃Cl₂). Fill to 1 l with UHQ water and store in an amber bottle at 4°C. Stable for up to a month.
- Reagent B: Salicylate Reagent
Dissolve 130 g of sodium salicylate (NaC₇H₅O₃) and 130 g of trisodium citrate (Na₃C₆H₅O₇·2H₂O) in 650 ml UHQ water. Add 0.970 g of disodium pentacyanonitrosoferric (III) dehydrate (Na₂[Fe(CN)₅NO]·2H₂O), shake, then add UHQ to 1 l. Store in an amber bottle, stable for at least a month.

Standards appropriate to the range of ammonia concentrations expected to be found were prepared using the 1000 ppm NH₃ standard. 1 ml of the 1000 ppm standard was pipetted into a 100 ml volumetric flask and filled with UHQ water to give a 10 ppm NH₃ standard. 250 µl, 500 µl, 1000 µl, 1500 µl and 2000 µl of this 10 ppm standard were then pipetted into test tubes and made up to 6 ml with UHQ water. 2 ml Reagent A and 2 ml Reagent B were then added, giving a total volume of 10 ml in each test tube and standards of 2.5 ppm, 5.0 ppm, 10.0 ppm, 15.0 ppm and 20.0 ppm. Blanks were prepared using 6 ml of UHQ water, with 2 ml of Reagent A and 2 ml of Reagent B added. These were left for an hour at room temperature (approx. 18 - 20°C) to allow the colour to develop.

Each sample ('sample' refers to either the 6 ml of solution from washing the glass flux tubes or 4ml of solution from the bubblers) was analysed in duplicate. 1 ml of the sample, 5 ml of 0.01 M NaOH (to bring the pH up to ~ 8), 2 ml of Reagent A and 2 ml of Reagent B were pipetted into a test tube. These were left for an hour at room temperature for the colour to develop.

Measurement was performed using UV-visible spectrophotometry, at a wavelength of 655 nm. Blanks were used to set a baseline reading, then the standards were used to produce a standard curve. Each duplicated sample was then run through the spectrophotometer to measure the absorption. As the absorption of the sample is directly proportional to its concentration, the concentration of ammonia in the sample can be determined.

APPENDIX 2: UNCERTAINTY OF FLUX MEASUREMENTS

Taylor (1997) states:

'If various quantities x, \dots, w are measured with small uncertainties $\delta x, \dots, \delta w$, and the measured values are used to calculate some quantity q , then the uncertainties in x, \dots, w cause an uncertainty in q as follows:

If q is the sum and difference, $q = x + \dots + z - (u + \dots + w)$, then

$$\delta q = \sqrt{(\delta x)^2 + \dots + (\delta z)^2 + (\delta u)^2 + \dots + (\delta w)^2} \quad (\text{A1})$$

..... If q is the product and quotient, $q = \frac{x \times \dots \times z}{u \times \dots \times w}$, then

$$\frac{\delta q}{|q|} = \sqrt{\left(\frac{\delta x}{x}\right)^2 + \dots + \left(\frac{\delta z}{z}\right)^2 + \left(\frac{\delta u}{u}\right)^2 + \dots + \left(\frac{\delta w}{w}\right)^2} \quad (\text{A2})$$

for independent random errors'.

When a number of measurements are taken to produce an estimate, the average uncertainty, δx , is defined as the standard deviation of the mean of a sample, or the standard error.

For the flux calculation in equation 14, the uncertainty can thus be calculated:

The mass of ammonia collected by each sampling tube is determined by UV-VIS spectrophotometry. A standard curve is used to calibrate the analyser before each run of samples is fed through, and this standard curve can be used to calculate the error in each measured concentration.

Standards of known concentration are analysed and a graph of absorbance against concentration is produced. This graph is then used by the analyser to determine the unknown concentration of each sample from its measured absorbance. Whilst the fit of the straight line to the absorbance against concentration ($A = a + bC$) graph was always very good (coefficient > 0.998), when the relationship is inverted (to concentration against absorbance, $C = \frac{A - a}{b}$) this fit changes.

The 95th percentile bands are ± 0.7 at the edges and ± 0.64 near the centre (see Figure A2.1), and thus the confidence limits of each concentration measurement are found. An approximate standard error based on this can then be found by dividing the worst confidence interval (0.7) by the t value for the slope (3.182). This gives a s.e. of 0.22. A fractional uncertainty for concentration and thus mass of ammonia captured can be estimated.

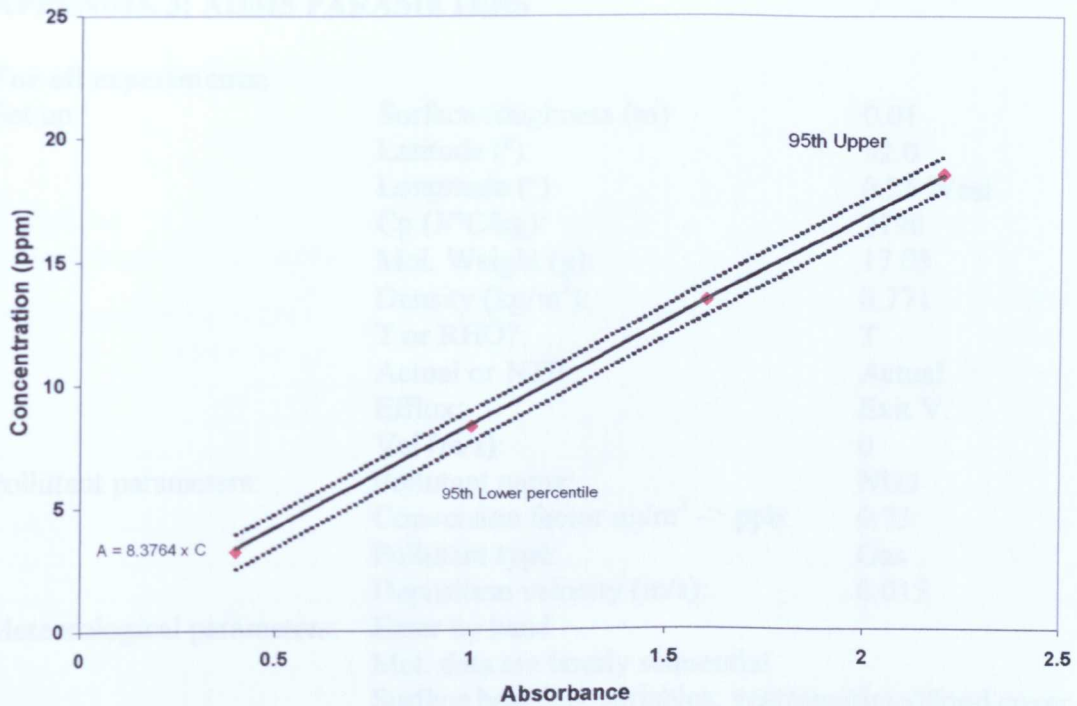


Figure A2.1: Concentration against absorbance graph typical of each analysis run.

Using equation A1, the error in ΔM is therefore:

$$\begin{aligned} \delta(\Delta M) &= \sqrt{(0.22)^2 + (0.22)^2} \\ &= 0.31 \end{aligned}$$

For a ΔM of 10 mg NH_3 , this is a fractional difference of 3.1%, whilst when ΔM is 1 mg NH_3 , this is a fractional difference of 31%.

The fractional difference on the r^2 term in equation 14 is:

$$0.5 \pm 0.025 \text{ mm} \quad = \pm 5\%$$

The fractional difference on the t term in equation 14 is, in the worst case (the shortest run):

$$3600 \pm 30 \text{ s} \quad = \pm 0.83\%$$

The fractional difference on the sampler constant, K , when it is used is:

$$0.71 \pm 0.04 \quad = \pm 6\%$$

Thus, using equation A2, for a high flux measurement, a low fractional difference is found ($\approx 8\%$) but for a low flux measurement, a high fractional difference is found ($\approx 32\%$). However, 32% of a negligible flux is still a negligible quantity.

APPENDIX 3: ADMS PARAMETERS

For all experiments:

Set up:	Surface roughness (m):	0.01
	Latitude (°):	52.0
	Longitude (°):	0.25 West
	Cp (J/°C/kg):	2190
	Mol. Weight (g):	17.03
	Density (kg/m ³):	0.771
	T or RHO?:	T
	Actual or NTP:	Actual
	Efflux:	Exit V.
	Vel (m/s):	0
Pollutant parameters:	Pollutant name:	NH3
	Conversion factor ug/m ³ -> ppb:	0.73
	Pollutant type:	Gas
	Deposition velocity (m/s):	0.015
Meteorological parameters:	Enter by hand	
	Met. data are hourly sequential	
	Surface heat flux variables: year/day/time/cloud cover	
Grids:	Cartesian co-ordinate system	
	Specified points	
Output:	Short/Long:	ST
	Averaging time:	1 Hr
	Units for output:	ug/m ³

Parameters specific to field experiments:

Meteorological parameters:	Height of recorded wind (m):	5.37
	Met parameters to be entered:	Lateral spread

Parameters specific to Frame 1:

Set up:	Source type:	P
	Height (m):	0.3
	Diam. (m):	0.004
Emissions:	Emission rate (g/s):	3.5 x 10 ⁻¹
Meteorological parameters:		

Wind speed (m/s)	Wind angle (degrees)	Year	Julian day number	Local time (hours)	Cloud cover (oktas)	Lateral spread (degrees)
5.48	258	2000	230	11	6	2.9
5.83	267	2000	230	12	6	7.48
5.35	260	2000	230	13	6	8.95
5.78	260	2000	230	14	6	6.26
5.61	263	2000	230	15	6	2.93
5.72	263	2000	230	16	6	10.55
4.17	281	2000	230	17	6	4.84
3.39	284	2000	230	18	6	3.41

Grids: Specified points: Frame 1 grid

Source point source: Include

Parameters specific to Frame 2:

Set up: Source type: P
 Height (m): 0.3
 Diam. (m): 0.004
 Emissions: Emission rate (g/s): 3.5×10^{-1}

Meteorological parameters:

Wind speed (m/s)	Wind angle (degrees)	Year	Julian day number	Local time (hours)	Cloud cover (oktas)	Lateral spread (degrees)
4.50	208	2000	249	12	6	3.09
3.58	215	2000	249	13	6	8.59
3.87	197	2000	249	14	6	7.59
2.68	209	2000	249	15	6	14.44
2.91	207	2000	249	16	6	10.08
2.91	186	2000	249	17	6	6.70
2.99	189	2000	249	18	6	4.98

Grids: Specified points: Frames 2/3 grid
 Source: point source: Include

Parameters specific to Frame 3:

Set up: Source type: P
 Height (m): 0.3
 Diam. (m): 0.004
 Emissions: Emission rate (g/s): 2.9×10^{-1}

Meteorological parameters:

Wind speed (m/s)	Wind angle (degrees)	Year	Julian day number	Local time (hours)	Cloud cover (oktas)	Lateral spread (degrees)
4.83	250	2000	256	10	4	5.48
5.85	245	2000	256	11	4	6.25
5.95	247	2000	256	12	4	6.32
5.57	252	2000	256	13	4	10.06
5.91	270	2000	256	14	4	10.87
5.47	269	2000	256	15	4	6.69
5.48	269	2000	256	16	4	6.51

Grids: Specified points: Frames 2/3 grid
 Source: point source: Include

Parameters specific to Frame 4:

Set up: Source type: P
 Height (m): 0.3
 Diam. (m): 0.004
 Emissions: Emission rate (g/s): 4.1×10^{-1}

Meteorological parameters:

Wind speed (m/s)	Wind angle (degrees)	Year	Julian day number	Local time (hours)	Cloud cover (oktas)	Lateral spread (degrees)
4.56	249	2000	278	11	5	13.5
4.49	234	2000	278	12	5	17.7
4.07	233	2000	278	13	5	13.4
4.48	247	2000	278	14	5	17.9
4.29	248	2000	278	15	5	12.2
4.29	249	2000	278	16	5	12.4

Grids: Specified points: Frames 4/5 grid
 Source: point source: Include

Parameters specific to Frame 5:

Set up: Source type: P
 Height (m): 0.3
 Diam. (m): 0.004
 Emissions: Emission rate (g/s): 4.2×10^{-1}

Meteorological parameters:

Wind speed (m/s)	Wind angle (degrees)	Year	Julian day number	Local time (hours)	Cloud cover (oktas)	Lateral spread (degrees)
6.21	248	2000	300	11	6	10.69
6.66	250	2000	300	12	6	11.68
7.92	258	2000	300	13	6	10.45
7.18	257	2000	300	14	6	11.68
5.83	260	2000	300	15	6	12.9

Grids: Specified points: Frames 4/5 grid
 Source: point source: Include

Parameters specific to Frame 6:

Set up: Source type: L
 Height (m): 0.3
 Emissions: Emission rate (g/m/s): 1.97×10^{-3}
 Geometry: Vertices:

x	y
-16	37
16	-37

Meteorological parameters:

Wind speed (m/s)	Wind angle (degrees)	Year	Julian day number	Local time (hours)	Cloud cover (oktas)	Lateral spread (degrees)
4.03	272.6	2001	232	12	2	14.89
3.98	276.7	2001	232	13	2	16.32
3.37	287.7	2001	232	14	2	29.7
2.94	296	2001	232	15	2	22.37
2.53	287.7	2001	232	16	2	22.09
2.88	290.7	2001	232	17	2	19.35

Grids: Specified points: Frames 6-12 grid
 Source: Line source: Include

Parameters specific to Frame 7:

Set up: Source type: L
 Height (m): 0.3
 Emissions: Emission rate (g/m/s): 2.49×10^{-3}
 Geometry: Vertices:

x	y
-16	37
16	-37

Meteorological parameters:

Wind speed (m/s)	Wind angle (degrees)	Year	Julian day number	Local time (hours)	Cloud cover (oktas)	Lateral spread (degrees)
5.08	276.1	2001	250	10	4	13.99
4.92	280.2	2001	250	11	4	12.45
5.31	280.7	2001	250	12	4	14.03
5.62	264.2	2001	250	13	4	18.53
6.25	260.5	2001	250	14	4	12.76
5.65	250.6	2001	250	15	4	13.1

Grids: Specified points: Frames 6-12 grid
 Source: Line source: Include

Parameters specific to Frame 8:

Set up: Source type: L
 Height (m): 0.3
 Emissions: Emission rate (g/m/s): 2.43×10^{-3}
 Geometry: Vertices:

x	y
-5	12
11	-25

Meteorological parameters:

Wind speed (m/s)	Wind angle (degrees)	Year	Julian day number	Local time (hours)	Cloud cover (oktas)	Lateral spread (degrees)
7.26	235.9	2001	276	11	4	12.55
7.36	238.6	2001	276	12	4	9.35
7.07	239.9	2001	276	13	4	11.53
7.21	236.7	2001	276	14	4	10.92
5.9	236.4	2001	276	15	4	17.13
6.66	242.8	2001	276	16	4	12.04

Grids:

Specified points:

Frames 6-12 grid

Source:

Line source:

Include

Parameters specific to Frame 10:

Set up:

Source type:

L

Height (m):

0.3

Emissions:

Emission rate (g/m/s):

5.28×10^{-3}

Geometry:

Vertices:

x	y
-4	9
4	-9

Meteorological parameters:

Wind speed (m/s)	Wind angle (degrees)	Year	Julian day number	Local time (hours)	Cloud cover (oktas)	Lateral spread (degrees)
6.03	252	2001	302	11	4	7.67
5.15	253	2001	302	12	4	6.52
3.86	241	2001	302	13	4	11.73
5.84	239	2001	302	14	4	4.65
5.63	243	2001	302	15	4	5.27

Grids:

Specified points:

Frames 6-12 grid

Source:

Line source:

Include

Parameters specific to Frame 11:

Set up:

Source type:

L

Height (m):

0.3

Emissions:

Emission rate (g/m/s):

6.94×10^{-3}

Geometry:

Vertices:

x	y
-4	9
4	-9

Meteorological parameters:

Wind speed (m/s)	Wind angle (degrees)	Year	Julian day number	Local time (hours)	Cloud cover (oktas)	Lateral spread (degrees)
5.60	206	2001	303	11	4	8.34
7.25	220	2001	303	12	4	5.32
7.41	224	2001	303	13	4	4.66
6.94	222	2001	303	14	4	6.68
5.85	224	2001	303	15	4	5.55

Grids: Specified points: Frames 6-12 grid
 Source: Line source: Include

Parameters specific to Frame 12:

Set up: Source type: L
 Height (m): 0.3
 Emissions: Emission rate (g/m/s): 9.57×10^{-3}
 Geometry: Vertices:

x	y
-4	9
4	-9

Meteorological parameters:

Wind speed (m/s)	Wind angle (degrees)	Year	Julian day number	Local time (hours)	Cloud cover (oktas)	Lateral spread (degrees)
7.95	233.3	2001	325	11	4	4.35
8.28	230.8	2001	325	12	4	3.91
8.43	234	2001	325	13	4	3.44
8.01	238.5	2001	325	14	4	3.72

Grids: Specified points: Frames 6-12 grid
 Source: Line source: Include

X (m)	Y (m)	Z (m)	X (m)	Y (m)	Z (m)	X (m)	Y (m)	Z (m)
24.51	-18.05	1.47	16.05	0.85	4.85	8.53	17.65	8.71
24.51	-18.05	4.37	16.05	0.85	6.78	8.53	17.65	10.64
24.51	-18.05	7.27	16.05	0.85	8.71	7.59	19.75	0.99
24.51	-18.05	10.17	16.05	0.85	10.64	7.59	19.75	2.92
23.57	-15.95	1.47	15.11	2.95	0.99	7.59	19.75	4.85
23.57	-15.95	4.37	15.11	2.95	2.92	7.59	19.75	6.78
23.57	-15.95	7.27	15.11	2.95	4.85	7.59	19.75	8.71
23.57	-15.95	10.17	15.11	2.95	6.78	7.59	19.75	10.64
22.63	-13.85	1.47	15.11	2.95	8.71	6.65	21.85	0.99
22.63	-13.85	4.37	15.11	2.95	10.64	6.65	21.85	2.92
22.63	-13.85	7.27	14.17	5.05	0.99	6.65	21.85	4.85
22.63	-13.85	10.17	14.17	5.05	2.92	6.65	21.85	6.78
21.69	-11.75	0.99	14.17	5.05	4.85	6.65	21.85	8.71
21.69	-11.75	2.92	14.17	5.05	6.78	6.65	21.85	10.64
21.69	-11.75	4.85	14.17	5.05	8.71	5.71	23.95	0.99
21.69	-11.75	6.78	14.17	5.05	10.64	5.71	23.95	2.92
21.69	-11.75	8.71	13.23	7.15	0.99	5.71	23.95	4.85
21.69	-11.75	10.64	13.23	7.15	2.92	5.71	23.95	6.78
20.75	-9.65	0.99	13.23	7.15	4.85	5.71	23.95	8.71
20.75	-9.65	2.92	13.23	7.15	6.78	5.71	23.95	10.64
20.75	-9.65	4.85	13.23	7.15	8.71	4.77	26.05	1.47
20.75	-9.65	6.78	13.23	7.15	10.64	4.77	26.05	4.37
20.75	-9.65	8.71	12.29	9.25	0.99	4.77	26.05	7.27
20.75	-9.65	10.64	12.29	9.25	2.92	4.77	26.05	10.17
19.81	-7.55	0.99	12.29	9.25	4.85	3.83	28.15	1.47
19.81	-7.55	2.92	12.29	9.25	6.78	3.83	28.15	4.37
19.81	-7.55	4.85	12.29	9.25	8.71	3.83	28.15	7.27
19.81	-7.55	6.78	12.29	9.25	10.64	3.83	28.15	10.17
19.81	-7.55	8.71	11.35	11.35	0.99	2.89	30.25	1.47
19.81	-7.55	10.64	11.35	11.35	2.92	2.89	30.25	4.37
18.87	-5.45	0.99	11.35	11.35	4.85	2.89	30.25	7.27
18.87	-5.45	2.92	11.35	11.35	6.78	2.89	30.25	10.17
18.87	-5.45	4.85	11.35	11.35	8.71			
18.87	-5.45	6.78	11.35	11.35	10.64			
18.87	-5.45	8.71	10.41	13.45	0.99			
18.87	-5.45	10.64	10.41	13.45	2.92			
17.93	-3.35	0.99	10.41	13.45	4.85			
17.93	-3.35	2.92	10.41	13.45	6.78			
17.93	-3.35	4.85	10.41	13.45	8.71			
17.93	-3.35	6.78	10.41	13.45	10.64			
17.93	-3.35	8.71	9.47	15.55	0.99			
17.93	-3.35	10.64	9.47	15.55	2.92			
16.99	-1.25	0.99	9.47	15.55	4.85			
16.99	-1.25	2.92	9.47	15.55	6.78			
16.99	-1.25	4.85	9.47	15.55	8.71			
16.99	-1.25	6.78	9.47	15.55	10.64			
16.99	-1.25	8.71	8.53	17.65	0.99			
16.99	-1.25	10.64	8.53	17.65	2.92			
16.05	0.85	0.99	8.53	17.65	4.85			
16.05	0.85	2.92	8.53	17.65	6.78			

FRAME 1

X (m)	Y (m)	Z (m)	X (m)	Y (m)	Z (m)	X (m)	Y (m)	Z (m)
33.61	-13.95	1.47	25.15	4.95	4.85	17.63	21.75	8.71
33.61	-13.95	4.37	25.15	4.95	6.78	17.63	21.75	10.64
33.61	-13.95	7.27	25.15	4.95	8.71	16.69	23.85	0.99
33.61	-13.95	10.17	25.15	4.95	10.64	16.69	23.85	2.92
32.67	-11.85	1.47	24.21	7.05	0.99	16.69	23.85	4.85
32.67	-11.85	4.37	24.21	7.05	2.92	16.69	23.85	6.78
32.67	-11.85	7.27	24.21	7.05	4.85	16.69	23.85	8.71
32.67	-11.85	10.17	24.21	7.05	6.78	16.69	23.85	10.64
31.73	-9.75	1.47	24.21	7.05	8.71	15.75	25.95	0.99
31.73	-9.75	4.37	24.21	7.05	10.64	15.75	25.95	2.92
31.73	-9.75	7.27	23.27	9.15	0.99	15.75	25.95	4.85
31.73	-9.75	10.17	23.27	9.15	2.92	15.75	25.95	6.78
30.79	-7.65	0.99	23.27	9.15	4.85	15.75	25.95	8.71
30.79	-7.65	2.92	23.27	9.15	6.78	15.75	25.95	10.64
30.79	-7.65	4.85	23.27	9.15	8.71	14.81	28.05	0.99
30.79	-7.65	6.78	23.27	9.15	10.64	14.81	28.05	2.92
30.79	-7.65	8.71	22.33	11.25	0.99	14.81	28.05	4.85
30.79	-7.65	10.64	22.33	11.25	2.92	14.81	28.05	6.78
29.85	-5.55	0.99	22.33	11.25	4.85	14.81	28.05	8.71
29.85	-5.55	2.92	22.33	11.25	6.78	14.81	28.05	10.64
29.85	-5.55	4.85	22.33	11.25	8.71	13.87	30.15	1.47
29.85	-5.55	6.78	22.33	11.25	10.64	13.87	30.15	4.37
29.85	-5.55	8.71	21.39	13.35	0.99	13.87	30.15	7.27
29.85	-5.55	10.64	21.39	13.35	2.92	13.87	30.15	10.17
28.91	-3.45	0.99	21.39	13.35	4.85	12.93	32.25	1.47
28.91	-3.45	2.92	21.39	13.35	6.78	12.93	32.25	4.37
28.91	-3.45	4.85	21.39	13.35	8.71	12.93	32.25	7.27
28.91	-3.45	6.78	21.39	13.35	10.64	12.93	32.25	10.17
28.91	-3.45	8.71	20.45	15.45	0.99	11.99	34.35	1.47
28.91	-3.45	10.64	20.45	15.45	2.92	11.99	34.35	4.37
27.97	-1.35	0.99	20.45	15.45	4.85	11.99	34.35	7.27
27.97	-1.35	2.92	20.45	15.45	6.78	11.99	34.35	10.17
27.97	-1.35	4.85	20.45	15.45	8.71			
27.97	-1.35	6.78	20.45	15.45	10.64			
27.97	-1.35	8.71	19.51	17.55	0.99			
27.97	-1.35	10.64	19.51	17.55	2.92			
27.03	0.75	0.99	19.51	17.55	4.85			
27.03	0.75	2.92	19.51	17.55	6.78			
27.03	0.75	4.85	19.51	17.55	8.71			
27.03	0.75	6.78	19.51	17.55	10.64			
27.03	0.75	8.71	18.57	19.65	0.99			
27.03	0.75	10.64	18.57	19.65	2.92			
26.09	2.85	0.99	18.57	19.65	4.85			
26.09	2.85	2.92	18.57	19.65	6.78			
26.09	2.85	4.85	18.57	19.65	8.71			
26.09	2.85	6.78	18.57	19.65	10.64			
26.09	2.85	8.71	17.63	21.75	0.99			
26.09	2.85	10.64	17.63	21.75	2.92			
25.15	4.95	0.99	17.63	21.75	4.85			
25.15	4.95	2.92	17.63	21.75	6.78			

FRAMES 2 + 3

X (m)	Y (m)	Z (m)	X (m)	Y (m)	Z (m)	X (m)	Y (m)	Z (m)
56.51	-3.85	1.47	48.05	15.05	4.85	40.53	31.85	8.71
56.51	-3.85	4.37	48.05	15.05	6.78	40.53	31.85	10.64
56.51	-3.85	7.27	48.05	15.05	8.71	39.59	33.95	0.99
56.51	-3.85	10.17	48.05	15.05	10.64	39.59	33.95	2.92
55.57	-1.75	1.47	47.11	17.15	0.99	39.59	33.95	4.85
55.57	-1.75	4.37	47.11	17.15	2.92	39.59	33.95	6.78
55.57	-1.75	7.27	47.11	17.15	4.85	39.59	33.95	8.71
55.57	-1.75	10.17	47.11	17.15	6.78	39.59	33.95	10.64
54.63	0.35	1.47	47.11	17.15	8.71	38.65	36.05	0.99
54.63	0.35	4.37	47.11	17.15	10.64	38.65	36.05	2.92
54.63	0.35	7.27	46.17	19.25	0.99	38.65	36.05	4.85
54.63	0.35	10.17	46.17	19.25	2.92	38.65	36.05	6.78
53.69	2.45	0.99	46.17	19.25	4.85	38.65	36.05	8.71
53.69	2.45	2.92	46.17	19.25	6.78	38.65	36.05	10.64
53.69	2.45	4.85	46.17	19.25	8.71	37.71	38.15	0.99
53.69	2.45	6.78	46.17	19.25	10.64	37.71	38.15	2.92
53.69	2.45	8.71	45.23	21.35	0.99	37.71	38.15	4.85
53.69	2.45	10.64	45.23	21.35	2.92	37.71	38.15	6.78
52.75	4.55	0.99	45.23	21.35	4.85	37.71	38.15	8.71
52.75	4.55	2.92	45.23	21.35	6.78	37.71	38.15	10.64
52.75	4.55	4.85	45.23	21.35	8.71	36.77	40.25	1.47
52.75	4.55	6.78	45.23	21.35	10.64	36.77	40.25	4.37
52.75	4.55	8.71	44.29	23.45	0.99	36.77	40.25	7.27
52.75	4.55	10.64	44.29	23.45	2.92	36.77	40.25	10.17
51.81	6.65	0.99	44.29	23.45	4.85	35.83	42.35	1.47
51.81	6.65	2.92	44.29	23.45	6.78	35.83	42.35	4.37
51.81	6.65	4.85	44.29	23.45	8.71	35.83	42.35	7.27
51.81	6.65	6.78	44.29	23.45	10.64	35.83	42.35	10.17
51.81	6.65	8.71	43.35	25.55	0.99	34.89	44.45	1.47
51.81	6.65	10.64	43.35	25.55	2.92	34.89	44.45	4.37
50.87	8.75	0.99	43.35	25.55	4.85	34.89	44.45	7.27
50.87	8.75	2.92	43.35	25.55	6.78	34.89	44.45	10.17
50.87	8.75	4.85	43.35	25.55	8.71			
50.87	8.75	6.78	43.35	25.55	10.64			
50.87	8.75	8.71	42.41	27.65	0.99			
50.87	8.75	10.64	42.41	27.65	2.92			
49.93	10.85	0.99	42.41	27.65	4.85			
49.93	10.85	2.92	42.41	27.65	6.78			
49.93	10.85	4.85	42.41	27.65	8.71			
49.93	10.85	6.78	42.41	27.65	10.64			
49.93	10.85	8.71	41.47	29.75	0.99			
49.93	10.85	10.64	41.47	29.75	2.92			
48.99	12.95	0.99	41.47	29.75	4.85			
48.99	12.95	2.92	41.47	29.75	6.78			
48.99	12.95	4.85	41.47	29.75	8.71			
48.99	12.95	6.78	41.47	29.75	10.64			
48.99	12.95	8.71	40.53	31.85	0.99			
48.99	12.95	10.64	40.53	31.85	2.92			
48.05	15.05	0.99	40.53	31.85	4.85			
48.05	15.05	2.92	40.53	31.85	6.78			

FRAMES 4+ 5

X (m)	Y (m)	Z (m)	X (m)	Y (m)	Z (m)	X (m)	Y (m)	Z (m)
33.61	-13.95	0.3	26.09	2.85	2.92	19.51	17.55	8.71
33.61	-13.95	1.47	26.09	2.85	4.85	19.51	17.55	10.64
33.61	-13.95	4.37	26.09	2.85	6.78	18.57	19.65	0.3
33.61	-13.95	7.27	26.09	2.85	8.71	18.57	19.65	0.99
33.61	-13.95	10.17	26.09	2.85	10.64	18.57	19.65	2.92
32.67	-11.85	0.3	25.15	4.95	0.3	18.57	19.65	4.85
32.67	-11.85	1.47	25.15	4.95	0.99	18.57	19.65	6.78
32.67	-11.85	4.37	25.15	4.95	2.92	18.57	19.65	8.71
32.67	-11.85	7.27	25.15	4.95	4.85	18.57	19.65	10.64
32.67	-11.85	10.17	25.15	4.95	6.78	17.63	21.75	0.3
31.73	-9.75	0.3	25.15	4.95	8.71	17.63	21.75	0.99
31.73	-9.75	1.47	25.15	4.95	10.64	17.63	21.75	2.92
31.73	-9.75	4.37	24.21	7.05	0.3	17.63	21.75	4.85
31.73	-9.75	7.27	24.21	7.05	0.99	17.63	21.75	6.78
31.73	-9.75	10.17	24.21	7.05	2.92	17.63	21.75	8.71
30.79	-7.65	0.3	24.21	7.05	4.85	17.63	21.75	10.64
30.79	-7.65	0.99	24.21	7.05	6.78	16.69	23.85	0.3
30.79	-7.65	2.92	24.21	7.05	8.71	16.69	23.85	0.99
30.79	-7.65	4.85	24.21	7.05	10.64	16.69	23.85	2.92
30.79	-7.65	6.78	23.27	9.15	0.3	16.69	23.85	4.85
30.79	-7.65	8.71	23.27	9.15	0.99	16.69	23.85	6.78
30.79	-7.65	10.64	23.27	9.15	2.92	16.69	23.85	8.71
29.85	-5.55	0.3	23.27	9.15	4.85	16.69	23.85	10.64
29.85	-5.55	0.99	23.27	9.15	6.78	15.75	25.95	0.3
29.85	-5.55	2.92	23.27	9.15	8.71	15.75	25.95	0.99
29.85	-5.55	4.85	23.27	9.15	10.64	15.75	25.95	2.92
29.85	-5.55	6.78	22.33	11.25	0.3	15.75	25.95	4.85
29.85	-5.55	8.71	22.33	11.25	0.99	15.75	25.95	6.78
29.85	-5.55	10.64	22.33	11.25	2.92	15.75	25.95	8.71
28.91	-3.45	0.3	22.33	11.25	4.85	15.75	25.95	10.64
28.91	-3.45	0.99	22.33	11.25	6.78	14.81	28.05	0.3
28.91	-3.45	2.92	22.33	11.25	8.71	14.81	28.05	0.99
28.91	-3.45	4.85	22.33	11.25	10.64	14.81	28.05	2.92
28.91	-3.45	6.78	21.39	13.35	0.3	14.81	28.05	4.85
28.91	-3.45	8.71	21.39	13.35	0.99	14.81	28.05	6.78
28.91	-3.45	10.64	21.39	13.35	2.92	14.81	28.05	8.71
27.97	-1.35	0.3	21.39	13.35	4.85	14.81	28.05	10.64
27.97	-1.35	0.99	21.39	13.35	6.78	13.87	30.15	0.3
27.97	-1.35	2.92	21.39	13.35	8.71	13.87	30.15	1.47
27.97	-1.35	4.85	21.39	13.35	10.64	13.87	30.15	4.37
27.97	-1.35	6.78	20.45	15.45	0.3	13.87	30.15	7.27
27.97	-1.35	8.71	20.45	15.45	0.99	13.87	30.15	10.17
27.97	-1.35	10.64	20.45	15.45	2.92	12.93	32.25	0.3
27.03	0.75	0.3	20.45	15.45	4.85	12.93	32.25	1.47
27.03	0.75	0.99	20.45	15.45	6.78	12.93	32.25	4.37
27.03	0.75	2.92	20.45	15.45	8.71	12.93	32.25	7.27
27.03	0.75	4.85	20.45	15.45	10.64	12.93	32.25	10.17
27.03	0.75	6.78	19.51	17.55	0.3	11.99	34.35	0.3
27.03	0.75	8.71	19.51	17.55	0.99	11.99	34.35	1.47
27.03	0.75	10.64	19.51	17.55	2.92	11.99	34.35	4.37
26.09	2.85	0.3	19.51	17.55	4.85	11.99	34.35	7.27
26.09	2.85	0.99	19.51	17.55	6.78	11.99	34.35	10.17

FRAMES 6-12

Parameters specific to AFL experiments:

Meteorological parameters: Height of recorded wind (m): 3
 Set up: Source type: P
 Diam. (m): 0.004
 Emissions: Emission rate (g/s): 2.57×10^{-2}
 Source: point source: Include

Parameters specific to Runs 10-15:

Set up: Height (m): 0.3
 Grids: Specified points: Run 10-15 grid

Meteorological parameters, Run 10:

Wind speed (m/s)	Wind angle (degrees)	Year	Julian day number	Local time (hours)	Could cover (oktas)
3.72	270	2001	204	10	8
3.75	270	2001	204	11	8
3.82	270	2001	204	12	8
3.78	270	2001	204	13	8
3.73	270	2001	204	14	8

Meteorological parameters, Run 11:

Wind speed (m/s)	Wind angle (degrees)	Year	Julian day number	Local time (hours)	Could cover (oktas)
2.1	270	2001	205	9	8
2.085	270	2001	205	10	8
2.095	270	2001	205	11	8
2.075	270	2001	205	12	8
2.055	270	2001	205	13	8

Meteorological parameters, Run 12:

Wind speed (m/s)	Wind angle (degrees)	Year	Julian day number	Local time (hours)	Could cover (oktas)
2.125	270	2001	206	9	8
2.095	270	2001	206	10	8
2.07	270	2001	206	11	8
1.95	270	2001	206	12	8
2.045	270	2001	206	13	8

Meteorological parameters, Run 13:

Wind speed (m/s)	Wind angle (degrees)	Year	Julian day number	Local time (hours)	Could cover (oktas)
3.715	270	2001	208	9	8
3.78	270	2001	208	10	8
3.705	270	2001	208	11	8
3.78	270	2001	208	12	8
3.725	270	2001	208	13	8

Meteorological parameters, Run 14:

Wind speed (m/s)	Wind angle (degrees)	Year	Julian day number	Local time (hours)	Could cover (oktas)
2.855	270	2001	215	10	8
2.905	270	2001	215	11	8
2.92	270	2001	215	12	8
2.86	270	2001	215	13	8

Meteorological parameters, Run 15:

Wind speed (m/s)	Wind angle (degrees)	Year	Julian day number	Local time (hours)	Could cover (oktas)
2.77	270	2001	218	9	8
2.77	270	2001	218	10	8
2.765	270	2001	218	11	8
2.71	270	2001	218	12	8

X (m)	Y (m)	Z (m)	X (m)	Y (m)	Z (m)
5	0.25	0.05	5	-0.25	0.05
5	0.25	0.3	5	-0.25	0.3
5	0.25	0.8	5	-0.25	0.8
5	0.25	1.3	5	-0.25	1.3
5	0.25	1.8	5	-0.25	1.8
5	0.25	2.3	5	-0.25	2.3
5	0.25	2.8	5	-0.25	2.8
5	0.25	3.3	5	-0.25	3.3
5	0.25	3.8	5	-0.25	3.8
5	0.75	0.05	5	-0.75	0.05
5	0.75	0.3	5	-0.75	0.3
5	0.75	0.8	5	-0.75	0.8
5	0.75	1.3	5	-0.75	1.3
5	0.75	1.8	5	-0.75	1.8
5	0.75	2.3	5	-0.75	2.3
5	0.75	2.8	5	-0.75	2.8
5	0.75	3.3	5	-0.75	3.3
5	0.75	3.8	5	-0.75	3.8
5	1.25	0.05	5	-1.25	0.05
5	1.25	0.3	5	-1.25	0.3
5	1.25	0.8	5	-1.25	0.8
5	1.25	1.3	5	-1.25	1.3
5	1.25	1.8	5	-1.25	1.8
5	1.25	2.3	5	-1.25	2.3
5	1.25	2.8	5	-1.25	2.8
5	1.25	3.3	5	-1.25	3.3
5	1.25	3.8	5	-1.25	3.8
5	1.75	0.05	5	-1.75	0.05
5	1.75	0.3	5	-1.75	0.3
5	1.75	0.8	5	-1.75	0.8
5	1.75	1.3	5	-1.75	1.3
5	1.75	1.8	5	-1.75	1.8
5	1.75	2.3	5	-1.75	2.3
5	1.75	2.8	5	-1.75	2.8
5	1.75	3.3	5	-1.75	3.3
5	1.75	3.8	5	-1.75	3.8
5	2.25	0.05	5	-2.25	0.05
5	2.25	0.3	5	-2.25	0.3
5	2.25	0.8	5	-2.25	0.8
5	2.25	1.3	5	-2.25	1.3
5	2.25	1.8	5	-2.25	1.8
5	2.25	2.3	5	-2.25	2.3
5	2.25	2.8	5	-2.25	2.8
5	2.25	3.3	5	-2.25	3.3
5	2.25	3.8	5	-2.25	3.8

Runs 10-15

Parameters specific to Runs 16-17:

Set up:	Source type:	P
	Height (m):	1.8
	Diam. (m):	0.004
Emissions:	Emission rate (g/s):	2.57×10^{-2}
Grids:	Specified points:	Run 16+17 grid
Source:	point source:	Include

Meteorological parameters, Run 16:

Wind speed (m/s)	Wind angle (degrees)	Year	Julian day number	Local time (hours)	Could cover (oktas)
2.835	270	2001	220	9	8
2.655	270	2001	220	10	8

Meteorological parameters, Run 17:

Wind speed (m/s)	Wind angle (degrees)	Year	Julian day number	Local time (hours)	Cloud cover (oktas)
2.78	270	2001	220	12	8
2.65	270	2001	220	13	8

Runs 18 and 19 were also modelled using the parameters for Runs 16 and 17, but using Run 18+19 grid for the grid parameters.

X (m)	Y (m)	Z (m)	X (m)	Y (m)	Z (m)
3	0.25	0.05	3	-0.25	0.05
3	0.25	0.3	3	-0.25	0.3
3	0.25	0.8	3	-0.25	0.8
3	0.25	1.3	3	-0.25	1.3
3	0.25	1.8	3	-0.25	1.8
3	0.25	2.3	3	-0.25	2.3
3	0.25	2.8	3	-0.25	2.8
3	0.25	3.3	3	-0.25	3.3
3	0.25	3.8	3	-0.25	3.8
3	0.75	0.05	3	-0.75	0.05
3	0.75	0.3	3	-0.75	0.3
3	0.75	0.8	3	-0.75	0.8
3	0.75	1.3	3	-0.75	1.3
3	0.75	1.8	3	-0.75	1.8
3	0.75	2.3	3	-0.75	2.3
3	0.75	2.8	3	-0.75	2.8
3	0.75	3.3	3	-0.75	3.3
3	0.75	3.8	3	-0.75	3.8
3	1.25	0.05	3	-1.25	0.05
3	1.25	0.3	3	-1.25	0.3
3	1.25	0.8	3	-1.25	0.8
3	1.25	1.3	3	-1.25	1.3
3	1.25	1.8	3	-1.25	1.8
3	1.25	2.3	3	-1.25	2.3
3	1.25	2.8	3	-1.25	2.8
3	1.25	3.3	3	-1.25	3.3
3	1.25	3.8	3	-1.25	3.8
3	1.75	0.05	3	-1.75	0.05
3	1.75	0.3	3	-1.75	0.3
3	1.75	0.8	3	-1.75	0.8
3	1.75	1.3	3	-1.75	1.3
3	1.75	1.8	3	-1.75	1.8
3	1.75	2.3	3	-1.75	2.3
3	1.75	2.8	3	-1.75	2.8
3	1.75	3.3	3	-1.75	3.3
3	1.75	3.8	3	-1.75	3.8
3	2.25	0.05	3	-2.25	0.05
3	2.25	0.3	3	-2.25	0.3
3	2.25	0.8	3	-2.25	0.8
3	2.25	1.3	3	-2.25	1.3
3	2.25	1.8	3	-2.25	1.8
3	2.25	2.3	3	-2.25	2.3
3	2.25	2.8	3	-2.25	2.8
3	2.25	3.3	3	-2.25	3.3
3	2.25	3.8	3	-2.25	3.8

Runs 16 + 17

X (m)	Y (m)	Z (m)	X (m)	Y (m)	Z (m)
3	0	0.3	3	-0.25	0.3
3	0	0.8	3	-0.25	0.8
3	0	1.3	3	-0.25	1.3
3	0	1.55	3	-0.25	1.55
3	0	1.8	3	-0.25	1.8
3	0	2.05	3	-0.25	2.05
3	0	2.3	3	-0.25	2.3
3	0	2.8	3	-0.25	2.8
3	0	3.3	3	-0.25	3.3
3	0.25	0.3	3	-0.5	0.3
3	0.25	0.8	3	-0.5	0.8
3	0.25	1.3	3	-0.5	1.3
3	0.25	1.55	3	-0.5	1.55
3	0.25	1.8	3	-0.5	1.8
3	0.25	2.05	3	-0.5	2.05
3	0.25	2.3	3	-0.5	2.3
3	0.25	2.8	3	-0.5	2.8
3	0.25	3.3	3	-0.5	3.3
3	0.5	0.3	3	-0.75	0.3
3	0.5	0.8	3	-0.75	0.8
3	0.5	1.3	3	-0.75	1.3
3	0.5	1.55	3	-0.75	1.8
3	0.5	1.8	3	-0.75	2.3
3	0.5	2.05	3	-0.75	2.8
3	0.5	2.3	3	-0.75	3.3
3	0.5	2.8	3	-1.25	0.3
3	0.5	3.3	3	-1.25	0.8
3	0.75	0.3	3	-1.25	1.3
3	0.75	0.8	3	-1.25	1.8
3	0.75	1.3	3	-1.25	2.3
3	0.75	1.8	3	-1.25	2.8
3	0.75	2.3	3	-1.25	3.3
3	0.75	2.8	3	-1.75	0.3
3	0.75	3.3	3	-1.75	0.8
3	1.25	0.3	3	-1.75	1.3
3	1.25	0.8	3	-1.75	1.8
3	1.25	1.3	3	-1.75	2.3
3	1.25	1.8	3	-1.75	2.8
3	1.25	2.3	3	-1.75	3.3
3	1.25	2.8			
3	1.25	3.3			
3	1.75	0.3			
3	1.75	0.8			
3	1.75	1.3			
3	1.75	1.8			
3	1.75	2.3			
3	1.75	2.8			
3	1.75	3.3			

Runs 18 + 19

APPENDIX 4: AMMONIA DEPOSITION RATE CALCULATION

Example deposition rate calculation:

Assuming that the plume is half a cone:

$$V_p = \frac{1}{6} \cdot \pi \cdot h^2 \cdot d$$

where: V_p is the volume of the plume upwind of the flux frame, h is the plume height and d is the distance between the source and the flux frame.

Plume height, $h = 2$ m; distance between the source and the flux frame = 7 m.

$$V_p = 14.66 \text{ m}^3$$

Using the log law relationship (equations 20-23), the wind speed at approximately half the height of the plume can be found from the measurement of air speed at a height of 2 m, and used as an approximate average wind speed for the plume.

Wind speed, $u_{2m} = 2.8 \text{ m s}^{-1}$.

$$u_{1m} = \frac{2.8 \times \ln\left(\frac{1}{0.01}\right)}{\ln\left(\frac{2}{0.01}\right)} = \frac{12.89}{5.298}$$

$$= 2.43 \text{ m s}^{-1}$$

From this and the distance the plume has to travel between source and flux frame (d), an Air Change Rate (ACR) can be determined:

$$\text{ACR} = \frac{d}{u_{1m}} = \frac{7}{2.43}$$

$$= 2.88 \text{ s}$$

The plume concentration can be determined using the ACR, the flow rate and the volume of the plume. The release rate (flow rate) is known in l min^{-1} , so must be converted to kg s^{-1} to enable the correct units, by converting first to l s^{-1} , then to $\text{m}^3 \text{ s}^{-1}$ (by multiplying by 10^{-3}) and then multiplying by the density of ammonia:

$$\text{Flow rate} = 2 \text{ l min}^{-1} = 0.033 \text{ l s}^{-1} = 0.033 \times 10^{-3} \text{ m}^3 \text{ s}^{-1}$$

$$\times \text{by density } (0.73 \text{ kg m}^{-3}) = 2.41 \times 10^{-5} \text{ kg s}^{-1}$$

$$C_p = \frac{ACR \times \text{flow rate}}{V_p} = \frac{2.88 \times (2.41 \times 10^{-5})}{14.66}$$

$$= 4.73 \times 10^{-6} \text{ kg m}^{-3}$$

Using the plume concentration and a deposition speed taken from literature (0.016 m s⁻¹), the deposition flux could be calculated:

$$F_D = C_p \times u_D = (4.73 \times 10^{-6}) \times 0.016$$

$$= 7.57 \times 10^{-8} \text{ kg m}^{-2} \text{ s}^{-1}$$

From the deposition flux and the area over which the plume can be found, a deposition rate can then be calculated:

$$\text{Deposition Rate} = F_D \times A_p$$

where A_p is the area of ground covered by the plume, calculated from half the width of the plume, b , and d :

$$A_p = b \times d = 2 \times 7$$

$$= 14 \text{ m}^2$$

Therefore:

$$\text{Deposition Rate} = (7.57 \times 10^{-8}) \times 14$$

$$= 1.06 \times 10^{-6} \text{ kg s}^{-1}$$

A percentage loss of ammonia can then be determined:

$$\% \text{ loss} = \frac{\text{Deposition Rate}}{\text{Flow Rate}} \times 100 = \frac{1.06 \times 10^{-6}}{2.41 \times 10^{-5}} \times 100$$

$$= 4.4 \%$$